Science Innovation
INTERNATIONAL SCIENTIFIC JOURNAL

ISSN: 2181-3337

SCIENCE & INNOVATION

INTERNATIONAL SCIENTIFIC JOURNAL

VOLUME 5 | ISSUE 7 | 2026
Series D: Medical Sciences

Science Innovation
INTERNATIONAL SCIENTIFIC JOURNAL

International Scientific Journal
SCIENCE AND INNOVATION

Series D
Volume 5 Issue 7
July 2026

Tashkent 2026

INTERNATIONAL PEER-REVIEWED SCIENTIFIC JOURNAL

SCIENCE & INNOVATION

Series D: Medical Sciences

VOLUME	ISSUE	PUBLICATION DATE	PLACE
5	7	31 JULY 2026	TASHKENT

ISSUE IDENTIFICATION

RECOMMENDED ISSUE CITATION

Science and Innovation. Series D: Medical Sciences. Volume 5, Issue 7, 31 July 2026. Tashkent: Science and Innovation LLC. ISSN 2181-3337.

Individual article DOIs are registered through Crossref under prefix 10.67620.

JOURNAL INFORMATION

Volume / issue	Volume 5 · Issue 7	**Publication date**	31 July 2026
ISSN	2181-3337	**Publisher**	Science and Innovation LLC
Established	2022	**Publication language**	English
Frequency	Monthly	**Publication format**	Electronic · Open Access
Peer review	Double-blind peer review	**License**	Creative Commons Attribution 4.0
DOI registration	Crossref · Prefix 10.67620	**Official website**	https://scientists.uz

AIMS AND SCOPE

Series D publishes original research and reviews in clinical and preclinical medicine, public health, pediatrics, dentistry, pharmacy and pharmacology, biomedical sciences, health education, healthcare management, and other interdisciplinary areas relevant to human health and medical practice.

EDITORIAL AND PUBLICATION STANDARDS

PEER REVIEW

Editorial screening, integrity checks, independent double-blind review, and a documented editorial decision.

ETHICS & CORRECTIONS

Conflicts of interest, authorship, misconduct, corrections, retractions, complaints, and appeals are handled under published journal policies.

AI TRANSPARENCY

Authors must disclose substantive use of generative AI. AI tools cannot be credited as authors; responsibility remains with the human authors.

EDITORIAL OFFICE

Bakhtiyor Rustamov	CEO Science and innovation LLC	**Kozim Ergashov**	Academic Editor
Gulira'no Rakhmatullayeva	Responsible Secretary	**Feruzabonu Mannonova**	Language Editor
Feruza Ollomurodova	Manuscript Coordinator	**Jahongir Bekmuradov**	Language Editor
Farangiz Sagdullaeva	Technical Editor	**Anvar Ergashev**	Digital Media Designer
Dilnoza Narzullayeva	Editorial Manager	**Asila Khaydaralieva**	Academic Editor
Sevara O'rinboyeva	Editorial Manager	**Bakhrom Qurbonov**	Digital Media Designer

PUBLISHER AND CONTACT

Science and Innovation LLC · Mass Media License No. 1597 (27 April 2022) Publishing License No. 455168 (21 November 2024)
150 Shota Rustaveli Street, Vega Business Center, 6th floor, Room 2, Tashkent 100121, Uzbekistan
info@scientists.uz · +998 90 125 96 54 · https://scientists.uz · https://science-innovation.org

© 2026 Authors. Published by Science and Innovation LLC under CC BY 4.0.

SCIENTIFIC EDITORIAL BOARD

Series D: Medical Sciences

EDITOR-IN-CHIEF: ABDURAKHMONOVA NILUFAR ZAYNOBIDDIN QIZI - DOCTOR OF PHILOLOGICAL SCIENCES, PROFESSOR

24 BOARD MEMBERS | **INTERNATIONAL REPRESENTATION** Uzbekistan · Russian Federation · Georgia · Tajikistan · Türkiye · India · United States

Members are listed by academic standing and editorial responsibility. Current institutional profiles and contact details are maintained on the journal website.

Sidikov Akmal Abdikakharovich DSc, Medical Sciences, Professor *Fergana Medical Institute of Public Health · Uzbekistan*	**Axmedova Dilorom Ilkhamovna** DSc, Medical Sciences, Professor, First-Degree State Prize Laureate of Uzbekistan *Tashkent State Medical University · Uzbekistan*	**Musayeva Dilfuza Makhmudovna** DSc, Medical Sciences, Professor *Central Asian Association of Pharmacologists and Clinical Pharmacologists · Uzbekistan*
Tursunov Sobir Turdiyevich Candidate of Medical Sciences, DSc, Pedagogical Sciences, Professor *Sergeli Abu Ali ibn Sino Public Health Technical College of Tashkent City · Uzbekistan*	**Khalimova Zamira Yusupovna** DSc, Medical Sciences, Professor *Republican Specialized Scientific and Practical Medical Center of Endocrinology · Uzbekistan*	**Novik Gennadiy Ayzikovich** DSc, Medical Sciences, Professor *Ministry of Health of the Russian Federation · Russia*
Sattarov Jamoliddin Bakhronovich DSc, Medical Sciences, Professor *Tashkent State Medical University · Uzbekistan*	**Rasulova Khurshidakhon Abduboriyevna** DSc, Medical Sciences, Professor *Termez Branch of Tashkent Medical Academy · Uzbekistan*	**Sodiqova Zumrat Shavkatovna** DSc, Medical Sciences, Professor *Tashkent Medical Academy · Uzbekistan*
Urinov Muso Boltayevich DSc, Medical Sciences, Professor *Abu Ali ibn Sino Bukhara State Medical Institute · Uzbekistan*	**Khalimova Khanifa Mukhsinovna** DSc, Medical Sciences, Professor *Tashkent Medical Academy · Uzbekistan*	**Ketevan Barabadze** DSc, Medical Sciences, Professor *Tbilisi State Medical University · Georgia*
Khajimuratov Abduqaxkhor Abdumutalovich DSc, Economic Sciences, Professor *Fergana Medical Institute of Public Health · Uzbekistan*	**Ilolov Ahmadsho Mahmadshoyevich** DSc, Chemical Sciences, Professor *International University of Tourism and Entrepreneurship of Tajikistan · Tajikistan*	**Abidov Hasankhodja Alisherovich** DSc, Medical Sciences, Assoc. Professor *Tashkent State Medical University · Uzbekistan*
Ibrohim Alatas DSc, Medical Sciences, Assoc. Professor *Beykent University · Türkiye*	**Javed Khon** DSc, Medical Sciences *Max Hospital · India*	**Nigmatova Iroda Maratovna** Candidate of Medical Sciences, Assoc. Professor *Tashkent State Dental Institute · Uzbekistan*
Abzalova Shahnoza Rustamovna Candidate of Medical Sciences, Assoc. Professor *Tashkent State Medical University · Uzbekistan*	**Jalolova Dilfuza Zukhridinovna** Candidate of Medical Sciences, Assoc. Professor *Samarkand State Medical University · Uzbekistan*	**Muqimov Odiljon Ahmadjonovich** PhD in Medical Sciences, Assoc. Professor *Tashkent State Dental Institute · Uzbekistan*
Pirlepesov Fakhriddin PhD in Radiation Oncology *St. Jude Children's Research Hospital (USA) · USA*	**Kalugina Vera Gennadyevna** Candidate of Medical Sciences *Research Institute of Pediatrics at the Russian National Surgical Center · Russia*	**Khasanova Guzaliya Marsovna** PhD in Medicine *Moscow Region State Budgetary Healthcare Institution (Russia) · Russia*

ISSN: 2181-3337 | SCIENTISTS.UZ VOLUME 5 ISSUE 7 JULY 2026

GROWTH AND NUTRITIONAL STATUS IN YOUNG CHILDREN WITH CONGENITAL HEART DISEASE

Agzamova Shoira[1], Khaybullina Zarina[2], Babadjanova Faniya[3]
D.M.Sc., Professor, Department of Family Medicine No.1,
Physical Education and Civil Defense, Tashkent State Medical University, Tashkent, Uzbekistan
Email: shoira_agzamova@mail.ru[1]
D.M.Sc., Professor, Head of the Department of Biochemistry with the Microbiology Group,
Republican Specialized Scientific and Practical Medical Center for Surgery named after Academician V. Vakhidov, Tashkent, Uzbekistan
Email: zrkhaybullina-1@gmail.com[2]
PhD, Associate Professor, Department of Pediatrics and Neonatology,
Urgench State Medical Institute, Urgench, Uzbekistan
Email: babadjanovafaniya@gmail.com[3]

DOI: 10.67620/sai.57d0001

ABSTRACT
Background. Congenital heart disease (CHD) is frequently accompanied by growth faltering and malnutrition during early childhood. Aim. To assess physical development and nutritional status in children aged 0–3 years with CHD according to age, sex, and defect phenotype. Materials and methods. This prospective observational study included 159 children with CHD and 58 age-comparable controls. Anthropometric indices were calculated with WHO Anthro and WHO AnthroPlus, including weight-for-age z score (WAZ), height-for-age z score (HAZ), weight-for-height z score (WHZ), and body mass index-for-age. Results. Children with CHD had significantly poorer anthropometric indices than controls. The greatest impairment occurred during the first 6 months of life, when severe underweight and wasting were especially frequent among boys. Indicators improved modestly at 6–12 months but deteriorated again at 1–3 years. Children with cyanotic defects had critically low WAZ and WHZ values more often than those with acyanotic defects. Conclusion. Children with CHD require early and regular standardized growth and nutritional monitoring. Infants, boys, and children with cyanotic defects represent the highest-risk groups.

ACCEPTED

20.07.26

Keywords: *congenital heart disease; children; physical development; nutritional status; underweight; stunting; wasting; WAZ; HAZ; WHZ; BMI.*

CC BY

INTRODUCTION

The global significance of this problem is determined by the fact that childhood malnutrition is recognized as one of the key public health challenges and is directly related to the achievement of Sustainable Development Goal 2.2 — ending all forms of malnutrition by 2030 [United Nations Children's Fund [UNICEF], World Health Organization [WHO], & World Bank Group, 2025]. According to joint estimates by UNICEF/WHO/World Bank, despite a decrease in the global prevalence of stunting among children under 5 years of age from 26.4% in 2012 to 23.2% in 2024, millions of children worldwide continue to suffer from chronic and acute malnutrition. In 2024, wasting was identified in 6.6% of children under 5 years of age, corresponding to 42.8 million children, while severe wasting was observed in 1.9%,

or 12.2 million children [UNICEF, WHO, & World Bank Group, 2025]. These data emphasize that WAZ, HAZ, and WHZ are not only anthropometric criteria but also important international indicators of child survival, health, and quality of development.

Nutritional status is of particular importance in children with CHD. In this category of patients, malnutrition develops under the influence of a complex combination of cardiac and non-cardiac factors, including hemodynamic overload, chronic hypoxemia, pulmonary hypertension, heart failure, increased energy requirements, sucking and feeding difficulties, gastroesophageal reflux, malabsorption, and frequent infectious complications [Centeno-Malfaz et al., 2023; Luca et al., 2022; Smith et al., 2024; Vazzana et al., 2025; Zhang et al., 2020]. As a result, a specific "vicious circle" develops in children with CHD: cardiovascular pathology aggravates nutritional deficiency, while body weight deficit and growth retardation, in turn, worsen disease tolerance, increase the risk of complications, and may negatively affect the outcomes of surgical treatment.

Current studies show that malnutrition among children with CHD occurs much more frequently than in the general population, and its severity depends on the child's age, the severity of hemodynamic disorders, and the phenotype of the defect [Centeno-Malfaz et al., 2023; Luca et al., 2022; Smith et al., 2024; Vazzana et al., 2025; Zhang et al., 2020]. The highest risk is typical for children in the first year of life, especially in the presence of cyanotic defects, pulmonary hypertension, heart failure, and delayed diagnosis. In this regard, assessment of physical development in children with CHD should be considered not as a secondary clinical indicator but as an essential component of comprehensive follow-up, early intervention, and preparation for cardiac surgery.

The relevance of this problem for the Republic of Uzbekistan is further strengthened by the fact that maternal and child health protection, early disease detection, improvement of the quality of medical care, and development of preventive medicine are important areas of state reforms. Presidential Decree of the Republic of Uzbekistan No. PF-60 dated January 28, 2022, "On the Development Strategy of New Uzbekistan for 2022–2026," pays special attention to improving the quality of medical and social services, as well as to measures aimed at strengthening children's health and well-being [President of the Republic of Uzbekistan, 2022]. It is also significant that, within the framework of this strategy, special social support measures for children are provided, including the organization of free meals for primary school pupils in the Republic of Karakalpakstan and Khorezm region, which reflects the state's intersectoral approach to issues of child health and nutrition [President of the Republic of Uzbekistan, 2022].

The further development of these priorities is reflected in the "Uzbekistan — 2030" Strategy and in Presidential Decree of the Republic of Uzbekistan No. PF-21 dated February 16, 2026, aimed at the consistent continuation of reforms and the alignment of national development with modern global challenges [President of the Republic of Uzbekistan, 2023, 2026]. These documents emphasize improving the quality of medical care and social protection, introducing measurable target indicators, and implementing digital monitoring of reform outcomes. Therefore, studies devoted to the early detection of physical developmental disorders in children with CHD fully correspond to national strategic objectives aimed at strengthening the health of the child population and improving the effectiveness of medical care [President of the Republic of Uzbekistan, 2023, 2026].

Against the background of the progress achieved in Uzbekistan in the field of child health protection, there remains a need for an in-depth study of vulnerable groups of children. According to UNICEF DATA, the under-five mortality rate in Uzbekistan in 2024 was 13.4 per 1,000 live births, reflecting a significant improvement compared with previous decades. At the same time, the modeled prevalence of stunting among children under 5 years of age is approximately 7%, early initiation of breastfeeding is observed in 40% of children, and the consumption of iodized salt is reported in 82% of households [UNICEF, n.d.]. These indicators demonstrate positive dynamics, but at the same time underline the need for targeted follow-up of children at high medical risk, including children with CHD.

ISSN: 2181-3337 | SCIENTISTS.UZ

The particular scientific and practical significance of the present study lies in its focus on the physical development of young children with CHD in the Khorezm region using standardized anthropometric indicators: WAZ, HAZ, WHZ, and BMI-for-age. The study included 159 children aged 0 to 3 years with CHD and 58 children in the control group; assessment was performed using WHO Anthro and WHO AnthroPlus, ensuring comparability of the obtained data with international standards for child growth and nutrition.

The obtained data show that most children with CHD are born with normal body weight and body length; however, during the first year of life, especially in the first 6 months, delayed physical development develops in these children. At the same time, abnormalities in WAZ, HAZ, and WHZ are more frequent and more pronounced in boys than in girls, while critically low WAZ and WHZ values occur significantly more often in children with cyanotic defects than in those with acyanotic defects.

Thus, the study of physical development in children with CHD is a relevant scientific and practical task of global, national, and regional importance. Early assessment of WAZ, HAZ, WHZ, and BMI in children with CHD allows timely detection of nutritional disorders, identification of high-risk groups, individualization of therapeutic and preventive measures, and improvement of the effectiveness of comprehensive follow-up in young children. Special attention should be paid to children in the first year of life, boys, and patients with cyanotic defects, since these groups have the highest risk of critical body weight deficit and impaired proportionality of physical development.

AIM

To assess physical development and nutritional status in young children with congenital heart disease according to age, sex, and defect phenotype.

MATERIALS AND METHODS

A prospective observational analytical cohort study was conducted among 159 children aged 0–3 years with congenital heart disease (CHD), including 91 boys (57.2%) and 68 girls (42.8%), who were born in Urgench and followed at the Departments of Cardiology and Cardiorheumatology of the Khorezm Regional Children's Multidisciplinary Medical Center from 2023 to 2026. The control group comprised 58 age-comparable children. Overall, 217 children were examined.

The inclusion criteria for the main group were as follows: age under 3 years, diagnosed congenital heart disease, absence of acute infections, and no antibacterial therapy within 14 days prior to examination. The exclusion criteria included prematurity of less than 36 weeks of gestation, inability to receive enteral nutrition, such as gastrostomy, ileostomy, or short bowel syndrome, as well as concomitant infectious diseases and viral hepatitis B and C.

The study was conducted in accordance with the Declaration of Helsinki after written informed consent had been obtained from the parents or legal guardians. Boys and girls accounted for 91 (57.2%) and 68 (42.8%) participants, respectively, giving a male-to-female ratio of 1.34. Ninety-six children (60.4%) were younger than 1 year, and 121 children (76.1%) were older than 6 months (Figure 1).

There were 6 newborns aged 0–30 days (3.8%), 32 children aged 1–6 months (20.1%), 58 children aged 6–12 months (36.5%), and 63 children aged 1–3 years (39.6%). The control group included 58 children. The most common defects were atrial and ventricular septal defects and Tetralogy of Fallot; other congenital heart defects occurred infrequently.

ISSN: 2181-3337 | SCIENTISTS.UZ

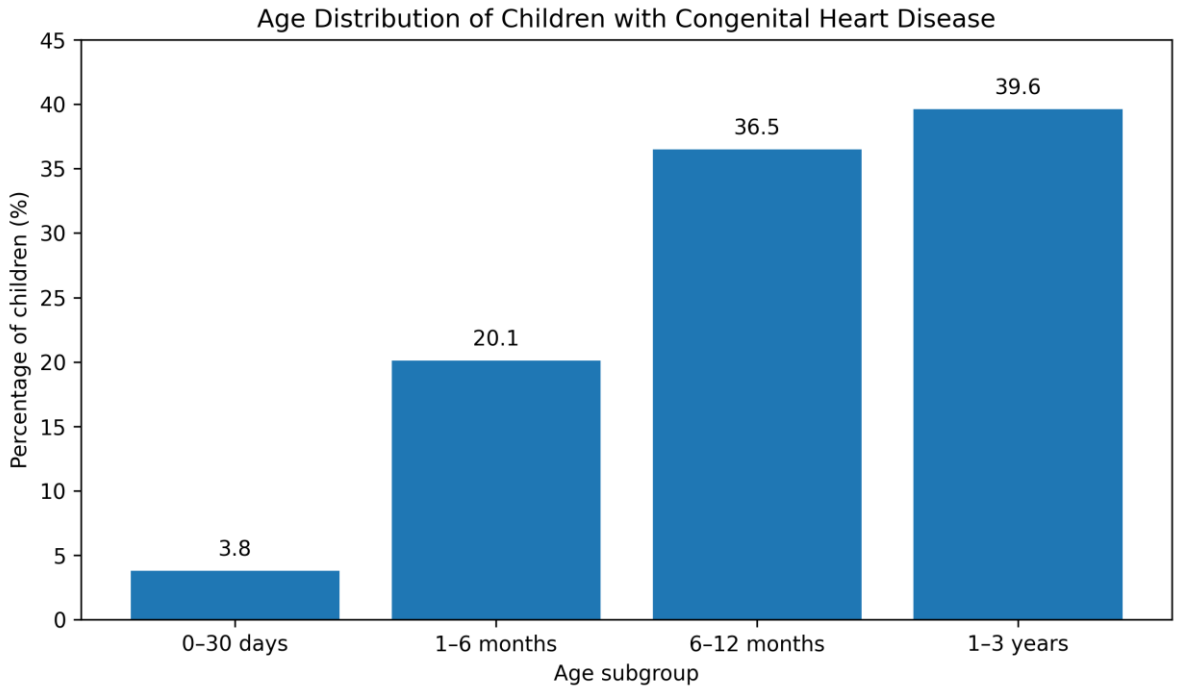


Figure 1. Age distribution of children with congenital heart disease (n = 159).

For analysis, defects were categorized as acyanotic or cyanotic according to anatomical and hemodynamic characteristics. Ventricular septal defect predominated among acyanotic lesions, whereas Tetralogy of Fallot was the most common cyanotic lesion. This grouping was preferred because administrative coding alone may not reliably capture anatomical CHD phenotypes (Ivey et al., 2023; Stephens et al., 2024).

Depending on the phenotype of the defect, we distinguished defects with left-to-right shunting, defects with right-to-left shunting, and combined defects. It was found that among acyanotic defects, VSD predominated, while among cyanotic defects, Tetralogy of Fallot was the most common. In addition, some children had CHD with potential transformation of an acyanotic defect into a defect with bidirectional shunting as a result of decompensation (Table 1).

Table 1. Distribution of children by age and CHD phenotype

Age Distribution of Children by Type of Congenital Heart Disease

Age subgroups	Cyanotic CHD, n	Cyanotic CHD, %	Acyanotic CHD, n	Acyanotic CHD, %	Total, n	Total, %
0–6 months, n (subgroup 1)	4	10.5	34	89.5	38	100
6–12 months, n (subgroup 2)	7	12.1	51	87.9	58	100
1–3 years, n (subgroup 3)	14	22.2	49	77.8	63	100
Total	25	15.7	134	84.3	159	100

A comprehensive examination of the children was conducted using standardized research methods. Analysis of life history and disease history was performed based on interviews with the children and their parents, as well as review of medical records, including Forms No. 111 and No. 25-u.

Assessment of anthropometric parameters was performed using the WHO Anthro software program (2009) and WHO AnthroPlus according to the following indicators: weight-for-age, weight-for-height, height-for-age, body mass index (BMI)-for-age, and z-score, reflecting the deviation of individual values from the mean reference values for the corresponding population.

Interpretation of the anthropometric measurement results in the observed patients was carried out according to the World Health Organization classification of malnutrition and ICD-10. Recent studies emphasize the importance of accurate anatomical and registry-based classification of congenital heart defects for epidemiological and outcome studies (Ivey et al., 2023; Stephens et al., 2024)

Anthropometric status was interpreted using World Health Organization growth standards. WAZ below −2 indicated underweight, HAZ below −2 indicated stunting, and WHZ or BMI-for-age below −2 indicated wasting or thinness. Values below −3 indicated severe impairment. Statistical analysis was performed in Statistica 10.0, SPSS 26.0, and Microsoft Excel. Quantitative variables are presented as mean

ISSN: 2181-3337 | SCIENTISTS.UZ

± standard error and 95% confidence intervals; categorical variables are presented as numbers and percentages. Student's t test was used for continuous variables, while the chi-square test or Fisher's exact test was used for categorical variables. A two-sided p value < 0.05 was considered statistically significant.

RESULTS

Among children aged 0–6 months, severe underweight (WAZ ≤ −3) was present in 62.5% of boys and 28.6% of girls, whereas moderate underweight (−3 < WAZ ≤ −2) occurred in 25.0% and 35.7%, respectively. Severe stunting (HAZ ≤ −3) was identified in 37.5% of boys and 21.4% of girls, and moderate stunting in 25.0% and 14.3%, respectively.

Normal-range HAZ values (−2 to +2) were found in 37.5% of boys and 64.3% of girls. Severe wasting (WHZ ≤ −3) affected 54.2% of boys and 28.6% of girls, while moderate wasting affected 33.3% and 42.9%, respectively.

Only 12.5% of boys and 28.5% of girls had WHZ values within the normal range (−2 to +2).

Girls aged 0–6 months showed a higher proportion of WAZ, HAZ, and WHZ values within the normal range than boys: 35.7% versus 12.5%, 64.3% versus 37.5%, and 28.5% versus 12.5%, respectively (Table 2).

Table 2. Distribution of children aged 0–6 months according to WHO growth z scores

Distribution of children with congenital heart defects according to their compliance with WHO growth curves at 0–6 months of age

Deviation (SD)	WAZ boys, n=24	WAZ girls, n=14	WAZ boys, %	WAZ girls, %	HAZ boys, n=24	HAZ girls, n=14	HAZ boys, %	HAZ girls, %	WHZ boys, n=24	WHZ girls, n=14	WHZ boys, %	WHZ girls, %
≤ −3 SD	15	4	62.5	28.6	9	3	37.5	21.4	13	4	54.2	28.6
−2 to −3 SD	6	5	25.0	35.7	6	2	25.0	14.3	8	6	33.3	42.9
−1 to −2 SD	3	4	12.5	28.6	3	2	12.5	14.3	3	3	12.5	21.4
−1 SD	0	1	0	7.1	5	6	20.8	42.9	0	1	0	7.1
Median	0	0	0	0	1	0	4.2	0	0	0	0	0
+1 SD	0	0	0	0	0	1	0	7.1	0	0	0	0
+1 to +2 SD	0	0	0	0	0	0	0	0	0	0	0	0
+2 to +3 SD	0	0	0	0	0	0	0	0	0	0	0	0
≥ +3 SD	0	0	0	0	0	0	0	0	0	0	0	0
Total	24	14	100	100	24	14	100	100	24	14	100	100

Note: WAZ — Weight-for-age z score, HAZ — Height-for-age z score, WHZ — Weight-for-height z score, SD — Standard deviation

Among children aged 6–12 months, severe underweight was present in 17.9% of boys and 20.0% of girls, while moderate underweight occurred in 17.9% and 16.7%, respectively. WAZ values within the normal range were observed in 64.3% of boys and 63.3% of girls.

Normal-range HAZ values were found in 89.3% of boys and 73.3% of girls. Severe stunting occurred in 3.6% of boys and 16.7% of girls, while moderate stunting was absent in boys and occurred in 10.0% of girls. Overall, linear growth was less impaired than body weight in this age subgroup.

Physical-development indices improved modestly during the second half of the first year. The proportion of boys with normal-range HAZ values increased from 37.5% to 89.3%, and the corresponding proportion among girls increased from 64.3% to 73.3% (Table 3).

ISSN: 2181-3337 | SCIENTISTS.UZ

Table 3. Distribution of children aged 6–12 months according to WHO growth z scores Distribution of children with CHD aged 6–12 months according to WHO growth curves,2nd subgroup, 6–12 months

Deviation (SD)	WAZ boys, n=28	WAZ girls, n=30	WAZ boys, %	WAZ girls, %	HAZ boys, n=28	HAZ girls, n=30	HAZ boys, %	HAZ girls, %	WHZ boys, n=28	WHZ girls, n=30	WHZ boys, %	WHZ girls, %
≤ −3 SD	5	6	17.9	20.0	1	5	3.6	16.7	12	3*	42.9	10.0
−3 to −2 SD	5	5	17.9	16.7	0	3	0	10.0	6	13*	21.4	43.3
−2 to −1 SD	13*	9	46.4	30.0	5*	3	17.9	10.0	6	9*	21.4	30.0
−1 SD	4*	9	14.3	30.0	9*	6	32.1	20.0	4	3	14.3	10.0
Median	0	0	0	0	1	0	3.6	0	0	0	0	0
+1 SD	1	1	3.6	3.3	4*	9	14.3	30.0	0	2*	0	6.7
+1 to +2 SD	0	0	0	0	6*	4	21.4	13.3	0	0	0	0
+2 to +3 SD	0	0	0	0	1	0	3.6	0	0	0	0	0
≥ +3 SD	0	0	0	0	1	0	3.6	0	0	0	0	0
Total	28	30	100	100	28	30	100	100	28	30	100	100

Note: * — statistically significant compared with girls at $p < 0.05$.

Among children aged 1–3 years with congenital heart disease (CHD), the proportion of boys with normal WAZ, HAZ, and WHZ values was 33.3%, 55.8%, and 53.9%, respectively, whereas among girls these values were 66.7%, 66.7%, and 66.7%, respectively. These data indicate that underweight and growth retardation/stunting were significantly more common among boys, with weight deficiency being more pronounced than growth retardation(Table 4).

Table 4. Distribution of children aged 1–3 years according to WHO growth z scores Distribution of children with CHD aged 1–3 years according to WHO growth curves,3rd subgroup, 1–3 years

Deviation (SD)	WAZ boys, n=39	WAZ girls, n=24	WAZ boys, %	WAZ girls, %	HAZ boys, n=39	HAZ girls, n=24	HAZ boys, %	HAZ girls, %	WHZ boys, n=39	WHZ girls, n=24	WHZ boys, %	WHZ girls, %
≤ −3 SD	12*	5	30.8	20.8	5*	1	12.8	4.2	12*	1	30.8	4.2
−3 to −2 SD	14*	3	35.9	12.5	11	5	28.2	20.8	6*	7	15.4	29.2
−2 to −1 SD	10*	12	25.6	50.0	11	6	28.2	25.0	12*	12	30.8	50.0
−1 SD	2*	2	5.1	8.3	5*	7	12.8	29.2	8	4	20.5	16.7
Median	0	0	0	0	2	0	5.1	0	0	0	0	0
+1 SD	0	1	0	4.2	3	2	7.7	8.3	1	0	2.6	0
+1 to +2 SD	1	1	2.6	4.2	1	1	2.6	4.2	0	0	0	0
+2 to +3 SD	0	0	0	0	0	0	0	0	0	0	0	0
≥ +3 SD	0	0	0	0	1	2	2.6	8.3	0	0	0	0
Total	39	24	100	100	39	24	100	100	39	24	100	100

Note: * — statistically significant compared with girls at $p < 0.05$.

In the control group, severe underweight and severe growth retardation/stunting were not detected. Changes in WAZ, HAZ, and WHZ within the range of −2Z to −3Z were observed only in 3.6% of cases among girls for HAZ and in 3.3% of boys for WHZ (Table5).

ISSN: 2181-3337 | SCIENTISTS.UZ

Table 5. Distribution of control-group children according to WHO growth z scores
Distribution of children in the control group according to WHO growth curves, Control group, n=58

Deviation (SD)	WAZ boys, n=30	WAZ girls, n=28	WAZ boys, %	WAZ girls, %	HAZ boys, n=30	HAZ girls, n=28	HAZ boys, %	HAZ girls, %	WHZ boys, n=30	WHZ girls, n=28	WHZ boys, %	WHZ girls, %
≤ −3 SD	0	0	0	0	0	0	0	0	0	0	0	0
−3 to −2 SD	0	0	0	0	0	1	0	3.6	1	0	3.3	0
−2 to −1 SD	11	3*	36.7	10.7	3	0	10.0	0	11*	7	36.7	25.0
−1 SD	15	12	50.0	42.9	20	14	66.7	50.0	9	11	30.0	39.3
Median	1	2*	3.3	7.1	0	1	0	3.6	2	1	6.7	3.6
+1 SD	2	11*	6.7	39.3	7*	12	23.3	42.9	4*	7	13.3	25.0
+1 to +2 SD	1	0	3.3	0	0	0	0	0	2*	1	6.7	3.6
+2 to +3 SD	0	0	0	0	0	0	0	0	1	1	3.3	3.6
≥ +3 SD	0	0	0	0	0	0	0	0	0	0	0	0
Total	30	28	100	100	30	28	100	100	30	28	100	100

Note: * — statistically significant compared with girls at $p < 0.05$.

Birth weight below 2,500 g was observed in 18 children (11.3%); among them, 2 children (11%) had cyanotic congenital heart defects, while 16 children (89%) had acyanotic congenital heart defects. Assessment of the mean values and 95% confidence intervals for WAZ, HAZ, and WHZ demonstrated statistically significant differences compared with the control group in all age subgroups. Although birth weight did not differ between children with and without congenital heart disease, weight deficiency progressed during subsequent growth and development (Table 6).

Table 6. Physical-development indices in newborns with CHD (subgroup 1a)

Parameters of physical development in newborns with congenital heart defects (subgroup 1a)

Indicator	Control group		Subgroup 1a, 0–30 days		p
	M±m	95% CI	M±m	95% CI	
Birth weight, g;	3562±256	2747; 4377	3642±72.8	3489; 3796	>0.05
WAZ	0.34±0.42	-1.01; +1.69	-2.01±0.29	-2.77; -1.27	<0.05
HAZ	-0.27±0.09	-0.58; +0.05	-0.73±0.45	-1.90; -0.43	<0.05
WHZ	0.89±0.14	-1.47; 1.26	-2.45±0.25	−2.91 to −2.01	<0.05
BMI	14.9±0.9	12.2; 17.8	10.1±0.9	9.21; 10.6	<0.05

Note: CHD — congenital heart disease; HAZ — height-for-age z score; WHZ — weight-for-height z score; SD — standard deviation.

As shown in the table, the mean WAZ values in children of subgroup 1a were within the 95% CI of −2.77 to −1.27; HAZ values were within the range of −1.90 to −0.43; and BMI values ranged from 9.21 to 10.6. In subgroup 1b, the 95% CIs for WAZ, HAZ, and WHZ were −3.1 to −4.6, −3.34 to −1.84, and −3.31 to −1.76, respectively. BMI increased over time but remained significantly lower than in the control group (Table 7).

Table 7. Physical-development indices in children aged 1–6 months with CHD (subgroup 1b)

Indicators of Physical Development in Children with Congenital Heart Disease (CHD), Subgroup 1b

ISSN: 2181-3337 | SCIENTISTS.UZ

Indicator	Control group		Subgroup 1 b (1–6 months)		p
	M±m	95% CI	M±m	95% CI	
WAZ	0.07±0.12	-0.19;+0.32	-3.8± 0.37*	−4.60 to −3.10	
HAZ	-0.28± 0.11	-0.51;+ 0.06	-2.59± 0.36*	-3.34; -1.84	
WHZ	0.07± 0.18	-0.31; +0.45	-2.5± 0.38*	-3.31; -1.76	
BMI	16.8± 0.38	16.0; 17.7	12.70±,28*	12.1; 13.2	

At the age of 1–6 months, there was a progression of both weight deficit, exceeding −3Z, and growth retardation, ranging from −2Z to −3Z. At the age of 6–12 months, the rate of lag in both growth and weight decreased, and children with congenital heart disease (CHD) showed WAZ and HAZ deviations within ±2Z. Moreover, the HAZ indicator was within ±1Z, while the decrease in BMI was mainly due to weight deficiency (Table 8).

Table 8. Physical-development indices in children aged 6–12 months with CHD (subgroup 2)

Indicators of Physical Development in Children with Congenital Heart Disease (CHD), Subgroup 2

Indicator	Control group		Subgroup 2 (6–12 months)		p
	M±m	95% CI	M±m	95% CI	
WAZ	-0.81±0.07	−0.96 to −0.67	-1.87± 0.16*	-2.20; -1.55	<0.05
HAZ	-0.03±0.10	-0.26;+0.19	-0.49± 0.23*	-0.97; -0.03	<0.05
WHZ	-1.07±0.03	−1.14 to −1.00	-1.82± 0.13*	-2.08; -1.57	<0.05
BMI	15.3±0.04	15.2; 15.4	14.1± 0.2	13.39; 14.89	<0.05

The trend toward a slight improvement in physical development indicators in children with congenital heart disease, which became evident in the second half of the first year of life, disappeared by the age of 2–3 years. Weight-for-age deficit remained stable at −2.30±0.17 Z-score, while the height-for-age indicator worsened almost twofold, decreasing from −0.49±0.23 Z-score to −1.14±0.21 Z-score (Table 9).

Table 9. Physical-development indices in children aged 1–3 years with CHD (subgroup 3)

Mean physical development parameters in children with congenital heart disease, subgroup 3

Indicator	Control group		Subgroup 3 (1–3 years)		p
	M±m	95% CI	M±m	95% CI	
WAZ	−0.24 ± 0.09	−0.44 to −0.09	-2.00±0.10*	-2.2; -1.83	<0.05
HAZ	0.08±0.05	-0.02; +0.18	-1.14±0.21*	-1.57; -0.71	<0.05
WHZ	-0.55±0.10	-0.77;+0.34	-2.30±0.17*	-2.67;-1.97	<0.05
BMI	15.1±0.1	14.8 to 15.5	13.5±0.2*	13.1;13.8	<0.05

The assessment of changes in mean physical development indicators among children with congenital heart disease revealed persistently reduced WAZ values, remaining below −2 Z-scores. In contrast, the mean HAZ values were generally within the acceptable −2 Z-score limits in both newborns with CHD and children older than 6 months. The most marked impairment in linear growth was recorded in the 6–12-month age group, where the HAZ value was −2.59±0.36 Z-score (Table 10, Figure 2).

ISSN: 2181-3337 | SCIENTISTS.UZ

Table 10. Mean physical-development indices by age subgroup

Dynamics of mean physical development parameters in children with congenital heart disease

Age subgroup	WAZ (M±m)	HAZ (M±m)	WHZ (M±m)	Linear-growth pattern	
0–30 days	-2.01±0.29	-0.73±0.45	-2.45±0.25	Underweight	Normal height
1–6 months	-3.8± 0.37	-2.59±0.36	-2.5±0.38	Underweight	Growth retardation / stunting
6–12 months	-1.87± 0.16	-0.49±0.23	-1.82± 0.13	Weight decrease within 2 Z-scores	Normal height
1–3 years	-2.00±0.10	-1.14±0.21	-2.30±0.17	Weight decrease within 2 Z-scores	Normal height

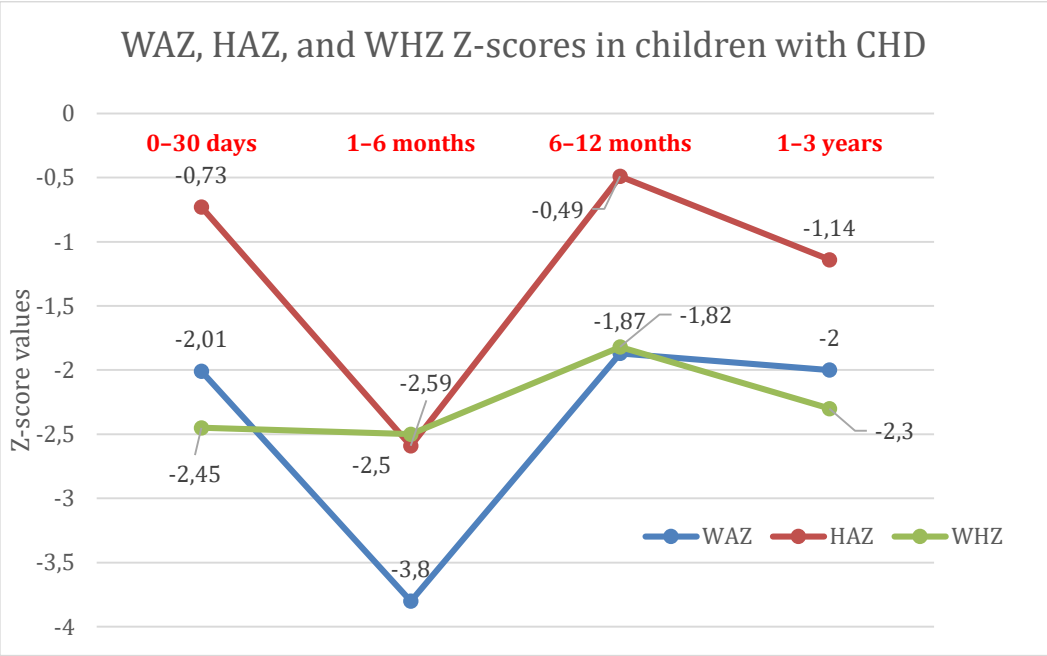


Figure 2

Figure 2 shows that nutritional impairment was greatest during the first 6 months of life. Among boys, severe underweight (WAZ ≤ −3) and severe stunting (HAZ ≤ −3) occurred in 62.5% and 37.5%, respectively; the corresponding proportions among girls were 28.6% and 21.4%. Normal-range WHZ values (−2 to +2) were found in only 12.5% of boys and 28.5% of girls ($p < 0.05$).

During the second six months of life, the parameters of physical development improved slightly: the proportion of boys without growth impairment increased 2.4-fold, from 37.5% to 89.3% ($p < 0.05$), while the proportion of girls without growth impairment increased from 64.3% to 73.3%. However, among children aged 1–3 years with CHD, the proportion of boys with normal WAZ values decreased 1.9-fold, from 64.3% in subgroup 2 to 33.3% ($p < 0.05$), and the proportion with normal HAZ values decreased 1.6-fold, from 89.3% to 55.8% ($p < 0.05$). In girls, the proportion with normal WAZ and HAZ values did not change significantly: the proportion of girls with normal WAZ values slightly increased from 63.3% to 66.7%, whereas the proportion with normal HAZ values slightly decreased from 73.3% to 66.7%. Normal WHZ values within ±2Z in subgroup 3 were observed in 53.9% of boys and 66.7% of girls.

These data indicate that, in children aged 1–3 years with CHD, underweight and growth retardation/stunting were significantly more common among boys, with weight deficiency being more pronounced than growth retardation. WHZ was −2.30±0.17, while the mean height-for-age z-score changed from −0.49±0.23Z to −1.14±0.21Z.

Most children with CHD (88.7%) had normal birth weight and length. During the first 6 months, however, severe underweight and wasting developed frequently, particularly among boys. Anthropometric indices improved modestly at 6–12 months but worsened again at 1–3 years, when weight deficit remained more pronounced than linear-growth impairment. These findings support intensified nutritional surveillance during infancy and early childhood.

ISSN: 2181-3337 | SCIENTISTS.UZ

DISCUSSION

Malnutrition is common among children with CHD and reflects increased energy expenditure, feeding difficulties, chronic hypoxemia, pulmonary hypertension, heart failure, gastrointestinal dysfunction, and recurrent infection (Centeno-Malfaz et al., 2023; Luca et al., 2022; Smith et al., 2024; Vazzana et al., 2025; Zhang et al., 2020). The present finding that most children were born with normal anthropometric measurements but developed nutritional deficits during infancy is consistent with previous reports. The higher frequency of severe WAZ and WHZ impairment in cyanotic CHD further supports the role of hypoxemia and hemodynamic burden in growth failure. Regular assessment of WAZ, HAZ, WHZ, and BMI-for-age should be integrated into cardiology follow-up and perioperative nutritional planning.

Approximately two thirds of children with CHD are born with normal body weight, while nutritional disorders develop during the first year of life. This is consistent with our data. As shown by our results, among full-term children with CHD, with prematurity being an exclusion criterion in the study, 141 children (89%) did not have fetal growth restriction syndrome, and their birth weight and length were normal and did not differ from those in the control group. At the same time, nutritional disorders developed in these children during the first year of life, especially during the first 6 months.

The type of heart defect has a strong influence on nutritional status. Early correction of patent ductus arteriosus, atrial septal defect, and pulmonary stenosis almost completely eliminates the risk of nutritional disorders. Pulmonary atresia, Tetralogy of Fallot, combined septal defects, transposition of the great arteries, and hypoplastic left heart syndrome are associated with a high risk for impaired nutritional status. In general, according to Vazzana GF et al. (2025), acyanotic defects are associated with a moderate and sometimes high risk of nutritional disorders, whereas defects with a right-to-left shunt, that is, cyanotic defects, always carry a high risk, especially in the presence of pulmonary hypertension and late diagnosis of the defect. The distribution of children according to the severity of nutritional disorders depending on the type of heart defect showed the following. Weight-for-age deficiency was more frequent and more severe in children with cyanotic congenital heart defects (C-CHD) compared with children with acyanotic congenital heart defects (A-CHD), since the proportion of children with WAZ deviations exceeding −3Z was 1.4 times higher among patients with C-CHD (Table11). Recent regional data also indicate that metabolic changes associated with short-chain fatty acids may be involved in the perioperative condition of children with congenital heart disease (Agzamova & Babadjanova, 2025).

Table 11. WAZ distribution according to CHD phenotype

Indicator	WAZ	A-CHD, n	C-CHD, n	A-CHD, %	C-CHD, %
Deviation (SD)	≤ −3 SD	40	10*	29.9	40.0
	−2 to −3 SD	34	4	25.4	16.0
	−1 to −2 SD	41	10	30.6	40.0
	−1 SD	14	1	10.4	4.0
	Median	0	0	0.0	0.0
	+1 SD	4	0	3.0	0.0
	+1 to +2 SD	1	0	0.7	0.0
	+2 to +3 SD	0	0	0.0	0.0
	≥ +3 SD	0	0	0.0	0.0
Total		134	25	100.0	100.0

Height-for-age deviations did not depend on the type of heart defect, whereas the proportion of children with WHZ deviations below −3Z was significantly higher among patients with cyanotic defects: 32% versus 22.4% ($p < 0.05$) (Table 12).

Table 12. HAZ and WHZ distributions in acyanotic and cyanotic CHD

Deviation (SD)	HAZ acyanotic CHD, n	HAZ cyanotic CHD, n	HAZ acyanotic CHD, %	HAZ cyanotic CHD, %	WHZ acyanotic CHD, n	WHZ cyanotic CHD, n	WHZ acyanotic CHD, %	WHZ cyanotic CHD, %
≤ −3 SD	20	3	14.9	12.0	30	8	22.4	32.0
−3 to −2 SD	24	4	17.9	16.0	32	8	23.9	32.0

ISSN: 2181-3337 | SCIENTISTS.UZ

Deviation (SD)	HAZ acyanotic CHD, n	HAZ cyanotic CHD, n	HAZ acyanotic CHD, %	HAZ cyanotic CHD, %	WHZ acyanotic CHD, n	WHZ cyanotic CHD, n	WHZ acyanotic CHD, %	WHZ cyanotic CHD, %
−2 to −1 SD	24	7	17.9	28.0	53	4	39.6	16.0
−1 SD	37	5	27.6	20.0	16	5	11.9	20.0
Median	0	0	0.0	0	0	0	0.0	0
+1 SD	15	4	11.2	16.0	2	0	1.5	0
+1 to +2 SD	9	1	6.7	4.0	0	0	0.0	0
+2 to +3 SD	2	0	1.5	0	0	0	0.0	0
≥ +3 SD	3	1	2.2	4.0	1	0	0.7	0
Total	134	25	100.0	100	134	25	100.0	100

Note: CHD — congenital heart disease; HAZ — height-for-age z score; WHZ — weight-for-height z score; SD — standard deviation.

CONCLUSION

Young children with CHD had substantially poorer growth and nutritional indices than controls. The greatest impairment occurred during the first 6 months of life, particularly among boys. Although some improvement was observed at 6–12 months, weight deficit persisted or re-emerged at 1–3 years. Cyanotic defects were associated with a higher frequency of critically low WAZ and WHZ values than acyanotic defects. Standardized, repeated anthropometric monitoring should begin early and should guide individualized nutritional, preventive, and therapeutic interventions.

REFERENCES

1. Allen, P., Zafar, F., Mi, J., Crook, S., Woo, J., Jayaram, N., Bryant, R., Karamlou, T., Tweddell, J., Dragan, K., Cook, S., Hannan, E. L., Newburger, J. W., Bacha, E. A., Vincent, R., Nguyen, K., Walsh-Spoonhower, K., Mosca, R., Devejian, N., … Anderson, B. R. (2022). Risk stratification for congenital heart surgery for ICD-10 administrative data (RACHS-2). Journal of the American College of Cardiology, 79(5), 465–478. https://doi.org/10.1016/j.jacc.2021.11.036
2. Agzamova, S. A., & Babadjanova, F. R. (2025). Dinamika korotkotsepochechnykh zhirnykh kislot u detey s vrozhdennymi porokami serdtsa v do- i posleoperatsionnom periode [Dynamics of short-chain fatty acids in children with congenital heart defects during the pre- and postoperative periods]. Aktual'nye voprosy prakticheskoy pediatrii, 1(1), 18–21. https://inconference.uz/index.php/congress-anesthes/article/view/708
3. Bourdon, G., Lenne, X., Godart, F., Storme, L., Theis, D., Subtil, D., Bruandet, A., & Rakza, T. (2024). Epidemiology of congenital heart defects in France from 2013 to 2022 using the PMSI-MCO database. PLOS ONE, 19(4), e0298234. https://doi.org/10.1371/journal.pone.0298234
4. Centeno-Malfaz, F., Moráis-López, A., Caro-Barri, A., Peña-Quintana, L., Gil-Villanueva, N., Redecillas-Ferreiro, S., Marcos-Alonso, S., Ros-Arnal, I., Tejero, M. Á., Sánchez, C. S., & Leis, R. (2023). Nutrition in congenital heart disease: Consensus document. Anales de Pediatría (English Edition), 98(5), 373–383. https://doi.org/10.1016/j.anpede.2023.02.022
5. Constantine, A., Dimopoulos, K., & Opotowsky, A. R. (2020). Congenital heart disease and pulmonary hypertension. Cardiology Clinics, 38(3), 445–456. https://doi.org/10.1016/j.ccl.2020.04.008
6. Fundora, M. P., Calamaro, C. J., Wu, Y., Brown, A. M., St John, A., Keiffer, R., Xiang, Y., Liu, K., Gillespie, S., Denning, P. W., Sanders-Lewis, K., Seitter, B., & Bai, J. (2024). Microbiome and growth in infants with congenital heart disease. The Journal of Pediatrics, 274, 114169. https://doi.org/10.1016/j.jpeds.2024.114169
7. Houyel, L., & Meilhac, S. M. (2021). Heart development and congenital structural heart defects. Annual Review of Genomics and Human Genetics, 22, 257–284. https://doi.org/10.1146/annurev-genom-083118-015012

8. Ivey, L. C., Rodriguez, F. H., III, Shi, H., Chong, C., Chen, J., Raskind-Hood, C. L., Downing, K. F., Farr, S. L., & Book, W. M. (2023). Positive predictive value of International Classification of Diseases, Ninth Revision, Clinical Modification, and International Classification of Diseases, Tenth Revision, Clinical Modification, codes for identification of congenital heart defects. Journal of the American Heart Association, 12(16), e030821. https://doi.org/10.1161/JAHA.123.030821
9. Luca, A. C., Miron, I. C., Mîndru, D. E., Curpăn, A. Ș., Stan, R. C., Țarcă, E., Luca, F. A., & Pădureț, A. I. (2022). Optimal nutrition parameters for neonates and infants with congenital heart disease. Nutrients, 14(8), 1671. https://doi.org/10.3390/nu14081671
10. Neunhaeuserer, D., Battista, F., Mazzucato, B., Vecchiato, M., Meneguzzo, G., Quinto, G., Niebauer, J., Gasperetti, A., Vida, V., Di Salvo, G., Varnier, M., & Ermolao, A. (2022). Exercise capacity and cardiorespiratory fitness in children with congenital heart diseases: A proposal for an adapted NYHA classification. International Journal of Environmental Research and Public Health, 19(10), 5907. https://doi.org/10.3390/ijerph19105907
11. Powell, A. W., Wittekind, S. G., Alsaied, T., Lubert, A. M., Chin, C., Veldtman, G. R., Cordina, R., Katz, D. A., Mays, W. A., Knecht, S. K., & Opotowsky, A. R. (2020). Body composition and exercise performance in youth with a Fontan circulation: A bio-impedance based study. Journal of the American Heart Association, 9(24), e018345. https://doi.org/10.1161/JAHA.120.018345
12. President of the Republic of Uzbekistan. (2022, January 28). Decree No. PF-60: On the Development Strategy of New Uzbekistan for 2022–2026. National Database of Legislation of the Republic of Uzbekistan.
13. President of the Republic of Uzbekistan. (2023, September 11). Decree No. PF-158: On the Uzbekistan–2030 Strategy. National Database of Legislation of the Republic of Uzbekistan.
14. President of the Republic of Uzbekistan. (2026, February 16). Decree No. PF-21: On additional measures for the consistent continuation and advancement of reforms within the priority areas of national development until 2030. National Database of Legislation of the Republic of Uzbekistan.
15. Silva-Gburek, J., Marroquín, A., Flores, S., Roddy, J., Ghanayem, N. S., Shekerdemian, L. S., & Coss-Bu, J. A. (2023). Perioperative nutritional status and organ dysfunction following surgery for congenital heart disease. Pediatric Cardiology, 44(6), 1350–1357. https://doi.org/10.1007/s00246-023-03111-2
16. Smith, R., Ntsiea, V., Brown, S., & Potterton, J. (2024). Undernutrition in young children with congenital heart disease undergoing cardiac surgery in a low-income environment. BMC Pediatrics, 24, Article 73. https://doi.org/10.1186/s12887-023-04508-x
17. Stephens, S. B., Benjamin, R. H., Lopez, K. N., Anderson, B. R., Lin, A. E., Shumate, C. J., Nembhard, W. N., Morris, S. A., & Agopian, A. J. (2024). Enhancing the classification of congenital heart defects for outcome association studies in birth defects registries. Birth Defects Research, 116(8), e2393. https://doi.org/10.1002/bdr2.2393
18. Sullivan, R. T., Raj, J. U., & Austin, E. D. (2023). Recent advances in pediatric pulmonary hypertension: Implications for diagnosis and treatment. Clinical Therapeutics, 45(9), 901–912. https://doi.org/10.1016/j.clinthera.2023.07.001
19. United Nations Children's Fund. (n.d.). Uzbekistan (UZB): Demographics, health & infant mortality. UNICEF Data. Retrieved July 18, 2026, from https://data.unicef.org/country/uzb/
20. United Nations Children's Fund, World Health Organization, & World Bank Group. (2025). Levels and trends in child malnutrition: UNICEF/WHO/World Bank Group Joint Child Malnutrition Estimates: Key findings of the 2025 edition. UNICEF and WHO.
21. Vazzana, G. F., Romano, A., & Romano, C. (2025). Nutritional issues in children with congenital heart diseases (CHDs). Nutrients, 17(24), 3936. https://doi.org/10.3390/nu17243936

ISSN: 2181-3337 | SCIENTISTS.UZ

22. Wacker, J., & Beghetti, M. (2025). Pulmonary hypertension in pediatrics: From clinical suspicion to management. European Journal of Pediatrics, 184(5), 288. https://doi.org/10.1007/s00431-025-06099-4
23. World Health Organization. (2009). WHO AnthroPlus for personal computers: Software for assessing growth of the world's children and adolescents. World Health Organization.
24. Zhang, M., Wang, L., Huang, R., Sun, C., Bao, N., & Xu, Z. (2020). Risk factors of malnutrition in Chinese children with congenital heart defect. BMC Pediatrics, 20, 213. https://doi.org/10.1186/s12887-020-02124-7
25. Zhang, Q.-L., Chen, X.-H., Zhou, S.-J., Lei, Y.-Q., Huang, J.-S., Chen, Q., & Cao, H. (2023). Relationship between disorders of the intestinal microbiota and heart failure in infants with congenital heart disease. Frontiers in Cellular and Infection Microbiology, 13, 1152349. https://doi.org/10.3389/fcimb.2023.1152349

ISSN: 2181-3337 | SCIENTISTS.UZ VOLUME 5 ISSUE 7 JULY 2026

ASSESSING THE EFFECTS OF MULTIMODAL PSYCHOMOTOR REHABILITATION ON MOTOR FUNCTION AND FUNCTIONAL INDEPENDENCE IN CHILDREN WITH CEREBRAL PALSY: A RANDOMIZED CONTROLLED TRIAL

Karimova Dilobar[1], **Ibodullaev Z.**[2]
E-mail: dilobarkarimov@gmail.com[1]
Tashkent State Medical University, Tashkent, Uzbekistan[2]

DOI: 10.67620/sai.57d0002

ABSTRACT

Cerebral palsy (CP) is a leading cause of childhood motor disability and is frequently accompanied by limitations in balance, self-care, mobility, and participation. Objective: To compare the clinical outcomes of a six-month multimodal psychomotor rehabilitation program with standard rehabilitation and to provide a preliminary economic assessment. Materials and Methods: Forty children with CP aged 3–12 years were randomly allocated to an intervention group (n = 20) or a control group (n = 20). Outcomes included the Gross Motor Function Measure-88 (GMFM-88), Pediatric Balance Scale (PBS), Modified Ashworth Scale, Manual Ability Classification System, and Pediatric Evaluation of Disability Inventory. EEG and MRI outcomes and economic estimates were exploratory. Results: The intervention group demonstrated larger improvements than the control group in GMFM-88 scores (30.8% vs. 13.1%; between-group change $p < .01$) and PBS scores (46.5% vs. 17.6%; $p < .01$). Modified Ashworth Scale scores decreased significantly in the intervention group ($p < .001$), and functional independence improved across PEDI domains. Exploratory EEG and MRI findings suggested neurophysiological and structural change, but these outcomes require independent confirmation. The preliminary economic analysis estimated a 94.4% return on investment and a 6.2-month payback period. Conclusion: Multimodal psychomotor rehabilitation was associated with greater motor, balance, and functional gains than standard therapy. The small sample, incomplete blinding, and exploratory imaging and economic analyses limit definitive inference.

ACCEPTED

20.07.26

Keywords: *cerebral palsy; psychomotor rehabilitation; motor function; GMFM-88; Pediatric Balance Scale; functional independence; randomized controlled trial.*

CC BY

Introduction.

Cerebral palsy (CP) comprises a group of permanent disorders of movement and posture caused by nonprogressive disturbances in the developing fetal or infant brain. Although motor impairment is the defining feature, CP is a lifelong, multisystem condition that may also involve cognition, communication, vision, hearing, epilepsy, behavior, pain, and participation restrictions (Graham et al., 2016; Gulati & Sondhi, 2018; Patel et al., 2020; Rosenbaum et al., 2007; Sadowska et al., 2020). Population-based estimates indicate that CP affects approximately 2 per 1,000 live births worldwide, with meaningful variation across regions, income settings, gestational age groups, and ascertainment methods (McIntyre et al., 2022; Vitrikas et al., 2020). European registry

data likewise demonstrate that associated impairments are common and should be considered when rehabilitation goals are formulated (Surveillance of Cerebral Palsy in Europe, 2000).

Contemporary rehabilitation emphasizes neuroplasticity, early identification, individualized goal setting, active practice, meaningful repetition, participation, and family involvement. International guidelines and systematic reviews support goal-directed, task-specific, activity-based, and sufficiently intensive interventions rather than reliance on any single named treatment approach (Hadders-Algra, 2021; Jackman et al., 2022; Morgan et al., 2021; Novak et al., 2020). Exercise and physical activity may improve fitness and selected functional outcomes, although intervention effects vary according to age, Gross Motor Function Classification System (GMFCS) level, treatment dose, and outcome measure (Ryan et al., 2017; Verschuren et al., 2016). Technology-assisted interventions are increasingly used; virtual reality, for example, has shown potential benefits for motor performance and balance, but the underlying evidence remains heterogeneous and is often based on small trials (Chen et al., 2018).

In Uzbekistan, strengthening access to coordinated, evidence-based pediatric rehabilitation and establishing locally relevant outcome and cost data remain important clinical and organizational priorities. A structured evaluation of multimodal psychomotor rehabilitation may therefore contribute to both clinical decision-making and service planning.

Aim of the Study. The primary objective was to compare changes in motor function, balance, muscle tone, manual ability, and functional independence between a multimodal psychomotor rehabilitation program and standard therapy. Secondary exploratory objectives were to describe EEG, MRI, parent-reported health-status, and preliminary economic outcomes.

Materials and Methods.

Study Design and Participants

This randomized controlled trial included 40 children aged 3–12 years (mean age, 6.8 ± 2.4 years) with a confirmed diagnosis of CP. Participants were allocated to an intervention group (n = 20), which received a comprehensive multimodal psychomotor rehabilitation program, or a control group (n = 20), which received standard rehabilitation therapy. The intervention period was six months. At baseline, the groups did not differ significantly in age, sex distribution, or GMFCS level ($p = .87$). Details of random-sequence generation, allocation concealment, prospective trial registration, and an a priori sample-size calculation were not available in the study records and are therefore acknowledged as reporting limitations.

Assessment Instruments

Gross motor function was classified using the five-level GMFCS, which describes self-initiated movement and mobility and has established reliability and content validity (Palisano et al., 1997, 2008). Quantitative gross motor performance was assessed using the Gross Motor Function Measure-88 (GMFM-88), which evaluates lying and rolling, sitting, crawling and kneeling, standing, and walking, running, and jumping (Russell et al., 2002).

Balance and postural control were evaluated with the Pediatric Balance Scale (PBS), a child-adapted modification of the Berg Balance Scale developed for school-age children with mild to moderate motor impairment (Franjoine et al., 2003). Spasticity was assessed using the Modified Ashworth Scale (Bohannon & Smith, 1987), and manual ability was classified using the Manual Ability Classification System (MACS; Eliasson et al., 2006). Because the Modified Ashworth Scale primarily measures resistance to passive movement, its scores were interpreted as an indirect clinical indicator of hypertonia rather than a complete physiological measure of spasticity (Pandyan et al., 1999).

Cognitive screening was performed with a study-specific age-adapted version of the Mini-Mental State Examination (MMSE). Because the original MMSE was developed for adults and the study-specific adaptation was not independently validated, cognitive scores were treated as exploratory and were not used as a primary efficacy endpoint (Folstein et al., 1975). Functional independence in activities of daily living was assessed using the Pediatric Evaluation of Disability Inventory (PEDI; Haley et al., 1992). For participants older than the PEDI's original normative age range, raw functional-domain scores were used descriptively rather than interpreted as age-normed values. Parent-reported health status was evaluated with the SF-36. Because the original SF-36 was developed for respondents aged 14 years and older, parent-proxy findings in this sample were treated as exploratory and not as validated pediatric quality-of-life outcomes (Ware & Sherbourne, 1992).

Neurophysiological and Neuroimaging Assessment

EEG was recorded according to the international 10–20 electrode placement system (Jasper, 1958).

ISSN: 2181-3337 | SCIENTISTS.UZ

Recordings used a low-frequency filter of 0.5–1 Hz, a high-frequency filter of 35–70 Hz, a sampling rate of 256–512 Hz, and a minimum duration of 20–30 minutes. Activation procedures included photic stimulation and hyperventilation. Background rhythm frequency and amplitude, epileptiform activity, and interhemispheric asymmetry were evaluated. Brain structure was assessed using MRI. T1-weighted, T2-weighted, fluid-attenuated inversion recovery, and diffusion-weighted sequences were used to evaluate cortical thickness, white matter integrity through fractional anisotropy, ventricular volume, corpus callosum thickness, and hippocampal volume.

Rehabilitation Program

The rehabilitation process was structured within the International Classification of Functioning, Disability and Health framework (World Health Organization, 2001). Following a multidimensional baseline assessment, individualized short-term goals (2–4 weeks) and long-term goals (3–12 months) were formulated using SMART principles (Bovend'Eerdt et al., 2009).

The multimodal program combined neuromotor treatment elements associated with the Bobath and Vojta approaches; exercises targeting attention, memory, and executive functioning; computer-based cognitive training; sensorimotor integration; and functional practice through play, sports, music, and art activities in home and school contexts. Consistent with contemporary evidence, the program emphasized active, goal-directed, task-specific, and participation-oriented practice rather than exclusive use of a single treatment concept (Anaby et al., 2013; Imms et al., 2017; Jackman et al., 2022; Novak et al., 2020). Progress was monitored monthly with standardized outcome measures. The intervention logic and assessment pathway are summarized in Figure 1.

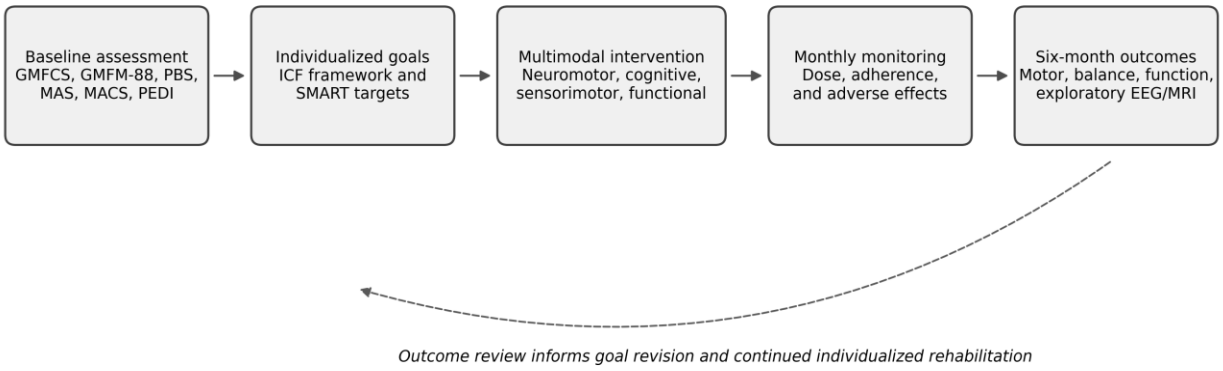


Figure 1. Multimodal psychomotor rehabilitation and outcome-assessment pathway.

Note. GMFCS = Gross Motor Function Classification System; GMFM-88 = Gross Motor Function Measure-88; PBS = Pediatric Balance Scale; MAS = Modified Ashworth Scale; MACS = Manual Ability Classification System; PEDI = Pediatric Evaluation of Disability Inventory; ICF = International Classification of Functioning, Disability and Health.

Statistical and Economic Analysis

Data were analyzed using SPSS version 25.0. Descriptive statistics included means, standard deviations, medians, and frequency distributions. Inferential analyses included paired- and independent-samples t tests as appropriate, the chi-square test, analysis of variance, correlation analysis, and regression analysis. Statistical significance was set at $p < .05$, and 95% confidence intervals were reported where available. Results are presented as mean ± standard deviation. Given the small sample and multiple exploratory outcomes, imaging, cognitive, parent-proxy health-status, and economic findings were interpreted cautiously. The economic analysis estimated incremental cost per additional GMFM-88 and PBS point, return on investment, and payback period. Because a full decision-analytic model and sensitivity analysis were not reported, the economic findings were treated as preliminary and interpreted against current reporting principles for health economic evaluation (Husereau et al., 2022).

Results

Baseline Characteristics

Baseline demographic and clinical characteristics were similar between the two groups. The intervention group included 12 boys (60%) and 8 girls (40%), whereas the control group included 11 boys (55%) and 9 girls (45%); the difference was not significant ($p > .05$). GMFCS levels were also balanced: levels I–II accounted for 40% of the intervention group and 45% of the control group, level III for 35% and 30%, respectively, and levels IV–V

ISSN: 2181-3337 | SCIENTISTS.UZ

for 25% in each group (p = .87).

Motor Function, Balance, Spasticity, and Manual Ability

After six months, GMFM-88 scores improved in both groups, with a greater increase in the intervention group. The mean score increased from 52.3 ± 18.7 to 68.4 ± 19.2 in the intervention group, corresponding to a 30.8% improvement (p < .001), and from 51.8 ± 17.9 to 58.6 ± 18.4 in the control group, corresponding to a 13.1% improvement (p < .05). The between-group difference in change was significant (p < .01), with a mean difference of 9.3 points (95% confidence interval, 4.7–14.9).

Analysis of individual GMFM-88 domains showed marked improvements in the intervention group. The sitting score increased from 65.3 ± 18.9 to 82.7 ± 14.2, and the crawling and kneeling score increased from 48.7 ± 22.4 to 71.3 ± 19.8 (both p < .001). Significant but smaller changes were observed in the standing and walking domains.

Independent sitting was achieved by 60% of children in the intervention group and 30% in the control group. Independent standing was achieved by 40% and 20%, respectively, and independent walking by 35% and 15%, respectively. PBS scores increased from 28.4 ± 12.7 to 41.6 ± 14.2 in the intervention group (46.5%, p < .001) and from 27.9 ± 13.1 to 32.8 ± 13.6 in the control group (17.6%, p < .05); the between-group difference was significant (p < .01). Modified Ashworth Scale scores decreased from 1.2 ± 0.8 to 0.7 ± 0.6 in the intervention group (p < .001) and from 1.3 ± 0.7 to 1.1 ± 0.7 in the control group (p > .05). MACS classification improved in 65% of children in the intervention group and 30% in the control group. Relative percentage improvements in GMFM-88 and PBS scores are shown in Chart 1.

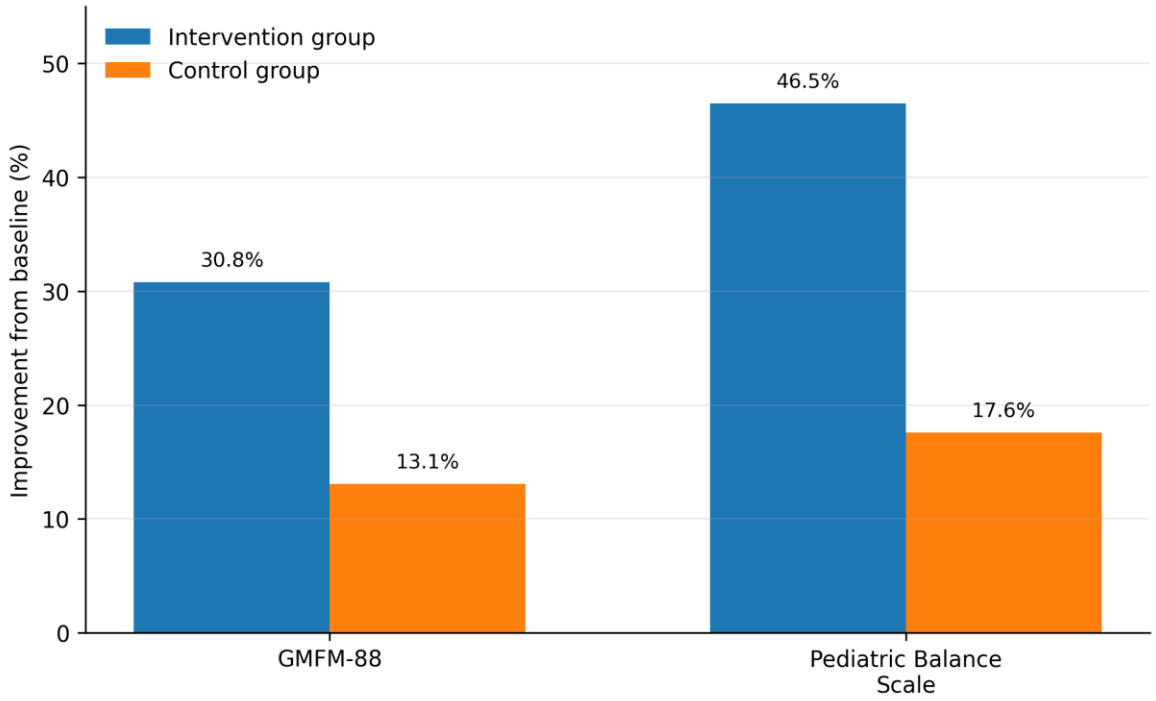


Chart 1. Percentage improvement in GMFM-88 and Pediatric Balance Scale scores after six months.

Note. Percentages were calculated from the baseline and six-month means reported for each group. GMFM-88 = Gross Motor Function Measure-88.

Table 1. Comparison of Key Clinical Outcomes Between Intervention and Control Groups

Outcome measure	Intervention group, baseline	Intervention group, 6 months	Control group, baseline	Control group, 6 months
GMFM-88, points	52.3 ± 18.7	68.4 ± 19.2*	51.8 ± 17.9	58.6 ± 18.4**
Pediatric Balance Scale (PBS), points	28.4 ± 12.7	41.6 ± 14.2*	27.9 ± 13.1	32.8 ± 13.6**
Modified Ashworth Scale, grade	1.2 ± 0.8	0.7 ± 0.6*	1.3 ± 0.7	1.1 ± 0.7

ISSN: 2181-3337 | SCIENTISTS.UZ

Outcome measure	Intervention group, baseline	Intervention group, 6 months	Control group, baseline	Control group, 6 months
PEDI self-care domain, points	45.7 ± 16.8	62.3 ± 18.4*	—	—

*Note. Values are mean ± SD. *p < .001 versus baseline; **p < .05 versus baseline. Between-group changes were significant for GMFM-88 and PBS (both p < .01). Dashes indicate values not reported.*

Functional Independence and Parent-Reported Health Status

PEDI scores improved significantly in all measured domains in the intervention group. Self-care increased from 45.7 ± 16.8 to 62.3 ± 18.4, mobility from 38.2 ± 19.6 to 56.8 ± 21.2, and social functioning from 52.4 ± 14.7 to 68.9 ± 16.3 (all p < .001). Improvements in each domain were reported as greater than those observed in the control group. Parent-proxy SF-36 physical-functioning scores increased from 34.2 ± 8.1 to 42.8 ± 7.6, and social-functioning scores increased from 28.6 ± 6.4 to 35.1 ± 6.9. Because the SF-36 proxy administration was not validated for this pediatric sample, these results are reported as exploratory parent-rated health-status findings rather than definitive quality-of-life outcomes.

EEG and MRI Outcomes

In the intervention group, the EEG alpha-rhythm index increased by 78.2%, from 23.4 ± 5.2% to 41.7 ± 6.8% (p < .001), and beta-rhythm activity increased by 52.2% (p < .001). Pathological delta/theta activity decreased by 45.3% (p < .001), and epileptiform activity decreased in 45% of the children. Corresponding changes in the control group were smaller and mostly nonsignificant.

MRI findings in the intervention group included an increase in cortical thickness of 0.23 ± 0.04 mm (8.7%, p < .001), an increase in fractional anisotropy and white matter integrity of 12.7 ± 3.2% (p < .001), a decrease in ventricular volume of 8.4 ± 2.1% (p < .01), and increases in corpus callosum thickness and hippocampal volume; hippocampal volume increased by 6.2 ± 1.8% (p < .01). These changes were greater than those recorded in the control group.

Adherence, Follow-Up, and Economic Outcomes

Mean attendance was 87.4 ± 6.8%, and parental satisfaction was 76.3 ± 8.4%. Mild fatigue was reported in 25% of the children, and 10% showed resistance to participation in some sessions. At six-month follow-up, 68.7 ± 9.2% of the gains achieved in the intervention group were maintained, compared with 52.4 ± 8.7% in the control group. Parent-reported activities of daily living improved by 15.7%–22.4% across the assessed domains.

The preliminary economic analysis estimated an incremental cost of approximately 7.7 million Uzbek soums per additional GMFM-88 point and 8.6 million Uzbek soums per additional Berg Balance Scale point. The estimated return on investment was 94.4%, with a payback period of approximately 6.2 months. The estimated savings were attributed mainly to a 40% reduction in hospitalization days and lower family out-of-pocket expenditure.

Discussion

The six-month multimodal psychomotor rehabilitation program was associated with greater improvement in gross motor function, balance, resistance to passive movement, functional independence, and selected quality-of-life domains than standard therapy alone. The direction of these findings is consistent with contemporary evidence favoring individualized, goal-directed, task-specific, activity-based, and adequately dosed interventions for children and young people with CP (Jackman et al., 2022; Novak et al., 2020). Exercise-based interventions can also support mobility, strength, fitness, and participation, although pooled effects are variable and depend on intervention content and participant characteristics (Ryan et al., 2017; Verschuren et al., 2016).

The improvement in balance is clinically relevant, but direct comparison with published percentage changes should be made cautiously because pediatric balance studies differ in age, CP subtype, GMFCS distribution, intervention dose, and scale administration. The PBS was developed as a child-adapted version of the Berg Balance Scale and provides an appropriate measurement framework for school-age children with motor impairment (Franjoine et al., 2003). The reduction in Modified Ashworth Scale scores suggests decreased resistance to passive movement; however, the scale has recognized limitations and does not isolate the neural component of spasticity from soft-tissue and biomechanical factors (Bohannon & Smith, 1987; Pandyan et al., 1999).

Improvements in PEDI domains are consistent with rehabilitation models that prioritize activity, participation, family goals, and performance in natural environments (Anaby et al., 2013; Imms et al., 2017). However, PEDI findings for participants beyond the original normative age range should be interpreted as descriptive raw functional scores rather than age-standardized estimates. Parent-proxy SF-36 findings also require caution because the instrument was not developed as a validated proxy measure for children aged 3–12 years. Future

ISSN: 2181-3337 | SCIENTISTS.UZ

studies should use a validated pediatric and CP-specific quality-of-life instrument, such as the PedsQL Cerebral Palsy Module (Varni et al., 2006).

The EEG and MRI changes may be compatible with experience-dependent neuroplastic adaptation, a concept that underpins early and intensive rehabilitation (Hadders-Algra, 2021; Morgan et al., 2021). However, the present data do not demonstrate neurogenesis or establish that structural changes were caused by the intervention. These outcomes should be regarded as exploratory until replicated using prespecified imaging pipelines, blinded analysis, test–retest reliability procedures, and longer follow-up.

The high attendance rate suggests that the program was feasible for many families. Nevertheless, children at different GMFCS levels have distinct developmental trajectories, assistance needs, and opportunities for participation; therefore, the same intervention dose and content cannot be assumed to be equally appropriate across GMFCS levels I–V (Hanna et al., 2009; Imms et al., 2017). Stratified analyses by age, CP distribution, GMFCS level, cognitive status, epilepsy, and family support would strengthen interpretation.

The preliminary economic estimates are promising, but they require cautious interpretation. A robust economic evaluation should clearly state the analytical perspective, time horizon, intervention and comparator costs, valuation methods, missing-data handling, uncertainty analysis, and whether downstream health and family costs were included (Husereau et al., 2022). The reported return on investment and payback period should therefore be validated prospectively in a larger sample.

Several limitations should be acknowledged. The study had a small single-center sample, outcome assessors were not fully blinded, and the inclusion of children across GMFCS levels I–V produced substantial clinical heterogeneity. The available records did not provide sufficient detail on random-sequence generation, allocation concealment, trial registration, or an a priori sample-size calculation. The intervention combined multiple components, so the contribution of each component could not be determined. Cognitive efficacy cannot be concluded because the study-specific MMSE adaptation was not independently validated and cognitive results were not presented as a primary outcome. PEDI scores for older participants and parent-proxy SF-36 results were descriptive rather than fully validated pediatric measures. EEG and MRI analyses lacked sufficient information on blinded processing, reproducibility, and correction for multiple comparisons. The economic evaluation did not include a fully specified perspective, uncertainty analysis, or sensitivity analysis. Larger multicenter trials with blinded assessment, validated pediatric cognitive and quality-of-life measures, prespecified imaging methods, and longer follow-up are needed.

Conclusion

This randomized controlled study suggests that a six-month multimodal psychomotor rehabilitation program may produce greater improvements than standard therapy alone in gross motor function, balance, resistance to passive movement, and functional independence in children with cerebral palsy. Exploratory EEG and MRI changes may reflect neuroplastic adaptation but require independent confirmation. Parent-proxy health-status and economic estimates should also be interpreted cautiously. The small sample and incomplete reporting of randomization procedures limit definitive inference. Structured, individualized, multidisciplinary rehabilitation with regular monitoring warrants evaluation in larger, prospectively registered multicenter trials.

REFERENCES

1. Anaby, D., Hand, C., Bradley, L., DiRezze, B., Forhan, M., DiGiacomo, A., & Law, M. (2013). The effect of the environment on participation of children and youth with disabilities: A scoping review. *Disability and Rehabilitation, 35*(19), 1589–1598. https://doi.org/10.3109/09638288.2012.748840
2. Bohannon, R. W., & Smith, M. B. (1987). Interrater reliability of a modified Ashworth scale of muscle spasticity. *Physical Therapy, 67*(2), 206–207. https://doi.org/10.1093/ptj/67.2.206
3. Bovend'Eerdt, T. J. H., Botell, R. E., & Wade, D. T. (2009). Writing SMART rehabilitation goals and achieving goal attainment scaling: A practical guide. *Clinical Rehabilitation, 23*(4), 352–361. https://doi.org/10.1177/0269215508101741
4. Chen, Y., Fanchiang, H. D., & Howard, A. (2018). Effectiveness of virtual reality in children with cerebral palsy: A systematic review and meta-analysis of randomized controlled trials. *Physical Therapy, 98*(1), 63–77. https://doi.org/10.1093/ptj/pzx107

ISSN: 2181-3337 | SCIENTISTS.UZ

5. Eliasson, A.-C., Krumlinde-Sundholm, L., Rösblad, B., Beckung, E., Arner, M., Öhrvall, A.-M., & Rosenbaum, P. (2006). The Manual Ability Classification System (MACS) for children with cerebral palsy: Scale development and evidence of validity and reliability. *Developmental Medicine & Child Neurology, 48*(7), 549–554. https://doi.org/10.1017/S0012162206001162
6. Folstein, M. F., Folstein, S. E., & McHugh, P. R. (1975). "Mini-mental state": A practical method for grading the cognitive state of patients for the clinician. *Journal of Psychiatric Research, 12*(3), 189–198. https://doi.org/10.1016/0022-3956(75)90026-6
7. Franjoine, M. R., Gunther, J. S., & Taylor, M. J. (2003). Pediatric Balance Scale: A modified version of the Berg Balance Scale for the school-age child with mild to moderate motor impairment. *Pediatric Physical Therapy, 15*(2), 114–128. https://doi.org/10.1097/01.PEP.0000068117.48023.18
8. Graham, H. K., Rosenbaum, P., Paneth, N., Dan, B., Lin, J.-P., Damiano, D. L., Becher, J. G., Gaebler-Spira, D., Colver, A., Reddihough, D. S., Crompton, K. E., & Lieber, R. L. (2016). Cerebral palsy. *Nature Reviews Disease Primers, 2*, Article 15082. https://doi.org/10.1038/nrdp.2015.82
9. Gulati, S., & Sondhi, V. (2018). Cerebral palsy: An overview. *Indian Journal of Pediatrics, 85*(11), 1006–1016. https://doi.org/10.1007/s12098-017-2475-1
10. Hadders-Algra, M. (2021). Early diagnostics and early intervention in neurodevelopmental disorders—Age-dependent challenges and opportunities. *Journal of Clinical Medicine, 10*(4), Article 861. https://doi.org/10.3390/jcm10040861
11. Haley, S. M., Coster, W. J., Ludlow, L. H., Haltiwanger, J. T., & Andrellos, P. J. (1992). Pediatric Evaluation of Disability Inventory (PEDI), version 1.0: Development, standardization, and administration manual. New England Medical Center Hospitals and PEDI Research Group.
12. Hanna, S. E., Rosenbaum, P. L., Bartlett, D. J., Palisano, R. J., Walter, S. D., Avery, L., & Russell, D. J. (2009). Stability and decline in gross motor function among children and youth with cerebral palsy aged 2 to 21 years. *Developmental Medicine & Child Neurology, 51*(4), 295–302. https://doi.org/10.1111/j.1469-8749.2008.03196.x
13. Husereau, D., Drummond, M., Augustovski, F., de Bekker-Grob, E., Briggs, A. H., Carswell, C., Caulley, L., Chaiyakunapruk, N., Greenberg, D., Loder, E., Mauskopf, J., Mullins, C. D., Petrou, S., Pwu, R.-F., & Staniszewska, S. (2022). Consolidated Health Economic Evaluation Reporting Standards 2022 (CHEERS 2022) statement: Updated reporting guidance for health economic evaluations. *BMJ, 376*, e067975. https://doi.org/10.1136/bmj-2021-067975
14. Imms, C., Granlund, M., Wilson, P. H., Steenbergen, B., Rosenbaum, P. L., & Gordon, A. M. (2017). Participation, both a means and an end: A conceptual analysis of processes and outcomes in childhood disability. *Developmental Medicine & Child Neurology, 59*(1), 16–25. https://doi.org/10.1111/dmcn.13237
15. Jackman, M., Sakzewski, L., Morgan, C., Boyd, R. N., Brennan, S. E., Langdon, K., Toovey, R. A. M., Greaves, S., Thorley, M., & Novak, I. (2022). Interventions to improve physical function for children and young people with cerebral palsy: International clinical practice guideline. *Developmental Medicine & Child Neurology, 64*(5), 536–549. https://doi.org/10.1111/dmcn.15055
16. Jasper, H. H. (1958). The ten-twenty electrode system of the International Federation. *Electroencephalography and Clinical Neurophysiology, 10*, 371–375.
17. McIntyre, S., Goldsmith, S., Webb, A., Ehlinger, V., Hollung, S. J., McConnell, K., Arnaud, C., Smithers-Sheedy, H., Oskoui, M., Khandaker, G., Himmelmann, K., & Global Cerebral Palsy Prevalence Group. (2022). Global prevalence of cerebral palsy: A systematic analysis. *Developmental Medicine & Child Neurology, 64*(12), 1494–1506. https://doi.org/10.1111/dmcn.15346
18. Morgan, C., Fetters, L., Adde, L., Badawi, N., Bancale, A., Boyd, R. N., Chorna, O., Cioni, G., Damiano, D. L., Darrah, J., de Vries, L. S., Dusing, S., Einspieler, C., Eliasson, A.-C., Ferriero, D., Fehlings, D., Forssberg, H., Gordon, A. M., Greaves, S., … Novak, I. (2021). Early intervention for children aged 0 to 2 years with or at high risk of cerebral palsy: International clinical practice guideline based on systematic reviews. *JAMA Pediatrics, 175*(8), 846–858. https://doi.org/10.1001/jamapediatrics.2021.0878

ISSN: 2181-3337 | SCIENTISTS.UZ

19. Novak, I., Morgan, C., Fahey, M., Finch-Edmondson, M., Galea, C., Hines, A., Langdon, K., McNamara, M., Paton, M. C. B., Popat, H., Shore, B., Khamis, A., Stanton, E., Finemore, O. P., Tricks, A., te Velde, A., Dark, L., Morton, N., & Badawi, N. (2020). State of the Evidence Traffic Lights 2019: Systematic review of interventions for preventing and treating children with cerebral palsy. *Current Neurology and Neuroscience Reports, 20*(2), Article 3. https://doi.org/10.1007/s11910-020-1022-z
20. Palisano, R., Rosenbaum, P., Walter, S., Russell, D., Wood, E., & Galuppi, B. (1997). Development and reliability of a system to classify gross motor function in children with cerebral palsy. *Developmental Medicine & Child Neurology, 39*(4), 214–223. https://doi.org/10.1111/j.1469-8749.1997.tb07414.x
21. Palisano, R. J., Rosenbaum, P., Bartlett, D., & Livingston, M. H. (2008). Content validity of the expanded and revised Gross Motor Function Classification System. *Developmental Medicine & Child Neurology, 50*(10), 744–750. https://doi.org/10.1111/j.1469-8749.2008.03089.x
22. Pandyan, A. D., Johnson, G. R., Price, C. I. M., Curless, R. H., Barnes, M. P., & Rodgers, H. (1999). A review of the properties and limitations of the Ashworth and modified Ashworth scales as measures of spasticity. *Clinical Rehabilitation, 13*(5), 373–383. https://doi.org/10.1191/026921599677595404
23. Patel, D. R., Neelakantan, M., Pandher, K., & Merrick, J. (2020). Cerebral palsy in children: A clinical overview. *Translational Pediatrics, 9*(Suppl. 1), S125–S135. https://doi.org/10.21037/tp.2020.01.01
24. Rosenbaum, P., Paneth, N., Leviton, A., Goldstein, M., Bax, M., Damiano, D., Dan, B., & Jacobsson, B. (2007). A report: The definition and classification of cerebral palsy April 2006. Developmental Medicine & Child Neurology, 49(Suppl. 109), 8–14. https://doi.org/10.1111/j.1469-8749.2007.tb12610.x
25. Russell, D. J., Rosenbaum, P. L., Avery, L. M., & Lane, M. (2002). *Gross Motor Function Measure (GMFM-66 & GMFM-88) user's manual*. Mac Keith Press.
26. Ryan, J. M., Cassidy, E. E., Noorduyn, S. G., & O'Connell, N. E. (2017). Exercise interventions for cerebral palsy. *Cochrane Database of Systematic Reviews, 2017*(6), Article CD011660. https://doi.org/10.1002/14651858.CD011660.pub2
27. Sadowska, M., Sarecka-Hujar, B., & Kopyta, I. (2020). Cerebral palsy: Current opinions on definition, epidemiology, risk factors, classification and treatment options. *Neuropsychiatric Disease and Treatment, 16*, 1505–1518. https://doi.org/10.2147/NDT.S235165
28. Surveillance of Cerebral Palsy in Europe. (2000). Surveillance of cerebral palsy in Europe: A collaboration of cerebral palsy surveys and registers. *Developmental Medicine & Child Neurology, 42*(12), 816–824. https://doi.org/10.1111/j.1469-8749.2000.tb00695.x
29. Varni, J. W., Burwinkle, T. M., Berrin, S. J., Sherman, S. A., Artavia, K., Malcarne, V. L., & Chambers, H. G. (2006). The PedsQL in pediatric cerebral palsy: Reliability, validity, and sensitivity of the Generic Core Scales and Cerebral Palsy Module. *Developmental Medicine & Child Neurology, 48*(6), 442–449. https://doi.org/10.1017/S001216220600096X
30. Verschuren, O., Peterson, M. D., Balemans, A. C. J., & Hurvitz, E. A. (2016). Exercise and physical activity recommendations for people with cerebral palsy. *Developmental Medicine & Child Neurology, 58*(8), 798–808. https://doi.org/10.1111/dmcn.13053
31. Vitrikas, K., Dalton, H., & Breish, D. (2020). Cerebral palsy: An overview. *American Family Physician, 101*(4), 213–220.
32. Ware, J. E., Jr., & Sherbourne, C. D. (1992). The MOS 36-item Short-Form Health Survey (SF-36): I. Conceptual framework and item selection. *Medical Care, 30*(6), 473–483. https://doi.org/10.1097/00005650-199206000-00002
33. World Health Organization. (2001). International classification of functioning, disability and health: ICF.

ISSN: 2181-3337 | SCIENTISTS.UZ

ISSN: 2181-3337 | SCIENTISTS.UZ VOLUME 5 ISSUE 7 JULY 2026

COMPARATIVE MORPHOBIOLOGICAL ASSESSMENT AND LENGTH–WEIGHT RELATIONSHIPS OF GRASS CARP (Ctenopharyngodon idella VALENCIENNES, 1844) BROODSTOCK FROM THREE POND FARMS IN THE TASHKENT REGION

Khudayberganova Khulkar[1]
Assistant Lecturer
Email: Zarazayka.1995.18@gmail.com

DOI: 10.67620/sai.57d0003

ABSTRACT

This study compared the morphobiological characteristics and length–weight relationships of grass carp (Ctenopharyngodon idella Valenciennes, 1844) broodstock maintained at three pond farms in the Tashkent region. Ninety-three mature fish were sampled in October 2025, with 31 individuals obtained from each farm. Total length, standard length, body weight, and Fulton's condition factor were determined. Pearson correlations, the regression model $W = aL^b$, and one-way analysis of variance were used. Khorrot Fish LLC recorded the highest mean total length (66.55 ± 1.16 cm), standard length (57.15 ± 1.13 cm), and body weight (3.88 ± 0.18 kg). Farm differences were significant for total length, standard length, and body weight, whereas Fulton's condition factor did not differ significantly. Total length was strongly correlated with body weight in all farms. The farm-specific allometric coefficients ranged from 1.866 to 2.209, and the pooled coefficient was 2.252, indicating negative allometric growth. The findings support the use of morphometric monitoring in broodstock assessment and selection, while causal interpretations of farm differences require controlled studies of feed, water quality, age, sex, and management.

ACCEPTED

20.07.26

Keywords: *grass carp; Ctenopharyngodon idella; broodstock; pond aquaculture; morphometry; length–weight relationship; Fulton's condition factor; selective breeding.*

CC BY

INTRODUCTION

Aquaculture is an increasingly important component of the global food system and contributes substantially to the supply of high-quality animal protein. The continued expansion of aquaculture increases the need for efficient production systems, reliable biological monitoring, and scientifically informed broodstock management (Food and Agriculture Organization of the United Nations [FAO], 2024). In Uzbekistan, the development of pond aquaculture and selective breeding is particularly relevant to food security and the sustainable growth of the fisheries sector.

Grass carp (*Ctenopharyngodon idella* Valenciennes, 1844) is widely cultured because of its rapid growth, effective utilization of plant biomass, ecological adaptability, and economic importance. The interpretation of fish condition and growth commonly relies on morphometric measurements, Fulton's condition factor, and length–weight models (Le Cren, 1951; Froese, 2006; Froese et al., 2011). Pond

productivity is influenced by the interaction of water quality, feeding, and husbandry practices (Boyd & Tucker, 1998). Studies of grass carp have further demonstrated that feeding rate, diet composition, and production system affect growth, feed efficiency, body composition, muscle quality, and survival (Du et al., 2006; Mahmood et al., 2018; Zhao et al., 2018; Kristan et al., 2019; Gharti et al., 2023).

Morphometric traits also provide useful information for broodstock selection. Quantitative-genetic and genomic investigations have identified exploitable variation in growth and body-shape traits in grass carp (Fu et al., 2016; Jiang et al., 2022; Guo et al., 2022; Chen et al., 2025). Regional research from the Tudakul Reservoir confirms the relevance of morphometric and length–weight analyses for grass carp in Uzbekistan (Sobirov et al., 2019). However, comparative evidence for broodstock maintained under different farm conditions in the Tashkent region remains limited. Therefore, this study aimed to compare total length, standard length, body weight, Fulton's condition factor, and length–weight relationships in grass carp broodstock from three pond farms and to assess the practical value of these indicators for broodstock monitoring and selection.

MATERIALS AND METHODS

Study design and sampling. The study was conducted during 2023–2025 at three pond fish farms in the Tashkent region: Khorrot Fish LLC, ZAFARASAD Farm, and Imkon Baliq Fayz LLC. Biometric sampling was performed in October 2025. A total of 93 sexually mature and apparently healthy grass carp were selected by random sampling, with 31 fish obtained from each farm. Fish showing visible deformities, mechanical injury, or clinical signs of disease were excluded.

Rearing and feeding conditions. Fish were maintained under intensive pond-culture conditions supported by the natural food base and commercial compound feeds. Khorrot Fish LLC used an Iranian common-carp feed containing approximately 32–35% protein; ZAFARASAD Farm used Aller Aqua feed containing approximately 30–35% protein; and Imkon Baliq Fayz LLC used Shench Jou feed produced through Chinese–Uzbek cooperation. The reported daily feeding rate was approximately 2% of body weight. Water temperature, dissolved oxygen, pH, and transparency were monitored by the farms, and routine fish-health and veterinary-preventive measures were implemented according to current production practices.

Morphometric measurements. Total length (TL, cm), standard length (SL, cm), and body weight (W, kg) were measured for each fish. Lengths were recorded to the nearest millimetre with an ichthyological measuring board. Total length was measured from the tip of the snout to the most posterior point of the caudal fin, whereas standard length was measured from the tip of the snout to the base of the caudal fin. Body weight was measured to the nearest gram using an electronic balance. Each measurement was repeated three times, and the mean value was used in the analysis.

Condition and growth calculations. Body proportions were evaluated using the SL/TL ratio. Fulton's condition factor was calculated as $K = 100W/L^3$, where W is body weight in grams and L is total length in centimetres. The length–weight relationship was estimated using $W = aL^b$, where a is the regression constant and b is the allometric coefficient (Le Cren, 1951; Froese, 2006). Growth was interpreted as isometric when $b = 3$, positively allometric when $b > 3$, and negatively allometric when $b < 3$.

Statistical analysis. Data were processed in Microsoft Excel 2021 and IBM SPSS Statistics. Descriptive statistics included the number of observations, mean, standard deviation, standard error, range, coefficient of variation, and 95% confidence interval. Associations among morphometric variables were assessed using Pearson's correlation coefficient. Length–weight parameters were estimated by least-squares regression, and model fit was summarized with the coefficient of determination (R^2). Differences among farms were evaluated using one-way analysis of variance. Statistical significance was set at $p < 0.05$.

ISSN: 2181-3337 | SCIENTISTS.UZ

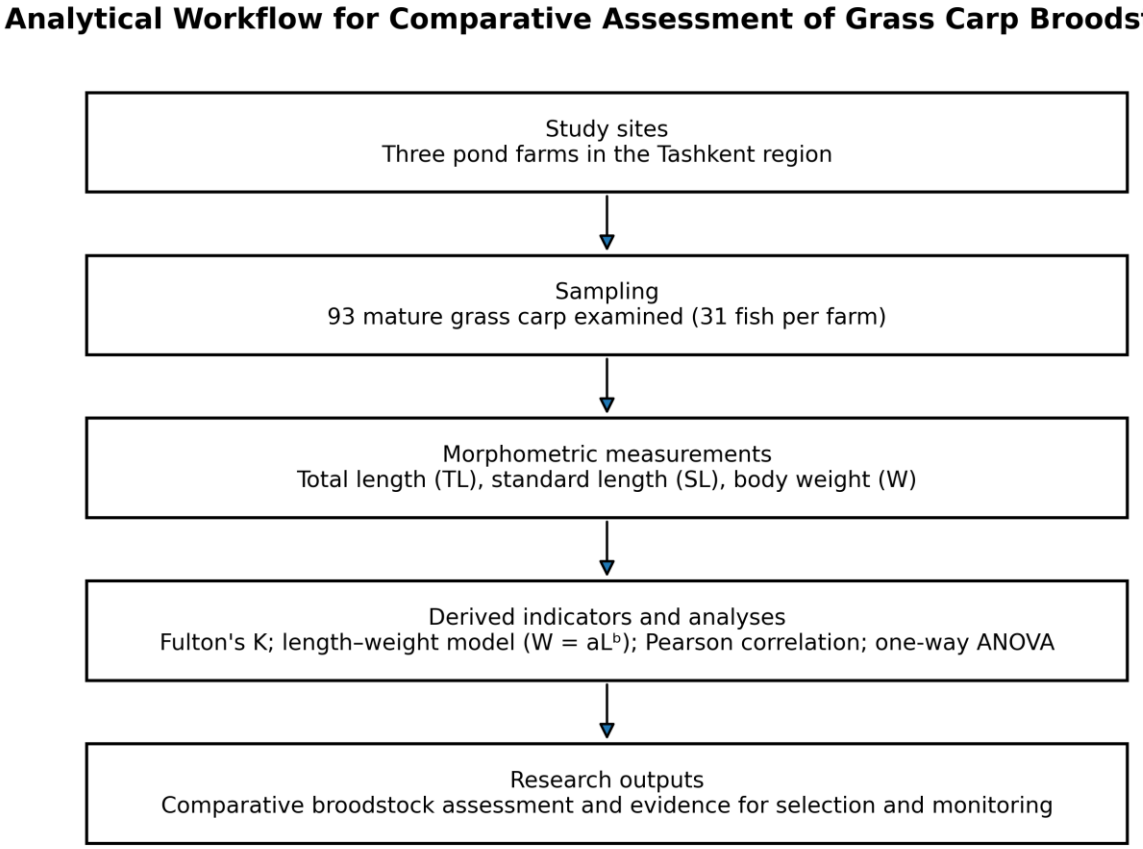


Figure 1. Analytical workflow for the comparative assessment of grass carp broodstock in the Tashkent region.

RESULTS

The three farms differed in broodstock size characteristics (Table 1). Khorrot Fish LLC had the highest mean total length (66.55 ± 1.16 cm), standard length (57.15 ± 1.13 cm), and body weight (3.88 ± 0.18 kg). ZAFARASAD Farm ranked second for these measurements, with a mean total length of 63.19 ± 0.94 cm, standard length of 53.90 ± 1.01 cm, and body weight of 3.38 ± 0.11 kg. Imkon Baliq Fayz LLC had the lowest means: 61.13 ± 0.81 cm for total length, 50.66 ± 0.80 cm for standard length, and 2.92 ± 0.10 kg for body weight. Fulton's condition factor ranged from 1.28 ± 0.03 to 1.35 ± 0.04.

Table 1. Descriptive statistics by farm (mean ± SE)

Farm	n	TL (cm)	SL (cm)	W (kg)	Fulton's K
Khorrot Fish LLC	31	66.55±1.16	57.15±1.13	3.88±0.18	1.31±0.03
ZAFARASAD Farm	31	63.19±0.94	53.90±1.01	3.38±0.11	1.35±0.04
Imkon Baliq Fayz LLC	31	61.13±0.81	50.66±0.80	2.92±0.10	**1.28±0.03**

Table 2. Variability of total length and body weight by farm

Farm	TL SD	TL CV (%)	W SD	W CV (%)
Khorrot Fish LLC	6.45	9.70	1.01	25.93
ZAFARASAD Farm	5.22	8.27	0.63	18.62
Imkon Baliq Fayz LLC	4.50	7.36	0.54	18.57

ISSN: 2181-3337 | SCIENTISTS.UZ

Table 3. Pearson correlation coefficients among morphometric variables			
Farm	**TL–SL**	**TL–W**	**SL–W**
Khorrot Fish LLC	0.953	0.855	0.838
ZAFARASAD Farm	0.935	0.789	0.695
Imkon Baliq Fayz LLC	0.954	0.853	0.770

Table 4. Length–weight regression models			
Farm	**Regression equation**	**b**	**R^2**
Khorrot Fish LLC	$W = 0.000369 \times TL^{2.201}$	2.201	0.779
ZAFARASAD Farm	$W = 0.001460 \times TL^{1.866}$	1.866	0.631
Imkon Baliq Fayz LLC	$W = 0.000328 \times TL^{2.209}$	2.209	0.706
Overall (n = 93)	$W = 0.000289 \times TL^{2.252}$	2.252	0.748

Table 5. One-way analysis of variance comparing farms		
Indicator	**F**	**p**
TL	7.800	0.00075
SL	10.913	0.00006
W	12.603	0.000015
Fulton K	1.117	0.332

DISCUSSION

Body-weight variability was highest at Khorrot Fish LLC (CV = 25.93%), whereas ZAFARASAD Farm and Imkon Baliq Fayz LLC showed similar coefficients of variation (18.62% and 18.57%, respectively; Table 2). This pattern indicates greater heterogeneity in the Khorrot Fish broodstock and may provide a broader phenotypic range for selection, although age and sex composition were not available for direct evaluation. Total length and standard length were very strongly correlated in all farms (r = 0.935–0.954), and total length was strongly associated with body weight (r = 0.789–0.855; Table 3). These relationships support the use of routine length measurements as practical indicators of broodstock size.

The length–weight models explained 63.1–77.9% of the within-farm variation in body weight (Table 4). The farm-specific b coefficients ranged from 1.866 to 2.209, and the pooled value was 2.252. Because every estimate was below 3, the broodstock exhibited negative allometric growth: weight increased with length, but less rapidly than expected under isometric growth. This interpretation is consistent with established recommendations for fish length–weight analysis (Le Cren, 1951; Froese, 2006; Froese et al., 2011).

One-way ANOVA identified significant farm differences in total length ($F = 7.800$, $p = 0.00075$), standard length ($F = 10.913$, $p = 0.00006$), and body weight ($F = 12.603$, $p = 0.000015$), whereas Fulton's condition factor did not differ significantly ($F = 1.117$, $p = 0.332$; Table 5). Thus, the farms differed in broodstock size but not in the measured condition index. The higher mean size at Khorrot Fish LLC and ZAFARASAD Farm may be associated with feeding regime, environmental conditions, stock structure, or broodstock-selection practices. However, because farms were not randomly assigned to treatments and feed type, water-quality measurements, age, and sex were not analysed as covariates, the present observational design cannot establish which factor caused the differences.

The biological plausibility of the observed farm variation is supported by research showing that water quality, feeding rate, diet composition, and culture system influence grass carp growth and performance (Boyd & Tucker, 1998; Du et al., 2006; Mahmood et al., 2018; Zhao et al., 2018; Kristan et al., 2019; Gharti et al., 2023). Furthermore, quantitative-genetic and genomic studies indicate that growth and body-shape measurements can contribute to broodstock improvement (Fu et al., 2016; Jiang et al., 2022; Guo et al., 2022; Chen et al., 2025). The present results are also broadly comparable with regional morphometric research on grass carp in Uzbekistan (Sobirov et al., 2019). Future work should use repeated seasonal sampling, record age and sex, report farm-level water-quality and feed-intake data, and apply multivariable or mixed-effects models to distinguish management effects from biological differences among stocks.

ISSN: 2181-3337 | SCIENTISTS.UZ

CONCLUSION

Grass carp broodstock from the three pond farms differed significantly in total length, standard length, and body weight, with Khorrot Fish LLC recording the highest mean values and Imkon Baliq Fayz LLC the lowest. Fulton's condition factor did not differ significantly among farms. Strong positive correlations among length and weight variables confirmed the practical value of morphometric monitoring, while all farm-specific and pooled b coefficients indicated negative allometric growth. These results can support routine broodstock assessment and the preliminary identification of large, phenotypically promising individuals. Nevertheless, selection decisions should combine morphometric evidence with reproductive performance, age, sex, health, genetic background, feed intake, and water-quality data. Controlled and longitudinal studies are required before farm differences can be attributed to specific feeding or management technologies.

REFERENCES

1. Boyd, C. E., & Tucker, C. S. (1998). *Pond aquaculture water quality management*. Springer. https://doi.org/10.1007/978-1-4615-5407-3
2. Chen, Y., Yu, Q., Lv, W., Sheng, T., Gui, L., Qiu, J., Xu, X., & Li, J. (2025). Genome-wide association analysis and genomic selection for growth traits in grass carp (*Ctenopharyngodon idella*). *Animals, 15*(13), 1888. https://doi.org/10.3390/ani15131888
3. Du, Z.-Y., Liu, Y.-J., Tian, L.-X., He, J.-G., Cao, J.-M., & Liang, G.-Y. (2006). The influence of feeding rate on growth, feed efficiency and body composition of juvenile grass carp (*Ctenopharyngodon idella*). *Aquaculture International, 14*(3), 247–257. https://doi.org/10.1007/s10499-005-9029-7
4. Food and Agriculture Organization of the United Nations. (2024). *The state of world fisheries and aquaculture 2024: Blue transformation in action*. FAO. https://doi.org/10.4060/cd0683en
5. Froese, R. (2006). Cube law, condition factor and weight-length relationships: History, meta-analysis and recommendations. *Journal of Applied Ichthyology, 22*(4), 241–253. https://doi.org/10.1111/j.1439-0426.2006.00805.x
6. Froese, R., Tsikliras, A. C., & Stergiou, K. I. (2011). Editorial note on weight-length relations of fishes. *Acta Ichthyologica et Piscatoria, 41*(4), 261–263. https://doi.org/10.3750/AIP2011.41.4.01
7. Fu, J., Shen, Y., Xu, X., & Li, J. (2016). Genetic parameter estimates for growth of grass carp, *Ctenopharyngodon idella*, at 10 and 18 months of age. *Aquaculture, 450*, 342–348. https://doi.org/10.1016/j.aquaculture.2015.08.018
8. Gharti, K., Yan, L., Li, K., Boonpeng, N., & Liu, L. (2023). Growth and muscle quality of grass carp (*Ctenopharyngodon idella*) in in-pond raceway aquaculture and traditional pond culture. *Water, 15*(9), 1771. https://doi.org/10.3390/w15091771
9. Guo, J., Zhang, M., Wang, S., Xu, X., Shen, Y., & Li, J. (2022). A high-density genetic linkage map and QTL mapping for growth-related traits in grass carp (*Ctenopharyngodon idella*). *Aquaculture, 552*, 738041. https://doi.org/10.1016/j.aquaculture.2022.738041
10. Jiang, P., Li, S., Fan, J., Du, J., Ma, D., & Lei, C. (2022). A novel morphological index applied to genetic improvement of body shape in grass carp *Ctenopharyngodon idella*. *Aquaculture, 548*, 737687. https://doi.org/10.1016/j.aquaculture.2021.737687
11. Kristan, J., Blecha, M., & Policar, T. (2019). Survival and growth rates of juvenile grass carp *Ctenopharyngodon idella* overwintered in ponds and recirculating aquaculture systems including a comparison of production economics. *Turkish Journal of Fisheries and Aquatic Sciences, 19*(3), 261–266. https://doi.org/10.4194/1303-2712-v19_3_09

ISSN: 2181-3337 | SCIENTISTS.UZ

12. Le Cren, E. D. (1951). The length-weight relationship and seasonal cycle in gonad weight and condition in the perch (*Perca fluviatilis*). *Journal of Animal Ecology*, *20*(2), 201–219. https://doi.org/10.2307/1540
13. Mahmood, S., Khan, N., Iqbal, K. J., Ashraf, M., & Khalique, A. (2018). Evaluation of water hyacinth (*Eichhornia crassipes*) supplemented diets on the growth, digestibility and histology of grass carp (*Ctenopharyngodon idella*) fingerlings. *Journal of Applied Animal Research*, *46*(1), 24–28. https://doi.org/10.1080/09712119.2016.1256291
14. Sobirov, J., Kanatbaeva, T., & Kamilov, B. (2019). Morphology, age and growth of grass carp (*Ctenopharyngodon idella*) in Tudakul Reservoir of Uzbekistan. *International Journal of Science and Research*, *8*(6), 1899–1905. https://doi.org/10.21275/ART20198881
15. Zhao, H., Xia, J., Zhang, X., He, X., Li, L., Tang, R., Chi, W., & Li, D. (2018). Diet affects muscle quality and growth traits of grass carp (*Ctenopharyngodon idellus*): A comparison between grass and artificial feed. *Frontiers in Physiology*, *9*, 283. https://doi.org/10.3389/fphys.2018.00283

ISSN: 2181-3337 | SCIENTISTS.UZ

ISSN: 2181-3337 | SCIENTISTS.UZ VOLUME 5 ISSUE 7 JULY 2026

CLINICAL PROGRESSION OF RHEUMATOID ARTHRITIS AND HEMOVASCULAR REMODELING: ASSOCIATIONS BETWEEN SEROSTATUS, FUNCTIONAL CLASS, ENDOTHELIAL DYSFUNCTION AND HEMOSTATIC ACTIVITY

Musaeva Nargiza
Tashkent State Medical University, Department of Hematology, Transfusiology and Laboratory Medicine

DOI: 10.67620/sai.57d0004

ABSTRACT

Rheumatoid arthritis is a systemic autoimmune disease whose progression is frequently accompanied by vascular inflammation, endothelial dysfunction, and hemostatic imbalance. This study assessed the relationships among disease duration, serological status, American College of Rheumatology functional class, platelet hemostasis, coagulation abnormalities, and endothelial dysfunction. The study included 85 patients with rheumatoid arthritis and 30 healthy controls. Patients were classified into three groups according to disease duration: up to 6 months (n = 24), 6 months to 1 year (n = 33), and more than 2 years (n = 28). Serostatus, functional class, platelet indices, coagulation parameters, and endothelial dysfunction markers were analyzed. The proportion of seronegative rheumatoid arthritis declined from 45.8% in the first group to 39.4% in the second and 28.6% in the third, whereas seropositive disease increased to 71.4% among patients with disease duration exceeding 2 years. The frequency of functional classes I and II decreased as disease duration increased, while classes III and IV became progressively more common. Platelet hemostatic activity was most pronounced during the first year of disease, whereas coagulation abnormalities became more prominent in patients with longer disease duration. Endothelial dysfunction persisted across all groups. These findings indicate that rheumatoid arthritis progression is associated with a transition from early platelet-dominant activation to later coagulation-dominant hypercoagulability, while endothelial dysfunction remains present throughout the disease course. Seropositive status and advanced functional limitation may therefore characterize a more severe hemovascular phenotype.

ACCEPTED

20.07.26

Keywords: *rheumatoid arthritis, serostatus, functional class, endothelial dysfunction, hemostasis, D-dimer, endothelin-1, von Willebrand factor.*

CC BY

Introduction

Rheumatoid arthritis is a chronic systemic autoimmune disease characterized by persistent synovial inflammation, progressive joint destruction and functional impairment [1,2]. Although joint involvement remains the main clinical feature of rheumatoid arthritis, increasing evidence shows that the disease also affects the vascular endothelium and hemostatic system [3,4,11-13].

Systemic inflammation in rheumatoid arthritis contributes to endothelial activation, platelet stimulation and coagulation imbalance. These changes may increase the risk of microcirculatory

disturbances, cardiovascular complications and thrombotic events [3,5-7,11-13,15]. Endothelial dysfunction is reflected by increased endothelin-1, soluble intercellular adhesion molecule and von Willebrand factor, while hemostatic activation is manifested by increased platelet adhesion and aggregation, elevated fibrinogen, increased D-dimer, shortened clotting times and higher prothrombin index [5-7,11-13,15].

Patients with rheumatoid arthritis have an increased risk of venous thromboembolism and cardiovascular complications, especially when systemic inflammation remains active [8-10,14]. Therefore, vascular and hemostatic risk assessment may have additional value in patients with different disease duration, serological status and functional limitation.

The present study was designed to evaluate how serostatus and ACR functional classes change with rheumatoid arthritis duration and how these changes relate to platelet hemostasis, coagulation hemostasis and endothelial dysfunction.

Materials and Methods

This clinical and laboratory study was conducted at the multidisciplinary clinic of Tashkent State Medical University during 2022-2025. The study included 85 patients with rheumatoid arthritis and 30 practically healthy individuals as a control group.

Patients were divided into three groups according to disease duration: group 1 included patients with rheumatoid arthritis up to 6 months, n=24; group 2 included patients with rheumatoid arthritis from 6 months to 1 year, n=33; and group 3 included patients with rheumatoid arthritis lasting more than 2 years, n=28.

Inclusion criteria were confirmed rheumatoid arthritis according to EULAR/ACR criteria, age above 18 years, moderate disease activity according to DAS28 and informed consent. Exclusion criteria included severe somatic diseases, acute infections, uncontrolled arterial hypertension, use of antiplatelet agents, anticoagulants or statins, and refusal to participate.

The following parameters were analyzed: seropositive and seronegative rheumatoid arthritis, ACR functional classes, platelet count, platelet adhesion, platelet aggregation, activated partial thromboplastin time, prothrombin index, thrombin time, fibrinogen, D-dimer, endothelin-1, sICAM and von Willebrand factor.

Quantitative values are presented as M±m. Differences compared with the control group were considered statistically significant at $p<0.05$.

Results

Serostatus and functional classes

Serostatus analysis demonstrated that seronegative rheumatoid arthritis became less frequent as disease duration increased. In group 1, seronegative rheumatoid arthritis was detected in 45.8% of patients. In group 2, this proportion decreased to 39.4%, and in group 3 it decreased further to 28.6%. In contrast, seropositive rheumatoid arthritis increased from 54.2% in group 1 to 60.6% in group 2 and 71.4% in group 3.

Functional status also worsened with disease duration. ACR functional class I was found in 33.3% of group 1 patients, 21.4% of group 2 patients and 14.3% of group 3 patients. Class II decreased from 41.6% to 38.4% and 28.6%, respectively. In contrast, class III increased from 21.0% in group 1 to 34.1% in group 2 and 46.4% in group 3. Class IV increased from 4.1% in group 1 to 6.1% in group 2 and 10.7% in group 3.

ISSN: 2181-3337 | SCIENTISTS.UZ

Table 1. Serostatus and ACR functional classes according to disease duration

Parameter	Group 1, n=24	Group 2, n=33	Group 3, n=28
Seropositive RA, %	54.2	60.6	71.4
Seronegative RA, %	45.8	39.4	28.6
ACR class I, %	33.3	21.4	14.3
ACR class II, %	41.6	38.4	28.6
ACR class III, %	21.0	34.1	46.4
ACR class IV, %	4.1	6.1	10.7

Platelet hemostasis and endothelial dysfunction

Platelet count increased from 254±28 in the control group to 332±30 in group 1 and 450±41 in group 2. In group 3, platelet count was 278±29 and did not differ substantially from the control value. Platelet adhesion increased from 30±4 in controls to 46±5 in group 1 and 52±6 in group 2, while in group 3 it was 26±3. Similar changes were observed in platelet aggregation.

Endothelial dysfunction markers showed a different pattern. Endothelin-1 progressively increased from 1.7±0.2 pg/ml in controls to 2.9±0.3 pg/ml in group 1, 3.5±0.4 pg/ml in group 2 and 4.1±0.4 pg/ml in group 3. sICAM increased from 220±24 ng/ml in controls to 298±26, 324±29 and 360±32 ng/ml, respectively. Von Willebrand factor increased from 98±10% to 139±13%, 152±16% and 148±11%.

Table 2. Platelet hemostasis and endothelial dysfunction markers

Parameter	Control, n=30	Group 1, n=24	Group 2, n=33	Group 3, n=28
Platelet count	254±28	332±30*	450±41***	278±29
Platelet adhesion	30±4	46±5*	52±6**	26±3
Maximum aggregation rate	33±4	46±4*	49±5*	30±3
Maximum aggregation degree	38±3	49±4*	52±5*	35±4
Endothelin-1, pg/ml	1.7±0.2	2.9±0.3**	3.5±0.4**	4.1±0.4**
sICAM, ng/ml	220±24	298±26*	324±29**	360±32***
Von Willebrand factor, %	98±10	139±13*	152±16**	148±11**

*Note: *p<0.05; **p<0.01; ***p<0.001 compared with the control group.*

Coagulation hemostasis

Coagulation parameters showed progressive hypercoagulability with increasing disease duration. APTT decreased from 30.0±2.8 s in controls to 24.2±2.2 s in group 1, 21.6±2.0 s in group 2 and 19.5±2.6 s in group 3. Prothrombin index increased from 97±8% in controls to 105±9%, 128±10% and 136±9%, respectively.

Thrombin time shortened from 18.8±1.0 s in controls to 16.6±1.3 s in group 1, 15.3±1.3 s in group 2 and 14.6±1.2 s in group 3. Fibrinogen increased from 2.83±0.22 g/L to 3.55±0.30 g/L, 4.46±0.43 g/L and 4.66±0.24 g/L. D-dimer increased from 254±29 ng/ml to 380±43, 460±41 and 450±49 ng/ml.

ISSN: 2181-3337 | SCIENTISTS.UZ

Table 3. Coagulation hemostasis according to rheumatoid arthritis duration

Parameter	Control, n=30	Group 1, n=24	Group 2, n=33	Group 3, n=28
APTT, s	30.0±2.8	24.2±2.2	21.6±2.0*	19.5±2.6**
Prothrombin index, %	97±8	105±9	128±10*	136±9**
Thrombin time, s	18.8±1.0	16.6±1.3	15.3±1.3*	14.6±1.2**
Fibrinogen, g/L	2.83±0.22	3.55±0.30	4.46±0.43**	4.66±0.24***
D-dimer, ng/ml	254±29	380±43*	460±41***	450±49***

*Note: *p<0.05; **p<0.01; ***p<0.001 compared with the control group.*

Figure 1 is provided below to visually summarize the central quantitative findings described in the Results section.

Figure 1. Disease progression, serostatus, and hemovascular remodeling in rheumatoid arthritis

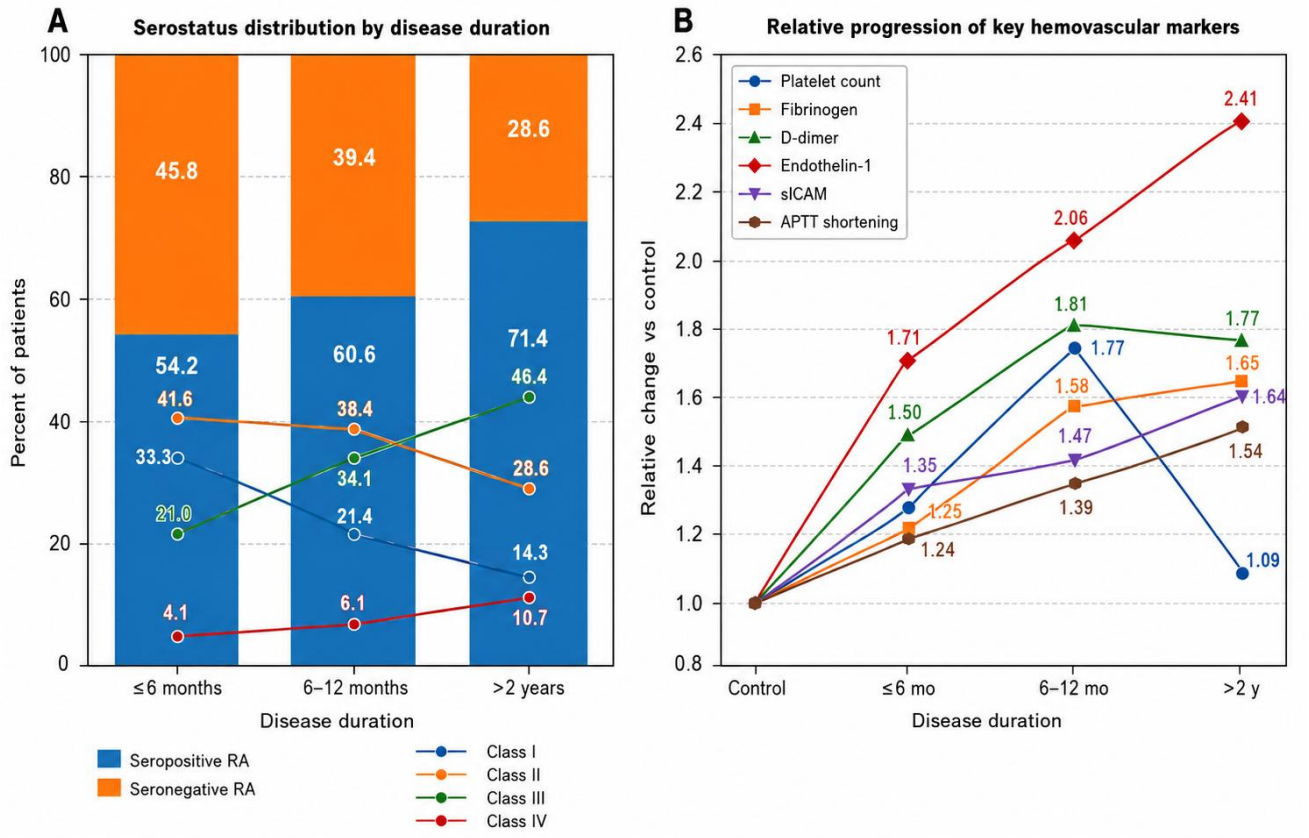


Figure 1. Disease progression, serostatus, and hemovascular remodeling in rheumatoid arthritis.

Note. Panel A shows the distribution of seropositive and seronegative rheumatoid arthritis together with ACR functional classes across disease-duration groups. Panel B illustrates relative changes versus the control group for selected platelet, coagulation, and endothelial markers. The figure was prepared from the summarized numerical data reported in Tables 1–3.

Discussion

The present study demonstrates that clinical progression of rheumatoid arthritis is accompanied by distinct hemovascular remodeling. The decrease in seronegative rheumatoid arthritis and increase in seropositive forms with disease duration suggest that longer disease course is associated with a more immunologically defined phenotype [1,2].

The worsening of ACR functional classes confirms progressive functional impairment. The proportion of patients with ACR classes III-IV increased with disease duration, while classes I-II decreased. This functional deterioration occurred in parallel with persistent endothelial dysfunction and increasing coagulation abnormalities.

The hemostatic pattern was not uniform. In patients with disease duration up to one year, platelet count, adhesion and aggregation were increased, indicating prominent platelet activation in early rheumatoid arthritis. In patients with disease duration longer than two years, platelet parameters were less pronounced, while coagulation disturbances became dominant. This suggests a transition from platelet-driven hemostatic activation to coagulation-dominant hypercoagulability [3,7,15].

Endothelial dysfunction persisted in all disease-duration groups. Endothelin-1, sICAM and von Willebrand factor were elevated even in the earliest group and remained increased in long-standing disease. This confirms that vascular endothelial involvement is not secondary only to late complications but is an early and persistent component of rheumatoid arthritis [3-7,11-13].

The combination of advanced seropositive disease, higher ACR functional classes, persistent endothelial dysfunction and coagulation activation may define a subgroup of patients with increased vascular and thrombotic risk. Therefore, assessment of endothelial and hemostatic markers may have practical value in addition to conventional rheumatologic evaluation [8-10,14].

Conclusions

1. Rheumatoid arthritis progression is associated with changes in serostatus, functional status and hemovascular parameters.

2. Seronegative rheumatoid arthritis decreased from 45.8% to 28.6% with increasing disease duration, while seropositive disease increased to 71.4%.

3. ACR functional classes III-IV became more frequent in long-standing disease, indicating progressive functional limitation.

4. Platelet hemostasis was most activated during the first year of rheumatoid arthritis.

5. Coagulation hyperactivity became more pronounced in patients with disease duration longer than two years.

6. Endothelial dysfunction persisted in all groups and increased with disease duration.

7. Serostatus, ACR functional class, endothelial dysfunction and hemostatic markers should be evaluated together for more complete clinical risk stratification in rheumatoid arthritis.

REFERENCES

1. Aletaha D, Neogi T, Silman AJ, Funovits J, Felson DT, Bingham CO, et al. 2010 rheumatoid arthritis classification criteria: an American College of Rheumatology/European League Against Rheumatism collaborative initiative. Ann Rheum Dis. 2010;69(9):1580-1588. https://doi.org/10.1136/ard.2010.138461.
2. Smolen JS, Landewé RBM, Bergstra SA, Kerschbaumer A, Sepriano A, Aletaha D, et al. EULAR recommendations for the management of rheumatoid arthritis with synthetic and biological disease-modifying antirheumatic drugs: 2022 update. Ann Rheum Dis. 2023;82(1):3-18. https://doi.org/10.1136/ard-2022-223356.
3. Yang XZ, Chang Y, Wei W. Endothelial dysfunction and inflammation: immunity in rheumatoid arthritis. Mediators Inflamm. 2016;2016:6813016. https://doi.org/10.1155/2016/6813016.
4. Anyfanti P, Gavriilaki E, Douma S, Gkaliagkousi E. Endothelial dysfunction in patients with rheumatoid arthritis: the role of hypertension. Curr Hypertens Rep. 2020;22(8):56. https://doi.org/10.1007/s11906-020-01064-y.
5. Klimiuk PA, Sierakowski S, Latosiewicz R, Cylwik JP, Cylwik B, Skowronski J, et al. Soluble adhesion molecules (ICAM-1, VCAM-1, and E-selectin) and vascular endothelial growth factor

ISSN: 2181-3337 | SCIENTISTS.UZ

(VEGF) in patients with distinct variants of rheumatoid synovitis. Ann Rheum Dis. 2002;61(9):804-809. https://doi.org/10.1136/ard.61.9.804.

6. Vischer UM. von Willebrand factor, endothelial dysfunction, and cardiovascular disease. J Thromb Haemost. 2006;4(6):1186-1193. https://doi.org/10.1111/j.1538-7836.2006.01949.x.
7. Manz XD, Doddaballapur A, Hynes RO, Wagner DD. Regulation of VWF (von Willebrand factor) in inflammatory thrombosis. Arterioscler Thromb Vasc Biol. 2022;42(11):1307-1320. https://doi.org/10.1161/ATVBAHA.122.318179.
8. Molander V, Bower H, Frisell T, Askling J. Risk of venous thromboembolism in rheumatoid arthritis, and its association with disease activity: a nationwide cohort study from Sweden. Ann Rheum Dis. 2021;80(2):169-175. https://doi.org/10.1136/annrheumdis-2020-218419.
9. Hu LJ, Ji B, Fan HX. Venous thromboembolism risk in rheumatoid arthritis patients: a systematic review and updated meta-analysis. Eur Rev Med Pharmacol Sci. 2021;25(22):7005-7013. https://doi.org/10.26355/eurrev_202111_27249.
10. Omair MA, Alkhelb SA, Ezzat SE, Boudal AM, Bedaiwi MK, Almaghlouth I. Venous thromboembolism in rheumatoid arthritis: the added effect of disease activity to traditional risk factors. Open Access Rheumatol. 2022;14:231-242. https://doi.org/10.2147/OARRR.S284757.
11. Södergren A, Karp K, Boman K, Eriksson C, Lundström E, Smedby T, et al. Atherosclerosis in early rheumatoid arthritis: very early endothelial activation and rapid progression of intima-media thickness. Arthritis Res Ther. 2010;12(4):R158. https://doi.org/10.1186/ar3116.
12. Vaudo G, Marchesi S, Gerli R, Allegrucci R, Giordano A, Siepi D, et al. Endothelial dysfunction in young patients with rheumatoid arthritis and low disease activity. Ann Rheum Dis. 2004;63(1):31-35. https://doi.org/10.1136/ard.2003.007740.
13. Bordy R, Totoson P, Prati C, Marie C, Wendling D, Demougeot C. Microvascular endothelial dysfunction in rheumatoid arthritis. Nat Rev Rheumatol. 2018;14(7):404-420. https://doi.org/10.1038/s41584-018-0022-8.
14. Solomon DH, Reed GW, Kremer JM, Curtis JR, Farkouh ME, Harrold LR, et al. Disease activity in rheumatoid arthritis and the risk of cardiovascular events. Arthritis Rheumatol. 2015;67(6):1449-1455. https://doi.org/10.1002/art.39098.
15. Jiang SZ, To JL, Hughes MR, McNagny KM, Kim H. Platelet signaling at the nexus of innate immunity and rheumatoid arthritis. Front Immunol. 2022;13:977828. https://doi.org/10.3389/fimmu.2022.977828.

ISSN: 2181-3337 | SCIENTISTS.UZ VOLUME 5 ISSUE 7 JULY 2026

PATHOGENETICALLY ORIENTED CORRECTION OF PLATELET ACTIVITY, COAGULATION IMBALANCE AND ENDOTHELIAL DYSFUNCTION IN RHEUMATOID ARTHRITIS

Musaeva Nargiza[1], Babadjanova Shaira[2]
Tashkent State Medical University, Department of Hematology, Transfusiology and Laboratory Medicine[1]
Tashkent State Medical University, Doctor of Medical Sciences, Professor[2]

DOI: 10.67620/sai.57d0005

ABSTRACT

Rheumatoid arthritis is frequently accompanied by platelet activation, coagulation imbalance, and endothelial dysfunction, which may persist despite standard anti-inflammatory treatment. This study evaluated the effects of standard therapy and pathogenetically oriented combined therapy on platelet function, coagulation parameters, and endothelial dysfunction markers in patients with rheumatoid arthritis. Patients without adverse thrombophilia-related genotypes received either standard treatment alone or standard treatment supplemented with endothelial, antiplatelet, and anticoagulant correction, whereas patients with adverse genotypes received genotype-oriented therapy that additionally included folate correction. Platelet count, adhesion, aggregation, activated partial thromboplastin time, prothrombin index, fibrinogen, D-dimer, endothelin-1, and soluble intercellular adhesion molecule were assessed before and after treatment. Platelet count decreased after therapy but did not normalize consistently. In contrast, platelet adhesion and aggregation improved more markedly with combined therapy than with standard treatment. Among patients without adverse genotypes, adhesion decreased from 46–52 to 28–30, while aggregation decreased from 49–52 to 31–33. Activated partial thromboplastin time increased from 19.5–24.2 seconds to 30.5–38.5 seconds, fibrinogen decreased from 3.55–4.66 g/L to 2.44–3.13 g/L, and D-dimer declined from 380–460 ng/mL to 291–332 ng/mL. Endothelin-1 and soluble intercellular adhesion molecule levels also decreased more substantially after combined therapy. These findings indicate that pathogenetically oriented combined treatment provides more pronounced correction of platelet hyperactivity, hypercoagulability, and endothelial dysfunction than standard therapy alone.

ACCEPTED

20.07.26

Keywords: *rheumatoid arthritis, combined therapy, platelet aggregation, hypercoagulation, endothelial dysfunction, D-dimer, fibrinogen, endothelin-1, sICAM.*

CC BY

Introduction

Rheumatoid arthritis is a systemic autoimmune inflammatory disease in which persistent immune activation affects not only the joints but also the vascular and hemostatic systems [1-3]. Platelet activation, coagulation imbalance and endothelial dysfunction contribute to the development of a prothrombotic state [3-7,15].

Traditional treatment of rheumatoid arthritis is primarily directed toward suppression of inflammation and control of joint damage [1]. However, clinical improvement may not always be accompanied by complete normalization of hemostatic and endothelial markers. Persistent hypercoagulation and endothelial dysfunction may maintain vascular risk even during anti-inflammatory therapy [4-7,15].

The pathogenesis of hemovascular disturbances in rheumatoid arthritis includes several interconnected mechanisms: platelet activation, increased fibrinogen and D-dimer, shortening of coagulation times, increased prothrombin index and elevation of endothelial dysfunction markers [3-7,15].

Folate cycle gene polymorphisms may influence homocysteine metabolism and endothelial function. Hyperhomocysteinemia can aggravate endothelial injury, platelet activation and procoagulant balance; therefore, genotype-oriented correction and prolonged laboratory monitoring may be important in selected patients [8-14].

The present study evaluates the dynamics of platelet, coagulation and endothelial markers under standard and combined therapeutic approaches in patients with rheumatoid arthritis.

Materials and Methods

The study included patients with rheumatoid arthritis who were evaluated before and after therapy. Laboratory assessment included platelet count, platelet adhesion, platelet aggregation, activated partial thromboplastin time, prothrombin index, fibrinogen, D-dimer, endothelin-1 and sICAM.

Patients without adverse thrombophilia-related genotypes received standard therapy alone or standard therapy combined with pathogenetically oriented correction aimed at endothelial protection, platelet inhibition and anticoagulant support. The combined protocol included L-arginine, rivaroxaban and clopidogrel for 10 days under physician supervision.

Patients with adverse thrombophilia-related genotypes received standard therapy combined with folate correction, endothelial support, low-molecular-weight heparin according to body weight and antiplatelet correction under physician supervision.

Patients were analyzed according to disease duration and genotype status. Quantitative values are presented according to the available study dataset. Statistical significance was accepted at $p<0.05$.

Results

Effect of therapy on platelet count

Platelet count decreased after both standard and combined therapy, but the changes were not statistically reliable. In patients without adverse genotypes, platelet count decreased from 332 to 296 after standard therapy and to 267 after combined therapy in group 1. In group 2, platelet count decreased from 450 to 418 after standard therapy and to 385 after combined therapy. In group 3, it decreased from 278 to 254 after standard therapy and to 266 after combined therapy.

In patients with adverse genotypes, platelet count also decreased after combined therapy: from 556 to 509 in group 2 heterozygous carriers, from 412 to 388 in group 3 heterozygous carriers and from 687 to 612 in group 3 homozygous carriers.

Table 1. Platelet count dynamics after therapy

Patient category	Before therapy	Standard therapy	Combined therapy
Group 1, without adverse genotype	332	296	267
Group 2, without adverse genotype	450	418	385
Group 3, without adverse genotype	278	254	266

ISSN: 2181-3337 | SCIENTISTS.UZ

Group 2, heterozygous genotype	556	NA	509
Group 3, heterozygous genotype	412	NA	388
Group 3, homozygous genotype	687	NA	612

Note: NA - not available / not applicable in the summarized dataset.

Effect of therapy on platelet adhesion and aggregation

Platelet adhesion and aggregation improved more clearly than platelet count. In patients without adverse genotypes, platelet adhesion decreased from 46 to 31 after standard therapy and to 28 after combined therapy in group 1. In group 2, adhesion decreased from 52 to 37 after standard therapy and to 30 after combined therapy.

Platelet aggregation showed similar dynamics. In group 1, aggregation decreased from 49 to 35 after standard therapy and to 31 after combined therapy. In group 2, aggregation decreased from 52 to 38 after standard therapy and to 33 after combined therapy.

In patients with adverse genotypes, combined therapy also reduced platelet functional activity. Adhesion decreased from 70 to 45 in group 2 heterozygous carriers, from 66 to 48 in group 3 heterozygous carriers and from 79 to 54 in homozygous carriers. Aggregation decreased from 66 to 44, from 70 to 48 and from 85 to 59, respectively.

Table 2. Platelet adhesion and aggregation after therapy

Parameter / category	Before therapy	Standard therapy	Combined therapy
Adhesion, group 1 without adverse genotype	46	31*	28**
Adhesion, group 2 without adverse genotype	52	37*	30**
Aggregation, group 1 without adverse genotype	49	35*	31**
Aggregation, group 2 without adverse genotype	52	38*	33**
Adhesion, group 2 heterozygous genotype	70	NA	45**
Adhesion, group 3 heterozygous genotype	66	NA	48**
Adhesion, group 3 homozygous genotype	79	NA	54**
Aggregation, group 2 heterozygous genotype	66	NA	44**
Aggregation, group 3 heterozygous genotype	70	NA	48**
Aggregation, group 3 homozygous genotype	85	NA	59**

*Note: *p<0.05; **p<0.01 compared with pre-treatment values.*

Effect of therapy on coagulation parameters

APTT increased more markedly after combined therapy than after standard therapy. In patients without adverse genotypes, group 1 APTT increased from 24.2 s to 28.2 s after standard therapy and to 38.5 s after combined therapy. In group 2, APTT increased from 21.6 s to 25.8 s after standard therapy and

ISSN: 2181-3337 | SCIENTISTS.UZ

to 32.3 s after combined therapy. In group 3, it increased from 19.5 s to 24.6 s after standard therapy and to 30.5 s after combined therapy.

Prothrombin index also improved. In group 1, it decreased from 105% to 80% after standard therapy and to 74% after combined therapy. In group 2, it decreased from 128% to 96% and 88%, respectively. In group 3, it decreased from 136% to 105% and 99%.

In patients with adverse genotypes, combined therapy improved but did not fully normalize coagulation parameters. APTT increased from 16.6 to 22.6 s in group 2 heterozygous carriers, from 17.8 to 23.5 s in group 3 heterozygous carriers and from 15.2 to 20.6 s in homozygous carriers. Prothrombin index decreased from 140% to 106%, from 168% to 112% and from 181% to 138%, respectively.

Table 3. APTT and prothrombin index after therapy

Parameter / category	Before therapy	Standard therapy	Combined therapy
APTT, group 1 without adverse genotype, s	24.2	28.2	38.5**
APTT, group 2 without adverse genotype, s	21.6	25.8*	32.3**
APTT, group 3 without adverse genotype, s	19.5	24.6	30.5**
APTT, group 2 heterozygous genotype, s	16.6	NA	22.6*
APTT, group 3 heterozygous genotype, s	17.8	NA	23.5*
APTT, group 3 homozygous genotype, s	15.2	NA	20.6*
Prothrombin index, group 1 without adverse genotype, %	105	80*	74**
Prothrombin index, group 2 without adverse genotype, %	128	96*	88**
Prothrombin index, group 3 without adverse genotype, %	136	105*	99*
Prothrombin index, group 2 heterozygous genotype, %	140	NA	106*
Prothrombin index, group 3 heterozygous genotype, %	168	NA	112**

ISSN: 2181-3337 | SCIENTISTS.UZ

Prothrombin index, group 3 homozygous genotype, %	181	NA	138*

*Note: *p<0.05; **p<0.01 compared with pre-treatment values.*

Effect of therapy on fibrinogen and D-dimer

Fibrinogen and D-dimer decreased after therapy, with stronger improvement after combined treatment. In patients without adverse genotypes, fibrinogen decreased from 3.55 to 2.75 g/L after standard therapy and to 2.44 g/L after combined therapy in group 1. In group 2, fibrinogen decreased from 4.46 to 3.25 g/L and 3.01 g/L, respectively. In group 3, it decreased from 4.66 to 3.64 g/L and 3.13 g/L.

D-dimer decreased from 380 to 320 and 312 ng/ml in group 1, from 460 to 349 and 332 ng/ml in group 2, and from 450 to 324 and 291 ng/ml in group 3.

In patients with adverse genotypes, combined therapy also reduced fibrinogen and D-dimer, although residual elevation remained. Fibrinogen decreased from 5.90 to 4.51 g/L, from 6.30 to 4.74 g/L and from 7.12 to 5.68 g/L in the corresponding genotype subgroups. D-dimer decreased from 820 to 652 ng/ml, from 780 to 608 ng/ml and from 1284 to 846 ng/ml.

Table 4. Fibrinogen after therapy

Patient category	Before therapy, g/L	Standard therapy, g/L	Combined therapy, g/L
Group 1, without adverse genotype	3.55	2.75*	2.44**
Group 2, without adverse genotype	4.46	3.25*	3.01**
Group 3, without adverse genotype	4.66	3.64*	3.13**
Group 2, heterozygous genotype	5.90	NA	4.51**
Group 3, heterozygous genotype	6.30	NA	4.74*
Group 3, homozygous genotype	7.12	NA	5.68*

*Note: *p<0.05; **p<0.01 compared with pre-treatment values.*

Table 5. D-dimer after therapy

Patient category	Before therapy, ng/ml	Standard therapy, ng/ml	Combined therapy, ng/ml
Group 1, without adverse genotype	380	320	312
Group 2, without adverse genotype	460	349*	332*
Group 3, without adverse genotype	450	324*	291**
Group 2, heterozygous genotype	820	NA	652*
Group 3, heterozygous genotype	780	NA	608*
Group 3, homozygous genotype	1284	NA	846**

ISSN: 2181-3337 | SCIENTISTS.UZ

*Note: *p<0.05; **p<0.01 compared with pre-treatment values.*

Effect of therapy on endothelial dysfunction

Endothelial dysfunction markers decreased after therapy. In patients without adverse genotypes, endothelin-1 decreased from 2.9 to 2.1 pg/ml after standard therapy and to 1.8 pg/ml after combined therapy in group 1. In group 2, endothelin-1 decreased from 3.5 to 2.4 and 2.0 pg/ml, respectively. In group 3, it decreased from 4.1 to 3.0 and 2.6 pg/ml.

sICAM also decreased after therapy. In group 1, it decreased from 298 to 234 and 226 ng/ml. In group 2, it decreased from 324 to 246 and 221 ng/ml. In group 3, it decreased from 360 to 271 and 255 ng/ml.

In patients with adverse genotypes, combined therapy reduced endothelin-1 from 4.5 to 3.2 pg/ml, from 4.8 to 3.6 pg/ml and from 5.2 to 4.1 pg/ml. sICAM decreased from 418 to 316 ng/ml, from 425 to 331 ng/ml and from 451 to 344 ng/ml.

Table 6. Endothelial dysfunction markers after therapy

Parameter / category	Before therapy	Standard therapy	Combined therapy
Endothelin-1, group 1 without adverse genotype, pg/ml	2.9	2.1*	1.8**
Endothelin-1, group 2 without adverse genotype, pg/ml	3.5	2.4*	2.0**
Endothelin-1, group 3 without adverse genotype, pg/ml	4.1	3.0*	2.6**
Endothelin-1, group 2 heterozygous genotype, pg/ml	4.5	NA	3.2*
Endothelin-1, group 3 heterozygous genotype, pg/ml	4.8	NA	3.6*
Endothelin-1, group 3 homozygous genotype, pg/ml	5.2	NA	4.1*
sICAM, group 1 without adverse genotype, ng/ml	298	234*	226*
sICAM, group 2 without adverse genotype, ng/ml	324	246*	221**
sICAM, group 3 without adverse genotype, ng/ml	360	271*	255*
sICAM, group 2 heterozygous genotype, ng/ml	418	NA	316*
sICAM, group 3 heterozygous genotype, ng/ml	425	NA	331*

ISSN: 2181-3337 | SCIENTISTS.UZ

sICAM, group 3 homozygous genotype, ng/ml	451	NA	344*

*Note: *p<0.05; **p<0.01 compared with pre-treatment values.*

Figure 1 is provided below to visually summarize the central quantitative findings described in the Results section.

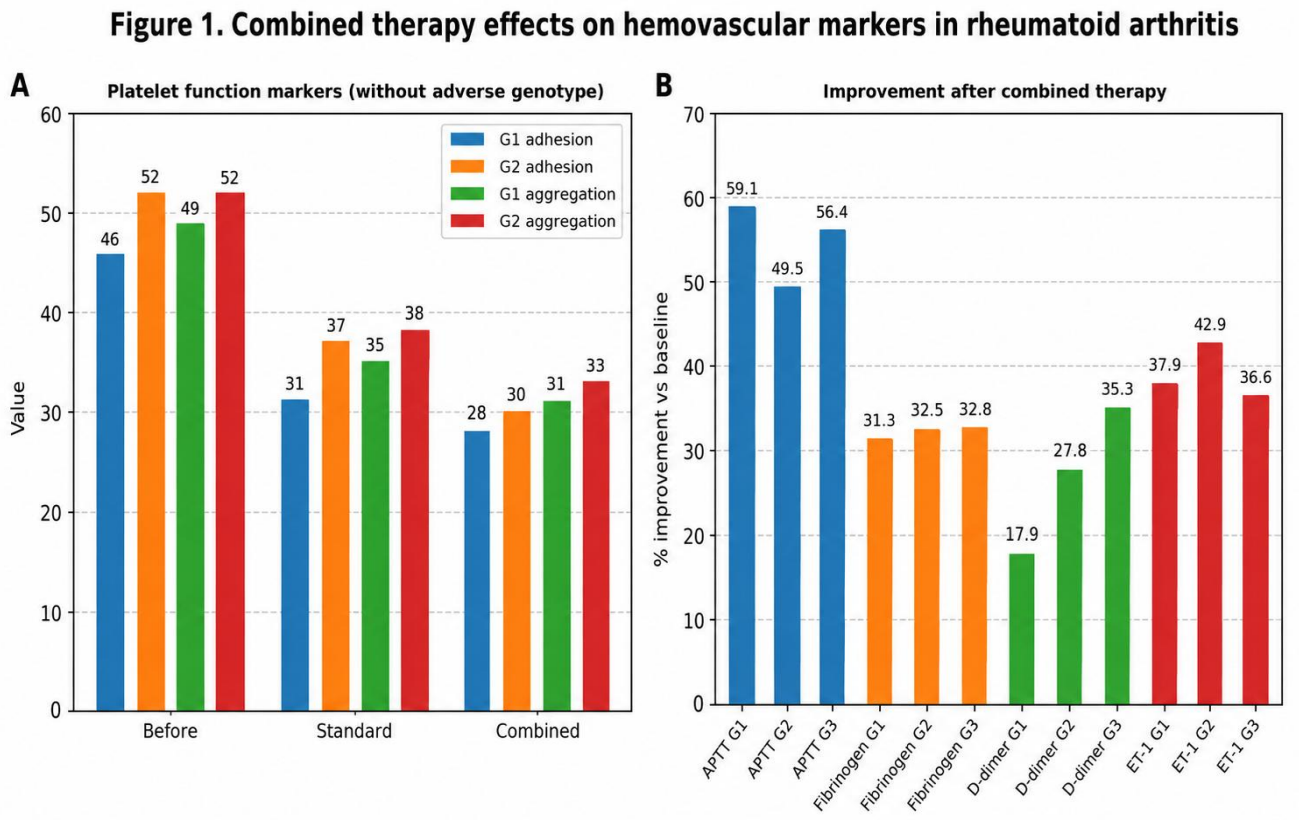


Figure 1. Visual summary of combined therapy effects on platelet function, coagulation markers, and endothelial dysfunction in rheumatoid arthritis.

Note. Panel A compares platelet adhesion and aggregation before treatment, after standard therapy, and after combined therapy in patients without adverse thrombophilia-related genotypes. Panel B presents percentage improvement from baseline after combined therapy for APTT, fibrinogen, D-dimer, and endothelin-1 across the summarized study groups. The figure was constructed from the numerical values reported in Tables 2–6.

Discussion

The results of this study show that combined pathogenetically oriented therapy has a more pronounced corrective effect on hemovascular disturbances in rheumatoid arthritis than standard therapy alone. The most evident improvements were observed in platelet adhesion and aggregation, APTT, prothrombin index, fibrinogen, D-dimer, endothelin-1 and sICAM.

Platelet count decreased after treatment, but these changes were not reliable. In contrast, platelet functional activity improved significantly. This suggests that platelet function may be a more sensitive marker of therapeutic response than platelet count alone.

The increase in APTT and decrease in prothrombin index after combined therapy indicate reduction of hypercoagulability. The decrease in fibrinogen and D-dimer further supports improvement of coagulation balance and reduction of fibrin formation and degradation activity [4-7,15].

Endothelial dysfunction markers also responded better to combined therapy. Reduction of endothelin-1 suggests improvement of endothelial vasoregulatory function, while reduction of sICAM indicates decreased inflammatory endothelial activation [3,9,15].

ISSN: 2181-3337 | SCIENTISTS.UZ

Patients with adverse thrombophilia-related genotypes improved after combined therapy, but their parameters did not fully normalize. This indicates that genetic predisposition may reduce the completeness of hemovascular correction and may require longer monitoring [8-14].

Overall, the findings support a personalized therapeutic model in rheumatoid arthritis. In patients with endothelial dysfunction and hypercoagulation, treatment assessment should include not only inflammatory and articular markers but also platelet, coagulation and endothelial parameters.

Conclusions

1. Standard therapy improves some hemostatic parameters in rheumatoid arthritis, but combined therapy has a stronger corrective effect.

2. Platelet adhesion and aggregation decreased more significantly after combined therapy than after standard therapy.

3. Combined therapy increased APTT, reduced prothrombin index and improved coagulation balance.

4. Fibrinogen and D-dimer decreased more markedly after combined therapy, indicating reduction of hypercoagulability.

5. Endothelin-1 and sICAM decreased after combined therapy, confirming improvement of endothelial dysfunction.

6. Patients with adverse thrombophilia-related genotypes improved after therapy but retained residual abnormalities.

7. Pathogenetically oriented therapy may be considered a promising adjunctive approach for correction of hemovascular disturbances in rheumatoid arthritis.

REFERENCES

1. Smolen JS, Landewé RBM, Bergstra SA, Kerschbaumer A, Sepriano A, Aletaha D, et al. EULAR recommendations for the management of rheumatoid arthritis with synthetic and biological disease-modifying antirheumatic drugs: 2022 update. Ann Rheum Dis. 2023;82(1):3-18. https://doi.org/10.1136/ard-2022-223356.
2. Aletaha D, Neogi T, Silman AJ, Funovits J, Felson DT, Bingham CO, et al. 2010 rheumatoid arthritis classification criteria: an American College of Rheumatology/European League Against Rheumatism collaborative initiative. Ann Rheum Dis. 2010;69(9):1580-1588. https://doi.org/10.1136/ard.2010.138461.
3. Yang XZ, Chang Y, Wei W. Endothelial dysfunction and inflammation: immunity in rheumatoid arthritis. Mediators Inflamm. 2016;2016:6813016. https://doi.org/10.1155/2016/6813016.
4. Adamantidi T, Pisioti MS, Pitsouni S, Chatzikamari M, Karamanis G, Dania V, et al. The inflammatory link of rheumatoid arthritis and thrombosis: pathogenic molecular circuits and treatment approaches. Curr Issues Mol Biol. 2025;47(4):291. https://doi.org/10.3390/cimb47040291.
5. Molander V, Bower H, Frisell T, Askling J. Risk of venous thromboembolism in rheumatoid arthritis, and its association with disease activity: a nationwide cohort study from Sweden. Ann Rheum Dis. 2021;80(2):169-175. https://doi.org/10.1136/annrheumdis-2020-218419.
6. Hu LJ, Ji B, Fan HX. Venous thromboembolism risk in rheumatoid arthritis patients: a systematic review and updated meta-analysis. Eur Rev Med Pharmacol Sci. 2021;25(22):7005-7013. https://doi.org/10.26355/eurrev_202111_27249.
7. Manz XD, Doddaballapur A, Hynes RO, Wagner DD. Regulation of VWF (von Willebrand factor) in inflammatory thrombosis. Arterioscler Thromb Vasc Biol. 2022;42(11):1307-1320. https://doi.org/10.1161/ATVBAHA.122.318179.

ISSN: 2181-3337 | SCIENTISTS.UZ

8. Bagheri-Hosseinabadi Z, Imani D, Yousefi H, Abbasifard M. MTHFR gene polymorphisms and susceptibility to rheumatoid arthritis: a meta-analysis based on 16 studies. Clin Rheumatol. 2020;39(8):2267-2279. https://doi.org/10.1007/s10067-020-05031-5.
9. Głuszek J, Wierzowiecka M, Niklas K, Niklas A. The importance of homocysteine in the development of cardiovascular complications in patients with rheumatoid arthritis. Reumatologia. 2020;58(5):282-288. https://doi.org/10.5114/reum.2020.99732.
10. Palomino-Morales R, Gonzalez-Juanatey C, Vazquez-Rodriguez TR, Rodriguez L, Miranda-Filloy JA, Fernandez-Gutierrez B, et al. A1298C polymorphism in the MTHFR gene predisposes to cardiovascular risk in rheumatoid arthritis. Arthritis Res Ther. 2010;12(2):R71. https://doi.org/10.1186/ar2989.
11. Fujimaki C, Hayashi H, Tsuboi S, Matsuyama T, Kosuge K, Yamada H, et al. Plasma total homocysteine level and methylenetetrahydrofolate reductase 677C>T genetic polymorphism in Japanese patients with rheumatoid arthritis. Biomarkers. 2009;14(1):49-54. https://doi.org/10.1080/13547500902730664.
12. Yxfeldt A, Wållberg-Jonsson S, Hultdin J, Rantapää-Dahlqvist S. Homocysteine in patients with rheumatoid arthritis in relation to inflammation and B-vitamin treatment. Scand J Rheumatol. 2003;32(4):205-210. https://doi.org/10.1080/03009740310003686.
13. van Ede AE, Laan RFJM, Blom HJ, Boers GHJ, Haagsma CJ, Thomas CMG, et al. Homocysteine and folate status in methotrexate-treated patients with rheumatoid arthritis. Rheumatology (Oxford). 2002;41(6):658-665. https://doi.org/10.1093/rheumatology/41.6.658.
14. Shea B, Swinden MV, Tanjong Ghogomu E, Ortiz Z, Katchamart W, Rader T, et al. Folic acid and folinic acid for reducing side effects in patients receiving methotrexate for rheumatoid arthritis. J Rheumatol. 2014;41(6):1049-1060. https://doi.org/10.3899/jrheum.130738.
15. Vona R, Di Franco M, Gambardella L, Di Lollo AC, Iannuccelli C, Valesini G, et al. Potential role of platelets for atherosclerotic events in rheumatoid arthritis. FEBS Open Bio. 2018;8(12):1888-1896. https://doi.org/10.1002/2211-5463.12531.

ISSN: 2181-3337 | SCIENTISTS.UZ

ISSN: 2181-3337 | SCIENTISTS.UZ VOLUME 5 ISSUE 7 JULY 2026

COTTON YIELD AND IRRIGATION WATER PRODUCTIVITY UNDER DRIP AND SURFACE IRRIGATION REGIMES IN CALCISOLS OF UZBEKISTAN

Sarimsakov Maksudkhon[1], **Seitbayev Kuandik**[2]
Corresponding author: engenering67@gmail.com
Research Institute of Plant Genetic Resources, Tashkent Region, Uzbekistan[1]
Sherkhan Murtaza International Taraz University, Taraz, Kazakhstan[2]

DOI: 10.67620/sai.57d0006

ABSTRACT

Water scarcity constrains cotton production in Central Asia, where irrigation strategies must balance yield with water conservation. A three-season field experiment (2018–2020) in Qibray District, Tashkent Region, compared surface and drip irrigation at three pre-irrigation soil-moisture threshold regimes: 65–65–60%, 70–70–65%, and 75–75–65% of field capacity across sequential crop-development periods. The experiment was reported as a randomized block design with three replications and 120 m² plots. Because the available analytical record contained treatment-level summaries rather than replicate- and year-level observations, results were evaluated descriptively and no inferential significance claims were retained. Drip irrigation used 2,900–3,560 m³ ha⁻¹ compared with 5,264–5,996 m³ ha⁻¹ under surface irrigation, corresponding to 40.6–44.9% less irrigation water for matched moisture regimes. Cotton yield was 3.06–3.49 t ha⁻¹ under drip irrigation and 2.66–3.07 t ha⁻¹ under surface irrigation, a 13.7–15.0% increase for matched regimes. Irrigation water productivity was highest under drip irrigation at 65–65–60% field capacity (1.06 kg m⁻³), whereas the highest yield occurred at 75–75–65% field capacity (3.49 t ha⁻¹). The findings indicate a trade-off: the wetter drip regime favored yield, while the drier drip regime maximized output per unit of irrigation water.

ACCEPTED

21.07.26

Keywords: *cotton; drip irrigation; irrigation scheduling; irrigation water productivity; field capacity; Calcisols; Uzbekistan.*

CC BY

Introduction

Agriculture is the largest global user of freshwater, and improving the productivity of irrigation water is central to food production in water-limited regions (Food and Agriculture Organization of the United Nations [FAO], 2017). The distinction between water-use efficiency based on evapotranspiration and productivity based on irrigation water applied is important because the two measures answer different management questions (Howell, 2001). At the field scale, drip irrigation can reduce non-beneficial surface losses and improve control over the timing and location of water delivery, although the magnitude of any saving depends on system design, scheduling, soil conditions, and the accounting boundary used (Ayars et al., 1999; Playán & Mateos, 2006).

Cotton is a major irrigated crop in Uzbekistan, and its production is closely linked to the availability and management of irrigation water. Previous field research in Uzbekistan reported that drip irrigation could reduce applied water and increase cotton yield relative to furrow irrigation under locally calibrated soil-moisture schedules (Ibragimov et al., 2007). A later study showed that improved irrigation termination using wetting-front detectors could further reduce water losses and improve irrigation crop water productivity (Ibragimov et al., 2021). A review of water-management practices in Uzbekistan likewise identified drip irrigation as one of the most promising approaches for increasing cotton water productivity, while emphasizing that technical performance and farm-level feasibility must be evaluated together (Mirshadiev et al., 2018).

Soil properties also influence the response to irrigation scheduling. The experimental site in the present study was described as typical gray soil corresponding to Calcisols, with carbonate accumulation and a deep groundwater table. Because water movement and storage in calcareous soils may differ from those in coarser or non-calcareous soils, locally derived treatment comparisons remain useful for irrigation planning. The present study therefore compared three pre-irrigation moisture-threshold regimes under drip and surface irrigation over three growing seasons. The objectives were to quantify treatment-level differences in seasonal irrigation water applied, cotton yield, and irrigation water productivity, and to distinguish the regime associated with the highest yield from the regime associated with the highest output per unit of irrigation water.

Materials and Methods

Study Site

Field experiments were conducted during the 2018, 2019, and 2020 cotton-growing seasons at the Central Experimental Farm of the Research Institute of Plant Genetic Resources in Qibray District, Tashkent Region, Uzbekistan. The site lies in the foothill zone and has a semi-arid continental climate with hot summers. The field record described growing-season air temperatures of approximately 18–32 °C, precipitation of 260–340 mm, and reference evapotranspiration of 850–950 mm across the study period. The soil was described as an automorphic typical gray soil corresponding to Calcisols. Groundwater depth was approximately 15 m, so direct groundwater contribution to root-zone water was considered negligible.

Experimental Design and Irrigation Treatments

The experiment used a randomized block design with three replications. Each plot covered 120 m². Two irrigation methods were compared: conventional surface irrigation and drip irrigation. Within each method, three pre-irrigation soil-moisture threshold regimes were evaluated: 65–65–60%, 70–70–65%, and 75–75–65% of field capacity. The three values in each treatment code represent sequential crop-development periods in the field protocol. Cotton was planted at 60 cm between rows and 20 cm between plants. For drip-irrigated plots, emitters were spaced at 30 cm and had a nominal discharge of 2 L h^{-1}. All treatments received the same general crop-management program so that irrigation method and threshold regime were the intended treatment contrasts.

Measurements and Derived Indicators

Soil moisture was monitored gravimetrically to determine when the assigned pre-irrigation threshold had been reached. The number of irrigation events and the seasonal volume of irrigation water applied were obtained from field irrigation records. Cotton yield was measured at harvest and reported in tonnes per hectare. Because the denominator available in the field record was irrigation water applied rather than crop evapotranspiration, the efficiency metric was defined as irrigation water productivity (IWP), not evapotranspiration-based water-use efficiency.

$$IWP\ (kg\ m^{-3}) = cotton\ yield\ (kg\ ha^{-1}) / seasonal\ irrigation\ water\ applied\ (m^3\ ha^{-1})$$

Water saving for each drip treatment was calculated relative to the surface-irrigated treatment with the same moisture-threshold regime: water saving (%) = 100 × [1 − (drip water applied / surface water applied)]. The percentage yield difference was calculated in the same matched-treatment manner.

ISSN: 2181-3337 | SCIENTISTS.UZ

Statistical Treatment and Verification Scope

The supplied analytical record contained one summary value per irrigation-method × moisture-regime combination and did not include replicate-level or year-level observations, variance estimates, model output, or reproducible statistical files. Consequently, analysis of variance, Tukey multiple-comparison groupings, p values, and error bars could not be independently reconstructed and are not reported. The present analysis is therefore limited to internally verified arithmetic and descriptive comparisons of the six treatment summaries. All water-saving percentages, yield differences, and IWP values were recalculated directly from the reported water and yield totals.

Ethical Considerations

The study involved field-grown cotton and did not include human participants or vertebrate animals; human-subject or animal-research ethical approval was therefore not applicable.

Results

Seasonal Irrigation Water Application

Surface-irrigated treatments received 5,264–5,996 $m^3\ ha^{-1}$ over five to seven irrigation events, whereas drip-irrigated treatments received 2,900–3,560 $m^3\ ha^{-1}$ over seven to ten events (Table 1). Thus, drip irrigation applied smaller volumes more frequently. For matched moisture-threshold regimes, the reduction in seasonal irrigation water was 44.9% at 65–65–60%, 43.8% at 70–70–65%, and 40.6% at 75–75–65%. Absolute water saving ranged from 2,364 to 2,516 $m^3\ ha^{-1}$.

Table 1

Seasonal irrigation water applied and water saving by treatment

Irrigation method	Threshold regime (% FC)	Irrigation events	Water applied ($m^3\ ha^{-1}$)	Water saving (%)
Surface	65–65–60	5	5,264	—
Surface	70–70–65	6	5,746	—
Surface	75–75–65	7	5,996	—
Drip	65–65–60	7	2,900	44.9
Drip	70–70–65	8	3,230	43.8
Drip	75–75–65	10	3,560	40.6

Note. FC = field capacity. Water saving for each drip treatment was calculated relative to the surface treatment with the same threshold regime.

ISSN: 2181-3337 | SCIENTISTS.UZ

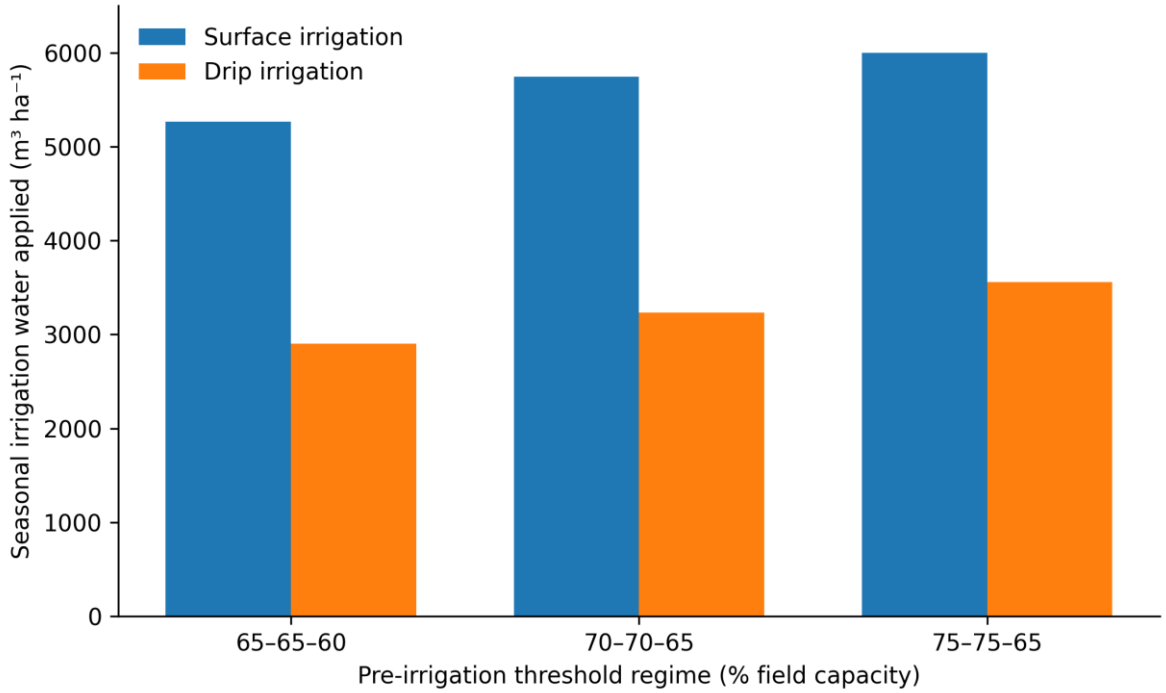


Figure 1. Seasonal irrigation water applied under surface and drip irrigation at three pre-irrigation threshold regimes. Values are treatment-level summaries; no error bars are shown because replicate-level variance estimates were not available.

Cotton Yield and Irrigation Water Productivity

Cotton yield increased across the three moisture-threshold regimes under both irrigation methods (Table 2). For matched regimes, drip-irrigated yield exceeded surface-irrigated yield by 15.0%, 14.0%, and 13.7%, respectively. The highest reported yield was 3.49 t ha^{-1} under drip irrigation at 75–75–65% field capacity (Figure 2). However, this treatment did not have the highest IWP. Because water application rose more rapidly than yield across the drip regimes, IWP declined from 1.06 kg m^{-3} at 65–65–60% to 0.98 kg m^{-3} at 75–75–65%. Surface-irrigated IWP remained near 0.50–0.51 kg m^{-3}. Thus, all drip treatments approximately doubled output per unit of irrigation water, but the driest drip regime produced the greatest IWP.

Table 2

Cotton yield, matched-treatment yield difference, and irrigation water productivity

Irrigation method	Threshold regime (% FC)	Yield (t ha^{-1})	Yield difference (%)	IWP (kg m^{-3})
Surface	65–65–60	2.66	—	0.51
Surface	70–70–65	2.85	—	0.50
Surface	75–75–65	3.07	—	0.51
Drip	65–65–60	3.06	15.0	1.06
Drip	70–70–65	3.25	14.0	1.01
Drip	75–75–65	3.49	13.7	0.98

Note. FC = field capacity; IWP = irrigation water productivity. Yield difference compares each drip treatment with the surface treatment at the same threshold regime. IWP was recalculated as yield in kg ha^{-1} divided by seasonal irrigation water applied in m^3 ha^{-1}.

ISSN: 2181-3337 | SCIENTISTS.UZ

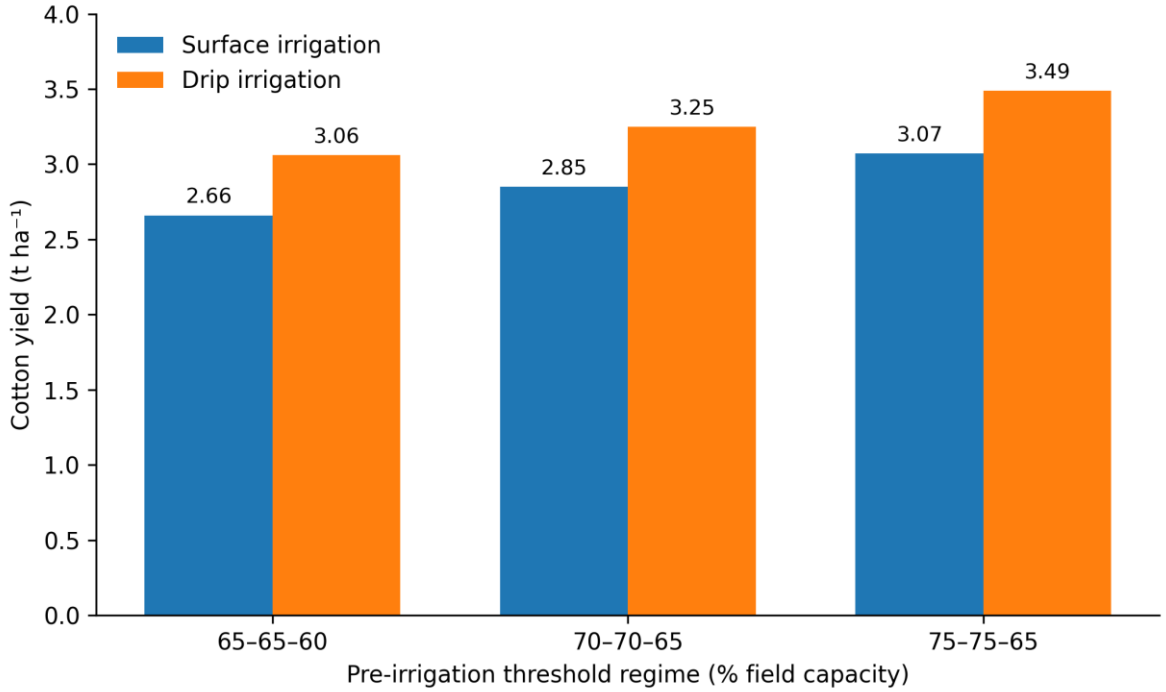


Figure 2. *Cotton yield under surface and drip irrigation at three pre-irrigation threshold regimes. Values are treatment-level summaries; inferential group letters and error bars are not shown because the underlying replicate-level data were not available for verification.*

Discussion

The treatment summaries show a consistent descriptive advantage of drip irrigation over surface irrigation in both seasonal water application and cotton yield. The 40.6–44.9% reduction in applied irrigation water is at the upper end of the 18–42% range reported in an earlier Uzbekistan field study, whereas the 13.7–15.0% yield increase falls within that study's reported 10–19% range (Ibragimov et al., 2007). The agreement in direction and approximate magnitude strengthens the practical plausibility of the present treatment summaries, although it does not replace statistical verification of the current experiment.

The main agronomic result is not a single universal optimum but a clear yield–water-productivity trade-off. The 75–75–65% drip regime produced the highest yield, but the 65–65–60% drip regime produced the highest IWP. This pattern is expected when additional irrigation continues to raise yield but with diminishing output per unit of applied water. Deficit-irrigation literature similarly shows that maximizing yield and maximizing water productivity can require different schedules (Cheng et al., 2021; Fereres & Soriano, 2007; Geerts & Raes, 2009). Accordingly, the preferred treatment depends on the management objective: maximizing harvested output favors the wetter drip regime, whereas maximizing output per cubic metre of irrigation water favors the drier drip regime.

The use of IWP rather than a generic water-use-efficiency label is also consequential. The reported denominator was seasonal irrigation water applied, not measured crop evapotranspiration. Therefore, the values quantify farm-level output per unit of supplied irrigation water and should not be interpreted as physiological efficiency or evapotranspiration-based crop water productivity (Howell, 2001; Pereira et al., 2002). This distinction improves comparability and prevents an overstatement of true consumptive water savings, particularly because reductions in field application do not necessarily translate one-for-one into basin-scale water savings.

Higher irrigation frequency under drip irrigation was accompanied by lower total seasonal application. This is consistent with the operational purpose of drip systems: smaller, localized applications can maintain the assigned soil-moisture threshold while reducing excess surface wetting and uncontrolled percolation. However, the present summary data cannot isolate the mechanisms responsible for the

ISSN: 2181-3337 | SCIENTISTS.UZ

observed differences. Detailed measurements of evapotranspiration, drainage, salinity, and root-zone water distribution would be required to quantify the water balance and to evaluate whether the apparent field-scale saving is sustained over longer periods.

Limitations

Several limitations constrain interpretation. First, only pooled treatment summaries were available; replicate-level and year-specific data were not supplied. Consequently, year-to-year variability, block effects, uncertainty intervals, and inferential significance could not be assessed. Second, the field record did not provide a complete description of the exact crop-development stages represented by the three moisture thresholds, fertilizer rates, cultivar, planting dates, harvest protocol, or instrument calibration. Third, the yield measure was reported generically as cotton yield and was not explicitly distinguished as seed cotton or lint yield. Fourth, the available water accounting covered irrigation water applied rather than a complete evapotranspiration or soil-water balance. Finally, economic claims were excluded because the original cost and return values did not include reproducible price assumptions and were internally inconsistent with the stated additional income. These limitations mean that the results should be treated as descriptive treatment evidence rather than a fully reproducible optimization analysis.

Conclusions

Across three reported growing seasons in Calcisols of the Tashkent Region, drip irrigation used 40.6–44.9% less seasonal irrigation water than the corresponding surface-irrigation regimes while producing 13.7–15.0% higher cotton yield. The 75–75–65% field-capacity regime under drip irrigation produced the highest yield (3.49 t ha^{-1}), whereas the 65–65–60% drip regime produced the highest irrigation water productivity (1.06 kg m^{-3}). The results therefore support drip irrigation as a promising field-level water-management approach at the study site, but they do not justify naming one regime as universally optimal. Selection should depend on whether the production objective prioritizes maximum yield or maximum output per unit of irrigation water. Future work should report year- and replicate-level data, complete crop and soil protocols, full water-balance measurements, and transparent economic assumptions.

Data Availability

The corrected analysis is based on the treatment-level water-application and yield summaries contained in the study record. Replicate-level and year-level datasets were not available with the supplied manuscript.

REFERENCES

26. Ayars, J. E., Phene, C. J., Hutmacher, R. B., Davis, K. R., Schoneman, R. A., Vail, S. S., & Mead, R. M. (1999). Subsurface drip irrigation of row crops: A review of 15 years of research at the Water Management Research Laboratory. Agricultural Water Management, 42(1), 1–27. https://doi.org/10.1016/S0378-3774(99)00025-6
27. Cheng, M., Wang, H., Fan, J., Zhang, S., Wang, Y., Li, Y., Sun, X., Yang, L., & Zhang, F. (2021). Water productivity and seed cotton yield in response to deficit irrigation: A global meta-analysis. Agricultural Water Management, 255, 107027. https://doi.org/10.1016/j.agwat.2021.107027
28. Food and Agriculture Organization of the United Nations. (2017). Water for sustainable food and agriculture: A report produced for the G20 Presidency of Germany. FAO.
29. Fereres, E., & Soriano, M. A. (2007). Deficit irrigation for reducing agricultural water use. Journal of Experimental Botany, 58(2), 147–159. https://doi.org/10.1093/jxb/erl165
30. Geerts, S., & Raes, D. (2009). Deficit irrigation as an on-farm strategy to maximize crop water productivity in dry areas. Agricultural Water Management, 96(9), 1275–1284. https://doi.org/10.1016/j.agwat.2009.04.009

ISSN: 2181-3337 | SCIENTISTS.UZ

31. Howell, T. A. (2001). Enhancing water use efficiency in irrigated agriculture. Agronomy Journal, 93(2), 281–289. https://doi.org/10.2134/agronj2001.932281x
32. Ibragimov, N., Avliyakulov, M., Durdiev, N., Evett, S. R., Gopporov, F., & Yakhyoeva, N. (2021). Cotton irrigation scheduling improvements using wetting front detectors in Uzbekistan. Agricultural Water Management, 244, 106538. https://doi.org/10.1016/j.agwat.2020.106538
33. Ibragimov, N., Evett, S. R., Esanbekov, Y., Kamilov, B. S., Mirzaev, L., & Lamers, J. P. A. (2007). Water use efficiency of irrigated cotton in Uzbekistan under drip and furrow irrigation. Agricultural Water Management, 90(1–2), 112–120. https://doi.org/10.1016/j.agwat.2007.01.016
34. Mirshadiev, M., Fleskens, L., van Dam, J., & Pulatov, A. (2018). Scoping of promising land management and water use practices in the dry areas of Uzbekistan. Agricultural Water Management, 207, 15–25. https://doi.org/10.1016/j.agwat.2018.05.015
35. Pereira, L. S., Oweis, T., & Zairi, A. (2002). Irrigation management under water scarcity. Agricultural Water Management, 57(3), 175–206. https://doi.org/10.1016/S0378-3774(02)00075-6
36. Playán, E., & Mateos, L. (2006). Modernization and optimization of irrigation systems to increase water productivity. Agricultural Water Management, 80(1–3), 100–116. https://doi.org/10.1016/j.agwat.2005.07.007
37. Wanjura, D. F., Upchurch, D. R., Mahan, J. R., & Burke, J. J. (2002). Cotton yield and applied water relationships under drip irrigation. Agricultural Water Management, 55(3), 217–237. https://doi.org/10.1016/S0378-3774(01)00175-5

ISSN: 2181-3337 | SCIENTISTS.UZ VOLUME 5 ISSUE 7 JULY 2026

MATERNAL PRE-PREGNANCY BODY MASS INDEX AMONG TERM NEWBORNS WITH PROLONGED JAUNDICE: CLINICAL AND LABORATORY FINDINGS

Xudayberganov Munis[1], **Sharipova Sarvinoz**[2]
[1]Head of the Department of Pediatrics and Neonatology,
Candidate of Medical Sciences, Associate Professor
[2]Assistant, Department of Pediatrics and Neonatology, Urgench State Medical Institute

DOI: 10.67620/sai.57d0007

ABSTRACT

Background: Prolonged neonatal jaundice requires careful assessment because persistent unconjugated hyperbilirubinemia must be distinguished from conjugated hyperbilirubinemia and hepatobiliary disease. Maternal overweight and obesity may alter maternal and neonatal metabolic conditions, but evidence regarding prolonged jaundice remains limited. Objective: To describe maternal body mass index distribution and clinical–laboratory findings among term newborns with prolonged jaundice. Methods: This clinical and laboratory study included 140 full-term newborns with jaundice persisting beyond 14 days and total bilirubin above 85 μmol/L. Newborns were grouped according to maternal pre-pregnancy BMI. Maternal and neonatal hematological and biochemical indicators were assessed, and Spearman correlations were calculated. Results: Of 140 newborns, 100 (71.4%) were male. Maternal BMI categories were overweight in 57 cases (40.7%), class I–II obesity in 21 (15.0%), underweight in 25 (17.9%), and normal weight in 37 (26.4%). Maternal AST was higher in the overweight and obesity groups than in the normal-BMI group. Mean neonatal biochemical values did not differ significantly across groups. Within the overweight group, platelet count correlated positively with direct bilirubin (ρ=0.63), ALT (ρ=0.95), and AST (ρ=0.79). Conclusion: Overweight or obesity was present in 55.7% of mothers in this case series. The observed laboratory correlations are exploratory and support structured hepatobiliary assessment rather than causal inference..

ACCEPTED

20.07.26

Keywords: *prolonged neonatal jaundice; maternal body mass index; overweight; obesity; hyperbilirubinemia; neonatal cholestasis; liver enzymes.*

CC BY

1. Introduction

The neonatal period, defined as the first 28 days of life, remains the most vulnerable stage of childhood. Global estimates indicate that 2.3 million children died during the first month of life in 2024, corresponding to approximately 6,200 neonatal deaths each day, and neonatal deaths accounted for 47% of all deaths before five years of age [11,12]. These figures provide a broad public-health context for improving recognition and management of conditions that may initially appear common or benign but can occasionally signal serious disease.

Jaundice is among the most frequent clinical findings in newborns. More than 80% of newborn infants develop visible jaundice during the first weeks after birth, usually because bilirubin production is high and hepatic conjugation and excretion are still maturing [1]. Most neonatal jaundice is transient and predominantly unconjugated. Nevertheless, severe unconjugated hyperbilirubinemia can cause acute bilirubin encephalopathy or kernicterus, while persistent jaundice can be the first sign of hemolysis, endocrine disease, infection, inherited metabolic disease, biliary obstruction, or another hepatobiliary disorder [1–5]. For this reason, clinical appearance alone is insufficient; bilirubin values must be interpreted according to the infant's age, gestational maturity, clinical status, and the direct or conjugated fraction.

Prolonged neonatal jaundice is commonly defined as jaundice persisting beyond 14 days in a term infant. International guidance emphasizes that infants who remain jaundiced at or after two weeks should undergo fractionated bilirubin measurement so that cholestasis is not missed [2–5]. The 2017 joint NASPGHAN–ESPGHAN guideline states that a direct bilirubin concentration above 1.0 mg/dL (17 μmol/L) warrants timely evaluation and, when appropriate, referral to pediatric gastroenterology or hepatology [3]. Timely recognition is particularly important because some causes, including biliary atresia, require rapid diagnostic and surgical decision-making. More recent reviews likewise recommend a stepwise evaluation that combines history, physical examination, total and direct bilirubin, liver enzymes, coagulation measures, targeted imaging, and metabolic or genetic testing when indicated [4,5].

The determinants of neonatal hyperbilirubinemia are heterogeneous. A meta-analysis identified exclusive breastfeeding, glucose-6-phosphate dehydrogenase deficiency, maternal–fetal ABO incompatibility, and preterm birth as important factors [10]. Large cohort work has also shown that hemolytic and nonhemolytic jaundice have different maternal and pregnancy risk profiles, with maternal obesity among the factors associated with nonhemolytic neonatal jaundice [9]. These findings indicate that maternal characteristics can contribute to the clinical context of neonatal jaundice, although the strength and mechanism of each association may differ across populations.

Maternal overweight and obesity are increasingly common. The World Health Organization estimated that 2.5 billion adults were overweight in 2022, including more than 890 million living with obesity [13]. In pregnancy, excess adiposity is associated with insulin resistance, chronic low-grade inflammation, altered lipid metabolism, nonalcoholic fatty liver disease, gestational diabetes, hypertensive disorders, and changes in placental function. These maternal conditions may affect neonatal metabolic adaptation directly or through associated obstetric and feeding factors. Maternal BMI is therefore a clinically accessible characteristic that may help identify newborns who merit closer surveillance, but it should not be interpreted in isolation.

Several studies have examined maternal weight and bilirubin outcomes. Rougée and colleagues reported an association between obstetric obesity and higher maternal and neonatal unconjugated bilirubin concentrations in a multiethnic sample [6]. Özdek and colleagues prospectively observed higher bilirubin values on postnatal days 5 and 15 among infants whose mothers gained more weight than recommended during pregnancy [7]. In a retrospective study of 3,594 healthy term newborns, Domosud and Kulik-Rechberger assessed maternal pre-pregnancy BMI and gestational weight gain in relation to early jaundice [8]. Although designs and outcomes differ, these studies support further investigation of maternal metabolic status as one component of neonatal jaundice assessment.

Important distinctions are required when interpreting a sample composed only of infants who already have prolonged jaundice. Such a sample can describe the maternal BMI distribution among cases and compare clinical or laboratory patterns between BMI-defined groups. It cannot, however, estimate the incidence of prolonged jaundice among all infants born to overweight or obese mothers unless the number and characteristics of all births are known. It also cannot establish that maternal BMI caused the jaundice.

ISSN: 2181-3337 | SCIENTISTS.UZ

The present study is therefore framed as a descriptive clinical and laboratory analysis of term newborns with prolonged jaundice rather than a population-based risk study.

The objective of this study was to describe the distribution of maternal pre-pregnancy BMI among full-term newborns with prolonged jaundice, compare the available maternal and neonatal laboratory findings across BMI groups, examine reported correlations within the overweight group, and formulate a cautious, guideline-informed approach to further hepatobiliary assessment.

2. Materials and Methods

2.1 Study design and participants

A clinical and laboratory study was conducted in 140 full-term newborns with prolonged jaundice. The available study record defined prolonged jaundice as persistence of visible jaundice after the 14th day of life together with a serum total bilirubin concentration above 85 μmol/L. All included infants were born at term. The sample comprised 100 boys (71.4%) and 40 girls (28.6%).

Maternal pre-pregnancy body mass index was used to classify the mother–infant pairs into four groups. Group 1 included 57 newborns born to overweight mothers; group 2 included 21 newborns born to mothers with class I–II obesity; group 3 included 25 newborns born to underweight mothers; and group 4 included 37 newborns born to mothers with normal body weight. The BMI thresholds applied by the investigators were not specified in the source record; for interpretation, the categories correspond to the conventional adult BMI group labels used in clinical practice.

Because all participants had prolonged jaundice, the study was treated as a case series with internal comparisons by maternal BMI. The design did not include a control group of infants without prolonged jaundice or information on the maternal BMI distribution among all deliveries. Accordingly, analyses of group proportions were interpreted descriptively and were not used to calculate relative risk, odds ratios, incidence, or population prevalence.

2.2 Clinical and laboratory assessment

Maternal assessment included complete blood count and biochemical blood testing. The recorded indicators were hemoglobin, erythrocyte count, platelet count, leukocyte count and differential, erythrocyte sedimentation rate, total protein, glucose, urea, creatinine, total bilirubin and bilirubin fractions, alanine aminotransferase (ALT), and aspartate aminotransferase (AST).

All newborns underwent complete blood count and biochemical testing. The neonatal biochemical panel included ALT, AST, total bilirubin, direct bilirubin, indirect bilirubin, urea, creatinine, calcium, total protein, and glucose. The study record did not provide assay manufacturers, analytical coefficients of variation, exact postnatal age at sampling, or reference intervals. Consequently, the present report focuses on the between-group patterns and correlations explicitly available in the source data rather than reconstructing unreported laboratory procedures.

For clinical interpretation, direct bilirubin was treated as the key screening measure for possible cholestasis, whereas ALT and AST were considered indicators of hepatocellular injury or stress rather than specific markers of biliary obstruction. Platelet count was interpreted as a nonspecific hematological measure that can vary with inflammatory, reactive, hematologic, and technical factors.

2.3 Statistical analysis

Absolute numbers and percentages were calculated for categorical variables. Continuous laboratory variables were summarized using means and the dispersion measures reported in the source manuscript. A two-sided significance threshold of $p<0.05$ was stated in the original analysis. Spearman rank correlation coefficients (ρ) were used to examine monotonic relationships among maternal BMI, neonatal bilirubin fractions, liver enzymes, and platelet count.

The correlation analysis within the overweight group was exploratory. Several pairwise correlations were examined, and no adjustment for multiple testing was reported. Therefore, the magnitude, direction,

ISSN: 2181-3337 | SCIENTISTS.UZ

and clinical coherence of the correlations were considered alongside their p values. Correlation was not interpreted as evidence of causation, prediction, or a validated diagnostic threshold.

2.4 Ethical reporting

The source manuscript did not state the approving ethics committee, approval number, or the procedure used to obtain parental informed consent. These details must be supplied by the authors before submission to a journal that requires formal ethics reporting.

3. Results

3.1 Characteristics of the study sample

Among the 140 full-term newborns with prolonged jaundice, boys predominated, accounting for 100 cases (71.4%), while girls accounted for 40 cases (28.6%). The study record did not provide sex distributions for every maternal BMI group, although the overweight group contained 37 boys, representing 64.9% of that group.

The largest maternal BMI category was overweight: 57 newborns (40.7%) were born to overweight mothers. A further 21 infants (15.0%) were born to mothers with class I–II obesity. Thus, 78 of 140 infants (55.7%) in the case series had mothers classified as overweight or obese. Twenty-five infants (17.9%) were born to underweight mothers, and 37 (26.4%) were born to mothers with normal BMI. These percentages describe the composition of the prolonged-jaundice sample and should not be interpreted as the incidence of prolonged jaundice within each maternal BMI category.

Table 1.

Study sample and distribution by maternal pre-pregnancy BMI

Characteristic / group	Definition in the study	n	% of total
Male newborns	Full-term newborns with prolonged jaundice	100	71.4
Female newborns	Full-term newborns with prolonged jaundice	40	28.6
Group 1	Maternal overweight	57	40.7
Group 2	Maternal class I–II obesity	21	15.0
Group 3	Maternal underweight	25	17.9
Group 4	Maternal normal BMI	37	26.4
Groups 1 + 2	Maternal overweight or obesity	78	55.7

Note. The table describes the composition of a case series. No denominator of all births was available for estimating BMI-specific incidence or risk.

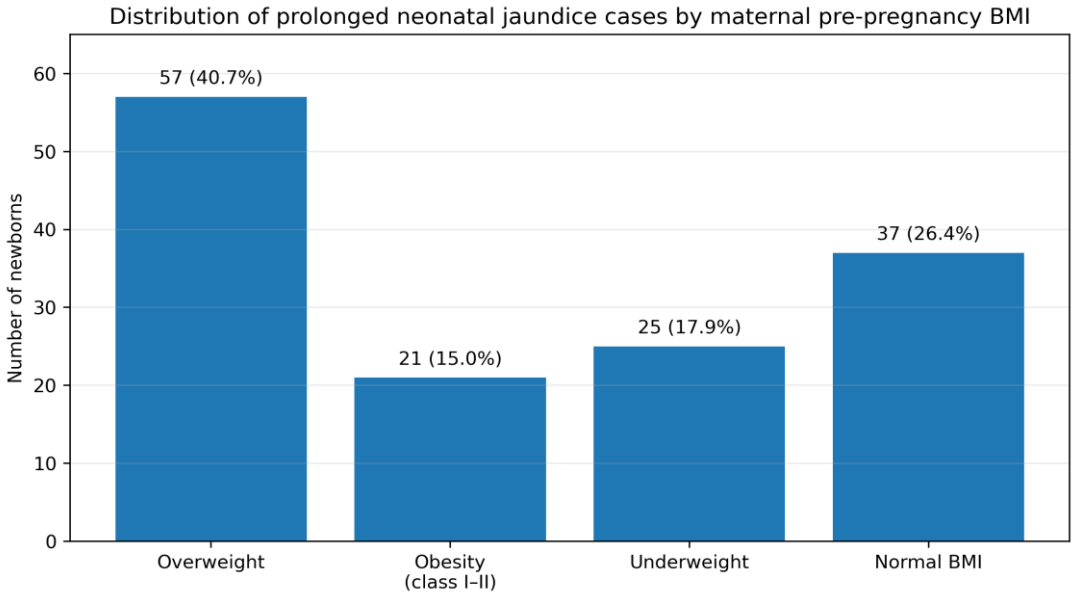


Chart 1. Distribution of prolonged neonatal jaundice cases by maternal pre-pregnancy BMI. Values are numbers and percentages of the 140 included newborns.

3.2 Maternal laboratory findings

Most routinely measured maternal hematological indicators did not differ significantly between BMI groups in the source analysis. Lymphocyte measures were reported to vary among women with abnormal body weight, but the manuscript did not provide complete numerical estimates for each group. Without those estimates, the direction and clinical magnitude of the lymphocyte differences cannot be independently evaluated.

The clearest reported maternal biochemical difference involved AST. Mean AST activity was 35.3±5.6 U/L in mothers in the overweight group and 35.3±5.5 U/L in mothers with class I–II obesity. The corresponding mean among mothers with normal BMI was 17.7±1.4 U/L. The underweight-group value was not reported. The approximately twofold difference between the overweight/obesity groups and the normal-BMI group may be compatible with greater hepatic or metabolic stress, but AST is nonspecific and can be affected by hepatic, muscular, hemolytic, and pre-analytical factors. The finding therefore requires interpretation with ALT, clinical history, and other liver-related measures.

Table 2.

Available maternal AST results by pre-pregnancy BMI group

Maternal BMI group	n	AST, mean ± reported dispersion (U/L)
Overweight	57	35.3 ± 5.6
Class I–II obesity	21	35.3 ± 5.5
Underweight	25	Not reported
Normal BMI	37	17.7 ± 1.4

Note. The source record did not specify whether the dispersion measure was a standard deviation or standard error and did not provide the underweight-group AST estimate.

3.3 Neonatal biochemical findings

The analysis reported no statistically significant between-group differences in neonatal ALT, AST, total bilirubin, direct bilirubin, indirect bilirubin, urea, creatinine, calcium, glucose, or total protein. This indicates that group means for the measured neonatal biochemical variables were broadly similar despite differences in maternal BMI category. It does not exclude clinically important abnormalities in individual infants, nor does it show equivalence between groups because equivalence testing and confidence intervals for group differences were not reported.

The absence of mean differences is relevant when interpreting the subsequent correlation analysis. A correlation observed within one BMI-defined group can coexist with similar group averages, because correlation concerns the joint ordering of two variables within individuals rather than the difference between group means. The results therefore address two distinct questions: whether average laboratory values differed by maternal BMI group, and whether specific neonatal markers moved together within the overweight group.

3.4 Correlation analysis in the maternal-overweight group

Within the 57 mother–infant pairs in the overweight group, maternal BMI showed only weak or negligible correlations with neonatal biochemical indicators. The reported coefficients were $\rho=0.166$ for maternal BMI and total bilirubin, $\rho=0.131$ for maternal BMI and direct bilirubin, $\rho=-0.093$ for maternal BMI and indirect bilirubin, $\rho=0.014$ for maternal BMI and ALT, and $\rho=0.052$ for maternal BMI and AST. These values do not support a strong monotonic relationship between incremental BMI variation within the overweight category and the neonatal bilirubin or aminotransferase measures.

ISSN: 2181-3337 | SCIENTISTS.UZ

By contrast, neonatal platelet count was positively correlated with direct bilirubin (ρ=0.63), ALT (ρ=0.95), and AST (ρ=0.79); the source analysis reported p<0.001 for these three associations. Strong positive correlations were also reported among biochemical indicators: total bilirubin with direct bilirubin (ρ=0.77), direct bilirubin with ALT (ρ=0.75), direct bilirubin with AST (ρ=0.62), and ALT with AST (ρ=0.84). These findings describe a cluster of laboratory values that increased together among infants in the overweight-maternal-BMI group.

The very high platelet–ALT coefficient (ρ=0.95) deserves particular caution. Such a large correlation may represent a strong biological pattern, but it can also arise from a restricted sample, influential observations, duplicated measurements, data-entry errors, or a shared relationship with another unmeasured factor. A scatterplot review, influence analysis, and replication in an independent sample would be necessary before platelet count could be proposed as a diagnostic or prognostic marker.

Table 3.

Reported Spearman correlations within the overweight maternal BMI group (n=57)

Variable 1	Variable 2	Spearman ρ	Reported significance
Maternal BMI	Total bilirubin	0.166	Not reported
Maternal BMI	Direct bilirubin	0.131	Not reported
Maternal BMI	Indirect bilirubin	−0.093	Not reported
Maternal BMI	ALT	0.014	Not reported
Maternal BMI	AST	0.052	Not reported
Platelet count	Direct bilirubin	0.63	p<0.001
Platelet count	ALT	0.95	p<0.001
Platelet count	AST	0.79	p<0.001
Total bilirubin	Direct bilirubin	0.77	Not reported
Direct bilirubin	ALT	0.75	Not reported
Direct bilirubin	AST	0.62	Not reported
ALT	AST	0.84	Not reported

Note. ALT=alanine aminotransferase; AST=aspartate aminotransferase. The source analysis did not report multiplicity-adjusted p values or confidence intervals for the correlations.

4. Discussion

This study describes maternal BMI categories and selected clinical–laboratory findings in 140 full-term newborns with prolonged jaundice. The largest single maternal BMI group was overweight, and overweight plus class I–II obesity accounted for 55.7% of the cases. Maternal AST values were higher in the overweight and obesity groups than in the normal-BMI group. Neonatal mean biochemical indicators did not differ significantly by maternal BMI category, but a set of strong within-group correlations was observed among platelet count, direct bilirubin, ALT, and AST in infants born to overweight mothers.

The case-series design is central to interpretation. The proportion of cases born to overweight or obese mothers cannot be compared with the proportion among all mothers who delivered during the same period because that denominator was not available. If overweight and obesity were similarly common in the underlying obstetric population, the observed 55.7% might simply reflect background maternal BMI distribution. Conversely, if those categories were uncommon among all deliveries, the case proportion might suggest overrepresentation. Without a non-jaundiced comparison group or population denominator, neither inference can be made reliably. The correct conclusion is therefore that overweight or obesity was common among mothers in this sample, not that it increased the incidence of prolonged jaundice by a quantified amount.

The finding remains clinically relevant because previous studies provide a plausible basis for considering maternal weight status during neonatal assessment. Rougée et al. found that obstetric obesity

ISSN: 2181-3337 | SCIENTISTS.UZ

was associated with higher maternal and neonatal unconjugated bilirubin concentrations and proposed reduced UGT1A1-mediated bilirubin clearance as a possible mechanism [6]. Özdek et al. reported higher postnatal bilirubin concentrations among term infants whose mothers gained more weight than recommended during pregnancy [7]. Domosud and Kulik-Rechberger also examined pre-pregnancy BMI and gestational weight gain in a large population of healthy term newborns [8]. A population-based analysis of hemolytic and nonhemolytic jaundice identified maternal obesity among the strongest maternal factors for nonhemolytic jaundice [9]. Together, these studies suggest that maternal adiposity or excessive gestational weight gain may be associated with bilirubin outcomes, while also showing that neonatal jaundice is multifactorial.

Several pathways could connect maternal metabolic status with neonatal jaundice, but the present data cannot distinguish among them. Maternal obesity is associated with insulin resistance, inflammation, altered placental nutrient transfer, higher rates of diabetes and operative delivery, and changes in breastfeeding initiation or neonatal weight loss. Each of these could influence bilirubin production, enterohepatic circulation, hydration, feeding, or hepatic conjugation. Maternal liver enzyme elevation could reflect steatotic liver disease or another source of metabolic stress, but AST alone is not specific. Mechanistic claims should therefore remain hypotheses until supported by better-characterized maternal metabolic, obstetric, placental, and neonatal data.

The elevated maternal AST values in the overweight and obesity groups were one of the clearest numerical differences. Their magnitude was approximately twice the reported mean in the normal-BMI group. Nevertheless, the clinical meaning is uncertain because complete ALT values, AST reference intervals, the dispersion measure, medication history, muscle injury, hemolysis indices, and diagnoses such as fatty liver disease were not provided. The result supports attention to maternal liver-related findings but does not establish maternal hepatic dysfunction or prove a pathway to neonatal jaundice.

The neonatal group means did not differ significantly across maternal BMI categories. This finding argues against a simple model in which maternal overweight or obesity uniformly increases the average bilirubin concentration or aminotransferase activity among all affected infants. It is possible that maternal BMI influences only a subgroup, that associated factors rather than BMI itself are responsible, or that the sample lacked power to detect modest differences. It is also possible that once prolonged jaundice is present, the range of neonatal laboratory values is driven more strongly by the infant's immediate clinical condition than by maternal BMI category.

The correlation cluster involving direct bilirubin, ALT, AST, and platelet count is potentially important but should be treated as exploratory. Direct bilirubin is relevant because conjugated hyperbilirubinemia is a marker of cholestasis and warrants prompt evaluation [3–5]. ALT and AST may rise with hepatocellular injury, although they do not identify the cause or severity of cholestasis by themselves. A positive relationship among these indicators can therefore be clinically coherent. Platelet count, however, is not a specific marker of neonatal cholestasis. Reactive thrombocytosis may occur with inflammation or recovery from illness, while thrombocytopenia can accompany severe liver disease, infection, or portal hypertension. The direction of the association may depend on age, disease stage, and underlying diagnosis.

The platelet–ALT correlation of $\rho=0.95$ is unusually high for independent clinical laboratory measurements. Before this association is used to support a screening algorithm, the raw data should be reviewed for outliers, repeated values, transcription errors, nonlinearity, and restricted ranges. Confidence intervals should be calculated, and the analysis should be repeated after robust or influence-sensitive checks. Because several correlations were tested, multiplicity should also be considered. Replication in a larger, prospectively enrolled sample is essential.

Clinical care should continue to follow established prolonged-jaundice pathways regardless of maternal BMI. NICE guidance recommends assessment of prolonged jaundice and measurement of

ISSN: 2181-3337 | SCIENTISTS.UZ

conjugated bilirubin, with further tests guided by clinical suspicion [2]. The NASPGHAN–ESPGHAN guideline emphasizes total and direct bilirubin measurement after two weeks and timely specialist evaluation when direct bilirubin is elevated [3]. Contemporary reviews recommend assessment of stool and urine color, feeding and growth, hepatosplenomegaly, bleeding, infection, endocrine disease, metabolic disorders, and biliary obstruction, followed by targeted laboratory and imaging investigations [4,5]. Maternal overweight or obesity can be used as contextual information that may lower the threshold for careful review, but it should not replace these standard steps.

Figure 1 presents a practical workflow based on the study's focus and current guidance. It begins with clinical confirmation of persistent jaundice and proceeds to fractionated bilirubin and core laboratory assessment. Infants without conjugated hyperbilirubinemia or clinical red flags may be managed according to the likely benign or noncholestatic cause with planned follow-up. Infants with elevated direct bilirubin, pale stools, dark urine, hepatomegaly, poor growth, coagulopathy, infection signs, or other red flags require urgent hepatobiliary investigation and referral. The workflow is a proposed clinical organization tool and was not prospectively validated in this study.

The study has several strengths. It includes a defined sample of 140 full-term newborns with prolonged jaundice, applies the same maternal BMI grouping across the cohort, assesses both maternal and neonatal laboratory parameters, and examines bilirubin fractions rather than total bilirubin alone. The reporting of correlation coefficients provides information about relationships that may be obscured by group means. The study also addresses a clinically relevant question in a setting where maternal metabolic disorders are becoming more common.

The limitations are substantial. First, the case-only design prevents estimation of risk, incidence, or causal effects. Second, recruitment dates, clinical setting, sampling method, and exclusion criteria were not reported in the available record. Third, the analysis did not account for major neonatal jaundice determinants such as ABO or Rh incompatibility, glucose-6-phosphate dehydrogenase deficiency, breastfeeding pattern, postnatal weight loss, cephalohematoma, infection, thyroid disease, phototherapy, delivery mode, or age at laboratory sampling. Fourth, maternal gestational weight gain, diabetes, hypertension, and detailed liver assessment were not included in the reported analysis. Fifth, complete numerical results and confidence intervals were unavailable for many laboratory comparisons. Sixth, the exploratory correlation analysis involved multiple tests without reported adjustment, and the very high coefficients require raw-data verification. Finally, ethics approval and consent information must be added before submission.

Future research should use a prospective cohort design that enrolls all eligible term births and follows infants beyond 14 days. Maternal pre-pregnancy BMI and gestational weight gain should be measured using standardized definitions. Important confounders should be recorded, including maternal diabetes, hypertension, medications, delivery mode, infant sex, gestational age, birth weight, bruising, blood-group incompatibility, G6PD status, feeding, weight loss, and treatment. The primary outcome should distinguish prolonged unconjugated jaundice from conjugated hyperbilirubinemia or confirmed cholestasis. Multivariable models could then estimate whether maternal BMI independently predicts prolonged jaundice after adjustment for these factors. External validation would be required before any maternal-BMI-based clinical score is used.

ISSN: 2181-3337 | SCIENTISTS.UZ

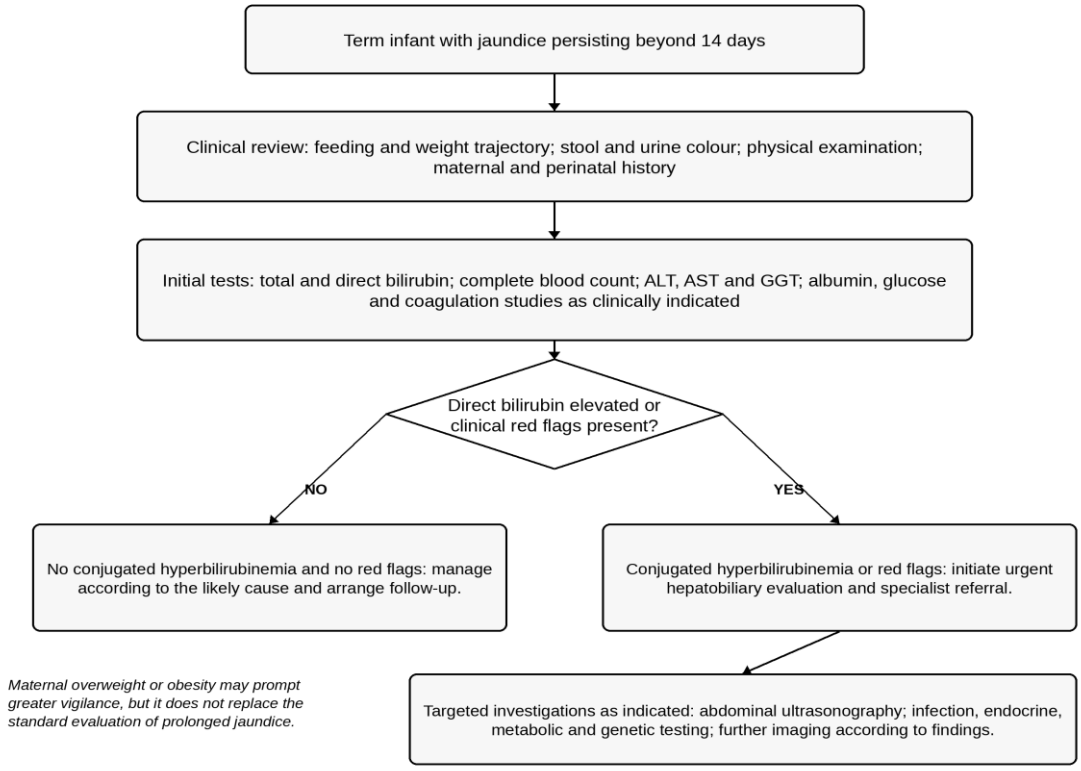


Figure 1. Guideline-informed clinical evaluation pathway for a term infant with prolonged jaundice. The pathway is an original synthesis for this manuscript and was not validated as a diagnostic algorithm in the present study.

Table 4.

Interpretation of the main findings and appropriate level of inference

Observed finding	Supported interpretation	Interpretation not supported by the design
55.7% of cases had mothers with overweight or obesity	Overweight/obesity was common among mothers in this case series	Maternal overweight/obesity increased population incidence or caused prolonged jaundice
Maternal AST was higher in overweight and obesity groups	Maternal BMI groups differed in reported AST values	AST proves fatty liver disease or a causal maternal–neonatal mechanism
No significant differences in neonatal group means	Average measured neonatal biochemical values were similar across BMI groups	The groups are clinically equivalent or individual abnormalities are absent
Strong platelet, bilirubin, ALT, and AST correlations	Markers co-varied within the overweight group	Platelet count is a validated diagnostic biomarker or predictor of cholestasis

5. Conclusion

Among 140 full-term newborns with prolonged jaundice, 40.7% were born to overweight mothers and 15.0% to mothers with class I–II obesity; together these groups accounted for 55.7% of the case series. Maternal AST was higher in the overweight and obesity groups than in the normal-BMI group, whereas the available neonatal biochemical means did not differ significantly across maternal BMI categories.

Within the overweight group, platelet count showed strong positive correlations with direct bilirubin, ALT, and AST, and several bilirubin and aminotransferase measures were also strongly correlated. These findings may indicate a coordinated laboratory pattern in a subgroup of infants, but they remain exploratory and require raw-data verification, adjustment for confounding, and independent replication.

ISSN: 2181-3337 | SCIENTISTS.UZ

Maternal BMI can be considered contextual information during assessment of prolonged neonatal jaundice, but the present design does not establish increased risk or causality. Every term infant with jaundice persisting beyond 14 days should receive clinically appropriate assessment, including fractionated bilirubin and timely evaluation for cholestasis when direct bilirubin is elevated or red flags are present.

Declarations

Ethics approval and consent to participate. The approving committee, approval number, and parental consent procedure were not included in the source manuscript and must be supplied by the authors before submission.

Conflict of interest. The authors should insert their conflict-of-interest declaration.

Funding. The authors should state whether the study received specific funding.

Data availability. The authors should state whether de-identified data are available and under what conditions.

Author contributions. The authors should provide contribution statements that reflect their actual roles.

REFERENCES

1. Kemper AR, Newman TB, Slaughter JL, Maisels MJ, Watchko JF, Downs SM, et al. Clinical Practice Guideline Revision: Management of Hyperbilirubinemia in the Newborn Infant 35 or More Weeks of Gestation. Pediatrics. 2022;150(3):e2022058859. doi:10.1542/peds.2022-058859.

2. National Institute for Health and Care Excellence. Jaundice in newborn babies under 28 days. NICE guideline CG98. Published 19 May 2010; updated 31 October 2023. https://www.nice.org.uk/guidance/cg98

3. Fawaz R, Baumann U, Ekong U, Fischler B, Hadzic N, Mack CL, et al. Guideline for the Evaluation of Cholestatic Jaundice in Infants: Joint Recommendations of NASPGHAN and ESPGHAN. Journal of Pediatric Gastroenterology and Nutrition. 2017;64(1):154–168. doi:10.1097/MPG.0000000000001334.

4. Feldman AG, Sokol RJ. Neonatal Cholestasis: Updates on Diagnostics, Therapeutics, and Prevention. NeoReviews. 2021;22(12):e819–e836. doi:10.1542/neo.22-12-e819.

5. Ranucci G, Della Corte C, Alberti D, Bondioni MP, Boroni G, Calvo PL, et al. Diagnostic approach to neonatal and infantile cholestasis: A position paper by the SIGENP liver disease working group. Digestive and Liver Disease. 2022;54(1):40–53. doi:10.1016/j.dld.2021.09.011.

6. Rougée LRA, Miyagi SJ, Collier AC. Obstetric Obesity is Associated with Neonatal Hyperbilirubinemia with High Prevalence in Native Hawaiians and Pacific Island Women. Hawai‘i Journal of Medicine & Public Health. 2016;75(12):373–378.

7. Özdek S, Kul M, Akcan AB, Çekmez F, Aydemir G, Aydınöz S, et al. The effect of the pre-pregnancy weight of the mother and the gestational weight gain on the bilirubin level of term newborn. Journal of Maternal-Fetal & Neonatal Medicine. 2016;29(15):2434–2437. doi:10.3109/14767058.2015.1086743.

8. Domosud J, Kulik-Rechberger B. Maternal pre-pregnancy BMI and gestational weight gain as risk factors of jaundice in healthy newborns ≥37 weeks of gestation. Journal of Health Inequalities. 2022;8(2):137–144. doi:10.5114/jhi.2022.121530.

9. Lee BK, Le Ray I, Sun JY, Wikman A, Reilly M, Johansson S. Haemolytic and nonhaemolytic neonatal jaundice have different risk factor profiles. Acta Paediatrica. 2016;105(12):1444–1450. doi:10.1111/apa.13470.

10. Lin Q, Zhu D, Chen C, Feng Y, Shen F, Wu Z. Risk factors for neonatal hyperbilirubinemia: a systematic review and meta-analysis. Translational Pediatrics. 2022;11(6):1001–1009. doi:10.21037/tp-22-229.

11. UNICEF. Under-five mortality. UNICEF Data. Updated March 2026. https://data.unicef.org/topic/child-survival/under-five-mortality/

12. UNICEF. Neonatal mortality. UNICEF Data. Updated March 2026. https://data.unicef.org/topic/child-survival/neonatal-mortality/
13. World Health Organization. Obesity and overweight. Fact sheet. 8 December 2025. https://www.who.int/news-room/fact-sheets/detail/obesity-and-overweight
14. Yokoda RT, Rodriguez EA. Review: Pathogenesis of cholestatic liver diseases. World Journal of Hepatology. 2020;12(8):423–435. doi:10.4254/wjh.v12.i8.423.

ISSN: 2181-3337 | SCIENTISTS.UZ

ISSN: 2181-3337 | SCIENTISTS.UZ VOLUME 5 ISSUE 7 JULY 2026

LOCAL MULTIFUNCTIONAL HYDROGEL THERAPY IN EXPERIMENTAL FIBRINOPURULENT PERITONITIS: ANTIBACTERIAL, FIBRINOLYTIC, AND REPARATIVE EFFECTS OF A NOVEL LEVOFLOXACIN-CUCUMAZINE-NA-CMC COMPOSITE

Turakulov Uktamjon[1,4], Mardonov Jamshid[4,5], Ergashev Farhod[2,4], Kurbonova Dilnoza[3], Sadikov Rustam[4,5]

D.M.Sc., associate professor[1,4]
PhD, associate professor[4,5]
Independent researcher[2,4]
medical doctor[3]
D.M.Sc., professor[4,5]
1 - Center for the development of professional qualifications of medical workers (Tashkent, Uzbekistan).
2 - Central hospital of the Kokand city medical association (Kokand, Uzbekistan).
3 - Kokand city infectious diseases hospital (Kokand, Uzbekistan).
4 - Republican Specialized Scientific and Practical Medical Center of Surgery named after Academician V. Vakhidov (Tashkent, Uzbekistan).
5 - Tashkent State Medical University (Tashkent, Uzbekistan).

DOI: 10.67620/sai.57d0008

ABSTRACT

Fibrinopurulent peritonitis (FPP) remains one of the most severe and life-threatening forms of intra-abdominal infection, with mortality rates ranging from 20% to 30% despite substantial advances in surgical source control, antimicrobial therapy, and intensive care management. The formation of extensive fibrinous deposits and bacterial biofilms within the peritoneal cavity creates a physical and biological barrier that significantly impairs the penetration and effectiveness of systemic antimicrobial agents, promotes persistent infection, enhances local inflammatory responses, and contributes to the development of postoperative adhesions and intra-abdominal abscesses. Objective: To develop and experimentally evaluate the therapeutic efficacy, biocompatibility, and reparative potential of a novel multifunctional composite hydrogel containing levofloxacin, cucumazine, and sodium carboxymethylcellulose (LCSC) for local treatment of fibrinopurulent peritonitis. Materials and Methods: The efficacy study was performed on 84 adult white rats with experimentally induced fibrinopurulent peritonitis using a modified distal cecal ligation and puncture (DCLP) model that closely reproduces the clinical and morphological features of diffuse peritonitis in humans. Animals were randomly assigned to three groups: control (saline lavage), levofloxacin (0.1% levofloxacin solution), and experimental (local application of LCSC hydrogel).

ACCEPTED

20.07.26

Keywords:
fibrinopurulent peritonitis, hydrogel, levofloxacin, cucumazine, sodium carboxymethylcellulose, local therapy, fibrinolysis, biofilms, morphology, adhesions, mesothelial regeneration.

CC BY

Clinical, microbiological, histological, and morphometric assessments were performed on postoperative days 3, 7, 14, and 21. The evaluated parameters included mortality, bacterial contamination of peritoneal exudate, adhesion formation, serosal thickness, fibrosis area, inflammatory cell density, and degree of mesothelial epithelialization. Results: Local administration of the LCSC hydrogel resulted in improvements in the evaluated outcomes compared with standard treatment. Mortality decreased from 41.7% in the control group to 8.3% in the experimental group ($p < 0.05$). Bacterial contamination of the peritoneal exudate decreased from 10^5-10^6 CFU/mL to $\leq 10^4$ CFU/mL, while exudate volume was reduced by 30-40%. Morphometric analysis demonstrated a 46% reduction in fibrosis area, a 62% decrease in inflammatory cell infiltration, and an increase in epithelialization from 38 ± 5% to 72 ± 6% ($p < 0.001$). Histological examination revealed accelerated angiogenesis, early maturation of granulation tissue, and restoration of mesothelial integrity; no dense intra-abdominal adhesions were observed by day 21. Conclusions: The newly developed LCSC composite hydrogel demonstrated pronounced antibacterial, fibrinolytic, anti-inflammatory, anti-adhesive, and reparative properties in an experimental model of fibrinopurulent peritonitis. The combination of sustained local antimicrobial delivery, enzymatic fibrin degradation, and promotion of mesothelial regeneration provides a multifactorial pathogenetic effect that may represent a promising strategy for improving the outcomes of local treatment of severe intra-abdominal infections.

Introduction

Fibrinopurulent peritonitis (FPP) remains one of the most challenging and life-threatening complications in emergency abdominal surgery and continues to be associated with considerable morbidity and mortality worldwide. Despite substantial advances in surgical techniques, perioperative intensive care, and antimicrobial therapy, mortality rates in diffuse and generalized forms of peritonitis still range from 20% to 30%, while in patients with severe abdominal sepsis and multiple organ dysfunction syndrome they may exceed 40% [1,2,15-17]. Furthermore, survivors frequently experience serious postoperative complications, including intra-abdominal abscesses, adhesive disease, intestinal fistulas, and recurrent septic episodes, which can prolong hospitalization [13,19-25].

The pathogenesis of fibrinopurulent peritonitis is multifactorial and involves a complex interaction between microbial invasion, systemic inflammatory response syndrome (SIRS), microcirculatory dysfunction, and impaired local immune defense mechanisms [11,15,16]. One of the central morphological and pathogenetic events during the progression of peritonitis is the formation of extensive fibrinous deposits on the serosal surfaces of abdominal organs [11,14]. Initially, fibrin deposition serves as a protective mechanism aimed at localizing the infectious process and limiting bacterial dissemination within the abdominal cavity. However, persistent fibrin accumulation subsequently creates a favorable microenvironment for bacterial colonization, biofilm formation, and chronic inflammation [4,5,12].

Bacterial biofilms formed on fibrin matrices represent highly organized three-dimensional microbial communities embedded within an extracellular polymeric substance that protects microorganisms from host immune responses and antimicrobial agents [4-6,12,18]. Numerous studies have demonstrated that bacteria residing within biofilms exhibit antibiotic resistance levels that are 100 to 1000 times greater than those of planktonic bacterial forms [4,5,12]. Consequently, systemic antibiotic therapy often fails to achieve adequate drug concentrations within the infected fibrinous microenvironment,

ISSN: 2181-3337 | SCIENTISTS.UZ

resulting in persistent infection, abscess formation, delayed tissue repair, and adhesion development [11,15].

The limitations of conventional treatment strategies have stimulated increasing interest in local therapeutic approaches capable of directly targeting the pathological substrate of fibrinopurulent inflammation [11]. Current concepts of local therapy emphasize the necessity of combining several pathogenetically important mechanisms, including enzymatic degradation of fibrin deposits, suppression of bacterial growth, adsorption of inflammatory mediators and tissue degradation products, and stimulation of mesothelial regeneration [6,8]. Such multifunctional therapeutic systems may simultaneously address several key components of peritoneal inflammation that remain inaccessible to systemic treatment alone.

Hydrogel-based drug delivery systems have emerged as one of the most promising directions in modern abdominal surgery and regenerative medicine [8-10]. Biocompatible polymers such as sodium carboxymethylcellulose (Na-CMC) and chitosan can form biodegradable matrices that provide sustained release of active compounds and may act as temporary physical barriers between injured surfaces [8,9,19,20]. Experimental and clinical studies have demonstrated that local hydrogel formulations may significantly improve antimicrobial efficacy, accelerate tissue regeneration, and reduce postoperative complications in purulent-inflammatory conditions [7-10].

Based on these considerations, a novel multifunctional composite hydrogel consisting of levofloxacin, cucumazine, and sodium carboxymethylcellulose (LCSC) was developed. The rationale behind this formulation was to combine prolonged local antibacterial activity provided by levofloxacin with the fibrinolytic properties of cucumazine and the biocompatible controlled-release matrix formed by Na-CMC [7,8]. Such a combination was expected to provide antibacterial, fibrinolytic, anti-inflammatory, anti-adhesive, and reparative effects within the peritoneal cavity.

The present study aimed to develop and experimentally evaluate the effectiveness of the LCSC composite hydrogel in the treatment of fibrinopurulent peritonitis using a clinically relevant modified distal cecal ligation and puncture (DCLP) model. Particular attention was paid to the assessment of mortality, bacterial contamination, adhesion formation, histological dynamics of peritoneal healing, and morphometric indicators of tissue repair in order to determine the therapeutic potential of this novel local treatment strategy.

MATERIALS AND METHODS

Study Design and Experimental Setting

This experimental study was conducted at the Department of Experimental Surgery and the Laboratory of Pathomorphology of the Republican Specialized Scientific and Practical Medical Center of Surgery named after Academician V. Vakhidov, Tashkent, Uzbekistan, between 2024 and 2025. The study was designed to evaluate the fibrinolytic activity, biocompatibility, antibacterial efficacy, and reparative potential of a newly developed multifunctional hydrogel composed of levofloxacin, cucumazine, and sodium carboxymethylcellulose (LCSC) in experimental fibrinopurulent peritonitis.

Ethical Approval

All experimental procedures involving laboratory animals were performed in accordance with the European Convention for the Protection of Vertebrate Animals Used for Experimental and Other Scientific Purposes (Strasbourg, 1986) and international guidelines for animal welfare and biomedical research. The study protocol was reviewed and approved by the Local Ethics Committee of the Republican Specialized Scientific and Practical Medical Center of Surgery named after Academician V. Vakhidov.

Experimental Animals

The study included 92 adult outbred white rats of both sexes. Of these, 84 underwent induction of fibrinopurulent peritonitis and eight intact rats were used for the biocompatibility assessment. The animals were aged 8-12 weeks and weighed between 220 and 250 g. Animals were housed under standard vivarium conditions with a controlled temperature of 21-23°C, relative humidity of 50-60%, and a 12-hour light/dark

ISSN: 2181-3337 | SCIENTISTS.UZ

cycle. Standard laboratory chow and water were provided ad libitum throughout the experiment. Prior to the study, all animals underwent a seven-day acclimatization period.

Experimental Groups

The animals were randomly assigned to three equal groups consisting of 28 animals each:

1. **Control group (n=28):** Peritoneal lavage with warmed isotonic saline solution only.
2. **Levofloxacin group (n=28):** Peritoneal lavage followed by intraperitoneal instillation of 0.1% levofloxacin solution.
3. **LCSC group (n=28):** Peritoneal lavage followed by local application of the composite hydrogel containing levofloxacin (0.5%), cucumazine (0.01%), and sodium carboxymethylcellulose (Na-CMC) as a polymeric carrier matrix.

In addition, an independent biocompatibility group consisting of eight intact animals received intraperitoneal administration of the LCSC gel without induction of peritonitis to evaluate local tolerance and possible toxic effects.

Preparation of the LCSC Hydrogel

The LCSC hydrogel was developed as a multifunctional local therapeutic formulation combining antimicrobial, fibrinolytic, and reparative activities. The preparation consisted of:

- levofloxacin - 0.5%;
- cucumazine - 0.01%;
- sodium carboxymethylcellulose (Na-CMC) as a biodegradable polymeric matrix.

Levofloxacin served as a broad-spectrum antimicrobial agent, cucumazine provided proteolytic and fibrinolytic activity facilitating degradation of fibrin deposits and bacterial biofilms, while Na-CMC ensured prolonged local retention and controlled release of active components within the peritoneal cavity.

In Vitro Evaluation of Fibrinolytic Activity

The fibrinolytic activity of the hydrogel was evaluated using human fibrin clots obtained from freshly coagulated venous blood. After centrifugation at 3,000 rpm for five minutes, fibrin clots were washed with isotonic saline and divided into fragments weighing approximately 40 mg each.

Four experimental conditions were studied:

- control (saline only);
- LCSC gel containing 2 U of cucumazine;
- LCSC gel containing 5 U of cucumazine;
- LCSC gel containing 10 U of cucumazine.

Samples were incubated in 2 mL of physiological saline at 37°C, and clot weight was measured every 15 minutes for 240 minutes. Visual assessment of fragmentation and liquefaction was additionally performed.

Experimental Model of Fibrinopurulent Peritonitis

Fibrinopurulent peritonitis was induced using a modified distal cecal ligation and puncture (DCLP) technique based on the model originally described by Singleton and Wischmeyer [26]. Under inhalational anesthesia with sevoflurane vapor, a midline laparotomy measuring 2.5-3 cm was performed.

A distal 1-cm segment of the cecum was ligated together with its vascular supply to induce ischemia. Subsequently, the cecal wall was punctured twice using a sterile 0.6-mm needle, allowing controlled leakage of fecal contents into the abdominal cavity. The abdominal wall was closed in two layers using Vicryl and Prolene sutures.

This model provided reproducible induction of progressive fibrinopurulent peritonitis closely resembling the clinical course of diffuse peritonitis in humans.

Treatment Protocol

Following induction of peritonitis and abdominal lavage, the corresponding treatment protocol was applied according to group allocation.

ISSN: 2181-3337 | SCIENTISTS.UZ

The LCSC hydrogel was administered locally into the peritoneal cavity during the early toxic phase of inflammation, when fibrin deposition and purulent exudation became macroscopically evident. The hydrogel was distributed evenly over affected serosal surfaces to ensure prolonged contact with the inflammatory substrate.

Clinical Evaluation

Animals were monitored daily for (Figure 1):

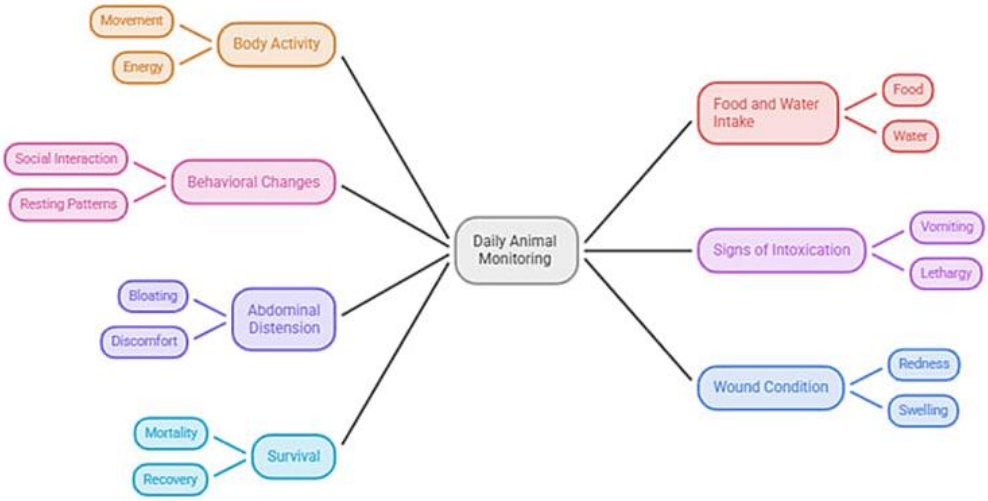


Figure 1. Daily animal monitoring parameters

Mortality was recorded throughout the observation period and analyzed as one of the primary outcome measures.

Macroscopic Assessment

At necropsy, the following parameters were evaluated:

- volume and character of peritoneal exudate;
- extent of fibrin deposition;
- severity of adhesions;
- presence of abscesses;
- intestinal distension and paralysis;
- restoration of anatomical relationships between abdominal organs.

Observations were performed on postoperative days 3, 7, 14, and 21.

Histological and Morphometric Analysis

Samples of peritoneum, omentum, and intestinal loops were fixed in 10% neutral buffered formalin, embedded in paraffin, sectioned at 4-5 μm, and stained with hematoxylin and eosin.

Microscopic examination was performed using a DN-300M light microscope equipped with a digital imaging system. Morphometric measurements were obtained using ImageJ software.

The following parameters were evaluated:

- serosal thickness (μm);
- fibrosis area (mm^2);
- inflammatory cell density (cells per high-power field);
- epithelialization index (%).

Measurements were performed in ten randomly selected microscopic fields at magnifications of ×200 and ×400.

ISSN: 2181-3337 | SCIENTISTS.UZ

Microbiological Analysis

Peritoneal exudate samples were collected aseptically and cultured to determine bacterial contamination levels expressed as colony-forming units per milliliter (CFU/mL). Quantitative bacterial load was compared between groups during the observation period.

Statistical Analysis

Statistical analysis was performed using standard biomedical statistical methods. Continuous variables were expressed as mean ± standard error of the mean (mean ± SEM). Intergroup comparisons were performed using Student's t-test. Differences were considered statistically significant at $\mathbf{p < 0.05}$. Statistical calculations were performed using standard statistical software packages.

RESULTS

In Vitro Fibrinolytic Activity of the LCSC Hydrogel

One of the principal objectives in the development of the LCSC hydrogel was to provide not only effective local antibacterial activity but also targeted fibrinolytic action against fibrin deposits, which represent a major structural component of fibrinopurulent peritonitis and a critical substrate for bacterial biofilm formation. Therefore, the first stage of the investigation involved an in vitro assessment of the fibrinolytic properties of the developed formulation.

The experiments demonstrated a clear dose-dependent fibrinolytic activity of cucumazine incorporated into the hydrogel matrix (Table 1, Figure 2). The most pronounced fibrin degradation was observed in the formulation containing 10 U of cucumazine, where the fibrin clot mass decreased from 52.7 ± 1.2 mg to 25.2 ± 1.3 mg after 120 minutes of incubation, corresponding to a reduction of approximately 52.2% ($p < 0.001$ versus control).

The formulation containing 5 U of cucumazine produced a moderate but significant effect, reducing clot mass by 42.3% ($p < 0.01$ versus control), whereas the 2 U formulation demonstrated a weaker but still measurable fibrinolytic response with a reduction of 20.4% ($p < 0.05$ versus control).

In contrast, control samples exposed to physiological saline alone showed only a minimal decrease in clot mass (10.2%), which was attributable to physiological clot retraction processes rather than enzymatic fibrinolysis.

Table 1.

Dose-dependent fibrinolytic activity of the LCSC hydrogel in vitro

Group	Initial clot mass (mg)	120 min (mg)	Reduction (%)
Control	50.2 ± 1.3	45.1 ± 1.4	10.2
LCSC + 2 U cucumazine	51.9 ± 1.6	41.3 ± 1.6	20.4
LCSC + 5 U cucumazine	52.3 ± 1.4	30.2 ± 1.2	42.3
LCSC + 10 U cucumazine	52.7 ± 1.2	25.2 ± 1.3	52.2

ISSN: 2181-3337 | SCIENTISTS.UZ

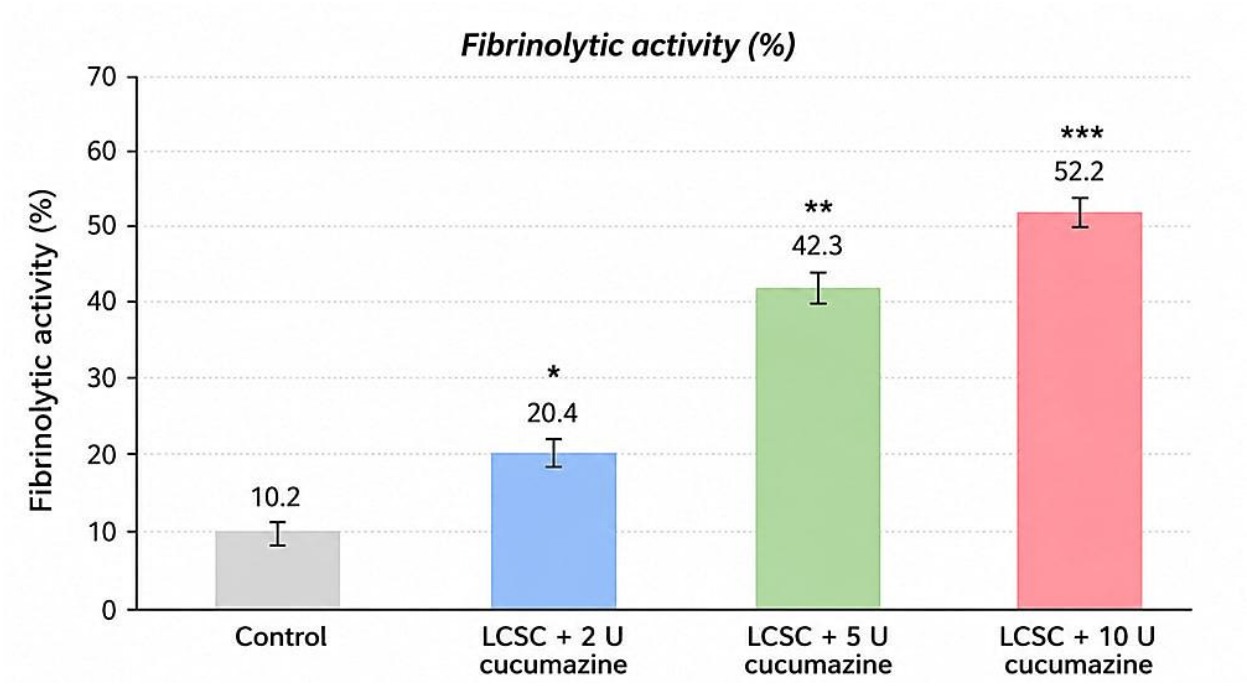


Figure 2. Dose-dependent fibrinolytic activity of the LCSC hydrogel in vitro. Data are presented as mean ± standard deviation (SD). *p < 0.05, **p < 0.01, ***p < 0.001 versus control.

These findings confirmed that the enzymatic component retained its biological activity after incorporation into the hydrogel matrix and provided effective degradation of fibrin structures under physiological conditions. Furthermore, the observed dose-dependent response supports the potential use of cucumazine as a local fibrinolytic agent for disrupting fibrin barriers and improving antimicrobial penetration into infected peritoneal tissues.

Biocompatibility of the LCSC Hydrogel

The safety profile of the developed formulation was evaluated in a separate group of intact animals receiving intraperitoneal administration of the hydrogel without induction of peritonitis.

During the entire observation period, no mortality, behavioral abnormalities, feeding disturbances, or signs of abdominal discomfort were observed. Macroscopic examination revealed no evidence of inflammatory reactions, serosal irritation, fibrin deposition, or adhesion formation. Histological assessment confirmed preservation of normal mesothelial architecture without inflammatory infiltration or vascular disturbances.

These findings demonstrated no detectable local toxicity under the study conditions, supporting further evaluation of the formulation in pathological conditions.

Clinical Course of Experimental Fibrinopurulent Peritonitis

The modified DCLP model produced highly reproducible progressive fibrinopurulent peritonitis closely resembling the clinical course of diffuse peritonitis in humans.

Day 1. Animals remained relatively active despite mild anorexia and decreased mobility. Laparotomy revealed localized inflammatory infiltration surrounding the ischemic cecal segment without evidence of diffuse contamination or generalized inflammation. These findings corresponded to the reactive phase of peritonitis.

Day 3. Signs of systemic intoxication became evident, including reduced activity, rough fur, and diminished responses to external stimuli. Macroscopically, inflammatory infiltrates involved approximately one-third of the intestinal loops and were associated with fibrin deposits and limited purulent exudation. Omental involvement and initial diffuse inflammatory changes became apparent (Figure 3A).

ISSN: 2181-3337 | SCIENTISTS.UZ



Figure 3A. Macroscopic appearance of experimental fibrinopurulent peritonitis on postoperative day 3 showing localized fibrin deposition and inflammatory infiltration of intestinal loops.

Day 4. Progressive abdominal distension, anorexia, and behavioral suppression were observed. Laparotomy demonstrated increasing exudate volume, diffuse hyperemia, vascular congestion, and loss of normal serosal transparency, indicating transition to the toxic phase of peritonitis.

Days 5-7. Animals developed severe intoxication characterized by tachypnea, dehydration, and complete loss of appetite. The abdominal cavity contained abundant foul-smelling purulent exudate associated with extensive fibrin deposits, intestinal paralysis, and multiple intra-abdominal abscesses. Mortality reached approximately 30% during this period (Figure 3B).



Figure 3B. Advanced fibrinopurulent peritonitis on postoperative day 7 characterized by diffuse fibrin deposits, purulent exudate, intestinal edema, and multiple intra-abdominal abscesses.

Clinical Efficacy of LCSC Therapy

Local administration of the LCSC hydrogel significantly improved survival and clinical outcomes compared with standard treatment protocols (Table 2, Figure 3C).

Mortality decreased significantly from 41.7% in the control group to 8.3% in LCSC-treated animals, corresponding to an approximately fivefold reduction in lethality ($p < 0.05$). Furthermore, treated animals demonstrated earlier recovery of spontaneous activity and feeding behavior, with normalization occurring approximately 2-3 days earlier than in untreated controls.

Table 2.

Clinical outcomes following treatment

Parameter	Control	LCSC group
Mortality	41.7%	8.3%
Adhesions	41.7%	0%
Exudate reduction	-	30-40%
Recovery acceleration	-	2-3 days

ISSN: 2181-3337 | SCIENTISTS.UZ

The incidence of postoperative adhesions was reduced from 41.7% in the control group to 0% following LCSC treatment ($p < 0.05$). In addition, the volume of inflammatory exudate decreased by 30-40%, while the severity of systemic intoxication was markedly attenuated.

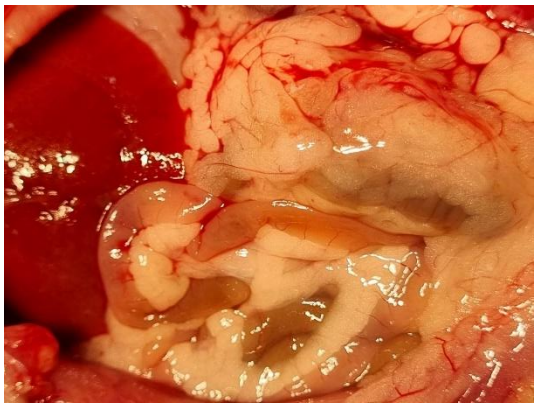


Figure 3C. Macroscopic appearance of the abdominal cavity following LCSC treatment demonstrating marked reduction of exudate, fibrin deposits, and inflammatory changes (Experimental group. Postoperative day 3).

Macroscopic examination of the abdominal cavity demonstrated a substantial reduction in fibrin deposits, inflammatory exudate, intestinal edema, and diffuse inflammatory changes in the experimental group compared with untreated animals (Figure 3C).

Comparative efficacy of local treatment strategies

To determine whether the observed therapeutic effects were attributable solely to local antibiotic administration or to the combined action of the composite hydrogel components, a comparative analysis between the control, levofloxacin, and LCSC groups was performed (Table 3).

Although local levofloxacin treatment resulted in moderate improvements in microbiological and inflammatory parameters, the LCSC hydrogel demonstrated greater improvements across the evaluated outcomes.

Mortality decreased from 41.7% in the control group to 25.0% in the levofloxacin group and further to 8.3% following LCSC treatment ($p < 0.05$). Similarly, bacterial contamination of peritoneal exudate decreased from 10^5-10^6 CFU/mL in untreated animals to 10^4-10^5 CFU/mL in the levofloxacin group and to $\leq 10^4$ CFU/mL in the LCSC group ($p < 0.01$).

The incidence of dense intra-abdominal adhesions decreased from 41.7% in controls to 16.7% after local levofloxacin administration and was not observed in animals treated with the LCSC hydrogel ($p < 0.05$).

Morphometric analysis demonstrated progressive improvements across treatment groups. Serosal thickness decreased from 980 ± 38 μm in controls to 900 ± 36 μm in the levofloxacin group and to 820 ± 35 μm following LCSC therapy ($p < 0.001$). Similarly, fibrosis area was reduced from 2.8 ± 0.2 mm² to 2.1 ± 0.2 mm² and 1.5 ± 0.1 mm², respectively ($p < 0.01$), while inflammatory cell density decreased from 52 ± 4 cells/HPF to 34 ± 3 cells/HPF and 20 ± 2 cells/HPF ($p < 0.001$).

In contrast, mesothelial epithelialization progressively increased from 38 ± 5% in untreated animals to 56 ± 5% following levofloxacin treatment and reached 72 ± 6% in the LCSC group ($p < 0.001$).

ISSN: 2181-3337 | SCIENTISTS.UZ

Table 3.

Comparative efficacy of different local treatment strategies in experimental fibrinopurulent peritonitis

Parameter	Control	Levofloxacin	LCSC Hydrogel	p-value
Mortality (%)	41.7	25.0	8.3	<0.05
Bacterial contamination (CFU/mL)	10^5-10^6	10^4-10^5	$\leq 10^4$	<0.01
Dense adhesions (%)	41.7	16.7	0	<0.05
Exudate volume reduction (%)	-	15-20	30-40	<0.05
Recovery acceleration (days)	-	1-2	2-3	<0.05
Serosal thickness (μm)	980 ± 38	900 ± 36	820 ± 35	<0.001
Fibrosis area (mm^2)	2.8 ± 0.2	2.1 ± 0.2	1.5 ± 0.1	<0.01
Inflammatory cells/HPF	52 ± 4	34 ± 3	20 ± 2	<0.001
Epithelialization (%)	38 ± 5	56 ± 5	72 ± 6	<0.001

The comparative analysis demonstrated that although local levofloxacin administration improved bacterial control and partially reduced inflammatory activity, the multifunctional LCSC hydrogel produced greater therapeutic benefits. These findings indicate that the superior outcomes observed in the experimental group were attributable not only to antimicrobial activity but also to the combined fibrinolytic, anti-adhesive, and reparative effects provided by cucumazine and the Na-CMC hydrogel matrix.

Microbiological Findings

Quantitative microbiological analysis demonstrated a substantial reduction in bacterial contamination within the peritoneal cavity following local hydrogel treatment (Table 4).

In untreated animals, bacterial contamination remained high throughout the observation period, reaching concentrations of 10^5-10^6 CFU/mL by postoperative day 7. Local administration of levofloxacin reduced bacterial counts to approximately 10^4-10^5 CFU/mL, whereas animals treated with the LCSC hydrogel exhibited bacterial loads not exceeding 10^4 CFU/mL, corresponding to at least a tenfold reduction in microbial burden compared with untreated controls ($p < 0.01$).

These findings indicate that the sustained local release of levofloxacin from the Na-CMC matrix, combined with enzymatic disruption of fibrin barriers by cucumazine, significantly enhanced antibacterial efficacy within the infected peritoneal cavity.

Table 4.

Bacterial contamination of peritoneal exudate

Group	Bacterial load (CFU/mL)
Control	10^5-10^6
Levofloxacin	10^4-10^5
LCSC	$\leq 10^4$

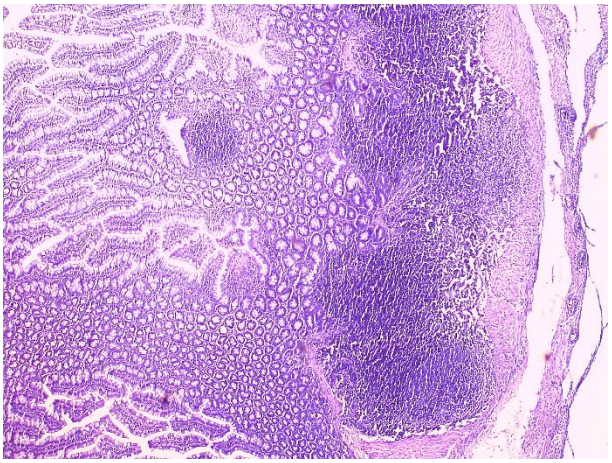
ISSN: 2181-3337 | SCIENTISTS.UZ

The microbiological findings suggest that the superior antibacterial effect of the LCSC hydrogel was not solely attributable to local antibiotic administration but also to improved penetration of antimicrobial agents following enzymatic fibrinolysis and disruption of bacterial biofilm-associated fibrin matrices.

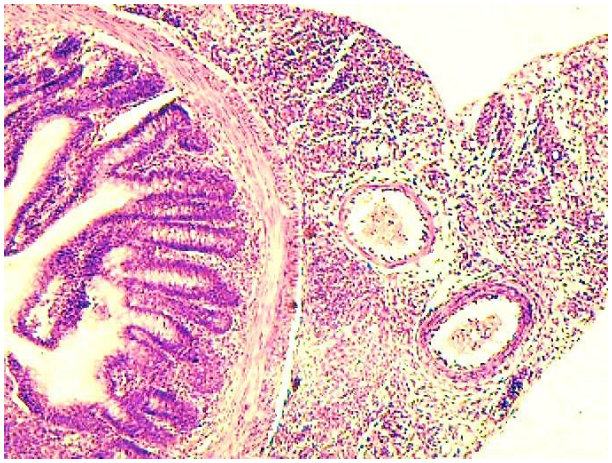
Morphological Findings

Histological examination demonstrated substantial differences in the dynamics of peritoneal tissue repair between the control and LCSC-treated groups (Figures 4-7).

Postoperative Day 3. On postoperative day 3, control animals exhibited extensive fibrinopurulent exudation characterized by diffuse neutrophilic infiltration, mesothelial destruction, vascular congestion, and early fibroblast proliferation (Figure 4A). In contrast, LCSC-treated animals demonstrated significantly thinner fibrin deposits, predominance of macrophages over neutrophils, and early development of granulation tissue (Figure 4B), indicating attenuation of the acute inflammatory response and initiation of reparative processes.



A: Control group demonstrating extensive fibrin deposition, diffuse neutrophilic infiltration, vascular congestion, and mesothelial destruction. Hematoxylin and eosin staining, ×100.



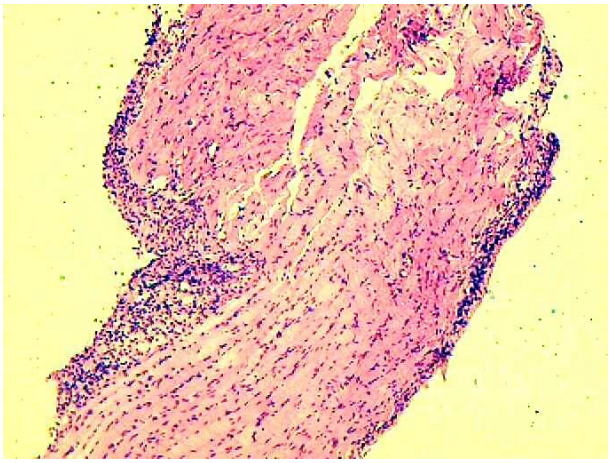
B: LCSC-treated group showing reduced inflammatory infiltration and early granulation tissue formation. H&E, ×100.

Figure 4. Representative histological sections on postoperative day 3.

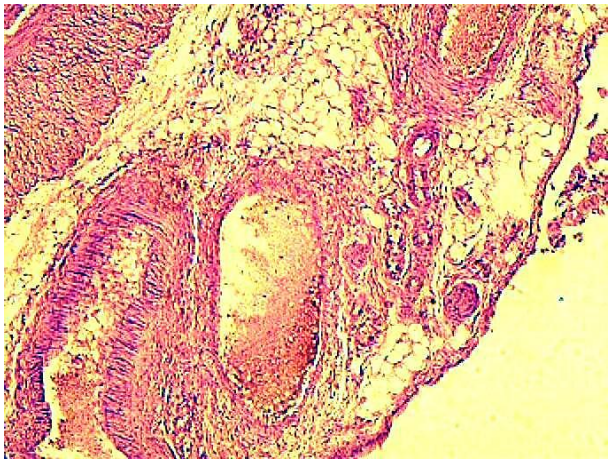
Postoperative Day 7. By postoperative day 7, control specimens continued to demonstrate extensive inflammatory infiltration and disorganized immature connective tissue. Conversely, LCSC-treated tissues exhibited active angiogenesis, orderly fibroblast orientation, and early mesothelial regeneration, suggesting accelerated maturation of reparative tissue and improved organization of the healing process.

Postoperative Day 14. On postoperative day 14, mature granulation tissue with well-developed capillary networks and regularly oriented collagen fibers predominated in the LCSC group (Figure 5B). Nearly complete restoration of the mesothelial lining was observed, whereas control animals continued to exhibit chronic inflammatory infiltration and progressive fibrosis (Figure 5A).

ISSN: 2181-3337 | SCIENTISTS.UZ



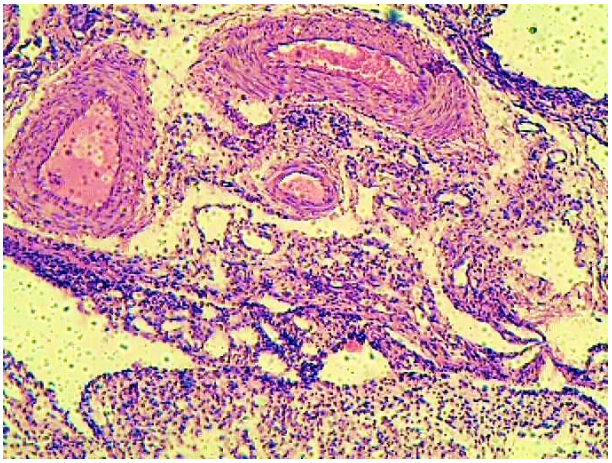
A: Chronic inflammatory changes and fibrosis in controls. H&E, ×100.



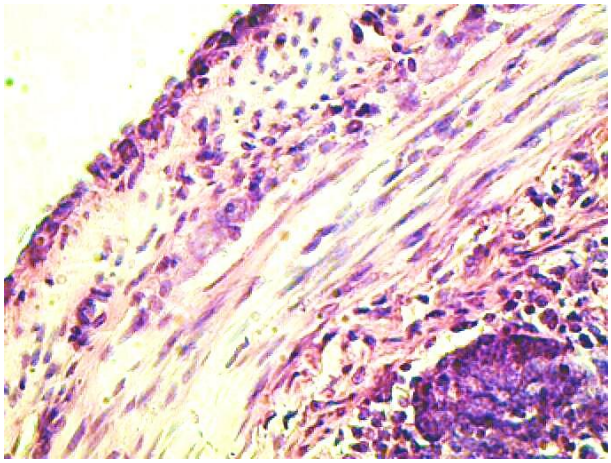
B: Mature granulation tissue and advanced mesothelial regeneration in the LCSC-treated animals. H&E, ×200.

Figure 5. Histological appearance on postoperative day 14.

Postoperative Day 21. By postoperative day 21, control animals developed dense fibrous adhesions and scar formation associated with incomplete epithelial recovery (Figure 6A). In contrast, the LCSC group demonstrated complete mesothelial regeneration, restoration of normal vascular architecture, and absence of inflammatory infiltrates or adhesions (Figure 6B). Histologically, the peritoneal surface closely resembled that of healthy animals.



A: Dense fibrous adhesions and incomplete epithelial recovery in controls. H&E, ×100.



B: Complete mesothelial restoration and normal peritoneal architecture in the LCSC group. H&E, ×200.

Figure 6. Histological appearance on postoperative day 21.

Collectively, the histological findings demonstrated that local administration of the LCSC hydrogel significantly accelerated the transition from the inflammatory phase to the reparative phase of healing, promoted early mesothelial regeneration, reduced fibrosis, and no adhesions were observed within the peritoneal cavity.

Morphometric Analysis

Quantitative morphometric analysis objectively confirmed the histological findings and demonstrated significant improvements in peritoneal healing following LCSC treatment (Table 5, Figure 7).

ISSN: 2181-3337 | SCIENTISTS.UZ

Table 5.

Morphometric parameters after treatment

Parameter	Control	LCSC	p-value
Serosal thickness (μm)	980 ± 38	820 ± 35	<0.001
Fibrosis area (mm²)	2.8 ± 0.2	1.5 ± 0.1	<0.01
Inflammatory cells/HPF	52 ± 4	20 ± 2	<0.001
Epithelialization (%)	38 ± 5	72 ± 6	<0.001

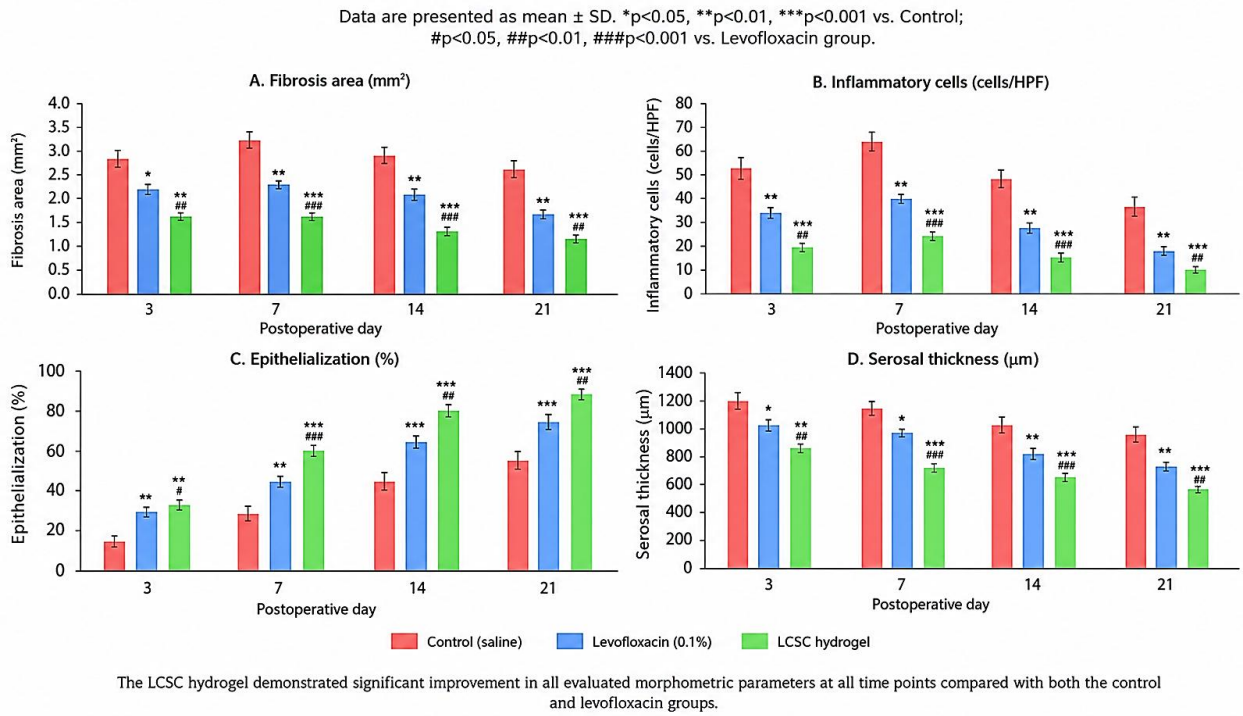


Figure 7. Comparative morphometric parameters of peritoneal healing following local treatment of experimental fibrinopurulent peritonitis. ***(A)*** Fibrosis area (mm²); ***(B)*** Inflammatory cell density (cells/high-power field, HPF); ***(C)*** Degree of mesothelial epithelialization (%); and ***(D)*** Serosal thickness (μm). Data are presented as mean ± standard deviation (SD). *p < 0.05, **p < 0.01, ***p < 0.001 versus the control group; #p < 0.05, ##p < 0.01, ###p < 0.001 versus the Levofloxacin group.

Compared with the control group, animals treated with the LCSC hydrogel exhibited a significant reduction in serosal thickness from 980 ± 38 μm to 820 ± 35 μm ($p < 0.001$), indicating attenuation of inflammatory edema and restoration of normal peritoneal architecture.

Similarly, the fibrosis area decreased by 46%, from 2.8 ± 0.2 mm² in controls to 1.5 ± 0.1 mm² in the LCSC group ($p < 0.01$). The density of inflammatory cells was reduced from 52 ± 4 cells/HPF to 20 ± 2 cells/HPF, corresponding to a 62% decrease in inflammatory infiltration ($p < 0.001$).

In contrast, mesothelial epithelialization increased significantly from 38 ± 5% in untreated animals to 72 ± 6% following hydrogel administration ($p < 0.001$), indicating accelerated regeneration of the peritoneal surface.

These quantitative findings support the pronounced anti-inflammatory, anti-fibrotic, and reparative effects of the LCSC hydrogel in experimental fibrinopurulent peritonitis (Table 5, Figure 7).

DISCUSSION

The present study demonstrates that local administration of the newly developed levofloxacin-cucumazine-sodium carboxymethylcellulose (LCSC) hydrogel provides a significant therapeutic advantage in the management of experimental fibrinopurulent peritonitis by simultaneously targeting several key pathogenetic mechanisms involved in the progression of intra-abdominal infection. The

obtained results indicate that the combination of prolonged local antimicrobial delivery, enzymatic fibrin degradation, suppression of inflammatory activity, and stimulation of mesothelial regeneration contributes to substantial improvements in both clinical and morphological outcomes (Tables 3-5, Figures 3-7).

Fibrin deposition is recognized as one of the earliest and most important protective responses of the peritoneum during bacterial contamination of the abdominal cavity [19,20]. Initially, fibrin formation serves to localize the infectious process and limit microbial dissemination. However, persistent fibrin accumulation subsequently becomes a major pathogenic factor contributing to the development of bacterial biofilms, chronic inflammation, impaired tissue repair, and adhesion formation [4,5,19,20]. Biofilm-associated matrices can limit antimicrobial penetration into infected tissues, thereby reducing treatment efficacy and facilitating microbial persistence [4,5,18].

Previous experimental and clinical studies have demonstrated that bacteria embedded within biofilms exhibit resistance to antimicrobial agents that may exceed that of planktonic bacteria by several hundred-fold [4-6,12,18]. Consequently, even high-dose systemic antibiotic therapy frequently fails to eradicate microorganisms located within biofilm-associated material and necrotic tissue fragments [4,12]. This phenomenon explains the persistent incidence of postoperative abscesses, recurrent infections, and adhesive complications despite apparently adequate antimicrobial treatment and surgical source control [15-17,19,20].

The concept underlying the development of the LCSC hydrogel was based on overcoming these limitations through simultaneous local intervention at multiple stages of the pathological process. The antibacterial component, levofloxacin, provides broad-spectrum antimicrobial activity directly within the inflammatory focus, achieving local concentrations substantially higher than those attainable through systemic administration without increasing systemic toxicity [7,8]. This mechanism likely explains the at least a tenfold reduction in bacterial contamination observed in the experimental group (Table 4) as well as the significant reduction in mortality and adhesion formation (Table 3).

Importantly, although local administration of levofloxacin alone improved microbiological and inflammatory parameters, its therapeutic effects remained consistently inferior to those achieved with the multifunctional LCSC hydrogel (Table 3). This finding indicates that the superior outcomes observed in the experimental group cannot be attributed solely to local antibiotic delivery but rather to the combined antimicrobial, fibrinolytic, anti-adhesive, and reparative effects.

The second essential component of the formulation is cucumazine, a proteolytic enzyme possessing fibrinolytic activity. The in vitro experiments demonstrated a clear dose-dependent ability of cucumazine to induce fibrin degradation (Table 1, Figure 2), with the highest concentration resulting in more than a 50% reduction in clot mass within two hours of incubation. These findings strongly support the hypothesis that local enzymatic destruction of fibrin deposits may improve antibiotic penetration, reduce bacterial protection within biofilms, and facilitate physiological clearance mechanisms [6,12]. The rapid disappearance of fibrin deposits and absence of dense adhesions in the treated animals (Table 3, Figure 3C) provide further in vivo confirmation of this mechanism.

The role of sodium carboxymethylcellulose as a polymeric matrix should also be emphasized. In addition to functioning as a biocompatible carrier system for active substances, Na-CMC provides prolonged retention of therapeutic components at the site of inflammation and creates a temporary protective barrier over damaged serosal surfaces [8-10]. Such local retention may be particularly important during the early phases of peritoneal inflammation, when exudation, fibrin formation, and bacterial proliferation occur most intensively. Furthermore, temporary physical barriers may contribute to adhesion prevention by mechanically separating injured serosal surfaces during the critical phases of peritoneal healing [3,19-21].

One of the most important findings of the present study is the marked improvement in reparative processes within the peritoneum. Histological analysis demonstrated accelerated angiogenesis, earlier

ISSN: 2181-3337 | SCIENTISTS.UZ

maturation of granulation tissue, and rapid restoration of mesothelial integrity in animals treated with the LCSC hydrogel (Figures 5-7). By postoperative day 14, nearly complete mesothelial recovery was observed in the experimental group (Figure 5B), whereas control animals continued to exhibit chronic inflammatory infiltration and active fibrosis (Figure 5A). By day 21, treated animals demonstrated complete restoration of normal peritoneal architecture without evidence of pathological adhesions or residual inflammation (Figure 6B).

The morphometric findings objectively confirmed these histological observations (Table 5, Figure 7). The 46% reduction in fibrosis area, 62% decrease in inflammatory cell infiltration, and nearly twofold increase in epithelialization provide quantitative evidence supporting the histological findings and indicate a profound influence of the hydrogel on tissue remodeling and regeneration.

The anti-adhesive effect observed in this study deserves particular attention. Adhesive disease remains one of the most common long-term complications following diffuse peritonitis and abdominal surgery, with reported incidences ranging from 40% to 60% [3,19-25]. Adhesions are responsible for a substantial proportion of postoperative bowel obstructions, chronic abdominal pain syndromes, infertility, and repeated surgical interventions [20-25]. In the present investigation, dense adhesions developed in 41.7% of untreated animals, whereas no dense adhesions were observed following LCSC treatment (Table 3). This finding suggests that simultaneous fibrin degradation and mesothelial preservation may be substantially more effective than mechanical anti-adhesion barriers alone [14,19,21].

The reduction in mortality from 41.7% to 8.3% represents perhaps the most clinically relevant outcome of the study (Table 3). Mortality in diffuse peritonitis is determined not only by bacterial contamination but also by the severity of systemic inflammatory response syndrome, endotoxemia, and multiple organ dysfunction [1,2,15-17]. By reducing bacterial burden, accelerating elimination of fibrinous exudates, and limiting the duration of local inflammation, the LCSC hydrogel appears to influence several determinants of survival simultaneously.

Several limitations of the study should be acknowledged. First, the investigation was conducted exclusively in an experimental animal model and therefore cannot fully reproduce the complexity of human diffuse peritonitis [15,16]. Second, the study focused primarily on morphological and microbiological outcomes without detailed assessment of cytokine profiles or molecular pathways involved in inflammation and tissue repair. Third, long-term evaluation beyond 21 days was not performed, which limits conclusions regarding very late adhesive complications or chronic inflammatory changes.

Despite these limitations, the present findings provide experimental evidence supporting the use of multifunctional local hydrogel systems in the treatment of severe intra-abdominal infections [8-10]. The combination of antimicrobial, fibrinolytic, anti-inflammatory, anti-adhesive, and reparative effects within a single formulation represents a promising direction in modern abdominal surgery and may contribute to improved outcomes in patients with complicated peritonitis.

The results of this study suggest that the LCSC hydrogel should be considered not merely as a local antimicrobial carrier but as a pathogenetically oriented therapeutic platform capable of modifying the biological environment of the inflamed peritoneal cavity and promoting physiological tissue recovery. Such an approach may represent an important step toward the development of next-generation local treatment strategies for fibrinopurulent peritonitis and other severe purulent-inflammatory diseases of the abdominal cavity.

CONCLUSIONS

1. The modified distal cecal ligation and puncture (DCLP) model demonstrated high reproducibility and reliably reproduced the principal clinical, microbiological, and morphological features of fibrinopurulent peritonitis, including extensive fibrin deposition, purulent exudation, bacterial contamination, and progressive systemic intoxication.

ISSN: 2181-3337 | SCIENTISTS.UZ

2. The newly developed levofloxacin-cucumazine-sodium carboxymethylcellulose (LCSC) hydrogel exhibited pronounced dose-dependent fibrinolytic activity in vitro and was associated with reduced fibrin deposits in vivo, supporting improved local sanitation of the inflammatory focus (Table 1, Figure 2).

3. Local administration of the LCSC hydrogel significantly improved clinical outcomes, reducing mortality from 41.7% to 8.3%, decreasing exudate volume by 30-40%, and accelerating recovery of spontaneous activity and feeding behavior by approximately 2-3 days compared with untreated controls (Tables 2 and 3, Figure 3C).

4. The hydrogel demonstrated substantial antimicrobial efficacy, reducing bacterial contamination of peritoneal exudate from 10^5-10^6 CFU/mL to $\leq 10^4$ CFU/mL, corresponding to at least a tenfold reduction in microbial burden (Table 4).

5. Morphological and morphometric analyses demonstrated marked acceleration of reparative processes, including a 46% reduction in fibrosis area, a 62% decrease in inflammatory cell infiltration, enhancement of mesothelial epithelialization, and no dense intra-abdominal adhesions observed by postoperative day 21 (Figures 4-6, Table 5, Figure 7).

6. The LCSC hydrogel demonstrated no detectable local toxic effects under the study conditions, supporting further preclinical investigation for severe intra-abdominal infections.

REFERENCES

38. Sartelli M, Coccolini F, Kluger Y, Abu-Zidan FM, Ansaloni L, Bala M, et al. WSES/GAIS/SIS-E/WSIS/AAST global clinical pathways for patients with intra-abdominal infections. World J Emerg Surg. 2021;16:49.
39. Ceresoli M, Coccolini F, Fugazzola P, Tomasoni M, Sartelli M, Catena F. Enhanced perioperative care in emergency general surgery: the WSES position paper. World J Emerg Surg. 2023;18:47.
40. Ouaïssi M, Gaujoux S, Veyrie N, Denève E, Brigand C, Castel B, et al. Postoperative adhesions after digestive surgery: their incidence and prevention: review of the literature. J Visc Surg. 2012;149(2):e104-e114.
41. Bi Y, Li J, Yu Y, Wang Y, Zhang X, Chen H. Therapeutic strategies against bacterial biofilms. Fundam Res. 2021;1(2):193-212.
42. Flemming HC, Wingender J, Szewzyk U, Steinberg P, Rice SA, Kjelleberg S. Biofilms: an emergent form of bacterial life. Nat Rev Microbiol. 2016;14(9):563-575.
43. Fleming D, Chahin L, Rumbaugh K. Glycoside hydrolases degrade polymicrobial bacterial biofilms in wounds. Antimicrob Agents Chemother. 2017;61(2):e01998-16.
44. Ishida H, Ishida Y, Kurosaka Y, Otani T, Sato K, Kobayashi H. In vitro and in vivo activities of levofloxacin against biofilm-producing Pseudomonas aeruginosa. Antimicrob Agents Chemother. 1998;42(7):1641-1645.
45. Elviri L, Bianchera A, Bergonzi MC, Bettini R. Controlled local drug delivery strategies from chitosan hydrogels for wound healing. Expert Opin Drug Deliv. 2017;14(7):897-908.
46. Liang X, Huang C, Liu H, Chen H, Shou J, Cheng H, Liu G. Natural hydrogel dressings in wound care: design, advances, and perspectives. Chin Chem Lett. 2024;35(10):109442.
47. Alberts A, Moldoveanu ET, Niculescu AG, Grumezescu AM. Hydrogels for wound dressings: applications in burn treatment and chronic wound care. J Compos Sci. 2025;9(3):133.
48. Andresen AK, Felding MS, Sacramento MMA, Nielsen LH. Hydrogel-based drug delivery systems for localized eradication of bacterial biofilms: advances, challenges and future directions. J Control Release. 2026;390:114509.
49. Mirghani R, Saba T, Khaliq H, Mitchell J, Do L, Chambi L, et al. Biofilms: formation, drug resistance and alternatives to conventional approaches. AIMS Microbiol. 2022;8(3):239-277.

ISSN: 2181-3337 | SCIENTISTS.UZ

50. Singh B, Dahiya M, Kumar V, Ayyagari A, Chaudhari DN, Ahire JJ. Biofilm and antimicrobial resistance: mechanisms, implications, and emerging solutions. Microbiol Res. 2025;16(8):183.
51. Fang CC, Chou TH, Lin GS, Yen ZS, Lee CC, Chen SC. Peritoneal infusion with cold saline decreased postoperative intra-abdominal adhesion formation. World J Surg. 2010;34(4):721-727.
52. Mazuski JE, Tessier JM, May AK, et al. The Surgical Infection Society revised guidelines on the management of intra-abdominal infection. Surg Infect. 2017;18(1):1-76.
53. Solomkin JS, Mazuski JE, Bradley JS, et al. Diagnosis and management of complicated intra-abdominal infection in adults and children: guidelines by the Surgical Infection Society and the Infectious Diseases Society of America. Clin Infect Dis. 2010;50(2):133-164.
54. Montravers P, Dupont H, Leone M, Constantin JM, Mimoz O, Veber B, et al. Guidelines for management of intra-abdominal infections. Anaesth Crit Care Pain Med. 2015;34(2):117-130.
55. Hall-Stoodley L, Costerton JW, Stoodley P. Bacterial biofilms: from the natural environment to infectious diseases. Nat Rev Microbiol. 2004;2(2):95-108.
56. Hellebrekers BWJ, Kooistra T. Pathogenesis of postoperative adhesion formation. Br J Surg. 2011;98(11):1503-1516.
57. Arung W, Meurisse M, Detry O. Pathophysiology and prevention of postoperative peritoneal adhesions. World J Gastroenterol. 2011;17(41):4545-4553.
58. Diamond MP, Wexner SD, diZerega GS, Korell M, Zmora O, Van Goor H, Kamar M. Adhesion prevention and reduction: current status and future recommendations of a multinational interdisciplinary consensus conference. Surg Innov. 2010;17(3):183-188.
59. ten Broek RPG, Issa Y, van Santbrink EJP, Bouvy ND, Kruitwagen RFPM, Jeekel J, et al. Burden of adhesions in abdominal and pelvic surgery: systematic review and meta-analysis. BMJ. 2013;347:f5588.
60. Van Goor H. Consequences and complications of peritoneal adhesions. Colorectal Dis. 2007;9(Suppl 2):25-34.
61. Parker MC, Wilson MS, Menzies D, et al. Clinical and economic consequences of postoperative adhesions. Eur J Surg Suppl. 2001;577:5-9.
62. Attard JA, MacLean AR. Adhesive small bowel obstruction: epidemiology, biology and prevention. Can J Surg. 2007;50(4):291-300.
63. Singleton KD, Wischmeyer PE. Distance of cecum ligated influences mortality, tumor necrosis factor-alpha and interleukin-6 expression following cecal ligation and puncture in the rat. Eur Surg Res. 2003;35(6):486-491.

ISSN: 2181-3337 | SCIENTISTS.UZ

ISSN: 2181-3337 | SCIENTISTS.UZ VOLUME 5 ISSUE 7 JULY 2026

EVALUATION OF THE CLINICAL EFFECTIVENESS OF PROFESSIONAL AND PERSONAL ORAL HYGIENE MEASURES IN THE TREATMENT OF CHRONIC CATARRHAL GINGIVITIS IN ADOLESCENTS

Jovliyev Behruz
Master's Student at Termez University
of Economics and Service

DOI: 10.67620/sai.57d0009

ABSTRACT

Chronic catarrhal gingivitis is one of the most common periodontal conditions among adolescents, and its development is primarily associated with the accumulation of microbial dental plaque and inadequate personal oral hygiene. This study aimed to evaluate the clinical effectiveness of professional and personal oral hygiene measures in treating chronic catarrhal gingivitis in adolescents. A prospective clinical study was conducted at the Surkhandarya Regional Pediatric Dental Clinic in 2025–2026 and included 30 adolescents aged 12–17 years. All participants underwent professional oral hygiene procedures, including the removal of soft and hard dental deposits, and received practical instruction in proper toothbrushing techniques. Clinical status was assessed before treatment and 14 days later using gingival bleeding, redness, swelling, halitosis, the Simplified Oral Hygiene Index (OHI-S), and the Gingival Index (GI). After the therapeutic and preventive interventions, the prevalence of gingival bleeding decreased from 83.3% to 23.3%, redness from 90.0% to 26.7%, swelling from 70.0% to 16.7%, and halitosis from 60.0% to 13.3%. The mean OHI-S score decreased from 2.41 ± 0.48 to 0.86 ± 0.31, while the mean GI score decreased from 1.72 ± 0.36 to 0.52 ± 0.21. These findings indicate that professional oral hygiene combined with individualized hygiene education was associated with short-term reductions in the clinical signs of gingivitis among adolescents.

ACCEPTED

31.07.26

Keywords: *adolescents, chronic catarrhal gingivitis, professional oral hygiene, personal oral hygiene, gingival bleeding, OHI-S, Gingival Index.*

CC BY

INTRODUCTION

Adolescence is characterized by rapid physical growth, hormonal changes, and the development of the permanent dentition. During this period, inadequate oral hygiene, microbial dental plaque accumulation, poor dietary habits, and the use of orthodontic appliances may create conditions conducive to gingival inflammation. In gingivitis, inflammation is largely confined to the gingival tissues and is clinically manifested by redness, swelling, and bleeding during toothbrushing or probing.

Chronic catarrhal gingivitis is one of the most common periodontal diseases among adolescents. Epidemiological studies have demonstrated a high prevalence of plaque-induced gingivitis in this age group. In particular, a study of schoolchildren aged 12–15 years identified localized or generalized gingivitis in 47.3% of the examined participants [1]. Although early-stage gingivitis does not involve

destructive changes in periodontal attachment or alveolar bone, prolonged inflammation may impair oral health and contribute to gingival bleeding, halitosis, and dental discomfort.

Eliminating microbial dental plaque, the primary etiological factor, is essential in the treatment of gingivitis. Removing soft and hard dental deposits through professional oral hygiene procedures helps reduce gingival inflammation. However, the long-term effectiveness of treatment also depends on adolescents' adherence to daily personal oral hygiene practices, proper toothbrushing techniques, and regular use of interdental cleaning aids. Current clinical guidelines recommend combining professional tooth cleaning with personalized oral hygiene instruction and regular follow-up for the treatment of gingivitis [2].

Nevertheless, local evidence on clinical changes following the combined use of professional and personal oral hygiene measures among adolescents remains limited. Comparing gingival bleeding, redness, swelling, halitosis, and oral hygiene indices before and after treatment can help determine the practical effectiveness of the therapeutic and preventive measures applied.

The aim of this study was to evaluate the clinical effectiveness of professional and personal oral hygiene measures in the treatment of chronic catarrhal gingivitis in adolescents.

LITERATURE REVIEW

The development of gingivitis in adolescents is often associated with microbial dental plaque accumulation and inadequate personal oral hygiene. Because habits established during adolescence may persist into adulthood, the early detection of gingival inflammation, removal of dental plaque, and instruction in proper oral hygiene practices are essential.

Diamanti et al. investigated oral hygiene and periodontal status in 2,478 adolescents aged 12 and 15 years. The researchers used the Simplified Plaque Index and periodontal indices. Gingival bleeding on probing was detected in 23.6% of the 12-year-old participants and 21.6% of the 15-year-old participants. Dental calculus was recorded in 46.2% and 44.3% of the participants, respectively. Adolescents who brushed their teeth less than twice daily and did not use interdental cleaning aids had poorer oral hygiene and periodontal health. The authors emphasized the need to strengthen preventive programs aimed at developing personal oral hygiene skills among adolescents [3].

Soldo et al. evaluated the effects of a motivational oral hygiene lecture and a practical demonstration of proper toothbrushing techniques on dental plaque levels among adolescents. The mean plaque index was 3.52 at baseline, decreased to 2.64 one week after oral hygiene education, and declined further to 1.44 after three months. However, at the six-month follow-up, the index increased to 2.52. The authors demonstrated that oral hygiene education produced positive short-term outcomes; however, adolescents' knowledge and skills require regular review and reinforcement to maintain these improvements [4].

Dimenäs et al. compared a person-centered educational program with conventional verbal instructions among adolescents with poor oral hygiene. The person-centered program considered each adolescent's existing oral hygiene habits, individual difficulties, motivation, and abilities. At the six-month follow-up, dental plaque and gingival bleeding had decreased in both groups; however, the improvement was greater among adolescents who received individualized, behavior-based education. The findings indicated that individualized work with each adolescent and active participation in the treatment process were more effective than general recommendations alone [5].

Al-Hassan, Kazlak, and Kateeb investigated the effectiveness of an interactive, school-based oral health program among adolescents. After two months, mean periodontal and oral hygiene index values were significantly lower in the intervention group than in the control group. Toothbrushing skills, frequency, and duration also improved in the intervention group. The authors found that combining theoretical information with practical activities, interactive teaching methods, and repeated follow-up had a positive effect on adolescents' periodontal health [6].

ISSN: 2181-3337 | SCIENTISTS.UZ

The reviewed literature demonstrates that professional oral hygiene reduces microbial dental plaque, the principal local factor contributing to gingival inflammation, while personal oral hygiene education helps maintain these improvements. Nevertheless, a single educational session or toothbrushing demonstration does not always produce stable, long-term outcomes. Treatment effectiveness depends on adolescents' motivation, regular and proper toothbrushing, use of interdental cleaning aids, and attendance at follow-up dental examinations.

Although the reviewed studies examined various educational programs and long-term follow-up periods, assessing short-term clinical outcomes after combining professional oral hygiene procedures with basic personal oral hygiene instruction is also of practical importance. Therefore, comparing gingival bleeding, redness, swelling, halitosis, OHI-S scores, and Gingival Index scores before treatment and 14 days after treatment can help determine the clinical effectiveness of the therapeutic and preventive measures.

RESEARCH METHODOLOGY

This single-group prospective clinical study evaluated the clinical effectiveness of professional and personal oral hygiene measures in treating chronic catarrhal gingivitis in adolescents. Participants' oral health status before treatment was compared with their status 14 days after the therapeutic and preventive interventions.

The study was conducted at the Surkhandarya Regional Pediatric Dental Clinic. It included 30 adolescents aged 12–17 years who underwent dental examinations and were diagnosed with chronic catarrhal gingivitis in 2025–2026. Before the study began, the examination and treatment procedures were explained to the adolescents and their parents, and written informed consent was obtained.

The inclusion criteria were redness and swelling of the gingival margin, bleeding during toothbrushing or periodontal probing, and soft dental plaque on tooth surfaces. Additional inclusion criteria were the absence of clinical attachment loss, pathological periodontal pockets, and alveolar bone destruction. Adolescents with severe systemic diseases; those who had taken antibiotics or antiseptic medications during the month preceding the examination; those with acute inflammatory conditions in the oral cavity; those undergoing orthodontic treatment with fixed appliances; and those who did not attend the recommended follow-up examination were excluded.

The initial dental examination was performed under natural and artificial lighting with a dental mirror and periodontal probe. Gingival color and shape, swelling severity, bleeding on probing, soft and hard dental deposits, and halitosis were assessed. Each participant's clinical findings were recorded on a specially designed examination form.

Oral hygiene status was assessed using the Simplified Oral Hygiene Index (OHI-S) developed by Greene and Vermillion. This index measures the amount of soft debris and dental calculus on the surfaces of six selected index teeth. The OHI-S score was calculated by adding the Debris Index-Simplified (DI-S) and Calculus Index-Simplified (CI-S) scores. A lower OHI-S score indicated better oral hygiene [7].

The severity of gingival inflammation was assessed using the Löe Gingival Index (GI). The vestibular, lingual or palatal, mesial, and distal gingival surfaces of each tooth were examined, and each site was scored from 0 to 3. A score of 0 indicated healthy gingiva; 1 indicated mild redness and swelling; 2 indicated moderate inflammation with bleeding on probing; and 3 indicated severe inflammation with a tendency toward spontaneous bleeding. The final GI score was calculated as the mean score across all examined surfaces [8].

Following the initial examination, all adolescents underwent professional oral hygiene procedures. Soft and hard dental deposits were removed, and tooth surfaces were polished with a specialized brush and prophylactic paste. Each participant then received a practical demonstration of the correct toothbrushing technique. The adolescents were advised to brush their teeth twice daily, pay particular attention to the gingival margins and interdental areas, and use personal oral hygiene aids correctly.

ISSN: 2181-3337 | SCIENTISTS.UZ

Fourteen days after the therapeutic and preventive interventions, the adolescents underwent a follow-up clinical examination. The same assessment criteria used at baseline were applied at follow-up. Gingival bleeding, redness, swelling, halitosis, OHI-S scores, and GI scores were compared before and after treatment.

Qualitative variables, including gingival bleeding, redness, swelling, and halitosis, were expressed as frequencies and percentages. OHI-S and GI scores were presented as mean values. Reductions in the prevalence of clinical signs and decreases in oral hygiene and gingival index scores were interpreted as evidence of short-term clinical improvement following the therapeutic and preventive interventions.

Participant confidentiality was maintained throughout the study. Examination forms were coded using unique identification numbers, and participants' names were not disclosed during data analysis. The study was conducted with authorization from the administration of the Surkhandarya Regional Pediatric Dental Clinic.

ANALYSIS AND RESULTS

The study included 30 adolescents aged 12–17 years who were diagnosed with chronic catarrhal gingivitis at the Surkhandarya Regional Pediatric Dental Clinic in 2025–2026. Sixteen participants were boys and 14 were girls, and the mean age was 14.6 years. At baseline, all participants underwent professional oral hygiene procedures, during which soft and hard dental deposits were removed. They also received practical instruction in proper toothbrushing techniques. Clinical indicators were assessed before treatment and 14 days later.

At the initial examination, most adolescents presented with gingival redness, bleeding during probing or toothbrushing, gingival swelling, and soft plaque on tooth surfaces. Fourteen days after the interventions, the clinical signs of inflammation had decreased, and oral hygiene and Gingival Index scores had improved.

Table 1.

Clinical indicators of chronic catarrhal gingivitis in adolescents before treatment and 14 days after treatment

Clinical indicator	Before treatment	14 days after treatment
Gingival bleeding, n (%)	25 (83.3%)	7 (23.3%)
Gingival redness, n (%)	27 (90.0%)	8 (26.7%)
Gingival swelling, n (%)	21 (70.0%)	5 (16.7%)
Halitosis, n (%)	18 (60.0%)	4 (13.3%)
OHI-S score, mean value	2.41 ± 0.48	0.86 ± 0.31
Gingival Index (GI), mean value	1.72 ± 0.36	0.52 ± 0.21

Before treatment, gingival bleeding was observed in 25 adolescents (83.3%). After 14 days, this clinical sign persisted in 7 participants (23.3%), representing a decrease of 60 percentage points. Gingival redness was initially recorded in 27 adolescents (90.0%) and persisted in 8 participants (26.7%) at follow-up.

Before treatment, gingival swelling was detected in 21 participants (70.0%); after 14 days, it was observed in 5 adolescents (16.7%). Halitosis was initially recorded in 18 adolescents (60.0%) and persisted in 4 participants (13.3%) at follow-up. These changes indicate that professional dental cleaning combined with daily oral hygiene instruction was associated with short-term reductions in the clinical signs of gingival inflammation.

A randomized study involving adolescents and young adults found that visual plaque disclosure and individualized oral hygiene recommendations improved plaque control and reduced gingival

ISSN: 2181-3337 | SCIENTISTS.UZ

inflammation [9]. These findings are consistent with the reductions in gingival bleeding, redness, and swelling observed in the present study.

Before treatment, the mean OHI-S score was 2.41 ± 0.48, indicating poor oral hygiene. Fourteen days after professional oral hygiene procedures and individualized instruction, the mean score decreased to 0.86 ± 0.31. This change indicates a substantial reduction in soft plaque and dental calculus on tooth surfaces. Similarly, a randomized study involving children aged 12–15 years demonstrated that oral hygiene education delivered by a dentist or trained peers improved plaque and gingival index scores [10].

The baseline mean Gingival Index score was 1.72 ± 0.36, indicating moderate gingival inflammation. Fourteen days after treatment, the mean GI score decreased to 0.52 ± 0.21. This change was consistent with a considerable reduction in gingival redness, swelling, and bleeding on probing. D'Cruz and Aradhya found that oral hygiene education and practical toothbrushing demonstrations reduced plaque and gingival index scores among schoolchildren aged 13–15 years [11].

The findings highlight the importance of combining professional dental cleaning with active adolescent involvement, instruction in proper toothbrushing techniques, and encouragement to maintain oral hygiene at home. Experiential and practice-based oral hygiene education has been reported to improve clinical outcomes among adolescents more effectively than conventional lectures [12].

Overall, gingival bleeding, redness, swelling, and halitosis decreased during the 14-day follow-up period. The reductions in the OHI-S score from 2.41 to 0.86 and the GI score from 1.72 to 0.52 indicate the short-term clinical effectiveness of professional oral hygiene procedures combined with individualized oral hygiene education. However, the persistence of inflammatory signs in some adolescents indicates a need for continued monitoring of toothbrushing practices and reinforcement of individualized recommendations.

Because this study used a single-group prospective design and included only 30 adolescents, its findings reflect short-term clinical changes following professional and personal oral hygiene interventions. The absence of a control group limits comparisons with other treatment approaches and prevents definitive causal inference. The small sample size also requires caution when generalizing the findings to the broader adolescent population. Future research should include multicenter controlled studies with sample sizes determined a priori. Paired t-tests or Wilcoxon signed-rank tests should be used for quantitative variables based on individual-level paired observations, while McNemar's test should be used for qualitative variables. Future studies should also report p-values, 95% confidence intervals, and effect sizes.

CONCLUSIONS AND RECOMMENDATIONS

The study findings showed substantial short-term improvements following the combined use of professional and personal oral hygiene measures in adolescents with chronic catarrhal gingivitis. Before treatment, gingival bleeding was observed in 83.3% of participants, gingival redness in 90.0%, gingival swelling in 70.0%, and halitosis in 60.0%. Fourteen days after the therapeutic and preventive interventions, these rates had decreased to 23.3%, 26.7%, 16.7%, and 13.3%, respectively.

Professional oral hygiene procedures, removal of soft and hard dental deposits, and practical demonstrations of proper toothbrushing techniques were followed by substantial improvements in participants' oral hygiene status. The mean OHI-S score decreased from 2.41 ± 0.48 to 0.86 ± 0.31, while the mean Gingival Index score decreased from 1.72 ± 0.36 to 0.52 ± 0.21. These changes were consistent with reduced gingival inflammation and positive short-term clinical outcomes.

However, gingival bleeding, redness, and other signs of inflammation persisted in some adolescents after 14 days. This finding highlights the need for consistent daily personal oral hygiene, reinforcement of proper toothbrushing practices, and regular follow-up dental examinations to support the long-term stability of treatment outcomes.

ISSN: 2181-3337 | SCIENTISTS.UZ

Practical Recommendations

1. In adolescents diagnosed with chronic catarrhal gingivitis, professional oral hygiene procedures should be combined with practical, individualized toothbrushing instruction.
2. Adolescents should be advised to brush their teeth correctly at least twice daily, pay particular attention to the gingival margins and interdental areas, and use appropriate personal oral hygiene aids.
3. A follow-up clinical examination should be conducted 14 days after treatment and repeated after three months. Adolescents with persistent gingival bleeding or other signs of inflammation should receive additional oral hygiene instruction.

REFERENCES

1. Wang W., Feng X., Tai B., Hu D., Lin H., Wang B. et al. Epidemiology of Plaque-Induced Gingivitis Among 12–15-Year-Old Chinese Schoolchildren: A Study Based on the 2018 Case Definition // Journal of Clinical Periodontology. - 2024. - Vol. 51, No. 3. - P. 299–308. - DOI: 10.1111/jcpe.13904.
2. American Academy of Pediatric Dentistry. Periodontal Conditions in Pediatric Dental Patients // The Reference Manual of Pediatric Dentistry. - Chicago, IL: American Academy of Pediatric Dentistry, 2025. - P. 527–544.
3. Diamanti I., Berdouses E. D., Kavvadia K., Arapostathis K. N., Polychronopoulou A., Oulis C. J. Oral Hygiene and Periodontal Condition of 12- and 15-Year-Old Greek Adolescents: Socio-Behavioural Risk Indicators, Self-Rated Oral Health and Changes in 10 Years // European Journal of Paediatric Dentistry. - 2021. - Vol. 22, No. 2. - P. 98–106. - DOI: 10.23804/ejpd.2021.22.02.3.
4. Soldo M., Matijević J., Malčić Ivanišević A., Čuković-Bagić I., Marks L., Nikolov Borić D., Jukić Krmek S. Impact of Oral Hygiene Instructions on Plaque Index in Adolescents // Central European Journal of Public Health. - 2020. - Vol. 28, No. 2. - P. 103–107. - DOI: 10.21101/cejph.a5066.
5. Dimenäs S. L., Jönsson B., Andersson J. S., Lundgren J., Petzold M., Abrahamsson I., Abrahamsson K. H. A Person-Centred, Theory-Based, Behavioural Intervention Programme for Improved Oral Hygiene in Adolescents: A Randomized Clinical Field Study // Journal of Clinical Periodontology. - 2022. - Vol. 49, No. 4. - P. 378–387. - DOI: 10.1111/jcpe.13601.
6. Al-Hassan S., Kazlak M., Kateeb E. Effectiveness of an Interactive School-Based Oral Health Educational Program on Periodontal Status Among Palestinian Adolescents: An Intervention Study // Children. - 2025. - Vol. 12, No. 10. - Art. 1302. - DOI: 10.3390/children12101302.
7. Greene J. C., Vermillion J. R. The Simplified Oral Hygiene Index // Journal of the American Dental Association. - 1964. - Vol. 68. - P. 7–13. - DOI: 10.14219/jada.archive.1964.0034.
8. Löe H. The Gingival Index, the Plaque Index and the Retention Index Systems // Journal of Periodontology. - 1967. - Vol. 38, No. 6. - P. 610–616. - DOI: 10.1902/jop.1967.38.6.610.
9. Peng Y., Wu R., Qu W., Wu W., Chen J., Fang J. et al. Effect of Visual Method versus Plaque Disclosure in Enhancing Oral Hygiene in Adolescents and Young Adults: A Single-Blind Randomized Controlled Trial // American Journal of Orthodontics and Dentofacial Orthopedics. - 2014. - Vol. 145, No. 3. - P. 280–286. - DOI: 10.1016/j.ajodo.2013.10.021.
10. Vangipuram S., Jha A., Raju R., Bashyam M. Effectiveness of Peer Group and Conventional Method (Dentist) of Oral Health Education Programme Among 12–15-Year-Old School Children: A Randomized Controlled Trial // Journal of Clinical and Diagnostic Research. - 2016. - Vol. 10, No. 5. - P. ZC125–ZC129. - DOI: 10.7860/JCDR/2016/17725.7844.
11. D'Cruz A. M., Aradhya S. Impact of Oral Health Education on Oral Hygiene Knowledge, Practices, Plaque Control and Gingival Health of 13- to 15-Year-Old School Children in Bangalore City // International Journal of Dental Hygiene. - 2013. - Vol. 11, No. 2. - P. 126–133. - DOI: 10.1111/j.1601-5037.2012.00563.x.

ISSN: 2181-3337 | SCIENTISTS.UZ

ISSN: 2181-3337 | SCIENTISTS.UZ

ISSN: 2181-3337 | SCIENTISTS.UZ VOLUME 5 ISSUE 7 JULY 2026

EVALUATION OF THE CLINICAL AND RADIOGRAPHIC OUTCOMES OF PULPITIS TREATMENT IN PRIMARY MOLARS USING DEVITALIZING PASTES

Ziyodullayev Samarddin
Master's Student at Termez University of Economics and Service

DOI: 10.67620/sai.57d0010

ABSTRACT

Pulpitis in primary teeth may cause pain, spread inflammation to the periodontal tissues, and result in premature tooth loss. Therefore, preserving primary molars until physiological exfoliation and evaluating treatment effectiveness using both clinical and radiographic criteria are important. This study aimed to evaluate the 3- and 6-month clinical and radiographic outcomes of pulpitis treatment in primary molars using devitalizing pastes. This retrospective observational study was conducted at the Surkhandarya Regional Pediatric Dental Clinic in 2025–2026. It included 44 primary molars from 38 children aged 4–9 years that had been treated with a devitalizing paste. Treatment outcomes were assessed according to the presence or absence of spontaneous pain, pain during mastication, tenderness to percussion, swelling, sinus tract formation, pathological mobility, furcation or periapical changes, and pathological root resorption. Three months after treatment, the overall clinical success rate was 90.9%, the radiographic success rate was 88.6%, and the combined clinical and radiographic success rate was 86.4%. At the 6-month follow-up, these rates decreased to 86.4%, 81.8%, and 79.5%, respectively. Complicated or unsuccessful cases accounted for 13.6% at 3 months and 20.5% at 6 months. The findings indicate that treatment with devitalizing pastes provides satisfactory short-term outcomes in primary molars with pulpitis. However, the higher proportion of radiographic complications at the longer follow-up indicates the need for regular clinical and radiographic monitoring of treated teeth.

ACCEPTED

31.07.26

Keywords: *primary teeth, primary molars, pulpitis, devitalizing paste, devital method, clinical outcome, radiographic outcome, root resorption.*

CC BY

INTRODUCTION

The timely treatment of dental caries and its complications in primary teeth is an important clinical responsibility in pediatric dentistry. Primary teeth play essential roles in mastication, speech development, normal craniofacial growth, and maintaining adequate space for the eruption of permanent teeth. Untreated pulpitis in a primary tooth may cause pain, spread inflammation to the periodontal tissues, induce pathological root resorption, and result in premature tooth loss. Therefore, selecting an appropriate treatment method and regularly evaluating post-treatment outcomes are important aspects of pediatric dental practice.

The anatomy and physiology of primary teeth differ considerably from those of permanent teeth. Primary teeth have relatively thin enamel and dentin, large pulp chambers, and pulp horns located close to the tooth surface. In addition, numerous accessory canals occur between the roots of primary molars, facilitating the rapid spread of inflammation to the furcation area. A child's age, psychological and emotional state, and level of cooperation during dental procedures also influence the choice of treatment. Therefore, the main objective of treating pulpitis in primary teeth is not only to relieve pain but also to preserve the tooth in a functional condition until physiological exfoliation.

The devital method involves devitalizing inflamed pulp tissue with a specialized paste and treating the devitalized tissue at a subsequent visit. This method has traditionally been used when adequate local anesthesia is difficult to achieve, when a child cannot cooperate sufficiently during the procedure, or when treatment must be completed over several visits. However, the composition and quantity of the devitalizing paste, the quality of the hermetic seal, and the duration of contact between the material and the pulp directly affect treatment safety. In particular, leakage of paraformaldehyde-containing preparations into the surrounding soft tissues may cause cytotoxic effects, gingival necrosis, periodontal tissue damage, and inflammatory changes in the alveolar bone [2].

Modern pediatric dentistry places particular emphasis on accurately assessing pulp status through clinical signs and radiographic findings. Evaluating treatment outcomes solely on the basis of pain relief is insufficient. A successful clinical outcome requires the absence of spontaneous pain, pain during mastication, swelling, sinus tract formation, pathological mobility, and tenderness to percussion. Radiographic examination should reveal no pathological changes in the furcation or periapical areas, no pathological internal or external root resorption, and no signs of adverse effects on the underlying permanent tooth germ. The American Academy of Pediatric Dentistry guidelines also state that the overall success of pulp therapy in primary teeth should be determined through a combined assessment of clinical and radiographic outcomes [1].

Although vital pulp therapy with highly biocompatible calcium silicate cements has become increasingly common in contemporary pediatric dentistry, investigating the outcomes of primary teeth treated with devitalizing pastes remains scientifically relevant. Such analysis can identify favorable outcomes, potential complications, and the clinical and radiographic signs that require attention during follow-up. In particular, it is important to assess tooth retention over time, the absence of recurrent pain and inflammation, and changes in the root and furcation areas.

Accordingly, the aim of this study was to evaluate the clinical and radiographic outcomes of pulpitis treatment in primary molars using devitalizing pastes.

LITERATURE REVIEW

Treatment approaches for pulpitis in primary teeth have evolved to include methods that devitalize pulp tissue, partially preserve pulp vitality, or stimulate biological regeneration. The traditional devital method is based on the chemical devitalization of inflamed pulp tissue, followed by the removal or mummification of the coronal pulp. This approach has been used when adequate local anesthesia is difficult to achieve, when a child demonstrates limited cooperation during dental procedures, or when treatment must be completed in several stages. However, its clinical effectiveness depends on the composition and quantity of the preparation, the duration of exposure, the quality of the hermetic seal, and the initial condition of the pulp.

S. Vilella-Pastor et al. investigated the long-term outcomes of pulpotomies performed with mineral trioxide aggregate (MTA) and Biodentine in primary molars in a randomized clinical trial. A total of 84 pulpotomy cases were monitored clinically and radiographically at 6, 12, 18, and 24 months. At the end of the 24-month follow-up, the overall success rate was 99.4% in the Biodentine group and 97.2% in the MTA group, with no statistically significant difference between the groups. The authors identified the

ISSN: 2181-3337 | SCIENTISTS.UZ

absence of pain, swelling, pathological mobility, sinus tract formation, and pathological radiographic changes as the principal criteria for treatment success [3].

N. Tewari et al. synthesized evidence from systematic reviews of the medicaments and techniques used for pulpotomy in primary teeth and analyzed their clinical and radiographic effectiveness. The findings showed that most pulpotomy medicaments and techniques, except calcium hydroxide, achieved success rates above 80%. In several comparisons, MTA produced better outcomes than calcium hydroxide and formocresol. However, the authors emphasized that differences in follow-up duration, patient-selection criteria, medicaments, and methods of evaluating treatment success limited the generalizability of the conclusions [4].

In a randomized, double-blind clinical trial, A. Eshghi et al. compared pulpotomies performed with MTA and Biodentine in mandibular second primary molars diagnosed with irreversible pulpitis. The treated teeth were examined clinically every three months for 12 months and radiographically at 6 and 12 months. No statistically significant differences in clinical or radiographic success were found between the MTA and Biodentine groups. Kaplan–Meier analysis also demonstrated similar survival rates for teeth treated with the two materials. The study showed that treatment outcomes are influenced not only by the material used but also by the initial condition of the pulp, adequate bleeding control, and high-quality hermetic sealing of the tooth cavity [5].

A network meta-analysis conducted by J. Guo, N. Zhang, and Y. Cheng synthesized the findings of 43 randomized clinical trials of pulpotomy in primary molars. The analysis compared the clinical and radiographic effectiveness of formocresol, ferric sulfate, sodium hypochlorite, calcium hydroxide, MTA, Biodentine, and laser techniques. MTA was associated with higher clinical and radiographic success rates than many other medicaments and techniques and had the highest probability of being the optimal treatment material. Calcium hydroxide produced less favorable outcomes than the other materials. The authors identified the absence of spontaneous pain, swelling, sinus tract formation, pathological mobility, tenderness to percussion, and radiographic pathology as essential criteria for treatment success [6].

The reviewed literature demonstrates that contemporary studies of pulp therapy in primary teeth have focused mainly on vital pulpotomy techniques using biocompatible materials. In contrast, relatively few studies have directly evaluated the clinical and radiographic outcomes of primary molars treated with devitalizing pastes. Therefore, assessing recurrent pain, swelling, sinus tract formation, pathological mobility, furcation changes, pathological root resorption, and tooth retention after treatment with the devital method is of considerable scientific and practical importance.

This line of research can clarify the clinical outcomes of treatment with devitalizing pastes, facilitate the prompt identification of post-treatment complications, and establish clinically relevant criteria for the clinical and radiographic follow-up of treated primary molars.

RESEARCH METHODOLOGY

This retrospective observational study evaluated the clinical and radiographic outcomes of pulpitis treatment in primary molars using devitalizing pastes. The principal recommendations of the Strengthening the Reporting of Observational Studies in Epidemiology (STROBE) guidelines were considered during study design, participant selection, variable definition, and reporting [7]. The STROBE guidelines promote clear reporting of the study design, participants, variables, data-collection procedures, potential sources of bias, and findings.

The study was conducted at the Surkhandarya Regional Pediatric Dental Clinic. It reviewed the outpatient records and radiographs of children aged 4–9 years who had been treated for pulpitis in primary molars during 2025–2026. Each primary molar treated with a devitalizing paste was considered an individual unit of analysis. When a child had more than one treated tooth, each tooth was recorded as a separate clinical case.

ISSN: 2181-3337 | SCIENTISTS.UZ

Cases were eligible when they met all of the following criteria: the child was 4–9 years old; a first or second primary molar had been diagnosed with pulpitis; the tooth had been treated with a devitalizing paste; pre-treatment and post-treatment clinical findings were completely documented in the outpatient record; baseline and follow-up radiographs were available; and the treated tooth had been followed for at least six months.

Cases were excluded when documentation of the diagnosis, treatment stages, or follow-up findings was incomplete. Additional exclusion criteria were poor-quality radiographs, physiological root resorption exceeding one-third of the total root length, pathological changes affecting the permanent tooth germ, and extensive destructive lesions in the furcation or periapical area before treatment.

The following variables were entered into a specially designed data-collection form: the child's age and sex; the type of tooth treated; its maxillary or mandibular location; the type of devitalizing paste used; the treatment date; and the duration of follow-up. The treated teeth were classified as first or second primary molars and as maxillary or mandibular teeth.

Treatment followed the clinical protocol documented in the outpatient records. First, carious tissue was removed, the pulp chamber was opened, and the devitalizing paste was applied according to the manufacturer's instructions. The cavity was then hermetically sealed with a temporary restorative material. At the subsequent visit, the devitalized pulp tissue was treated according to the documented protocol; the cavity was then filled with an appropriate material, and a permanent restoration was placed. No additional procedures were performed for this study; only records of previously completed treatment were retrospectively analyzed.

Treatment outcomes were evaluated clinically and radiographically at the 3- and 6-month follow-up examinations. Previous studies of pulp therapy outcomes in primary molars have also used 3- and 6-month follow-up periods and combined clinical and radiographic criteria for success [8].

The clinical assessment included spontaneous pain, pain during mastication, tenderness to percussion, swelling of the gingiva and surrounding soft tissues, sinus tract formation, pathological mobility, and retention of the treated tooth in the dental arch. Cases without spontaneous pain, pain during mastication, tenderness to percussion, swelling, sinus tract formation, or pathological mobility were considered clinically successful. A case with at least one of these signs was classified as a clinical failure.

During the radiographic assessment, baseline intraoral radiographs were compared with follow-up radiographs. The assessment covered radiolucent lesions in the furcation area, periapical pathological changes, widening of the periodontal ligament space, internal root resorption, pathological external root resorption, and signs of adverse effects on the permanent tooth germ.

Teeth without furcation or periapical destruction, pathological internal or external root resorption, or adverse periodontal changes were considered radiographically successful. Cases in which pathological changes were detected radiographically, even in the absence of clinical signs, were included in the overall treatment-failure group.

Overall treatment success was determined through a combined assessment of clinical and radiographic criteria. Cases without clinical symptoms or radiographic pathology were classified as successful. Cases with at least one unfavorable clinical or radiographic finding were classified as complicated or unsuccessful.

The data were analyzed using descriptive statistical methods. Categorical variables were expressed as absolute numbers (n) and percentages (%). A 95% confidence interval (95% CI) was calculated for each proportion using the Wilson method, which provides more reliable estimates in small samples. Because multiple teeth could come from the same patient and tooth-level paired follow-up data were unavailable, p-values were not calculated for comparisons between the follow-up periods. The findings were therefore presented as proportions with 95% confidence intervals. All confidence intervals were two-sided.

ISSN: 2181-3337 | SCIENTISTS.UZ

Patient confidentiality was maintained throughout the study. Data obtained from the outpatient records were coded, and the children's names were not disclosed during the analysis. The study was conducted with appropriate authorization from the administration of the Surkhandarya Regional Pediatric Dental Clinic.

ANALYSIS AND RESULTS

The outpatient records of patients treated at the Surkhandarya Regional Pediatric Dental Clinic during 2025–2026 were reviewed. Based on the established inclusion and exclusion criteria, 44 primary molars from 38 children aged 4–9 years were included in the study. When a child had more than one treated tooth, each tooth was evaluated as a separate unit of observation.

The participants were divided into two age groups: 4–6 years and 7–9 years. The treated teeth were classified by tooth type (first or second primary molar) and jaw location (maxilla or mandible). The general characteristics of the children and treated teeth are presented in Table 1.

Table 1.

General characteristics of the children and treated primary molars included in the study

Indicator	Group	Number, n	Proportion, %
Children	Total	38	100
Sex	Boys	20	52.6
	Girls	18	47.4
Age	4–6 years	23	60.5
	7–9 years	15	39.5
Treated teeth	Total primary molars	44	100
Tooth type	First primary molar	19	43.2
	Second primary molar	25	56.8
Location by jaw	Maxilla	20	45.5
	Mandible	24	54.5

Of the 38 participants, 20 (52.6%) were boys and 18 (47.4%) were girls. Children aged 4–6 years constituted the majority of the study population, with 23 participants (60.5%).

Of the 44 treated primary molars, 19 (43.2%) were first primary molars and 25 (56.8%) were second primary molars. Regarding jaw location, 24 teeth (54.5%) were mandibular and 20 (45.5%) were maxillary.

The outcomes of primary molars treated with devitalizing pastes were evaluated using clinical and radiographic criteria at 3 and 6 months after treatment. The clinical assessment included spontaneous pain, pain during mastication, tenderness to percussion, swelling, sinus tract formation, and pathological mobility. The radiographic assessment included pathological changes in the furcation and periapical areas and pathological root resorption.

Previous studies of pulp therapy in primary molars have defined clinical success by the absence of pain, swelling, sinus tract formation, pathological mobility, and tenderness to percussion. Furcation changes and pathological root resorption have been identified as signs of radiographic failure [9].

Table 2.

Clinical and radiographic outcomes of primary molars treated with devitalizing pastes at the 3- and 6-month follow-ups

Assessment indicator	After 3 months, n (%) [95% CI]	After 6 months, n (%) [95% CI]

ISSN: 2181-3337 | SCIENTISTS.UZ

No spontaneous pain	42 (95.5) [84.9–98.7]	40 (90.9) [78.8–96.4]
No pain during mastication	41 (93.2) [81.8–97.7]	39 (88.6) [76.0–95.0]
No tenderness to percussion	42 (95.5) [84.9–98.7]	40 (90.9) [78.8–96.4]
No swelling or sinus tract	43 (97.7) [88.2–99.6]	41 (93.2) [81.8–97.7]
No pathological mobility	43 (97.7) [88.2–99.6]	41 (93.2) [81.8–97.7]
No furcation or periapical changes	40 (90.9) [78.8–96.4]	37 (84.1) [70.6–92.1]
No pathological root resorption	41 (93.2) [81.8–97.7]	38 (86.4) [73.3–93.6]
Overall clinical success	40 (90.9) [78.8–96.4]	38 (86.4) [73.3–93.6]
Overall radiographic success	39 (88.6) [76.0–95.0]	36 (81.8) [68.0–90.5]
Overall combined clinical and radiographic success	38 (86.4) [73.3–93.6]	35 (79.5) [65.5–88.8]
Unsuccessful or complicated cases	6 (13.6) [6.4–26.7]	9 (20.5) [11.2–34.5]

At the 3-month follow-up, spontaneous pain was absent in 42 teeth (95.5%), pain during mastication was absent in 41 teeth (93.2%), and tenderness to percussion was absent in 42 teeth (95.5%). Swelling or sinus tract formation and pathological mobility were each absent in 43 teeth (97.7%).

At the 3-month follow-up, overall clinical success was recorded in 40 teeth (90.9%). Radiographic examination revealed no pathological furcation or periapical changes in 40 teeth, while pathological root resorption was absent in 41 teeth. Overall radiographic success was recorded in 39 teeth (88.6%).

When the clinical and radiographic findings were evaluated together, 38 teeth (86.4%) were classified as successful at the 3-month follow-up. Clinical or radiographic complications were identified in six teeth (13.6%).

At the 6-month follow-up, several outcome indicators had declined. Spontaneous pain was absent in 40 teeth (90.9%), pain during mastication was absent in 39 teeth (88.6%), and tenderness to percussion was absent in 40 teeth (90.9%). Swelling or sinus tract formation and pathological mobility were each absent in 41 teeth (93.2%).

At the 6-month follow-up, overall clinical success was observed in 38 teeth (86.4%). No pathological furcation or periapical changes were detected in 37 teeth, while seven teeth showed radiographic changes of varying severity in these areas. Pathological root resorption was absent in 38 teeth (86.4%).

Overall radiographic success was recorded in 36 teeth (81.8%). Some teeth were included in the overall treatment-failure group because pathological radiographic changes were detected despite the absence of clinical symptoms. Previous studies have likewise reported that clinical success rates may exceed radiographic success rates [10]. Therefore, radiographic monitoring of treated primary teeth is important even when patients have no clinical complaints.

At the 6-month follow-up, overall combined clinical and radiographic success was recorded in 35 teeth (79.5%). Unfavorable clinical or radiographic findings were identified in nine teeth (20.5%). Because multiple clinical and radiographic findings could occur simultaneously in a single tooth, the total number of individual complications did not necessarily equal the total number of unsuccessful cases.

Contemporary clinical studies have shown that, even when clinical outcomes are favorable after the use of certain pulpotomy materials, internal root resorption, furcation radiolucency, or other pathological signs may still be detected during radiographic follow-up [11]. Systematic reviews and meta-

ISSN: 2181-3337 | SCIENTISTS.UZ

analyses have likewise emphasized the importance of considering clinical and radiographic outcomes together when evaluating the effectiveness of pulp therapy in primary teeth [12].

The overall combined clinical and radiographic success rate for primary molars treated with devitalizing pastes was 86.4% at three months (95% CI: 73.3–93.6) and 79.5% at six months (95% CI: 65.5–88.8). The proportion of complicated cases was 13.6% (95% CI: 6.4–26.7) and 20.5% (95% CI: 11.2–34.5), respectively. Because no paired inferential comparison was performed and no control group was included, the observed reduction cannot be interpreted as a statistically confirmed effect of time or as evidence of superiority over another treatment method. These findings describe the outcomes of the devital method within the present sample.

This retrospective, single-center observational study did not include a control group treated with vital pulpotomy or another method. Therefore, the findings represent only the clinical and radiographic outcomes observed in this sample and do not demonstrate the comparative effectiveness of devitalizing pastes relative to other treatment approaches.

The sample was limited to 38 children and 44 primary molars. In addition, more than one tooth from some children was included as a unit of observation, which may have reduced the independence of the observations and limited the generalizability of the findings. Wilson 95% confidence intervals were provided for all principal proportions to indicate statistical uncertainty. However, because tooth-level paired outcome data at 3 and 6 months were unavailable, McNemar's test and regression analyses appropriate for clustered data were not performed. Future studies should include a larger sample with a prospectively determined sample size, an independent control group, individual paired data, and a statistical model that accounts for patient-level clustering.

CONCLUSIONS AND RECOMMENDATIONS

This retrospective observational study described the short-term clinical and radiographic outcomes of primary molars treated with devitalizing pastes. Three months after treatment, the overall clinical success rate was 90.9% (95% CI: 78.8–96.4), the radiographic success rate was 88.6% (95% CI: 76.0–95.0), and the combined clinical and radiographic success rate was 86.4% (95% CI: 73.3–93.6).

At the 6-month follow-up, the overall clinical success rate was 86.4% (95% CI: 73.3–93.6), the radiographic success rate was 81.8% (95% CI: 68.0–90.5), and the combined clinical and radiographic success rate was 79.5% (95% CI: 65.5–88.8). Because the study did not include a control group, these findings should not be interpreted as evidence that the devital method is superior to other treatment methods.

Clinical success rates were higher than radiographic success rates. In some teeth, clinical signs such as pain, swelling, sinus tract formation, and pathological mobility were absent, whereas radiographic examinations revealed furcation or periapical changes and pathological root resorption. Therefore, clinical symptoms alone are insufficient for evaluating primary molars treated with the devital method.

The findings indicate that treatment with devitalizing pastes may keep primary molars functional in the dental arch for a limited period. However, treatment effectiveness depends on correct application of the preparation, a high-quality hermetic seal, and regular clinical and radiographic monitoring.

Practical Recommendations

1. Before a devitalizing paste is applied, the clinical condition of the pulp, the degree of physiological root resorption, and the radiographic condition of the furcation area should be thoroughly evaluated.
2. Only the minimum amount required under the manufacturer's instructions should be applied. The tooth cavity should be hermetically sealed during both the temporary and permanent restoration stages.
3. Treated primary molars should undergo clinical and radiographic follow-up examinations at 3 and 6 months. If pathological changes are detected, the treatment strategy should be reconsidered.

ISSN: 2181-3337 | SCIENTISTS.UZ

REFERENCES

1. Coll J. A., Dhar V., Chen C. Y., Crystal Y. O., Guelmann M., Marghalani A. A. et al. Use of Vital Pulp Therapies in Primary Teeth 2024 // Pediatric Dentistry. - 2024. - Vol. 46, No. 1. - P. 13–26.
2. Lee C. H., Choi Y., Park S. Mandibular bone necrosis after use of paraformaldehyde-containing paste // Restorative Dentistry & Endodontics. - 2016. - Vol. 41, No. 4. - P. 332–337. - DOI: 10.5395/rde.2016.41.4.332.
4. Vilella-Pastor S., Sáez S., Veloso A., Guinot-Jimeno F., Mercadé M. Long-term Evaluation of Primary Teeth Molar Pulpotomies with Biodentine and MTA: A CONSORT Randomized Clinical Trial // European Archives of Paediatric Dentistry. - 2021. - Vol. 22, No. 4. - P. 685–692. - DOI: 10.1007/s40368-021-00616-3.
5. Tewari N., Goel S., Mathur V. P., O'Connell A. C., Johnson R. M., Rahul M. et al. Success of Medicaments and Techniques for Pulpotomy of Primary Teeth: An Overview of Systematic Reviews // International Journal of Paediatric Dentistry. - 2022. - Vol. 32, No. 6. - P. 828–842. - DOI: 10.1111/ipd.12963.
6. Eshghi A., Hajiahmadi M., Nikbakht M. H., Esmaeili M. Comparison of Clinical and Radiographic Success Between MTA and Biodentine in Pulpotomy of Primary Mandibular Second Molars with Irreversible Pulpitis: A Randomized Double-Blind Clinical Trial // International Journal of Dentistry. - 2022. - Vol. 2022. - Art. 6963944. - DOI: 10.1155/2022/6963944.
7. Guo J., Zhang N., Cheng Y. Comparative Efficacy of Medicaments or Techniques for Pulpotomy of Primary Molars: A Network Meta-analysis // Clinical Oral Investigations. - 2023. - Vol. 27. - P. 91–104. - DOI: 10.1007/s00784-022-04830-1.
8. von Elm E., Altman D. G., Egger M., Pocock S. J., Gøtzsche P. C., Vandenbroucke J. P. The Strengthening the Reporting of Observational Studies in Epidemiology (STROBE) Statement: Guidelines for Reporting Observational Studies // Annals of Internal Medicine. - 2007. - Vol. 147, No. 8. - P. 573–577. - DOI: 10.7326/0003-4819-147-8-200710160-00010.
9. Subramanyam D., Somasundaram S. Clinical and Radiographic Evaluation of Aloe vera versus Formocresol as a Pulpotomy Medicament in Primary Molars: A Double-Blinded Randomized Controlled Trial // International Journal of Clinical Pediatric Dentistry. - 2020. - Vol. 13, No. 2. - P. 138–143. - DOI: 10.5005/jp-journals-10005-1724.
10. Ramanandvignesh P., Gyanendra K., Dhillon J. K., Goswami M. Clinical and Radiographic Evaluation of Pulpotomy Using MTA, Biodentine and Er,Cr:YSGG Laser in Primary Teeth: A Clinical Study // Laser Therapy. - 2020. - Vol. 29, No. 1. - P. 29–34. - DOI: 10.5978/islsm.20-OR-03.
11. Chak R. K., Muthu M. S., Rathna Prabhu V. Clinical Radiographic Evaluation of 3Mixtatin and MTA in Primary Teeth Pulpotomies: A Randomized Controlled Trial // International Journal of Clinical Pediatric Dentistry. - 2022. - Vol. 15, Suppl. 1. - P. S82–S87. - DOI: 10.5005/jp-journals-10005-2216.
12. Gisour E. F., Jahanimoghadam F., Karimipour P. Clinical and Radiographic Comparison of Primary Molar Pulpotomy Using Formocresol, Portland Cement, and NeoMTA Plus: A Randomized Controlled Clinical Trial // Scientific Reports. - 2024. - Vol. 14. - Art. 29690. - DOI: 10.1038/s41598-024-81180-w.
13. Bastos M. C., Albuquerque F. G. A., Filho E. L. C., Silva P. G., Rolim J. P. M. L. Clinical and Radiographic Success of Pulpotomy and Pulpectomy in Primary and Permanent Teeth: A Systematic Review and Meta-Analysis // Journal of Clinical and Experimental Dentistry. - 2024. - Vol. 16, No. 9. - P. e1120–e1128. - DOI: 10.4317/jced.61346.

ISSN: 2181-3337 | SCIENTISTS.UZ

ISSN: 2181-3337 | SCIENTISTS.UZ VOLUME 5 ISSUE 7 JULY 2026

IN VIVO EVALUATION OF THE CHRONIC TOXIC EFFECTS OF REPEATED ADMINISTRATION OF THE C-4 COMPOSITION AT DIFFERENT DOSES IN RABBITS

Makhmudov Lazizbek[1], Yakubova Rana[1], Tagayalieva Nigora[1]

[1]Institute of Bioorganic Chemistry named after Academician O. S. Sodikov, Academy of Sciences of the Republic of Uzbekistan, Tashkent, Uzbekistan

DOI: 10.67620/sai.57d0011

ABSTRACT

Background: Repeated-dose toxicity studies are required to identify cumulative adverse effects, target-organ injury, dose-response patterns, and the reversibility of treatment-related changes before a pharmacologically active composition advances in development. Objective: This study evaluated the safety of the C-4 composition after once-daily oral administration to rabbits at 4, 8, or 16 mg/kg for 90 consecutive days. Methods: Rabbits were assigned to a distilled-water control group or one of three dose groups. Clinical condition, behavior, body weight, peripheral blood indices, serum biochemical markers, relative organ weights, gross pathology, and hematoxylin-eosin histology of major organs were assessed. Quantitative figures in the source study report mean ± SEM for four animals per group. Results: No statistically significant treatment-related differences were reported for hemoglobin, erythrocytes, leukocytes, platelets, selected erythrocyte indices, serum total protein, glucose, urea, alanine aminotransferase, aspartate aminotransferase, alkaline phosphatase, or body-weight gain ($p > 0.05$). Relative organ-weight coefficients were broadly comparable across groups. Most examined tissues retained normal architecture, with mild lymphoid activation and vascular congestion described as non-destructive findings. At 16 mg/kg, however, uneven myocardial congestion and microfoci of myolysis with little or no cellular reaction were reported. Conclusion: The available dataset shows no overt systemic, hematological, or serum-biochemical toxicity at 4-16 mg/kg over 90 days. The 4- and 8-mg/kg doses appear well tolerated. A definitive no-observed-adverse-effect level should not be assigned until the high-dose cardiac finding, sample-size discrepancy, and unreported recovery, coagulation, and renal-excretory outcomes are clarified.

ACCEPTED

02.08.26

Keywords: *C-4 composition; repeated-dose toxicity; rabbits; hematology; clinical chemistry; histopathology; preclinical safety.*

CC BY

INTRODUCTION

The development of a new pharmacologically active composition requires a staged evaluation of efficacy, exposure, and safety. Acute toxicity testing can identify immediate hazards and approximate dose-limiting effects, but it cannot adequately predict adverse reactions that arise through accumulation, repeated metabolic stress, adaptive responses, or delayed tissue injury. Repeated-dose studies are therefore designed to characterize the toxicological profile of a candidate substance, identify potential target organs,

evaluate exposure-response relationships, and determine whether observed effects persist or resolve after treatment is withdrawn [1-4]. A 90-day study in a non-rodent species is commonly classified as a subchronic repeated-dose investigation, even when the broader research programme refers to it as a chronic-toxicity assessment [1].

An integrated toxicological assessment normally combines daily clinical observations with body-weight and food-consumption data, hematology, clinical chemistry, urinalysis, gross necropsy, organ weights, and histopathology. Each domain contributes different information. Hematological variables may reveal effects on erythropoiesis, leukopoiesis, platelet production, inflammation, immune status, or oxygen-carrying capacity. Clinical chemistry can provide evidence of altered hepatocellular integrity, biliary function, protein synthesis, carbohydrate metabolism, or renal excretory function. Organ weights may identify treatment-related hypertrophy, atrophy, congestion, or proliferative change, while microscopic examination remains essential for detecting focal or subtle tissue lesions that are not reflected in circulating biomarkers [7-15].

The liver and kidneys are central to the disposition of xenobiotics and are consequently prominent targets in nonclinical safety assessment. Alanine aminotransferase (ALT) and aspartate aminotransferase (AST) are widely used indicators of hepatocellular injury, although AST is less organ-specific and both enzymes must be interpreted together with histopathology and other clinical-pathology findings [10,11]. Alkaline phosphatase (ALP), total protein, glucose, and urea add information concerning hepatobiliary function, hepatic synthetic capacity, intermediary metabolism, and nitrogen handling. Traditional renal indices can be insensitive to early structural damage; accordingly, contemporary toxicology increasingly supplements urea and creatinine with urinalysis, urinary proteins, and qualified kidney-injury biomarkers when the study design and resources permit [12,13].

Rabbits are used in selected pharmacological, toxicological, medical-device, and translational investigations, but interpretation requires species-appropriate reference information. Rabbit hematological and biochemical values may vary with age, strain, sex, diet, handling, stress, circadian rhythm, and laboratory methods [8,9]. For this reason, comparison with a concurrent control group is more informative than reliance on a single published reference interval. Transparent reporting of animal allocation, numbers analyzed, randomization, blinding, ethics approval, exclusions, and adverse events is also essential for reproducibility and critical appraisal under the ARRIVE 2.0 framework [6].

The C-4 composition is a multicomponent pharmacologically promising formulation intended for further preclinical development. Before advancement, its safety under prolonged daily exposure must be characterized, with particular attention to cumulative and dose-related effects. The present study examined rabbits receiving 4, 8, or 16 mg/kg orally for 90 days. The available study record included clinical observations, body-weight measurements, peripheral-blood indices, serum biochemistry, relative organ weights, macroscopic examination, and histological images of major organs. The objective was to determine whether repeated administration produced systemic, hematological, biochemical, or morphological evidence of toxicity and to evaluate whether the findings supported a safe dose range.

2. Materials and Methods

2.1. Test article

The test article was identified in the source study as the C-4 composition. It was administered in distilled water by intragastric gavage. Detailed information on the qualitative and quantitative composition, active constituents, purity, batch number, stability, storage conditions, and preparation of the dosing formulation was not included in the available document. These details should be added from the original laboratory records before journal submission because they are necessary for reproducibility and interpretation.

ISSN: 2181-3337 | SCIENTISTS.UZ

2.2. Experimental animals and allocation

Rabbits of the same sex, with a reported initial body weight of 2.4 ± 0.5 kg, were maintained under standard vivarium conditions. The study record describes four experimental groups with 10 animals allocated to each group. This allocation corresponds to 40 rabbits, although one sentence in the source document reports a total of 30 animals. The group-based allocation is used in the present revision, but the final total must be verified against the original animal log. The source also does not specify the rabbit strain, exact sex, age, acclimatization period, or method used to generate the random allocation sequence.

Group	Treatment	Dose	Schedule
1	Distilled-water control	0 mg/kg	Once daily for 90 days
2	C-4 composition	4 mg/kg	Once daily for 90 days
3	C-4 composition	8 mg/kg	Once daily for 90 days
4	C-4 composition	16 mg/kg	Once daily for 90 days

Table 1. Experimental groups and dosing regimen.

2.3. Husbandry, dosing, and clinical observations

Animals were housed at 22 ± 2 °C and 55-65% relative humidity, received a standard laboratory diet, and had ad libitum access to drinking water. The C-4 composition or an equivalent volume of distilled water was administered orally by gavage once daily, seven days per week, for 90 consecutive days. General condition, posture, activity, grooming, behavior, food and water consumption, and visible clinical signs of toxicity were monitored during the study. Body weight was recorded on days 10, 30, and 90. The source record does not provide cage density, light-dark cycle, gavage volume, individual dose calculations, food-consumption data, or a formal clinical-observation scoring system.

2.4. Hematological, biochemical, and coagulation assessment

Peripheral blood was examined on days 10, 30, and 90. The reported hematological panel included hemoglobin concentration, erythrocyte count, reticulocyte percentage, platelet count, leukocyte count, mean corpuscular volume (MCV), mean corpuscular hemoglobin concentration (MCHC), and mean corpuscular hemoglobin (MCH). The source figures report mean ± SEM for n = 4 animals per group, but the relationship between this analytical subset and the 10 animals allocated to each group is not described.

Serum biochemical testing included urea, glucose, total protein, ALT, AST, and ALP. Analyses were performed with a semi-automated biochemical analyzer manufactured by Rayto Life and Analytical Sciences Co., Ltd., using commercial reagent kits from Cypress Diagnostics, Belgium. Prothrombin time, activated partial thromboplastin time, and fibrinogen concentration were reportedly measured using a HUMACLOT Junior single-channel coagulometer and Cypress Diagnostics reagents. However, numerical coagulation results were not included in the available manuscript and are therefore not interpreted in the Results section.

2.5. Necropsy, organ weights, and recovery period

At the end of the 90-day dosing period, animals selected for terminal evaluation were anesthetized with ether and euthanized by decapitation, as reported in the source record. The thoracic and abdominal cavities were opened, organs were examined macroscopically, and tissues were collected. Relative organ-weight coefficients were reported for the heart, lungs, spleen, kidneys, stomach, liver, and small intestine. The normalization formula and units used for these coefficients were not specified. A subset of animals was reportedly retained without further dosing for a recovery period to assess reversibility or persistence, but the duration, group sizes, and recovery findings were not present in the available dataset.

2.6. Histological processing and evaluation

Samples were collected from the liver, heart, lungs, stomach, small intestine, spleen, kidneys, thymus, lymph nodes, and adrenal glands. Tissues were fixed in 10% neutral buffered formalin for 48

ISSN: 2181-3337 | SCIENTISTS.UZ

hours, washed in running tap water for 2-4 hours, dehydrated through graded ethanol, cleared in chloroform, and embedded in paraffin. Sections 5-8 μm thick were prepared. After deparaffinization, sections were stained with hematoxylin for approximately 3 minutes, washed under running water, counterstained with eosin for 0.2-3 minutes, dehydrated through 70-96% ethanol, cleared in carbol-xylene and xylene, and mounted in balsam. Hematoxylin stained nuclei blue to violet, whereas eosin stained cytoplasm and extracellular tissue components in shades of pink.

The available narrative describes the heart, lungs, kidneys, spleen, thymus, lymph nodes, adrenal glands, stomach, and small intestine. Although the liver was listed among collected tissues, a dedicated liver histology description or liver micrograph was not included. The record also does not specify whether the pathologist was blinded to treatment, whether lesions were graded for incidence and severity, or whether peer review was performed. These elements are recommended in toxicologic histopathology practice [14].

2.7. Ethical compliance

The source manuscript states that all experimental protocols were reviewed and approved by an Institutional Animal Care and Use Committee and that animal care complied with Directive 2010/63/EU on the protection of animals used for scientific purposes [5]. The committee name, approval number, approval date, and institution-specific protocol identifier were not provided and should be inserted from the original approval documentation. Reporting was revised with reference to ARRIVE 2.0 [6].

2.8. Statistical analysis

Experimental data were processed and visualized using OriginPro version 9.0 (OriginLab Corporation, USA). Results were expressed as mean ± standard error of the mean (SEM). At each observation time, groups were compared using one-way analysis of variance followed by Tukey's post hoc test. Statistical significance was defined as $p < 0.05$. The source document reports only the conclusion that group differences were not significant ($p > 0.05$); exact F statistics, degrees of freedom, adjusted p values, effect sizes, confidence intervals, assumptions checks, and individual-animal data were unavailable. No analysis of longitudinal within-animal correlation was reported.

3. Results

3.1. Clinical condition and body-weight dynamics

Throughout the 90-day administration period, rabbits in the control and C-4 groups were described as active and well groomed. Food and water intake appeared normal, coats remained smooth and glossy, and no visible treatment-related clinical signs were reported. Behavior in treated groups did not differ appreciably from that of control animals.

Body weight increased over time in all groups, consistent with expected growth during the study. Rabbits receiving C-4 showed a descriptive tendency toward greater weight gain than control animals, particularly at 4 mg/kg, but the differences were not statistically significant ($p > 0.05$). No dose-related loss of body mass or growth suppression was evident in the reported data. Because body weight is a broad indicator rather than an organ-specific endpoint, these findings support the absence of overt systemic intolerance but do not independently exclude focal tissue toxicity.

ISSN: 2181-3337 | SCIENTISTS.UZ

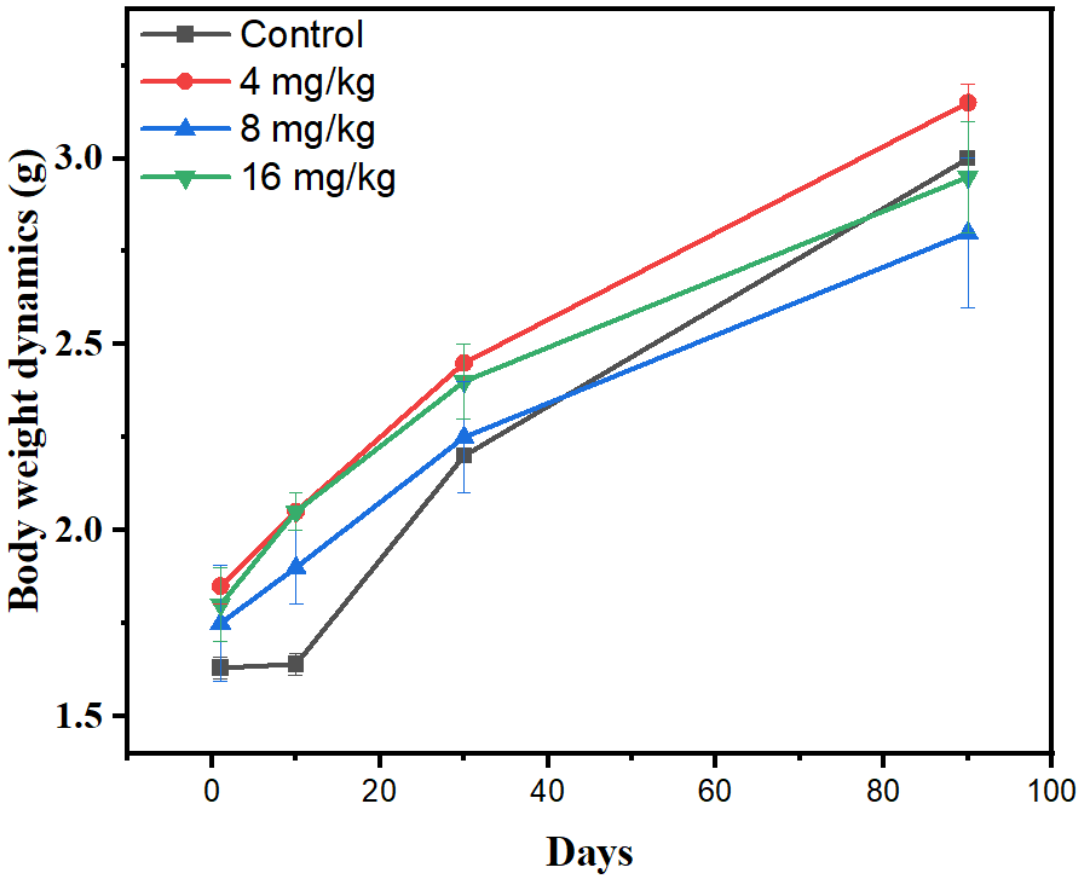


Figure 1. Body-weight dynamics in rabbits receiving distilled water or C-4 at 4, 8, or 16 mg/kg for 90 days. Data are presented as mean ± SEM, n = 4 per group as reported in the source figure.

3.2. Hematological findings

Repeated oral administration of C-4 did not produce statistically significant differences in the reported peripheral-blood variables at days 10, 30, or 90 compared with the control group ($p > 0.05$). Hemoglobin concentration, erythrocyte count, leukocyte count, platelet count, and erythrocyte indices were described as remaining within the physiological range for the study population. The absence of consistent dose-related changes suggests that the composition did not measurably suppress erythropoiesis, leukopoiesis, or thrombopoiesis under the conditions tested.

The reticulocyte-percentage panel in the source figure displays values of approximately 25-36%. These values are reproduced without reinterpretation because the underlying individual data and analyzer output were not available. The variable name, unit, and correspondence with the methods section should be checked against the laboratory worksheet before submission. This verification is important because species-specific hematological interpretation depends on both analytical methodology and correct parameter labeling [8,9].

ISSN: 2181-3337 | SCIENTISTS.UZ

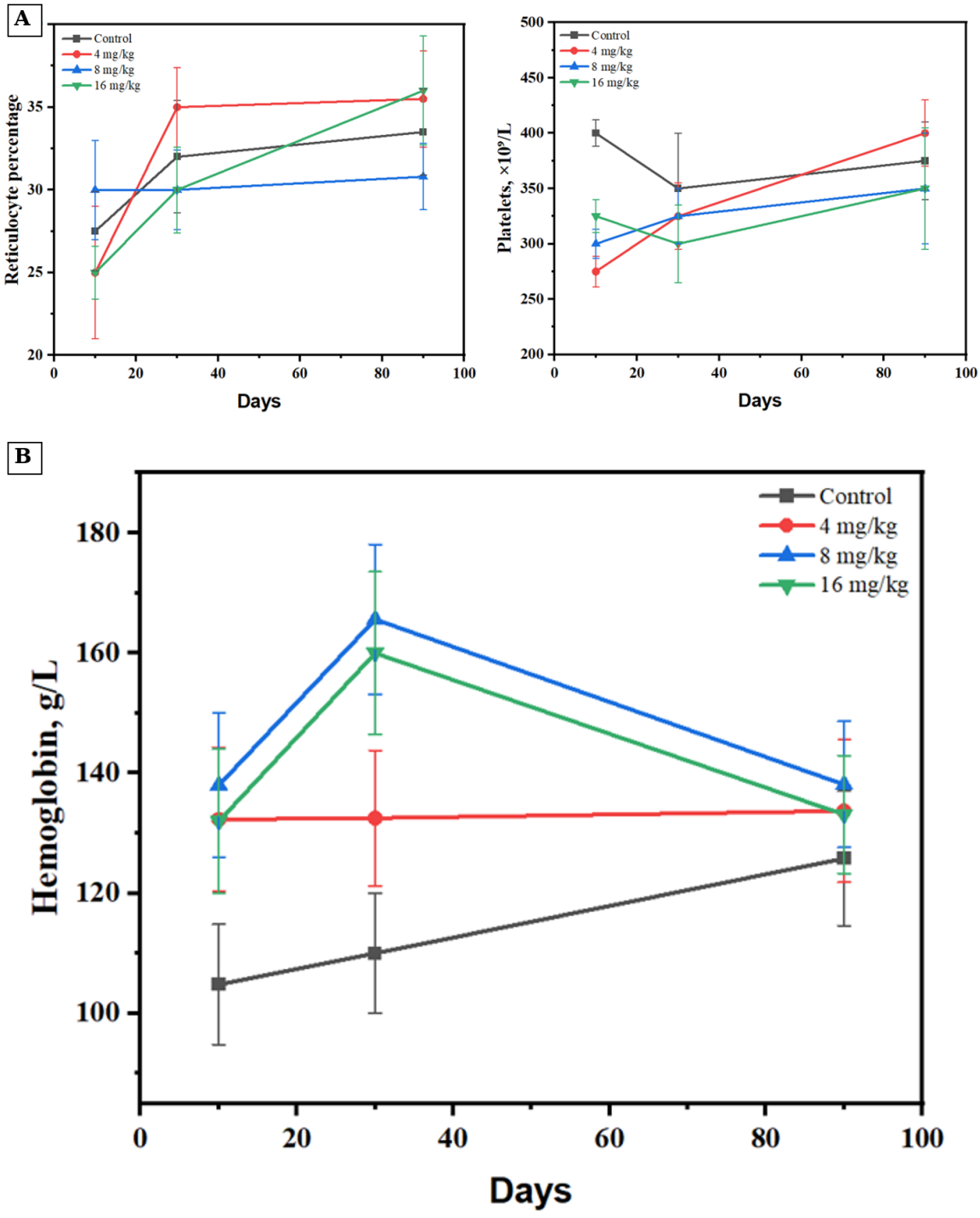


Figure 2. Selected hematological outcomes during repeated C-4 administration. (A) Reported reticulocyte percentage and platelet count; (B) hemoglobin concentration. Data are mean ± SEM, n = 4 per group as stated in the source figures. No statistically significant differences versus control were reported ($p > 0.05$).

3.3. Serum biochemical findings

Serum total protein, glucose, and urea concentrations and the activities of ALT, AST, and ALP did not differ significantly among the control and treated groups at the reported observation points ($p > 0.05$). Total protein remained comparatively stable, providing no evidence of a marked reduction in hepatic protein-synthetic function. The absence of a consistent elevation in ALT or AST provided no serum-biochemical signal of hepatocellular injury, while stable ALP activity provided no evidence of a major cholestatic or hepatobiliary disturbance. Glucose and urea also remained broadly comparable with control values.

ISSN: 2181-3337 | SCIENTISTS.UZ

These findings should be interpreted as an absence of detectable changes in the measured conventional markers, rather than proof that no microscopic or mechanistic injury occurred. ALT and AST are useful but imperfect indicators, and urea is relatively insensitive to early renal tubular injury [10-13]. The source introduction refers to renal excretory evaluation, but quantitative diuresis, urinalysis, creatinine, electrolyte, or urinary-biomarker results were not included in the document.

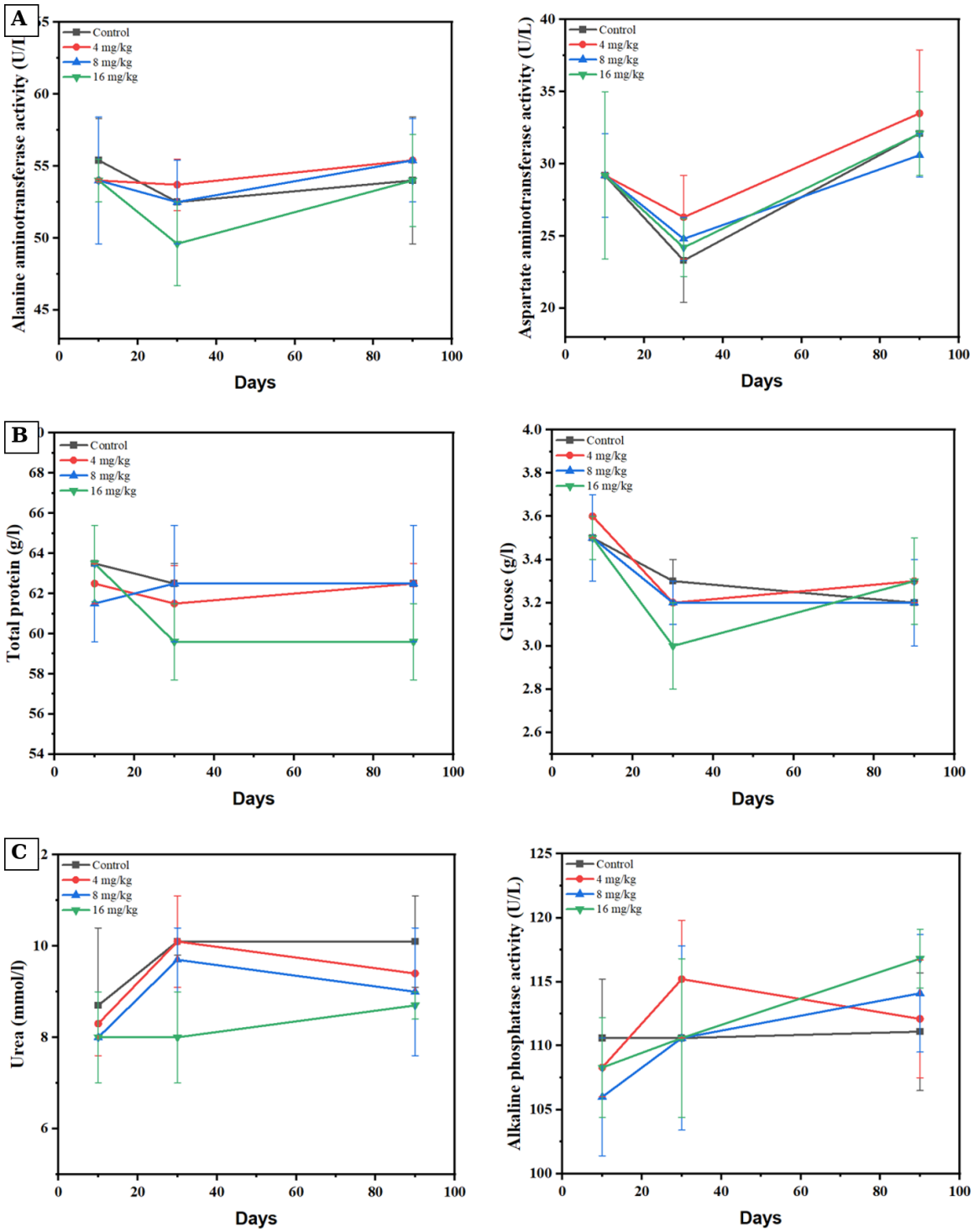


Figure 3. Serum biochemical parameters after 10, 30, and 90 days of repeated C-4 administration. Panels show ALT and AST activities, total protein and glucose concentrations, and urea and ALP values. Data are mean ± SEM, n = 4 per group as reported. No statistically significant differences from control were reported (p > 0.05).

3.4. Relative organ-weight coefficients

Relative organ-weight coefficients after 90 days were generally similar across the four groups (Table 2). No monotonic dose-related increase or decrease was apparent for the heart, kidneys, stomach,

ISSN: 2181-3337 | SCIENTISTS.UZ

liver, or small intestine. Lung and spleen coefficients were numerically lower in treated animals than in controls, but the source manuscript did not report statistical significance, confidence intervals, or the normalization formula. Organ-weight interpretation should integrate absolute weights, terminal body weights, macroscopic observations, and histopathology rather than rely on isolated relative coefficients [15].

Organ	Control	4 mg/kg	8 mg/kg	16 mg/kg
Heart	9.5 ± 1.0	9.0 ± 0.5	8.75 ± 0.75	8.85 ± 0.95
Lungs	13.29 ± 0.36	11.9 ± 0.6	11.95 ± 0.45	11.08 ± 0.725
Spleen	1.23 ± 0.025	1.15 ± 0.05	1.13 ± 0.025	1.08 ± 0.025
Kidneys	20.75 ± 1.25	19.50 ± 2.0	20.25 ± 2.25	19.35 ± 2.65
Stomach	36.0 ± 4.0	35.15 ± 3.1	35.82 ± 3.065	37.15 ± 1.55
Liver	99.1 ± 4.0	95.43 ± 4.5	98.10 ± 2.6	99.54 ± 7.24
Small intestine	3.01 ± 0.14	3.05 ± 0.75	2.9 ± 0.6	2.8 ± 0.5

Table 2. Relative organ-weight coefficients after 90 days of C-4 administration. Values are reproduced from the source document as mean ± SEM; the coefficient formula and units were not specified.

3.5. Macroscopic examination

At terminal necropsy, the major organs were reported to occupy normal anatomical positions. No free fluid was observed in the pleural or abdominal cavities. The mucosal surfaces of the oral, thoracic, and abdominal cavities were described as clean, moist, and normally colored, without visible hemorrhage. The lungs, stomach, and intestines showed no gross erosion, ulceration, or hemorrhage. No visible pathological changes were reported in the pancreas, kidneys, or adrenal glands.

3.6. Histopathological findings

3.6.1. Heart

At 4 and 8 mg/kg, the endocardial, myocardial, and epicardial layers were clearly distinguishable. Cardiomyocytes formed regularly oriented fibers with preserved transverse striations, centrally located oval or elongated nuclei, and visible intercalated discs. No morphological signs of myocardial ischemia or hypoxia were described at these doses. Mild reactive edema and occasional endothelial swelling were noted in some microvessels without marked alteration of the vascular wall.

At 16 mg/kg, the source histology caption reported uneven myocardial congestion and microfoci of myolysis accompanied by little or no cellular reaction. This is the most important potentially adverse microscopic observation in the dataset. The record does not provide lesion incidence, severity grade, distribution among animals, comparison with controls, or an independent pathology review. Consequently, the finding cannot be dismissed as non-treatment-related, but its biological and toxicological significance cannot be established from the available information.

3.6.2. Lungs

Pulmonary architecture was largely preserved. The walls of large, medium, and small intrapulmonary bronchi retained their expected tissue components, and no destructive changes were described in respiratory bronchioles, alveolar ducts, type I or type II pneumocytes, or interalveolar connective tissue. Moderate lymphoid-cell infiltration was present in the mucosa of some bronchi, together with isolated macrophages, mast cells, and plasma cells. Isolated macrophages containing dense cytoplasmic inclusions were observed in interalveolar tissue and air spaces. These observations were not accompanied by a clear dose-related inflammatory or destructive pattern.

3.6.3. Kidneys

The renal capsule was thin and intact, and the cortical region contained numerous renal corpuscles. Glomerular capillary loops remained patent, Bowman's spaces were of normal width, and no blood cells or pathological deposits were reported. Epithelial cells of the proximal, thin, and distal nephron segments retained their expected structure. Collecting ducts contained principal and intercalated cells in normal

ISSN: 2181-3337 | SCIENTISTS.UZ

proportions. Tubular lumina lacked cellular debris or abnormal deposits, and the cortical and medullary interstitium showed no edema or inflammatory infiltration. These findings provide no morphological evidence of overt nephrotoxicity in the examined sections.

3.6.4. Spleen, thymus, and lymph nodes

Splenic red and white pulp remained distinguishable and broadly maintained the normal adult proportion. Some follicles contained germinal or reactive centers with mitotic activity, and macrophages with hemosiderin pigment were present in the red pulp. At 8 mg/kg, foci of hyperplasia were described in subcapsular white pulp. The thymus preserved a clear cortico-medullary boundary, densely arranged cortical lymphocytes, medullary reticuloepithelial cells, and Hassall's corpuscles. Mild lymphocyte blast transformation was noted at 16 mg/kg.

Lymph nodes showed mild secondary activation of lymphoid, reticular, and macrophage populations, with activated lymphocytes and plasma cells in cortical and paracortical regions. These findings were not described as destructive and may represent reactive immune activity. Nevertheless, without incidence data, baseline infectious screening, or blinded lesion scoring, a treatment relationship cannot be established or excluded.

3.6.5. Adrenal glands

The adrenal capsule remained intact. The zona glomerulosa, zona fasciculata, and zona reticularis maintained their characteristic proportions, and chromaffin cells in the medulla retained their expected structure and dimensions. Venous sinusoids were unchanged or mildly dilated. No dystrophic or destructive alteration was reported.

3.6.6. Stomach and small intestine

The gastric surface epithelium and glands were largely preserved. The mucosal surface was covered by mucus and contained occasional exfoliated cells. The lamina propria contained isolated lymphocytes, plasma cells, and lymphoid follicles. Gastric glands retained their tubular structure. Mild stromal edema, vascular congestion, and focal neutrophil accumulation were described in the submucosa, but no ulceration, erosion, glandular destruction, or major disorganization was reported.

Small-intestinal villi were covered by a single layer of columnar epithelium with numerous goblet cells. The lamina propria contained lymphocytes, plasma cells, and lymphoid follicles, with moderate vascular congestion in some sections. The mucosal and submucosal architecture remained preserved, and no dystrophic change was described.

ISSN: 2181-3337 | SCIENTISTS.UZ

3.6.7. Histology plates

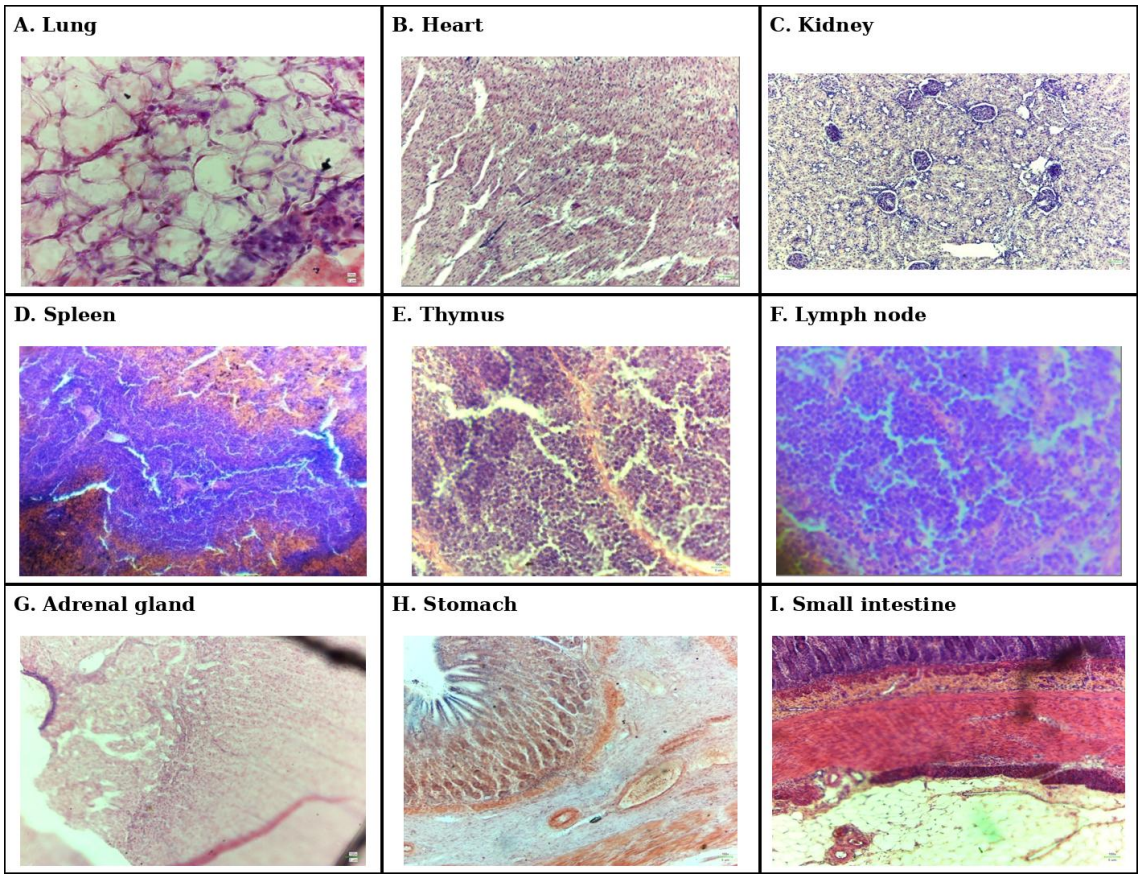


Figure 4. Representative hematoxylin-eosin micrographs after 90 days of C-4 at 4 mg/kg: (A) lung, (B) heart, (C) kidney, (D) spleen, (E) thymus, (F) lymph node, (G) adrenal gland, (H) stomach, and (I) small intestine. Original magnifications were reported as 10×40.

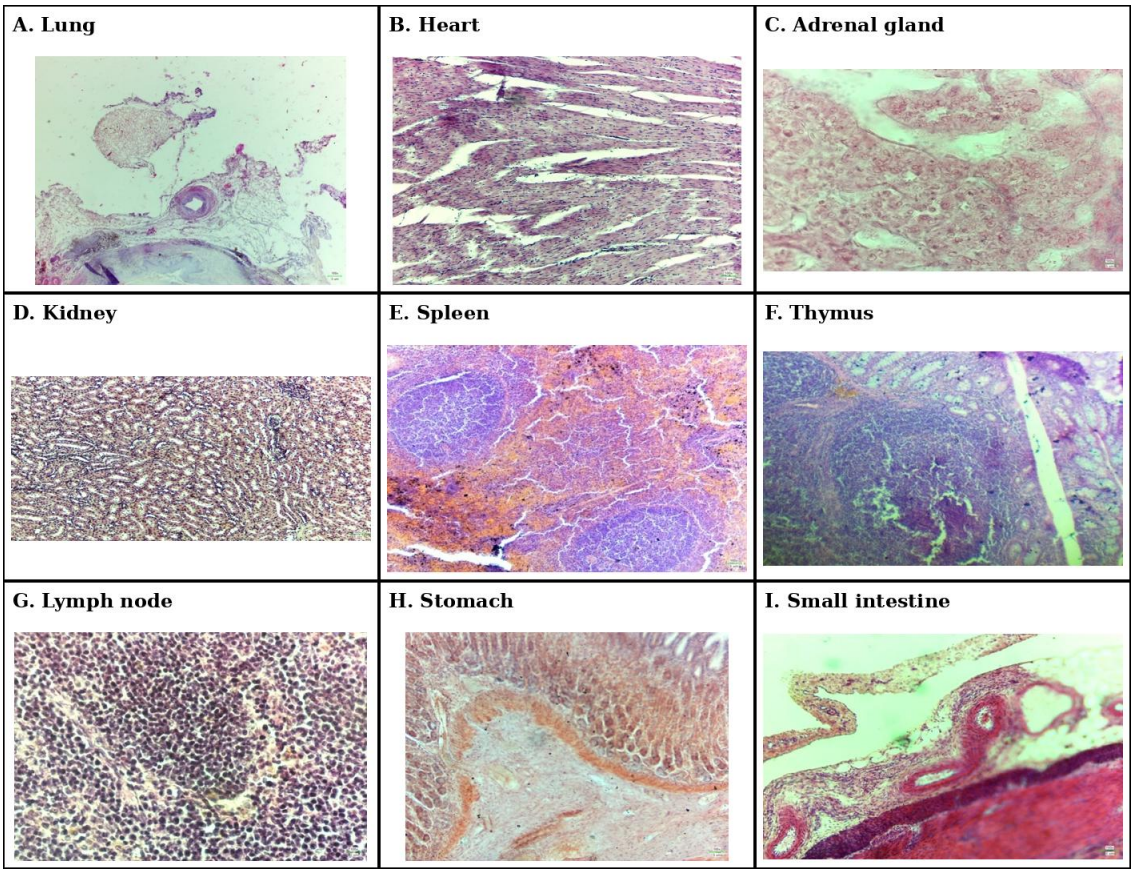


Figure 5. Representative hematoxylin-eosin micrographs after 90 days of C-4 at 8 mg/kg: (A) lung, (B) heart, (C) adrenal gland, (D) kidney, (E) spleen, (F) thymus, (G) lymph node, (H) stomach, and (I) small intestine. Reported magnifications varied from 10×4 to 10×40.

ISSN: 2181-3337 | SCIENTISTS.UZ

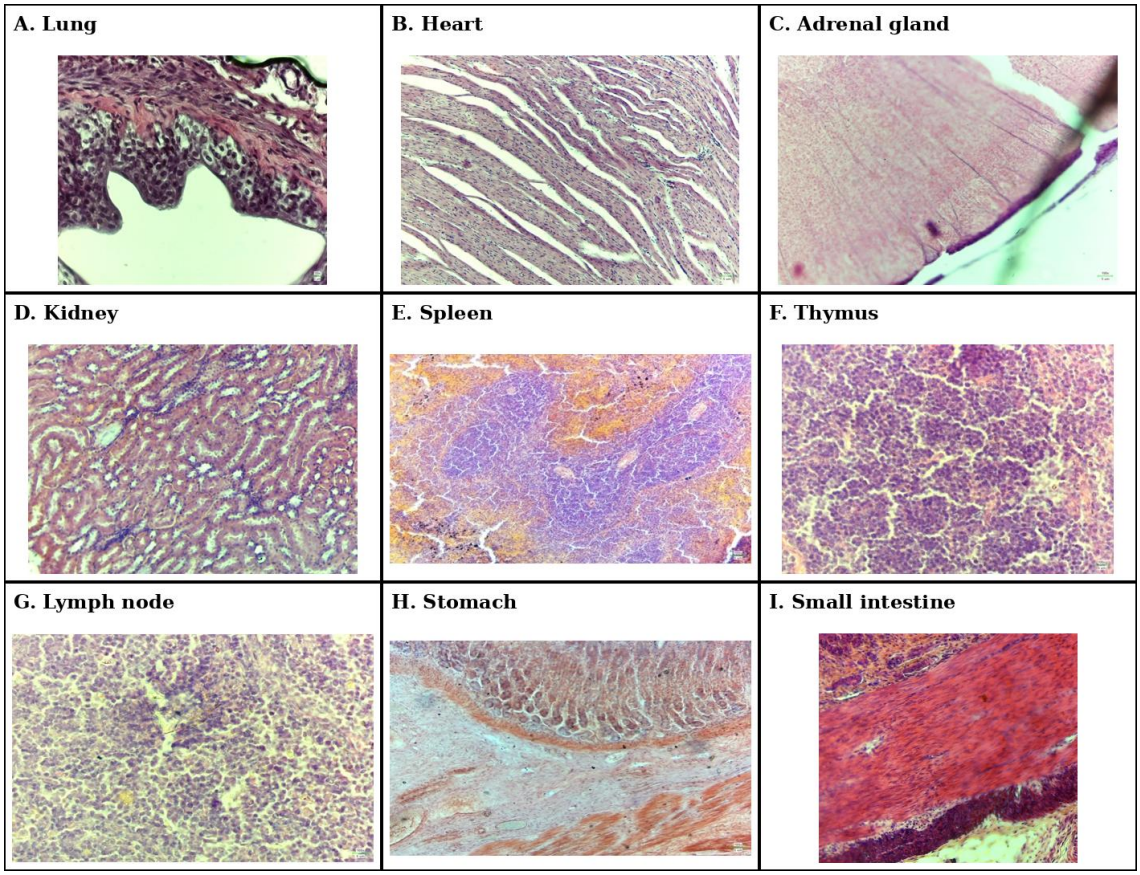


Figure 6. Representative hematoxylin-eosin micrographs after 90 days of C-4 at 16 mg/kg: (A) lung, (B) heart, (C) adrenal gland, (D) kidney, (E) spleen, (F) thymus, (G) lymph node, (H) stomach, and (I) small intestine. The heart panel was described as showing uneven congestion and microfoci of myolysis. Reported magnifications varied from 10×4 to 10×40.

4. Discussion

This 90-day repeated-dose study was intended to determine whether daily oral administration of the C-4 composition produced cumulative systemic toxicity in rabbits. Across the clinical, body-weight, hematological, and serum-biochemical endpoints reported, no statistically significant treatment-related differences were detected at 4, 8, or 16 mg/kg. The absence of reduced activity, impaired grooming, abnormal food or water consumption, weight loss, anemia, leukocyte disturbance, thrombocytopenia, or consistent liver-enzyme elevation suggests that the composition was generally tolerated during the dosing period. This broad pattern is relevant because repeated-dose guidelines emphasize integrated interpretation across in-life observations, clinical pathology, necropsy, organ weights, and histopathology rather than reliance on any single endpoint [1-4,7].

The hematological findings provide no clear evidence of bone-marrow suppression or peripheral blood-cell destruction. Stable hemoglobin and erythrocyte measures argue against clinically meaningful anemia, while the absence of consistent leukocyte and platelet changes argues against major leukopoietic or thrombopoietic toxicity. However, interpretation is limited by the lack of individual-animal data, differential leukocyte counts, blood-smear morphology, sex-specific results, and exact reference intervals for the colony. Rabbit blood parameters are particularly sensitive to handling and stress, and published reference values should be used cautiously because laboratory conditions and analytical platforms differ [8,9]. The apparent reticulocyte percentages in the figure also require confirmation of labeling and units before the result can be considered reliable.

The serum-biochemical results similarly show no conventional signal of hepatocellular or hepatobiliary injury. ALT is generally the most frequently used circulating indicator of hepatocyte membrane damage, whereas AST is less specific and can also increase after muscle injury. ALP may increase with cholestasis or other tissue sources, while total protein reflects a combination of hepatic

ISSN: 2181-3337 | SCIENTISTS.UZ

synthesis, hydration, and immunoglobulin status [10,11]. In the present study, no dose-related rise in ALT, AST, or ALP was reported, and total protein remained stable. These findings are reassuring, but they do not replace liver histopathology. The source record listed liver sampling and reported liver organ-weight coefficients, yet provided no dedicated liver microscopic description or micrograph. Accordingly, the conclusion should be restricted to the measured serum markers and organ weights rather than extended to a definitive absence of hepatic microscopic injury.

Renal assessment was more limited. Urea remained comparable across groups, and kidney histology did not show glomerular, tubular, or interstitial destruction in the representative sections. Nevertheless, urea and serum creatinine can remain unchanged until substantial functional reserve is lost, and modern preclinical safety programmes may incorporate urinalysis and qualified urinary biomarkers when renal liability is suspected [12,13]. The source manuscript refers to renal excretory function, but diuresis, urine chemistry, creatinine, electrolytes, or urinary biomarkers were not reported. The available evidence therefore supports the absence of overt histological nephrotoxicity, not a comprehensive demonstration of preserved renal function.

Organ-weight data did not reveal an obvious monotonic dose response. Liver and heart coefficients were similar to controls, and the small changes in lungs and spleen were not accompanied by a clear gross pathological correlate. Society of Toxicologic Pathology recommendations stress that organ weights should be interpreted with terminal body weight, absolute organ weight, relative weight, macroscopic findings, and microscopy [15]. Because the normalization formula, absolute weights, animal numbers, and statistical analysis were not provided, the coefficients in this manuscript are best regarded as descriptive supporting data.

Most histological descriptions were compatible with preserved tissue architecture. Mild bronchial lymphoid infiltration, reactive splenic follicles, lymph-node activation, mild thymic blast transformation, gastric vascular congestion, and scattered inflammatory cells can occur as background or reactive findings. Toxicological attribution usually requires a consistent increase in incidence or severity, a plausible dose response, concordant findings in related endpoints, and comparison with concurrent controls. The source record did not provide lesion tables or severity grades, so these mild observations cannot be classified definitively as spontaneous, adaptive, or treatment related. Best-practice toxicologic pathology also recommends clear diagnostic terminology, lesion incidence and severity, documentation of the pathologist's approach, and appropriate peer review when findings affect the study conclusion [14].

The high-dose cardiac observation deserves particular attention. Uneven myocardial congestion may be influenced by terminal procedures, anesthesia, agonal changes, tissue handling, or true cardiovascular effects. Microfoci of myolysis, however, describe focal loss or dissolution of myofibrillar structure and may represent a meaningful lesion depending on severity, distribution, and incidence. The absence of serum AST elevation does not eliminate the possibility of focal cardiac injury, especially because cardiac-specific biomarkers and electrocardiographic or functional data were not collected. Before the 16-mg/kg dose is declared non-adverse, the original slides should be reviewed blindly by an experienced toxicologic pathologist, with lesion grading and animal-level tabulation. If the finding is confirmed and exceeds the control background, the high dose may represent a lowest-observed-adverse-effect level rather than a no-observed-adverse-effect level.

The 4- and 8-mg/kg groups showed no comparable cardiac lesion in the available descriptions and no consistent adverse findings in the other measured systems. These doses therefore appear well tolerated under the conditions of the study. Formal assignment of a no-observed-adverse-effect level nevertheless requires a complete, internally consistent dataset, verified exposure, adequate group numbers, and clear distinction between incidental and treatment-related pathology. Toxicokinetic measurements were not reported, so systemic exposure and dose proportionality cannot be evaluated. This is important because

ISSN: 2181-3337 | SCIENTISTS.UZ

administered dose alone does not establish internal exposure, and multicomponent formulations can show nonlinear absorption, metabolism, or interaction among constituents.

The manuscript was revised to avoid the original overstatement that no pathological changes occurred at any dose. A more defensible interpretation is that no overt systemic toxicity or conventional serum-biochemical toxicity was demonstrated, most tissues appeared morphologically preserved, and the low and medium doses were tolerated. The 16-mg/kg group requires additional pathological clarification. This cautious interpretation is consistent with regulatory principles that repeated-dose studies should identify target organs, characterize dose-response relationships, and assess reversibility rather than simply classify a product as safe or unsafe [1-4].

5. Study Limitations

Several reporting limitations prevent a definitive regulatory conclusion. First, the test article is identified only as C-4; composition, purity, batch, stability, and formulation details are missing. Second, the stated total number of animals is inconsistent with the described group allocation. Third, the sex, strain, age, acclimatization, randomization method, blinding procedures, and sample-size justification are not reported. Fourth, the quantitative figures state n = 4 per group, although 10 animals per group were reportedly allocated, and no explanation is provided for the analytical subset.

Fifth, exact numerical hematological and biochemical tables, individual-animal data, effect sizes, confidence intervals, and complete statistical outputs are unavailable. Sixth, the reticulocyte panel requires verification of the parameter name and units. Seventh, coagulation outcomes, renal excretory measurements, urinalysis, and recovery-period results are mentioned in the methods or aims but are not reported. Eighth, the organ-weight coefficient formula and units are missing. Ninth, liver tissue was reportedly collected but no liver histology narrative or image was supplied. Tenth, the high-dose myocardial lesion lacks incidence, severity, animal identifiers, and pathology peer review.

These limitations do not invalidate the reported absence of major clinical or biochemical changes, but they substantially restrict reproducibility and the strength of the safety claim. The missing information should be recovered from laboratory notebooks, analyzer printouts, animal logs, raw-data files, and histopathology records. A revised statistical analysis using animal-level data and an appropriate repeated-measures or mixed-effects framework would strengthen the longitudinal interpretation. The final report should also include the ethical approval number, adverse-event record, inclusion and exclusion criteria, and a clear account of all animals analyzed in accordance with ARRIVE 2.0 [6].

6. Conclusions

Daily oral administration of the C-4 composition at 4, 8, and 16 mg/kg for 90 days produced no reported mortality, overt clinical toxicity, growth suppression, significant hematological disturbance, or significant change in the measured serum biochemical markers. Relative organ-weight coefficients were broadly comparable with control values, and most examined tissues retained their normal architecture.

The available evidence supports a favorable preliminary tolerability profile at 4 and 8 mg/kg. At 16 mg/kg, the reported myocardial congestion and microfoci of myolysis require confirmation and grading before the dose can be classified as non-adverse. Therefore, a definitive no-observed-adverse-effect level cannot be assigned from the current manuscript alone. Completion of the missing raw-data, pathology, recovery, coagulation, renal, and test-article documentation is necessary before the study is used to support subsequent clinical development.

REFERENCES

1. Organisation for Economic Co-operation and Development (OECD). Test No. 409: Repeated Dose 90-Day Oral Toxicity Study in Non-Rodents. OECD Guidelines for the Testing of Chemicals, Section 4. Paris: OECD Publishing; 1998. https://doi.org/10.1787/9789264070721-en

ISSN: 2181-3337 | SCIENTISTS.UZ

2. European Medicines Agency, Committee for Medicinal Products for Human Use. Guideline on repeated dose toxicity. CPMP/SWP/1042/99 Rev 1 Corr*. London: European Medicines Agency; 2010. https://www.ema.europa.eu/en/documents/scientific-guideline/guideline-repeated-dose-toxicity-revision-1_en.pdf
3. International Council for Harmonisation of Technical Requirements for Pharmaceuticals for Human Use. M3(R2): Nonclinical Safety Studies for the Conduct of Human Clinical Trials and Marketing Authorization for Pharmaceuticals. Geneva: ICH; 2009. https://database.ich.org/sites/default/files/M3_R2__Guideline.pdf
4. International Council for Harmonisation of Technical Requirements for Pharmaceuticals for Human Use. S4: Duration of Chronic Toxicity Testing in Animals (Rodent and Non-Rodent Toxicity Testing). Geneva: ICH; 1998. https://database.ich.org/sites/default/files/S4_Guideline.pdf
5. European Parliament and Council of the European Union. Directive 2010/63/EU of 22 September 2010 on the protection of animals used for scientific purposes. Official Journal of the European Union. 2010;L276:33-79. https://eur-lex.europa.eu/legal-content/EN/TXT/?uri=CELEX:32010L0063
6. Percie du Sert N, Hurst V, Ahluwalia A, et al. The ARRIVE guidelines 2.0: Updated guidelines for reporting animal research. PLoS Biology. 2020;18(7):e3000410. https://doi.org/10.1371/journal.pbio.3000410
7. Organisation for Economic Co-operation and Development (OECD). Guidance Document 116 on the Conduct and Design of Chronic Toxicity and Carcinogenicity Studies, Supporting Test Guidelines 451, 452 and 453. 2nd ed. OECD Series on Testing and Assessment No. 116. Paris: OECD Publishing; 2014. https://doi.org/10.1787/9789264221475-en
8. Wolford ST, Schroer RA, Gohs FX, et al. Reference range data base for serum chemistry and hematology values in laboratory animals. Journal of Toxicology and Environmental Health. 1986;18(2):161-188. https://doi.org/10.1080/15287398609530859
9. Melillo A. Rabbit clinical pathology. Journal of Exotic Pet Medicine. 2007;16(3):135-145. https://doi.org/10.1053/j.jepm.2007.06.002
10. Boone L, Meyer D, Cusick P, et al. Selection and interpretation of clinical pathology indicators of hepatic injury in preclinical studies. Veterinary Clinical Pathology. 2005;34(3):182-188. https://doi.org/10.1111/j.1939-165X.2005.tb00041.x
11. Ozer J, Ratner M, Shaw M, Bailey W, Schomaker S. The current state of serum biomarkers of hepatotoxicity. Toxicology. 2008;245(3):194-205. https://doi.org/10.1016/j.tox.2007.11.021
12. Dieterle F, Sistare F, Goodsaid F, et al. Renal biomarker qualification submission: a dialog between the FDA-EMEA and Predictive Safety Testing Consortium. Nature Biotechnology. 2010;28(5):455-462. https://doi.org/10.1038/nbt.1625
13. Vaidya VS, Ozer JS, Dieterle F, et al. Kidney injury molecule-1 outperforms traditional biomarkers of kidney injury in preclinical biomarker qualification studies. Nature Biotechnology. 2010;28(5):478-485. https://doi.org/10.1038/nbt.1623
14. Crissman JW, Goodman DG, Hildebrandt PK, et al. Best practices guideline: Toxicologic histopathology. Toxicologic Pathology. 2004;32(1):126-131. https://doi.org/10.1080/01926230490268756
15. Sellers RS, Morton D, Michael B, et al. Society of Toxicologic Pathology position paper: Organ weight recommendations for toxicology studies. Toxicologic Pathology. 2007;35(5):751-755. https://doi.org/10.1080/01926230701595300

ISSN: 2181-3337 | SCIENTISTS.UZ

ISSN: 2181-3337 | SCIENTISTS.UZ VOLUME 5 ISSUE 7 JULY 2026

AUTOMATIC SPEECH RECOGNITION AND CLINICAL DOCUMENTATION TIME IN TWO HEALTHCARE INSTITUTIONS IN BUKHARA, UZBEKISTAN: A WITHIN-CLINICIAN QUASI-EXPERIMENTAL STUDY

Teshayev Rajabbek
Westminster International University in Tashkent

DOI: 10.67620/sai.57d0012

ABSTRACT

Clinical documentation can consume a substantial proportion of physicians' working time and may limit the operational benefits of healthcare digitalisation. This study examined whether automatic speech recognition (ASR) reduced the time required to create medical documentation in two functioning healthcare institutions in Bukhara, Uzbekistan. A within-clinician quasi-experimental comparison was used: the same clinicians completed documentation by conventional keyboard entry and by ASR-supported voice input. The quantitative analysis covered more than 120 observed patient records. To account for differences in note length, documentation time was standardised as minutes required to produce 100 words. Mean time declined from 8.8 minutes with manual typing to 5.2 minutes with ASR, corresponding to a descriptive reduction of 3.6 minutes per 100 words, or 40.9%. The finding suggests that locally adapted speech input may reduce the labour-time cost of documentation in routine clinical practice. However, the available report did not include dispersion measures, confidence intervals, inferential statistics, transcription accuracy, correction time, or full ethical and technical details. The result should therefore be interpreted as preliminary real-world evidence rather than a definitive causal estimate. Future evaluation should combine time outcomes with note quality, clinically significant error rates, clinician workload, patient consent, privacy safeguards, and implementation costs.

ACCEPTED

02.08.26

Keywords: *automatic speech recognition; clinical documentation; electronic health records; workflow efficiency; digital health; Uzbekistan.*

CC BY

INTRODUCTION

Healthcare digitalisation is frequently presented as a route to improved continuity, accessibility, and organisational efficiency. In practice, however, the introduction of electronic health records (EHRs) can also shift a substantial clerical burden onto clinicians. Time-and-motion research has shown that physicians may spend as much or more time on EHR and desk work as on direct patient interaction, while event-log studies indicate that a considerable proportion of EHR activity continues after scheduled clinical hours (Arndt et al., 2017; Sinsky et al., 2016). Poor usability and intensive EHR interaction have also been associated with professional fatigue and burnout (Khairat et al., 2020; Melnick et al., 2020).

This tension is particularly important in health systems undergoing rapid digital transition. Uzbekistan has prioritised digital health development, but the practical value of digital reform depends on

whether new systems reduce rather than reproduce administrative friction. In facilities with limited specialist capacity, high patient volumes, and mixed paper–digital workflows, documentation time is not merely an individual inconvenience. It is an operational resource that affects scheduling stability, patient flow, clinician attention, and the feasibility of wider digital implementation.

Automatic speech recognition converts spoken language into text and may allow clinicians to enter information more quickly than by keyboard. Earlier clinical speech-recognition studies, however, have reported heterogeneous effects because performance depends on recognition accuracy, speaker adaptation, specialty vocabulary, background noise, correction requirements, and integration with the EHR (Hodgson & Coiera, 2016; Hodgson et al., 2019). More recent ambient documentation systems have renewed interest in voice-enabled workflows by reporting reductions in note-writing time and after-hours EHR work (Duggan et al., 2025; Stults et al., 2025; Tierney et al., 2024). These newer systems are technically different from conventional ASR, but they address the same managerial problem: the time cost of transforming clinical information into a usable medical record.

The linguistic context matters. Clinical ASR systems trained mainly on English-language data cannot be assumed to perform equally well with Uzbek speech, local accents, code-switching, abbreviations, drug names, and specialty-specific terminology. A system may transcribe ordinary language adequately while producing clinically important errors in diagnoses, dosages, anatomical terms, or medication names. Consequently, evaluation should consider both efficiency and documentation quality. Speed alone is insufficient if the generated text requires extensive editing or introduces clinically significant errors.

The present article focuses on a real-world comparison conducted as part of doctoral research in Bukhara. Its primary question is: how much did ASR-supported voice input reduce the time required to produce a standard quantity of medical text compared with manual keyboard entry? A secondary aim is to interpret the operational meaning of the observed difference while clearly distinguishing measured findings from projected managerial benefits.

2. Materials and Methods

2.1 Study design and setting

The study used a within-clinician quasi-experimental design in two functioning healthcare institutions in Bukhara, Uzbekistan. The same clinicians documented clinical information using conventional keyboard entry and ASR-supported voice input. This design reduced between-participant variation because each clinician served as his or her own practical comparator.

Full randomisation was not reported in the supplied manuscript. The design should therefore be regarded as quasi-experimental rather than a randomised trial. The available material also did not specify whether the order of manual and ASR conditions was counterbalanced. Order effects, learning, fatigue, and increasing familiarity with the ASR system may consequently have influenced performance.

2.2 Participants and observations

The quantitative analysis included more than 120 observed patient records. The exact number of participating clinicians, the exact record count, medical specialties, demographic characteristics, recruitment method, and the distribution of observations across the two institutions were not stated in the supplied manuscript. These details must be recovered from the dissertation and reported before journal submission.

Eligibility criteria should specify that participants were clinicians responsible for creating the relevant medical records and able to use both keyboard and voice input. Exclusion criteria should identify incomplete records, interrupted sessions, technical failures, training trials, and observations with missing timing or word-count data. Because these criteria were not included in the source manuscript, no exclusions have been assumed in this revision.

ISSN: 2181-3337 | SCIENTISTS.UZ

2.3 Intervention and comparison

The comparison condition was routine keyboard-based documentation. The intervention condition used ASR-supported voice entry to convert spoken medical narration into text. The supplied document did not identify the software, ASR model, application version, device, microphone, operating system, network requirements, vocabulary adaptation, or whether processing occurred locally or through a cloud service. These technical details are essential for reproducibility and data-governance assessment.

The final paper should also specify whether timing included dictation only or the complete workflow of dictation, recognition, correction, formatting, EHR transfer, and clinician approval. The present analysis can support only the reported measure of text-production time; it cannot establish end-to-end documentation efficiency if correction and verification were excluded.

2.4 Outcome measurement

The primary outcome was documentation time standardised to 100 words of medical text. Standardisation was appropriate because total completion time can be misleading when notes differ in length. For each observation, the preferred calculation is: time per 100 words = total documentation time in minutes divided by total word count, multiplied by 100.

The source manuscript reported mean values of 8.8 minutes per 100 words for manual typing and 5.2 minutes per 100 words for ASR. It did not report standard deviations, medians, interquartile ranges, clinician-level averages, confidence intervals, or the distribution of paired differences. Therefore, this revision presents the comparison descriptively and does not claim statistical significance.

2.5 Statistical analysis

The descriptive percentage reduction was calculated as $[(8.8 - 5.2) / 8.8] \times 100 = 40.9\%$. The phrase “up to 41%” has been replaced with “a descriptive mean reduction of 40.9%,” because the available values are group means rather than a reported maximum.

For a definitive analysis, record-level observations should not be treated as fully independent because multiple records were produced by the same clinicians and clinicians were nested within institutions. The preferred analysis is a linear mixed-effects model with documentation method as a fixed effect and random intercepts for clinician and institution. If distributional assumptions are not met, a log-transformed mixed model or a paired clinician-level nonparametric analysis may be appropriate. Results should include the mean paired difference, 95% confidence interval, effect size, test statistic, exact p value, and sensitivity analyses.

2.6 Ethics, consent, and data governance

The supplied manuscript did not include an ethics committee name, approval number, approval date, clinician-consent procedure, patient-consent procedure or waiver, de-identification process, audio-retention policy, or data-storage location. Because the study involved clinical documentation and potentially identifiable voice or health information, these omissions are critical and must be corrected from the original study records.

Before submission, the authors must state whether actual patient encounters were recorded, whether patient identifiers were captured, whether audio or text was transmitted to an external provider, how long recordings were retained, who had access, and how the final records were verified. Clinician responsibility for reviewing and approving the final note should be explicit.

3. Results

3.1 Documentation time

Across more than 120 observed patient records, the reported mean time required to produce 100 words of medical documentation was 8.8 minutes with manual keyboard entry and 5.2 minutes with ASR-supported voice input. The absolute descriptive difference was 3.6 minutes per 100 words. Relative to manual typing, this corresponds to a 40.9% reduction in mean documentation time.

ISSN: 2181-3337 | SCIENTISTS.UZ

The result indicates that voice input was faster under the observed conditions. It does not, by itself, demonstrate that ASR improved note accuracy, completeness, patient safety, total encounter duration, patient throughput, or clinician well-being. No inferential statistical conclusion is possible from the summary values alone.

Documentation method	Mean min/100 words	Absolute difference	Relative difference	Interpretation
Manual keyboard entry	8.8	Reference	Reference	Observed comparison
ASR-supported voice input	5.2	−3.6 min/100 words	−40.9%	Descriptive reduction

Table 1. Reported documentation-time comparison. Variability and inferential statistics were not available in the supplied manuscript.

3.2 Evidence not reported

The supplied study report did not provide recognition accuracy, word error rate, clinically significant error rate, number of corrections, correction time, note completeness, physician satisfaction, patient outcomes, or implementation cost. These outcomes should not be implied from the time result.

4. Discussion

The observed reduction is operationally important because documentation is repeated across many consultations. A saving of 3.6 minutes per 100 words could accumulate when clinicians produce multiple notes each day. Nevertheless, the study did not measure whether saved documentation time was converted into additional consultations, shorter queues, longer patient interaction, or reduced after-hours work. Such consequences should be presented as plausible hypotheses for future evaluation rather than as demonstrated outcomes.

The direction of the finding is compatible with international research showing that documentation support can reduce time spent on notes. Tierney et al. (2024) reported favourable clinician experiences with ambient documentation, while more recent evaluations have found reductions in EHR note time and documentation burden after implementation of ambient systems (Duggan et al., 2025; Stults et al., 2025). Human-scribe studies also suggest that reducing continuous keyboard entry can improve physician workflow and, in some settings, productivity or patient throughput (Mishra et al., 2018; Walker et al., 2019).

Direct numerical comparison is inappropriate because these studies evaluated different technologies, specialties, healthcare systems, and outcomes. Ambient systems may listen to an entire encounter and generate structured notes, whereas conventional ASR usually transcribes explicit dictation. Human scribes perform additional coordination tasks that speech-recognition software may not reproduce (Tran et al., 2020). The Uzbek study therefore contributes context-specific preliminary evidence rather than proof that all speech-enabled systems yield a 40.9% benefit.

A major unresolved issue is the trade-off between speed and quality. Clinical ASR performance cannot be judged only by general word accuracy because errors in medications, measurements, negation, or diagnoses may be clinically consequential. Clinically aware evaluation frameworks have been proposed to better reflect the medical importance of transcription errors (Shor et al., 2023). Future Uzbek-language evaluation should report general word error rate together with a clinician-rated measure of clinically significant errors and the time required for correction.

Language adaptation is central to implementation. Uzbek medical communication may include Russian terminology, international drug names, abbreviations, and code-switching. A specialised lexicon should therefore be developed and tested by specialty. However, a lexicon alone will not solve workflow problems. The system must also integrate with EHR templates, authentication, data fields, and approval

ISSN: 2181-3337 | SCIENTISTS.UZ

procedures. Otherwise, time saved during dictation may be lost through copying, formatting, or duplicate entry.

Governance is equally important. Speech-enabled documentation can involve sensitive health information and biometric voice data. Institutions should establish patient-notification or consent procedures, data-minimisation rules, secure transmission and storage, retention limits, audit trails, and contractual restrictions on secondary data use. Final responsibility for the clinical record must remain with the clinician. Human review is necessary because even high-performing systems may produce omissions, substitutions, or plausible but incorrect text.

The findings should also be interpreted within the study's methodological limits. The number and characteristics of clinicians were not reported, the sample was drawn from only two institutions, the condition order was not described, and no measure of statistical uncertainty was available. Participants may have differed in typing skill, speaking rate, digital literacy, specialty, and familiarity with the system. A novelty or training effect may also have influenced the observed times. These factors limit causal inference and national generalisability.

5. Practical Implications

A phased pilot strategy is preferable to immediate large-scale deployment. Pilot sites should use predefined success criteria covering total documentation time, correction time, clinically significant errors, note completeness, clinician acceptance, patient consent, technical reliability, and cost per completed note.

Implementation should begin in specialties with relatively structured and repetitive documentation, but performance must be evaluated separately for each specialty. The ASR model should be adapted to Uzbek medical vocabulary and tested under realistic background-noise conditions.

The technology should operate within a clinician-in-the-loop workflow. ASR-generated text should remain a draft until reviewed and approved by the responsible clinician. Institutions should document responsibility for errors and maintain an audit trail of edits and approvals.

Integration with the EHR is necessary. A system that saves time during dictation but requires manual transfer, reformatting, or duplicate entry may not reduce total workload. End-to-end time, rather than dictation time alone, should be the primary implementation outcome.

6. Limitations

This revision is limited by the information contained in the supplied manuscript. It was not possible to verify the exact number of clinicians or records, institutional identities, study dates, participant characteristics, technical configuration, condition order, ethics approval, consent process, or record-level data.

The reported result is based on two mean values without measures of variability. Statistical significance, confidence intervals, and effect size cannot be reconstructed without the original dataset. The study also did not report accuracy, correction burden, note quality, patient outcomes, or cost.

The findings are drawn from two institutions in Bukhara and should not be generalised to all Uzbek healthcare facilities, specialties, languages, or digital infrastructures. Replication with prespecified protocols, larger multisite samples, and complete reporting is required.

7. Conclusion

In two functioning healthcare institutions in Bukhara, ASR-supported voice input was associated with a lower reported mean time for producing medical text than manual keyboard entry. Time per 100 words declined from 8.8 to 5.2 minutes, an absolute descriptive difference of 3.6 minutes and a relative reduction of 40.9%. This finding supports further evaluation of locally adapted ASR as a potential workflow tool in Uzbekistan. It should not yet be interpreted as proof of improved patient throughput, care quality, cost-effectiveness, or national scalability. A submission-ready evaluation requires complete participant and technical reporting, ethics and data-governance documentation, record-level statistical analysis, and simultaneous assessment of speed, correction burden, and clinical accuracy.

ISSN: 2181-3337 | SCIENTISTS.UZ

Declarations

Ethics approval and consent to participate: [INSERT the approving committee, approval number and date, clinician consent procedure, and patient consent or waiver from the original study records.]

Consent for publication: [INSERT applicable statement.]

Data availability: The record-level dataset and analysis materials were not included with the supplied manuscript. The authors should state where de-identified data and code can be accessed, or provide a justified restriction.

Competing interests: The author should declare any financial, institutional, or technical relationship with the ASR software provider.

Funding: [INSERT funding source or state that the study received no specific funding.]

Author contributions: Rajabbek Kaxramonovich Teshayev: conceptualisation, investigation, analysis, and manuscript preparation. Revise this statement if additional contributors qualify for authorship.

REFERENCES

1. Arndt, B. G., Beasley, J. W., Watkinson, M. D., Temte, J. L., Tuan, W.-J., Sinsky, C. A., & Gilchrist, V. J. (2017). Tethered to the EHR: Primary care physician workload assessment using EHR event log data and time-motion observations. Annals of Family Medicine, 15(5), 419–426. https://doi.org/10.1370/afm.2121
2. Duggan, M. J., Gervase, J., Schoenbaum, A., et al. (2025). Clinician experiences with ambient scribe technology to assist with documentation burden and efficiency. JAMA Network Open, 8(2), e2460637. https://doi.org/10.1001/jamanetworkopen.2024.60637
3. Hodgson, T., & Coiera, E. (2016). Risks and benefits of speech recognition for clinical documentation: A systematic review. Journal of the American Medical Informatics Association, 23(e1), e169–e179. https://doi.org/10.1093/jamia/ocv152
4. Hodgson, T., Magrabi, F., & Coiera, E. (2019). Speech recognition for clinical documentation from 1990 to 2018: A systematic review. Journal of the American Medical Informatics Association, 26(4), 324–338. https://doi.org/10.1093/jamia/ocy179
5. Khairat, S., Coleman, C., Ottmar, P., Jayachander, D. I., Bice, T., & Carson, S. S. (2020). Association of electronic health record use with physician fatigue and efficiency. JAMA Network Open, 3(6), e207385. https://doi.org/10.1001/jamanetworkopen.2020.7385
6. Melnick, E. R., Dyrbye, L. N., Sinsky, C. A., Trockel, M., West, C. P., Nedelec, L., Tutty, M. A., & Shanafelt, T. (2020). The association between perceived electronic health record usability and professional burnout among US physicians. Mayo Clinic Proceedings, 95(3), 476–487. https://doi.org/10.1016/j.mayocp.2019.09.024
7. Mishra, P., Kiang, J. C., & Grant, R. W. (2018). Association of medical scribes in primary care with physician workflow and patient experience. JAMA Internal Medicine, 178(11), 1467–1472. https://doi.org/10.1001/jamainternmed.2018.3956
8. Pearlman, K., Wan, W., Shah, S., & Laiteerapong, N. (2025). Use of an AI scribe and electronic health record efficiency. JAMA Network Open, 8(10), e2537000. https://doi.org/10.1001/jamanetworkopen.2025.37000
9. Shor, J., Bi, R. A., Venugopalan, S., Ibara, S., Goldenberg, R., & Rivlin, E. (2023). Clinical BERTScore: An improved measure of automatic speech recognition performance in clinical settings. arXiv. https://doi.org/10.48550/arXiv.2303.05737

ISSN: 2181-3337 | SCIENTISTS.UZ

10. Sinsky, C., Colligan, L., Li, L., Prgomet, M., Reynolds, S., Goeders, L., Westbrook, J., Tutty, M., & Blike, G. (2016). Allocation of physician time in ambulatory practice: A time and motion study in 4 specialties. Annals of Internal Medicine, 165(11), 753–760. https://doi.org/10.7326/M16-0961
11. Stults, C. D., Deng, S., Martinez, M. C., et al. (2025). Evaluation of an ambient artificial intelligence documentation platform for clinicians. JAMA Network Open, 8(5), e258614. https://doi.org/10.1001/jamanetworkopen.2025.8614
12. Teshayev, R. K. (2025). Improving healthcare management tools in Uzbekistan based on foreign experience [Doctoral dissertation, Westminster International University in Tashkent]. [VERIFY the exact registered dissertation title and repository record.]
13. Tierney, A. A., Gayre, G., Hoberman, B., Mattern, B., Ballesca, M., Kipnis, P., Liu, V., & Lee, K. (2024). Ambient artificial intelligence scribes to alleviate the burden of clinical documentation. NEJM Catalyst Innovations in Care Delivery, 5(3). https://doi.org/10.1056/CAT.23.0404
14. Tran, B. D., Chen, Y., Liu, S., & Zheng, K. (2020). How does medical scribes' work inform development of speech-based clinical documentation technologies? A systematic review. Journal of the American Medical Informatics Association, 27(5), 808–817. https://doi.org/10.1093/jamia/ocaa020
15. Walker, K., Ben-Meir, M., Dunlop, W., Rosler, R., West, A., O'Connor, G., Chan, T., Badcock, D., Putland, M., & Hansen, K. (2019). Impact of scribes on emergency medicine doctors' productivity and patient throughput: Multicentre randomised trial. BMJ, 364, l121. https://doi.org/10.1136/bmj.l121

ISSN: 2181-3337 | SCIENTISTS.UZ

ISSN: 2181-3337 | SCIENTISTS.UZ VOLUME 5 ISSUE 7 JULY 2026

MECHANISM OF DENTAL ENAMEL DEMINERALIZATION: THE ROLE OF ORGANIC ACIDS, PH, AND HYDROXYAPATITE DISSOLUTION

Ismoilov Iqboljon[1], **Aliyeva G**[2]
[1]CAMU International Medical University
[2]Scientific adviser

DOI: 10.67620/sai.57d0013

ABSTRACT
Dental enamel demineralization is the initiating physicochemical event in the development of a carious lesion. This structured narrative review synthesizes evidence on the sequence linking carbohydrate metabolism in dental biofilm, organic-acid production, local pH decline, loss of mineral saturation, and dissolution of enamel apatite. Human enamel is a highly mineralized, carbonated apatite tissue that remains in dynamic equilibrium with calcium and phosphate in saliva and plaque fluid. Acidogenic and aciduric members of the dental biofilm convert fermentable carbohydrates to organic acids, creating repeated periods of undersaturation at the tooth surface. Although an enamel critical pH near 5.5 is commonly cited, the threshold is not a universal constant because it depends on calcium, phosphate, fluoride, and mineral composition. Experimental evidence further indicates that dissolution kinetics depend not only on pH but also on solution saturation, acid activity, acid identity, exposure time, and enamel architecture. At matched saturation and acid activity, lactic acid can produce faster enamel mineral loss than acetic or propionic acid, while time-lapse imaging demonstrates anisotropic lesion progression governed by enamel microstructure. Early mineral loss can be reversed when the environment becomes supersaturated again. Saliva contributes buffering, clearance, and mineral ions; fluoride primarily inhibits demineralization and accelerates remineralization at apatite surfaces, whereas calcium-phosphate systems provide additional mineral precursors. The evidence supports prevention strategies that reduce the frequency of acid challenges and maintain favorable oral-fluid chemistry rather than treating pH 5.5 or any single bacterial species as an absolute determinant of caries.

ACCEPTED

02.08.26

Keywords: *dental enamel, demineralization, dental caries, organic acids, critical pH, hydroxyapatite, remineralization.*

CC BY

Introduction

Dental caries is a biofilm-mediated, diet-modulated, dynamic disease in which repeated episodes of mineral loss and mineral gain occur at the tooth surface. Its earliest hard-tissue change is not an abrupt destruction of enamel but a shift in the chemical equilibrium between enamel mineral and the surrounding oral fluids. Enamel is approximately 96% mineral by weight and consists predominantly of substituted, carbonated apatite rather than perfectly stoichiometric hydroxyapatite. This distinction is important because substitutions within biological apatite influence crystal solubility and make enamel dissolution

more chemically complex than the dissolution of an ideal laboratory crystal (Abou Neel et al., 2016; Robinson et al., 2000).

The modern ecological view of caries also requires caution against assigning the disease to a single microorganism. Dental biofilm contains a diverse community whose composition and metabolic activity change in response to environmental conditions. Frequent exposure to fermentable carbohydrate favors organisms and metabolic pathways that are both acidogenic and aciduric, thereby increasing the duration and intensity of low-pH conditions. Streptococcus mutans can contribute to this ecology, but it is one member of a broader dysbiotic community rather than a sufficient cause by itself (Takahashi & Nyvad, 2011).

The mechanistic sequence that links this ecological shift to enamel mineral loss can be organized into three interdependent stages: production and transport of organic acids, reduction of plaque-fluid and tooth-surface pH with loss of mineral saturation, and dissolution of apatite crystallites. These stages are influenced by salivary flow and buffering, calcium and phosphate concentrations, fluoride availability, lesion diffusion pathways, enamel structure, and the frequency and duration of dietary challenges. The purpose of this review is to explain that sequence at a physicochemical level, critically compare the evidence that supports it, and identify implications for prevention and remineralization.

Methods

A structured narrative literature review was used because the objective was mechanistic synthesis rather than estimation of a pooled treatment effect. Relevant literature was identified through targeted searches of PubMed/MEDLINE and publisher databases, supplemented by backward citation searching from key papers. Search concepts included combinations of “enamel demineralization,” “hydroxyapatite dissolution,” “critical pH,” “dental biofilm pH,” “organic acid enamel,” “lactic acid enamel,” “saliva remineralization,” “fluoride mechanism caries,” and “amorphous calcium phosphate enamel.” The literature set was updated through August 2026.

Priority was given to peer-reviewed primary experimental studies that directly measured mineral loss, lesion depth, microhardness, or dissolution kinetics, together with authoritative mechanistic and clinical reviews. Seminal studies published before 2000 were retained when they provided foundational kinetic or chemical evidence that remained directly relevant. Educational webpages and duplicate or substantially overlapping secondary publications were not used as independent evidence. Because the search was iterative and designed for a narrative review, no PRISMA flow diagram, pooled effect estimate, or formal risk-of-bias score was generated. Accordingly, conclusions are framed as a mechanistic synthesis of the included literature rather than as a systematic estimate of the entire evidence base.

Mechanistic Basis of Enamel Demineralization

Enamel Mineral and the Mineral-Solution Equilibrium

The conventional formula $Ca_{10}(PO_4)_6(OH)_2$ is useful for representing ideal hydroxyapatite, but human enamel is a substituted biological apatite containing carbonate and other ions. Its crystallites are organized within enamel rods and interrod enamel, with water-filled microscopic pathways between crystallites. These pathways allow diffusion of acids and dissolved ions even though mature enamel is acellular and highly mineralized (Abou Neel et al., 2016; Robinson et al., 2000).

At the tooth surface, the direction of mineral exchange depends on the degree of saturation of plaque fluid or saliva with respect to enamel mineral. When the surrounding fluid is saturated or supersaturated, net dissolution is not thermodynamically favored and mineral may precipitate onto residual crystal surfaces. When acid production lowers phosphate activity and the solution becomes undersaturated, the chemical driving force reverses and apatite dissolves. Thus, pH is important because it changes the distribution of phosphate species and the saturation state; pH does not act as an isolated variable independent of calcium, phosphate, fluoride, and mineral composition (Dawes, 2003; Margolis et al., 1999).

ISSN: 2181-3337 | SCIENTISTS.UZ

Organic-Acid Production in Dental Biofilm

Fermentable carbohydrates entering dental biofilm are metabolized through microbial glycolytic and related pathways. The acids generated during this metabolism reduce extracellular pH and create selective pressure favoring acid-tolerant organisms. The resulting ecological feedback can increase both the capacity of the biofilm to generate acid and its ability to remain metabolically active under acidic conditions (Takahashi & Nyvad, 2011). Frequent carbohydrate intake is therefore mechanistically important because it increases the number of acidification episodes and reduces the interval available for salivary neutralization and mineral recovery.

Lactic acid is commonly prominent during rapid carbohydrate fermentation, but plaque contains multiple organic acids, including acetic and propionic acids. Weak acids can exist in both dissociated and undissociated forms, and their behavior within plaque and porous enamel is not determined by bulk pH alone. Margolis et al. (1999) demonstrated this point experimentally. Human enamel sections were exposed to partially saturated acid solutions while pH, degree of saturation, and acid activity were controlled. In the direct acid comparison performed at pH 4.3, demineralization rates were similar in acetic and propionic acid solutions but were higher in lactic acid at the same enamel saturation and acid activity. The result does not establish that lactic acid is universally "more cariogenic" in vivo; rather, it shows that acid-specific interactions can modify dissolution kinetics after major thermodynamic variables are controlled.

pH Decline and the Critical-pH Concept

After a carbohydrate challenge, plaque pH typically falls rapidly as acids accumulate and then recovers more gradually as substrates are cleared and acids are buffered or metabolized. Repeated excursions into an undersaturated state constitute the chemical episodes during which net enamel mineral loss can occur. This dynamic pattern is more informative than a single resting-pH measurement because caries reflects the cumulative balance of multiple demineralization and remineralization periods (Featherstone, 2004; Takahashi & Nyvad, 2011).

A value near pH 5.5 is often used as a practical approximation for the "critical pH" of enamel. However, the term should not be interpreted as a fixed biological constant. Dawes (2003) emphasized that the pH at which oral fluid becomes unsaturated with respect to enamel varies inversely with the calcium and phosphate concentrations of that fluid. Fluoride and the variable composition of biological apatite can shift the equilibrium further. Therefore, one plaque sample may remain mineral-saturated at a pH at which another sample is already undersaturated. The clinically relevant question is not simply whether pH crossed 5.5, but how far the fluid moved from saturation, for how long, and how frequently the challenge was repeated.

Hydroxyapatite Dissolution at the Crystal Surface

Acidification promotes protonation of phosphate and hydroxyl groups associated with apatite. As phosphate species shift toward HPO_4^{2-} and $H_2PO_4^-$, the activity of PO_4^{3-} falls and the surrounding solution becomes less saturated with respect to enamel mineral. The equilibrium then shifts toward dissolution, releasing calcium and phosphate species from the crystal surface. A simplified reaction for ideal hydroxyapatite can be represented as $Ca_{10}(PO_4)_6(OH)_2 + 8H^+ \rightarrow 10Ca^{2+} + 6HPO_4^{2-} + 2H_2O$, although real enamel dissolution involves substituted apatite, multiple aqueous calcium-phosphate species, diffusion, and possible reprecipitation (Robinson et al., 2000).

This chemistry corrects a common oversimplification: hydrogen ions do not merely "push calcium out" of the lattice by direct one-for-one displacement. Protonation changes the solution chemistry and mineral saturation, and mineral ions are subsequently released as the system approaches a new equilibrium. Margolis et al. (1999) showed that enamel mineral loss increased as pH decreased and as the degree of saturation decreased, demonstrating that the magnitude of undersaturation is a major kinetic determinant.

ISSN: 2181-3337 | SCIENTISTS.UZ

Enamel Structure, Lesion Pattern, and Duration of Acid Exposure

Enamel does not dissolve uniformly. Its crystallites are organized into rods, interrod regions, and larger decussating structures such as Hunter-Schreger bands. Using time-lapse microradiography and polarized-light imaging, Harper et al. (2021) demonstrated that mineral loss progressed anisotropically and was influenced by intrinsic enamel architecture. In their acid model, progression from the surface toward dentin was faster than lateral progression, and demineralization preferentially followed Hunter-Schreger bands once the lesion front reached them. These findings support a diffusion-reaction model in which local structure modifies the route and rate of mineral loss.

A relatively intact surface layer can coexist with substantial subsurface mineral loss. Margolis et al. (1999) observed well-defined surface layers in lesions produced at pH 4.3 and 5.0, whereas lesions formed at pH 6.0 lacked an apparent surface layer under their experimental conditions. Such observations show that early caries is not equivalent to uniform surface etching. Selective dissolution, diffusion gradients, and reprecipitation can preserve the outer surface while mineral is lost beneath it (Robinson et al., 2000).

Exposure time is also important. Ersen et al. (2025) reported, in an in vitro human-enamel model, that longer demineralization periods were associated with increasing lesion depth and decreasing surface microhardness. Their design does not reproduce the fluctuating chemistry of the oral cavity, but it reinforces the general principle that duration of an acid challenge changes the magnitude of tissue damage. In vivo, this duration is strongly influenced by salivary clearance and buffering.

Remineralization and Protective Oral-Fluid Factors

Saliva

Saliva is central to the reversal of early mineral loss. Its protective functions include dilution and clearance of fermentable substrates and acids, bicarbonate-dependent buffering, contribution to the acquired pellicle, and maintenance of calcium and phosphate in solution. When acid production declines and pH recovers, these ions can support supersaturation and redeposition onto partially dissolved crystals (Dawes et al., 2015). This is why salivary dysfunction increases caries susceptibility even when enamel composition is unchanged.

The demineralization-remineralization balance is therefore temporal. A brief episode of undersaturation does not inevitably produce a permanent lesion if sufficient recovery follows. Repeated or prolonged acid challenges, especially when salivary flow is low, can shift the cumulative balance toward mineral loss. Conversely, preserving or stimulating salivary flow supports both chemical neutralization and mineral availability (Featherstone, 2004).

Fluoride

Fluoride should not be described simply as converting bulk enamel into fluorapatite. Its principal anticaries effects are topical and occur at the mineral-fluid interface. During an acidic challenge, low concentrations of fluoride associated with apatite surfaces can reduce mineral dissolution. When pH rises again, fluoride increases the driving force for precipitation of less soluble fluoridated apatite and accelerates remineralization. Higher topical fluoride exposures can also create calcium-fluoride-like reservoirs that release fluoride during subsequent acidic challenges (Buzalaf et al., 2011).

This mechanism explains why regular exposure to topical fluoride is effective even though the fluoride concentration incorporated throughout the enamel crystal lattice is relatively small. The important clinical objective is to maintain biologically useful fluoride availability at the tooth-biofilm-fluid interface during repeated cycles of acidification and recovery.

Calcium-Phosphate Remineralizing Systems

Calcium-phosphate systems act through a different but complementary principle: they increase the availability of calcium and phosphate precursors that can participate in mineral reprecipitation. Amorphous calcium phosphate (ACP) is of interest because it can serve as a transient precursor to apatite, but its

ISSN: 2181-3337 | SCIENTISTS.UZ

instability in aqueous environments requires stabilization or delivery strategies. Yan et al. (2022) reviewed approaches including casein phosphopeptides, amelogenin-related systems, polymers, and other stabilizers designed to maintain ACP in a reactive state.

These agents should not be presented as mechanistically interchangeable with fluoride or as established substitutes for fluoride-based prevention. A recent systematic review of randomized trials evaluating CPP-ACP and bioactive glass for early enamel lesions found remineralizing potential but substantial heterogeneity and generally low-to-moderate certainty, with evidence insufficient to replace fluoride as the standard preventive therapy (Mishra et al., 2026). Their most defensible role is therefore as adjunctive or context-specific strategies rather than universal alternatives.

Comparative Synthesis and Critical Appraisal

The strongest mechanistic evidence in the literature comes from controlled physicochemical and imaging studies in which pH, acid activity, degree of saturation, or exposure time can be manipulated independently. Margolis et al. (1999) demonstrated that enamel dissolution kinetics depend simultaneously on pH, mineral saturation, and acid species. Harper et al. (2021) extended the mechanistic picture by showing that enamel architecture introduces directional differences in lesion progression. These studies provide direct evidence for causal chemical and structural determinants, but they remain laboratory models.

Clinical translation is more complex because oral biofilm is spatially heterogeneous and saliva continuously changes the local concentrations of acids, buffers, calcium, phosphate, and fluoride. Consequently, it would be inappropriate to infer a patient's caries risk from acid identity or a single pH threshold alone. Likewise, the observation that lactic acid produced faster mineral loss than acetic or propionic acid under matched in vitro conditions should be interpreted as evidence of acid-specific kinetics, not as a basis for assigning dietary recommendations to a particular acid species without clinical validation.

The evidence also clarifies the relationship between remineralizing interventions. Fluoride, calcium-phosphate systems, salivary support, and dietary modification act at different points within the same chemical cycle. Fluoride modifies dissolution and reprecipitation at apatite surfaces; calcium-phosphate agents increase mineral-ion availability; saliva governs buffering, clearance, and supersaturation; and dietary behavior determines the frequency of substrate-driven acid challenges. A mechanism-based prevention strategy should therefore combine these approaches according to caries risk rather than treating them as interchangeable products.

Table 1

Key Variables Governing Enamel Demineralization

Variable	Evidence-based interpretation	Representative source
Biofilm acid production	Fermentable carbohydrate drives acid production and selects for an acidogenic/aciduric ecology; no single species is sufficient to explain caries.	Takahashi & Nyvad (2011)
pH and saturation	A pH near 5.5 is only an approximation. The actual dissolution threshold depends on calcium, phosphate, fluoride, and mineral composition.	Dawes (2003)
Acid identity	At matched enamel saturation and acid activity at pH 4.3, lactic acid produced faster mineral loss than acetic or propionic acid; acetic and propionic rates were similar.	Margolis et al. (1999)
Enamel structure	Mineral loss is anisotropic; intrinsic rod architecture and Hunter-Schreger bands influence lesion progression.	Harper et al. (2021)
Exposure time	Longer sustained acid exposure increases lesion depth and reduces surface microhardness in vitro.	Ersen et al. (2025)

ISSN: 2181-3337 | SCIENTISTS.UZ

Variable	Evidence-based interpretation	Representative source
Remineralization	Recovery requires a return toward supersaturation. Saliva supplies buffering and mineral ions; fluoride inhibits dissolution and accelerates reprecipitation.	Dawes et al. (2015); Buzalaf et al. (2011)

Note. The table summarizes mechanistic evidence and does not imply that any single variable independently determines clinical caries risk.

Clinical Implications

The mechanistic evidence supports prevention strategies aimed at reducing the cumulative time during which enamel is exposed to an undersaturated environment. Reducing the frequency of fermentable-carbohydrate intake can reduce repeated acidification episodes; maintaining normal salivary flow supports clearance, buffering, and mineral availability; and regular topical fluoride exposure increases resistance to demineralization while promoting remineralization. These measures address the chemistry of the disease rather than relying solely on removal of a named microorganism (Buzalaf et al., 2011; Dawes et al., 2015; Featherstone, 2004).

For early noncavitated lesions, preservation of the surface layer is clinically important because residual mineral provides a scaffold for remineralization. Once structural integrity is lost and cavitation develops, simple mineral replacement becomes less capable of restoring original anatomy. This distinction supports early detection and nonoperative management of lesions that remain cleansable and structurally intact.

Limitations of the Evidence

Several limitations constrain interpretation. First, many mechanistic studies use sectioned or polished enamel exposed to simplified acid solutions, which cannot reproduce the spatial heterogeneity, microbial metabolism, salivary flow, pellicle, and intermittent dietary challenges of the oral cavity. Second, the frequently cited critical pH is context dependent; reporting it as an absolute threshold can obscure clinically important variation in mineral saturation. Third, evidence on newer calcium-phosphate systems remains heterogeneous, and in vitro remineralization does not automatically predict superior clinical outcomes. Finally, this paper is a structured narrative review rather than a systematic review; its purpose is to integrate mechanisms, not to establish exhaustive effect estimates or formal certainty ratings for every intervention.

These limitations also define useful research directions. Experimental work should increasingly combine controlled mineral chemistry with realistic biofilm and salivary conditions, and clinical studies should connect measurable physicochemical variables—such as plaque-fluid saturation, acid-challenge duration, and fluoride availability—to lesion progression over time. Such designs would strengthen the bridge between dissolution kinetics and patient-level outcomes.

Conclusion

Dental enamel demineralization is best understood as a dynamic mineral-solution process produced by the interaction of biofilm metabolism, oral-fluid chemistry, and enamel structure. Fermentable carbohydrates support acid production within a dysbiotic biofilm; the resulting fall in pH reduces phosphate activity and can make plaque fluid undersaturated with respect to enamel; and this undersaturation drives dissolution of substituted apatite crystals. The rate of mineral loss is modified by the degree of saturation, acid activity and identity, exposure duration, diffusion pathways, and enamel architecture.

The same framework explains why early lesions can recover. When acid production decreases and pH rises, saliva restores buffering and provides calcium and phosphate, while fluoride inhibits further dissolution and favors precipitation of less soluble fluoridated mineral. Calcium-phosphate technologies may supplement, but not automatically replace, fluoride. Effective prevention therefore depends on shifting

ISSN: 2181-3337 | SCIENTISTS.UZ

repeated demineralization-remineralization cycles toward net mineral gain through dietary control, salivary support, fluoride, and appropriate adjuncts.

REFERENCES

1. Abou Neel, E. A., Aljabo, A., Strange, A., Ibrahim, S., Coathup, M., Young, A. M., Bozec, L., & Mudera, V. (2016). Demineralization-remineralization dynamics in teeth and bone. *International Journal of Nanomedicine, 11*, 4743–4763. https://doi.org/10.2147/IJN.S107624
2. Buzalaf, M. A. R., Pessan, J. P., Honório, H. M., & ten Cate, J. M. (2011). Mechanisms of action of fluoride for caries control. In M. A. R. Buzalaf (Ed.), *Fluoride and the oral environment* (pp. 97–114). Karger. https://doi.org/10.1159/000325151
3. Dawes, C. (2003). What is the critical pH and why does a tooth dissolve in acid? *Journal of the Canadian Dental Association, 69*(11), 722–724.
4. Dawes, C., Pedersen, A. M. L., Villa, A., Ekström, J., Proctor, G. B., Vissink, A., Aframian, D., McGowan, R., Aliko, A., Narayana, N., Sia, Y. W., Joshi, R. K., Jensen, S. B., Kerr, A. R., & Wolff, A. (2015). The functions of human saliva: A review sponsored by the World Workshop on Oral Medicine VI. *Archives of Oral Biology, 60*(6), 863–874. https://doi.org/10.1016/j.archoralbio.2015.03.004
5. Ersen, M. C., Çelik, Z. C., Oztas, M., Sahin, M., Tagtekin, D., & Yanikoglu, F. (2025). Impact of demineralization time on enamel microhardness reduction and lesion depth: An in vitro study. *Cureus, 17*(2), e79441. https://doi.org/10.7759/cureus.79441
6. Featherstone, J. D. B. (2004). The caries balance: The basis for caries management by risk assessment. *Oral Health & Preventive Dentistry, 2*(Suppl. 1), 259–264.
7. Harper, R. A., Shelton, R. M., James, J. D., Salvati, E., Besnard, C., Korsunsky, A. M., & Landini, G. (2021). Acid-induced demineralisation of human enamel as a function of time and pH observed using X-ray and polarised light imaging. *Acta Biomaterialia, 120*, 240–248. https://doi.org/10.1016/j.actbio.2020.04.045
8. Margolis, H. C., Zhang, Y. P., Lee, C. Y., Kent, R. L., Jr., & Moreno, E. C. (1999). Kinetics of enamel demineralization in vitro. *Journal of Dental Research, 78*(7), 1326–1335. https://doi.org/10.1177/00220345990780070701
9. Mishra, A., Sharan, J., & Sivakumar, I. (2026). Remineralising efficacy of bioactive glass and casein phosphopeptide amorphous calcium phosphate in white spot lesions or early enamel caries: A systematic review of randomised controlled trials. *Japanese Dental Science Review, 62*, 205–215. https://doi.org/10.1016/j.jdsr.2026.05.004
10. Robinson, C., Shore, R. C., Brookes, S. J., Strafford, S., Wood, S. R., & Kirkham, J. (2000). The chemistry of enamel caries. *Critical Reviews in Oral Biology & Medicine, 11*(4), 481–495. https://doi.org/10.1177/10454411000110040601
11. Takahashi, N., & Nyvad, B. (2011). The role of bacteria in the caries process: Ecological perspectives. *Journal of Dental Research, 90*(3), 294–303. https://doi.org/10.1177/0022034510379602
12. Yan, J., Yang, H., Luo, T., Hua, F., & He, H. (2022). Application of amorphous calcium phosphate agents in the prevention and treatment of enamel demineralization. *Frontiers in Bioengineering and Biotechnology, 10*, 853436. https://doi.org/10.3389/fbioe.2022.853436

ISSN: 2181-3337 | SCIENTISTS.UZ

ISSN: 2181-3337 | SCIENTISTS.UZ VOLUME 5 ISSUE 7 JULY 2026

PSYCHOMOTOR THERAPY COMBINED WITH COGNITIVE-BEHAVIORAL TECHNIQUES FOR NEUROTIC SYMPTOMS IN VASCULAR DEMENTIA: A PROSPECTIVE COMPARATIVE PILOT STUDY

Karakhonova Sarvinoz

Department of Neurology and Medical Psychology, Tashkent State Medical University, Tashkent, Uzbekistan. Email: s.karakhanova@tashmeduni.uz

DOI: 10.67620/sai.57d0014

ABSTRACT

Neuropsychiatric symptoms are common in vascular cognitive impairment and can complicate rehabilitation and long-term care. This 30-day prospective comparative pilot study evaluated two multimodal regimens for neurotic symptoms in patients with mild-to-moderate vascular dementia. Forty-six patients were enrolled, and 42 had complete baseline and end-of-treatment records for comparative analysis: 20 received basic neuroprotective therapy, rational psychotherapy, and temgicoluril (Adaptol), whereas 22 received basic neuroprotective therapy, structured psychomotor therapy combined with cognitive-behavioral techniques, and the same temgicoluril regimen. The source manuscript contained internally inconsistent percentages and mislabeled figure rows; therefore, percentages were recalculated from stated denominators and post-treatment severity counts were provisionally reconstructed by matching group sample sizes and exact baseline distributions. Baseline distributions of the study-defined Heck-Hess symptom categories did not differ between groups, $\chi^2(2, N = 42) = 0.43$, $p = .806$, Cramér's $V = .10$. Reconstructed day-30 distributions also did not significantly differ, $\chi^2(2, N = 42) = 1.03$, $p = .597$, Cramér's $V = .16$; the proportion classified as normal was 70.0% in the rational-psychotherapy group and 77.3% in the psychomotor/cognitive-behavioral group (Fisher's exact $p = .730$). Both groups showed favorable descriptive shifts, but superiority of the psychomotor regimen was not established. These findings support further study of integrated motor-cognitive approaches using a preregistered, adequately powered randomized design with validated outcomes, standardized therapy exposure, blinded assessment, and longer follow-up.

ACCEPTED

07.08.26

Keywords: *vascular dementia, vascular cognitive impairment, psychomotor therapy, neuropsychiatric symptoms, cognitive-behavioral therapy, temgicoluril.*

CC BY

Introduction

Vascular dementia is a major clinical form within the broader spectrum of vascular cognitive impairment (VCI), in which cerebrovascular disease contributes to decline in cognition and everyday functioning. Contemporary guidance emphasizes the heterogeneity of VCI and the need for individualized management that addresses vascular risk, cognition, mood, behavior, functional ability, and caregiver needs (Heart and Stroke Foundation of Canada, 2024; O'Brien & Thomas, 2015). The World Health

Organization (2026a) also notes that dementia commonly includes changes in mood, emotional control, behavior, or motivation in addition to cognitive decline.

Behavioral and psychological symptoms can be substantial in vascular syndromes. A recent systematic review and meta-analysis found that apathy, depression, irritability, anxiety, sleep disturbance, and other neuropsychiatric manifestations occur across VCI subtypes, although prevalence varies by clinical phenotype (Santos et al., 2025). Such symptoms may amplify subjective somatic complaints, interfere with rehabilitation, reduce participation in care, and complicate communication when cognitive flexibility and verbal abstraction are already impaired.

Nonpharmacological interventions are therefore clinically attractive because they can target function and behavior without adding medication burden. Evidence in vascular cognitive disorders remains limited but suggests that structured exercise, cognitive stimulation, and combined motor-cognitive programs may produce benefits in selected cognitive, functional, or neuropsychiatric outcomes (Liu-Ambrose et al., 2016; Piras et al., 2017; Valencia-Quiroz et al., 2025). These approaches are consistent with broader recommendations to incorporate rehabilitation, physical activity, cognitive engagement, and person-centered nonpharmacological management into VCI care (Heart and Stroke Foundation of Canada, 2024; World Health Organization, 2026b).

Psychomotor therapy uses guided movement, breathing, relaxation, body awareness, and sensorimotor tasks to engage both motor and emotional regulation. Previous local work has also examined psychocorrection and psychodiagnostic approaches in psycho-emotional disorders and vascular dementia (Karakhonova, 2022; Karakhonova & Ernayeva, 2025). However, the independent efficacy of psychomotor therapy in vascular dementia has not been established, and interpretation is especially difficult when psychomotor techniques are delivered together with cognitive-behavioral methods and pharmacotherapy.

The present study compared rational psychotherapy plus temgicoluril with psychomotor therapy combined with cognitive-behavioral techniques plus the same temgicoluril regimen. The primary aim was to determine whether the two treatment approaches differed in neurotic symptom severity after 30 days. A secondary aim was to describe the autonomic and neurological findings observed at baseline.

Method

Design and Setting

This prospective comparative clinical study was conducted in the First and Second Neurological Departments of Clinic No. 1 of Tashkent Medical Academy. Treatment lasted 30 days, with assessments at baseline (Days 1-3) and at the end of treatment (Days 27-30). Details of random-sequence generation, allocation concealment, and assessor blinding were not described; therefore, the study is presented as a prospective comparative investigation.

Participants

Forty-six patients with vascular dementia and secondary neurotic symptoms were enrolled. Participants were 62-64 years of age, with a reported mean age of 63.5 years. Forty-two patients had complete baseline and follow-up assessments and were included in the comparative analysis. Four participants had incomplete follow-up records; their reasons for non-completion were not documented.

Inclusion criteria were (a) a diagnosis of mild-to-moderate vascular dementia according to ICD-10 criteria, (b) comorbid neurotic symptoms identified through medical-psychological screening, and (c) written informed consent from the patient or a legally authorized representative. Exclusion criteria were severe cognitive impairment defined as a Mini-Mental State Examination score below 10 with inability to communicate, acute cerebrovascular events or severe decompensated systemic disease, primary psychotic disorders, and severe endogenous depression.

Treatment Conditions

Group 1 (n = 20) received basic neuroprotective therapy, rational psychotherapy, and temgicoluril (Adaptol) 300-500 mg twice daily, with dose selected according to baseline anxiety intensity. Rational psychotherapy was delivered in 45- to 60-minute sessions once every 3-4 days, for a total of approximately 6-8 sessions during the 30-day course.

Group 2 (n = 22) received basic neuroprotective therapy, psychomotor therapy combined with cognitive-behavioral techniques, and the same temgicoluril dose range. Psychomotor components included breathing exercises, progressive muscle relaxation, sensorimotor coordination tasks, and structured movement-based emotional-regulation exercises. The number, frequency, and duration of Group 2 sessions

ISSN: 2181-3337 | SCIENTISTS.UZ

were not recorded in sufficient detail to confirm equal therapist-contact time between the two treatment groups.

Because both groups received temgicoluril, the study design cannot estimate the independent effect of that medication. Published evidence on temgicoluril/Adaptol remains largely observational and regionally conducted rather than based on a large international randomized evidence base (Taube et al., 2025). In this study, temgicoluril was therefore treated as a common co-intervention rather than as an independently evaluated treatment.

Measures

Neurological and autonomic examinations included tendon reflexes, skull-percussion tenderness, sensitivity at Vaale points, Danzig-Kunakov and Danini-Ashner signs, coordination tests, Romberg testing, dermographism, pupillary findings, sweating, and sensory symptoms. A medical-psychological questionnaire developed by Ibodullayev (Patent No. 001031) was also used, although sufficient validation information was not available for independent appraisal.

Neurotic symptoms were assessed with a 40-item binary Heck-Hess/BFB-type screening questionnaire. Scores were grouped into three study-defined categories: less than 13 (normal/non-neurotic), 13-24 (mild/situational), and 25-40 (pronounced). Because the exact language version and validation characteristics used in this cohort were not documented, these thresholds were used as analytic categories rather than as independent diagnostic criteria. Questionnaire categories were therefore interpreted as indicators of symptom severity and not as stand-alone clinical diagnoses.

Statistical Analysis

Categorical findings were summarized as absolute counts and percentages. Percentages for baseline autonomic and neurological findings were calculated using the enrolled cohort (N = 46). Descriptive baseline frequencies were reported without inferential p values when no prespecified comparison or null hypothesis was defined.

Neurotic symptom severity was analyzed in three categories at baseline and day 30 for Group 1 (n = 20) and Group 2 (n = 22). Analyses were based on the group-level counts available at each assessment. Because patient-level transition data were not available, within-person pre-post inferential testing was not performed.

Between-group differences in the three-category distributions were examined with Pearson chi-square tests and summarized with Cramér's V. Fisher's exact test was used for the dichotomous comparison of normal versus non-normal status because of small cell counts. Two-sided p values below .05 were considered statistically significant. Changes over time are described as shifts in group-level proportions rather than as statistically tested within-person change.

Ethical Considerations

Written informed consent was obtained from patients or their legally authorized representatives. The ethics committee approval number and date, trial registration identifier, capacity-assessment procedure, and formal adverse-event reporting plan were not reported.

Results

Participant Flow and Baseline Characteristics

Of 46 enrolled participants, 42 completed both baseline and end-of-treatment assessments and were included in the comparative analysis (Group 1, n = 20; Group 2, n = 22). The four incomplete cases represented 8.7% of the enrolled cohort. Their group assignments and reasons for missing follow-up were not reported, so attrition bias cannot be excluded. Participants were 62-64 years of age, with a reported mean age of 63.5 years.

Table 1

Baseline Autonomic Findings in the Enrolled Cohort

Finding	n	%
Red dermographism	34	73.9
White dermographism	8	17.4

ISSN: 2181-3337 | SCIENTISTS.UZ

Finding	n	%
Miosis	36	78.3
Mydriasis	6	13.0
Hyperhidrosis	40	87.0
Danini-Ashner reflex change	37	80.4

Note. Percentages were calculated from the reported counts using the initially enrolled cohort (N = 46).

The most frequently recorded autonomic findings were hyperhidrosis (87.0%), Danini-Ashner reflex changes (80.4%), and miosis (78.3%). Red dermographism was recorded in 73.9% of the enrolled cohort. These findings are descriptive; the study did not include a healthy control group or a prespecified inferential comparison for baseline autonomic prevalence.

Table 2

Baseline Neurological and Sensory Findings in the Enrolled Cohort

Finding	n	%
Tenderness on skull percussion	44	95.7
Positive Danzig-Kunakov sign	33	71.7
Tenderness at Vaale points	22	47.8
Increased tendon reflexes	35	76.1
Mild intention tremor on coordination testing	19	41.3
Mild staggering in the Romberg position	25	54.3
Hyperesthesia	28	60.9
Paresthesia	25	54.3
Hyperhidrosis	18	39.1

Note. Percentages were recalculated using N = 46. The original table contained percentages and p values that were not supported by the stated counts or a defined comparison.

Tenderness on skull percussion (95.7%) and increased tendon reflexes (76.1%) were among the most frequently reported neurological signs. Hyperesthesia was recorded in 60.9% and paresthesia in 54.3% of enrolled participants when percentages were calculated using N = 46. These findings describe the neurological and sensory profile of the enrolled cohort and were not compared with a healthy control group.

Neurotic Symptom Categories

Table 3

Study-Defined Neurotic Symptom Categories at Baseline and Day 30

Time and group	Pronounced, n (%)	Mild, n (%)	Normal, n (%)
Group 1 baseline (n = 20)	4 (20.0)	7 (35.0)	9 (45.0)
Group 2 baseline (n = 22)	6 (27.3)	8 (36.4)	8 (36.4)
Group 1 day 30 (n = 20)	1 (5.0)	5 (25.0)	14 (70.0)
Group 2 day 30 (n = 22)	2 (9.1)	3 (13.6)	17 (77.3)

ISSN: 2181-3337 | SCIENTISTS.UZ

Note. The category thresholds were study-defined. Day-30 counts are a provisional reconstruction from the embedded Figure 2 data after matching group sample sizes and exact narrative baseline distributions. Raw-data confirmation is required before submission.

At baseline, the three-category distribution did not differ significantly between groups, $\chi^2(2, N = 42) = 0.43$, $p = .806$, Cramér's $V = .10$. The proportion categorized as normal was 45.0% in Group 1 and 36.4% in Group 2; Fisher's exact comparison of normal versus non-normal status was not significant, $p = .754$.

At day 30, the three-category distribution did not differ significantly between groups, $\chi^2(2, N = 42) = 1.03$, $p = .597$, Cramér's $V = .16$. Normal-category status was present in 14 of 20 participants (70.0%) in Group 1 and 17 of 22 participants (77.3%) in Group 2. Fisher's exact test for normal versus non-normal status yielded $p = .730$. The corresponding odds ratio for normal status in Group 2 relative to Group 1 was 1.46 (approximate 95% CI [0.37, 5.80]), indicating substantial uncertainty around the between-group effect.

Descriptively, the proportion classified as normal increased by 25.0 percentage points in Group 1 and by 40.9 percentage points in Group 2, while pronounced-category proportions decreased in both groups. Because individual category transitions were not available, these changes should be interpreted as group-level descriptive shifts. The between-group analyses did not demonstrate statistically significant superiority of the psychomotor/cognitive-behavioral regimen over rational psychotherapy at 30 days.

Discussion

Both treatment regimens were associated with favorable descriptive shifts in neurotic symptom categories during the 30-day treatment period. However, the end-of-treatment difference between groups was not statistically significant. Normal-category status was observed in 70.0% of Group 1 and 77.3% of Group 2, and the effect estimate remained imprecise because of the small sample size. These results suggest a possible clinical benefit of both multimodal approaches while emphasizing the need for a larger study to determine whether the psychomotor/cognitive-behavioral program offers an additional advantage.

A cautious interpretation is still clinically plausible. Integrated motor-cognitive and cognitive stimulation interventions have shown potential in vascular cognitive disorders, although the evidence base is heterogeneous. Liu-Ambrose et al. (2016) reported cognitive benefits during a structured aerobic intervention in adults with mild VCI, while Piras et al. (2017) found benefits of cognitive stimulation therapy in vascular dementia. More recently, Valencia-Quiroz et al. (2025) described improvements or stability in cognitive, psychomotor, and selected neuropsychiatric outcomes after a combined psychomotor and cognitive stimulation program. These studies support continued investigation of body-based and cognitive interventions, but they do not justify assuming that any specific psychomotor protocol is superior without a properly controlled trial.

The current intervention contrast is also not a pure test of psychomotor therapy. Group 2 received psychomotor therapy combined with cognitive-behavioral techniques, whereas Group 1 received rational psychotherapy. Thus, any difference would reflect the entire psychotherapy package, not psychomotor therapy in isolation. In addition, Group 1 session exposure was described in detail, but Group 2 session frequency and duration were not. Unequal therapist contact is therefore a possible confounder. A future trial should manualize both interventions, match contact time, record therapist fidelity, and prespecify whether the scientific question concerns psychomotor therapy alone or an integrated psychomotor-CBT package.

The medication component requires similar caution. Both groups received temgicoluril, so the study cannot determine whether symptom changes were attributable to medication, psychotherapy, nonspecific treatment effects, or their combination. A 2025 noninterventional study reported improvement in anxiety and somatic symptoms during Adaptol use, but its observational design and disclosed manufacturer-related conflicts underscore the need for controlled evidence (Taube et al., 2025). For the present study, the medication is best treated as a common co-intervention rather than a tested causal factor.

Consistent use of the enrolled cohort denominator (N = 46) provided a clearer description of baseline autonomic and sensory findings. Hyperesthesia was present in 60.9% of participants and paresthesia in 54.3%. These frequencies indicate that sensory symptoms were common in the cohort, although their clinical significance should be interpreted within the broader neurological and psychological assessment.

ISSN: 2181-3337 | SCIENTISTS.UZ

Measurement validity is another consideration. The study used a 40-item Heck-Hess/BFB-type questionnaire, but the language version, validation sample, reliability characteristics, and supporting citation for the three severity thresholds were not documented. Screening measures should not be treated as equivalent to clinical diagnoses. Future work should therefore use a validated neuropsychiatric or anxiety measure appropriate for older adults with cognitive impairment, report reliability in the study sample where feasible, and distinguish screening severity from diagnostic terminology. Contemporary VCI guidance also supports multidomain assessment rather than reliance on a single symptom scale (Heart and Stroke Foundation of Canada, 2024).

Limitations

The study has several limitations that constrain causal interpretation. The sample was small and follow-up lasted only 30 days. Four enrolled participants were not included in the complete-case comparison, and their group assignments and reasons for missing follow-up were not documented. Details of randomization, allocation concealment, and assessor blinding were unavailable. Group 2 treatment exposure was incompletely specified, and actual temgicoluril dose distributions by group were not reported. The Heck-Hess symptom categories were study-defined and were not linked to a documented validated language version. Functional adaptation, adherence, and quality of life were not measured with reported instruments, and adverse-event results were not available. In addition, the analysis relied on group-level outcome counts rather than patient-level transition data. These limitations make the findings exploratory and preclude a definitive efficacy conclusion.

Implications for Future Research

A confirmatory study should use a preregistered parallel-group randomized design with concealed allocation, blinded outcome assessment where feasible, and an a priori sample-size calculation. The psychomotor protocol should be manualized and matched to the comparison intervention for therapist-contact time. Outcomes should include a validated neuropsychiatric or anxiety measure, a global cognitive measure, activities of daily living, functional mobility, quality of life, treatment adherence, and adverse events. Follow-up of at least 3-6 months would help determine whether short-term symptom changes persist. Patient-level data should be retained in a form that permits intention-to-treat analysis and transparent reporting consistent with clinical-trial standards.

Conclusion

During 30 days of multimodal treatment, both groups showed descriptive shifts toward lower study-defined neurotic symptom categories. The end-of-treatment data did not demonstrate statistically significant superiority of psychomotor therapy combined with cognitive-behavioral techniques over rational psychotherapy when both regimens also included temgicoluril and basic neuroprotective treatment. Psychomotor and motor-cognitive approaches remain promising candidates for further study in vascular dementia. Larger randomized studies with validated outcomes, standardized treatment exposure, and longer follow-up are needed to determine the magnitude and durability of any additional benefit.

Declarations

Ethics approval and consent to participate. Written informed consent was obtained from participants or legally authorized representatives. The ethics committee name, approval number, approval date, and capacity-assessment procedure were not reported.

Trial registration. No trial registration identifier was reported.

Funding. Funding information was not reported.

Conflicts of interest. A conflict-of-interest statement was not reported.

Data availability. The analysis was based on group-level study data; patient-level data were not available for the present analysis.

REFERENCES

1. Heart and Stroke Foundation of Canada. (2024). *Canadian Stroke Best Practice Recommendations: Vascular cognitive impairment* (7th ed.). https://www.strokebestpractices.ca/recommendations/vascular-cognitive-impairment

ISSN: 2181-3337 | SCIENTISTS.UZ

2. Karakhonova, S. A. (2022). The significance of the application of psycho-correction methods in the treatment of psycho-emotional disorder. *European Journal of Modern Medicine and Practice, 2*(12), 59-64.
3. Karakhonova, S. A., & Ernayeva, G. H. (2025). Evaluation of the effectiveness of psychodiagnostic methods in vascular dementia. *Integration of Education and Science: Global Challenges and Solutions, 1*(2), 1090-1094. https://worldconferences.us/index.php/iesg/article/view/781
4. Liu-Ambrose, T., Best, J. R., Davis, J. C., Eng, J. J., Lee, P. E., Jacova, C., Boyd, L. A., Brasher, P. M., Munkacsy, M., Cheung, W., & Hsiung, G.-Y. R. (2016). Aerobic exercise and vascular cognitive impairment: A randomized controlled trial. *Neurology, 87*(20), 2082-2090. https://doi.org/10.1212/WNL.0000000000003332
5. O'Brien, J. T., & Thomas, A. (2015). Vascular dementia. *The Lancet, 386*(10004), 1698-1706. https://doi.org/10.1016/S0140-6736(15)00463-8
6. Piras, F., Carbone, E., Faggian, S., Salvalaio, E., Gardini, S., & Borella, E. (2017). Efficacy of cognitive stimulation therapy for older adults with vascular dementia. *Dementia & Neuropsychologia, 11*(4), 434-441. https://doi.org/10.1590/1980-57642016dn11-040014
7. Santos, A. de P., Lôbo, A. de O. M., Santos, C. B. A. L., Carvalho, M. G. N. C., Ribeiro, M. M. C., Rodrigues, A. E. O., Santos, S. M., Costa Filho, B. H. C., Welkovic Junior, S., de Melo, E. S., & Barbosa, B. J. A. P. (2025). Behavioral and psychological symptoms of dementia associated with vascular impairment: A systematic review and meta-analysis. *Brazilian Journal of Psychiatry, 47*, e20254225. https://doi.org/10.47626/1516-4446-2025-4225
8. Taube, M., Dansone, G., & Troshina, Y. (2025). Efficacy of Adaptol 500 mg tablets in patients with anxiety and somatic symptoms of anxiety disorder: A noninterventional study. *Journal of Clinical Medicine, 14*(22), 7972. https://doi.org/10.3390/jcm14227972
9. Valencia-Quiroz, K., Maldonado-Paz, G., & Hernández-Galván, A. (2025). Effects of a coordinated program of psychomotricity and cognitive stimulation in vascular mild cognitive impairment and vascular dementia. *Dementia & Neuropsychologia, 19*, e20250293. https://doi.org/10.1590/1980-5764-DN-2025-0293
10. World Health Organization. (2026a, July 3). *Dementia*. https://www.who.int/news-room/fact-sheets/detail/dementia
11. World Health Organization. (2026b). *Risk reduction of cognitive decline and dementia: WHO guidelines* (2nd ed.). https://www.who.int/publications/i/item/9789240123557

ISSN: 2181-3337 | SCIENTISTS.UZ

ISSN: 2181-3337 | SCIENTISTS.UZ VOLUME 5 ISSUE 7 JULY 2026

EARLY OUTCOMES OF LIVING-RELATED DONOR KIDNEY TRANSPLANTATION WITH MULTIPLE RENAL ARTERIES: A RETROSPECTIVE COHORT STUDY WITH AN MSCT-GUIDED ARTERIAL RECONSTRUCTION FRAMEWORK

A. S. Suyumov[1], Z. T. Matkarimov[1], M. O. Rustamov[1], D. N. Komilova[1]

[1]State Institution "Republican Specialized Scientific and Practical Medical Center of Surgery named after Academician V. Vakhidov", Tashkent, Uzbekistan

DOI: 10.67620/sai.57d0015

ABSTRACT

Multiple renal arteries increase the technical complexity of living-donor kidney transplantation. This retrospective single-center cohort compared fixed-time outcomes in 578 living-related donor kidney transplantations: 471 grafts had one renal artery and 107 had two or more. All donors underwent preoperative multislice computed tomography angiography with three-dimensional reconstruction, and reconstruction was individualized according to vascular anatomy. Because outcome events were sparse, two-sided Fisher exact tests and absolute differences in survival proportions with 95% confidence intervals were used. Multiple-artery grafts accounted for 18.5% of the cohort, and 101 of 107 had two arteries. Six-month graft survival was 97.9% for single-artery grafts and 97.2% for multiple-artery grafts (difference, -0.7 percentage points; 95% CI [-5.9, 1.9]; p = .716). Twelve-month graft survival was 96.2% and 96.3%, respectively (difference, 0.1 percentage points; 95% CI [-5.6, 3.2]; p = 1.000). Recipient survival showed no statistically detectable difference at 6 months (96.8% vs. 96.3%; p = .765) or 12 months (95.5% vs. 94.4%; p = .613). These unadjusted analyses do not establish equivalence or noninferiority. Selected multiple-artery living-donor grafts were feasible in this experienced center, but the proposed MSCT-guided planning framework and area-equivalent ostial diameter remain descriptive tools requiring further validation.

ACCEPTED

10.08.26

Keywords: *kidney transplantation, living donor, multiple renal arteries, MSCT angiography, vascular reconstruction, bench surgery.*

CC BY

Introduction

Living-donor kidney transplantation is an established treatment for patients with end-stage kidney disease and offers advantages that include elective planning, reduced waiting time, and favorable graft outcomes. Expansion of the living-donor pool, however, increases the likelihood of evaluating donor kidneys with variant vascular anatomy, including grafts with multiple renal arteries. Multiple renal arteries are common anatomical variants and have historically raised concern because they may require additional bench reconstruction or arterial anastomoses and may increase technical complexity (Lentine et al., 2017; Zorgdrager et al., 2016).

Contemporary evidence suggests that multiple renal arteries should not automatically exclude an otherwise suitable living donor. In a patient-level meta-analysis of 8,400 recipients, Lim et al. (2023) found

no statistically significant difference in overall survival or graft survival between single- and multiple-artery living-donor grafts. Single-center reports have likewise described acceptable outcomes when vascular reconstruction is performed by experienced transplant teams (Garcia et al., 2021; Roth et al., 2024). At the same time, the literature is not uniformly reassuring. A recent systematic review and meta-analysis found slightly lower 1-year graft survival and higher overall and vascular complication rates for multiple-artery grafts, although absolute differences were small and living-donor multiple-artery grafts remained clinically usable (George et al., 2026). These findings underscore the need to distinguish feasibility from formal equivalence and to evaluate vascular complications in addition to survival.

Preoperative vascular imaging is central to this decision process. Computed tomography angiography is widely used to define renal arterial number, origin, diameter, course, branching, and relationships to the renal vein, collecting system, and renal hilum (Aghayev et al., 2019). Such information is particularly important when an accessory or polar artery may supply functionally important renal parenchyma or contribute to ureteral perfusion. Surgical options include separate anastomoses, side-to-side or pantaloon reconstruction, end-to-side reconstruction, and other individualized ex vivo techniques, each selected according to the specific anatomy (Muharia et al., 2025; Roth et al., 2024).

The present study therefore had two related but distinct aims. The primary aim was to compare unadjusted 6- and 12-month graft and recipient survival proportions between living-related donor grafts with one renal artery and grafts with multiple renal arteries. The secondary aim was to describe the center's preoperative MSCT-based anatomical assessment, vascular planning framework, reconstruction patterns, and a geometric area-equivalent ostial diameter calculation used as a technical guide during common-ostium reconstruction. The planning framework and ostial calculation were treated as descriptive tools rather than validated predictors of clinical outcome.

Methods

Study Design and Setting

This retrospective single-center cohort study included 578 living-related kidney transplantations performed at the State Institution "Republican Specialized Scientific and Practical Medical Center of Surgery named after Academician V. Vakhidov." Recipients were divided into a single renal artery group (n = 471) and a multiple renal artery group (n = 107). Primary outcomes were graft and recipient survival at 6 and 12 months.

Ethical Considerations

Donor evaluation and transplantation were performed according to institutional and national requirements. Legal and psychological assessment was completed for all donors.

Donor Evaluation

Donors underwent clinical, laboratory, functional, imaging, legal, and psychological assessment. Selection criteria included adult age, acceptable body mass index, preserved renal function, and absence of diabetes mellitus, uncontrolled hypertension, autoimmune disease, active urinary infection, or other contraindications. Renal assessment included estimated glomerular filtration rate, urinalysis, proteinuria testing, and radionuclide split renal function when indicated (Lentine et al., 2017).

MSCT Angiography

All donors underwent preoperative multislice computed tomography angiography with three-dimensional reconstruction. Assessment included the number and diameter of renal arteries, bifurcation level, arterial length, distance between ostia, polar arteries, segmental perfusion territory, and relationships with the renal vein, ureter, and renal hilum. MSCT findings were used to plan separate anastomoses, common-ostium formation, or individualized ex vivo reconstruction.

Surgical Reconstruction

Bench reconstruction was performed under cold preservation using atraumatic vascular techniques. Separate anastomoses were preferred when arteries were widely separated, whereas side-to-side or

ISSN: 2181-3337 | SCIENTISTS.UZ

pantaloon reconstruction was considered for closely positioned arteries. Three- and four-artery grafts were reconstructed using individualized 2+1, 1+1+1, or 2+2 strategies.

For combined arterial reconstruction, the area-equivalent ostial diameter was calculated as:

$D_eq = \sqrt{(d_1^2 + d_2^2)}$

This calculation was used as a morphometric guide rather than as a direct measurement of blood flow.

Descriptive Vascular-Anatomical Planning Framework

A four-level institutional planning framework was used to summarize anticipated technical complexity. Because the present study does not establish that the categories are mutually exclusive or predictive of outcomes, the framework is presented as a descriptive surgical planning aid rather than a validated risk score. Category-specific outcome analysis was not performed.

Table 1

Descriptive Vascular-Anatomical Planning Framework

Category	Arterial anatomy	Minimum diameter	Branching pattern	Planning implication
I	1 artery	>= 4 mm	Bifurcation > 1 cm from hilum	Low expected complexity; standard transplantation
II	2 arteries	2.5-4 mm	Near renal hilum	Moderate complexity; consider bench plasty and experienced vascular technique
III	2-3 arteries	2-3 mm	Intrahilar branching	High complexity; individualized ex vivo reconstruction by a specialized team
IV	>= 3 arteries	< 2 mm	Intrahilar or parenchymal branching	Very high complexity; multidisciplinary review, individualized protocol, consideration of contralateral kidney or nonuse

Note. The framework summarizes the institutional approach to vascular-anatomical planning. It has not been externally validated and should not be interpreted as a prognostic classification.

Surgical Strategy and Bench Reconstruction

The donor nephrectomy approach was selected according to donor anatomy, anticipated technical complexity, and institutional experience. Open retroperitoneal nephrectomy was preferred for the most complex arterial variants. After explantation, the graft was immediately perfused with cold preservation solution. In grafts with multiple arteries, each arterial lumen was perfused to assess patency and segmental perfusion. Bench reconstruction was performed under cold ischemic conditions using atraumatic handling, magnification, fine monofilament polypropylene sutures, and attention to avoiding stenosis, twisting, and tension.

For two arteries located sufficiently close to permit reconstruction without tension, side-to-side or pantaloon reconstruction could be considered; more widely separated arteries could be implanted separately. For three arteries, the center used either a 2+1 approach, in which two arteries were combined and the third implanted separately, or a 1+1+1 approach with three separate arterial anastomoses. For four arteries, the described approach paired upper and lower arterial branches into two reconstructed arterial complexes (2+2). These strategies should be interpreted as anatomy-dependent technical options rather than evidence that one technique is superior to another (Muharia et al., 2025).

Area-Equivalent Ostial Diameter

When two arterial lumens were combined into a common ostium, the reconstructed opening was assessed geometrically. Assuming circular cross-sections, the luminal area of an artery is $S = \pi(d^2)/4$. For two arteries, conservation of total cross-sectional area yields an area-equivalent diameter of $D_eq = \sqrt{(d_1^2 + d_2^2)}$. Thus, arteries measuring 4 mm and 3 mm correspond to an area-equivalent circular diameter of 5 mm. D_eq was treated as a morphometric area-equivalence calculation, not as a validated measure of

ISSN: 2181-3337 | SCIENTISTS.UZ

hemodynamic adequacy. Actual flow depends on anastomotic geometry, vessel compliance, downstream resistance, and other factors. Clinical validation would require direct flow, Doppler, angiographic, or stenosis outcome data.

Statistical Analysis

Categorical variables were summarized as counts and percentages. Because the number of graft and recipient deaths or failures was small, two-sided Fisher exact tests were used for comparisons of survival status between the single-artery and multiple-artery groups at 6 and 12 months. Absolute differences in survival proportions were calculated as the multiple-artery proportion minus the single-artery proportion, with 95% confidence intervals estimated using the Newcombe method. Statistical significance was defined as $p < .05$. The analyses were unadjusted. No formal equivalence or noninferiority margin was prespecified; therefore, a nonsignificant result was interpreted only as failure to detect a difference and not as proof of equivalence. Time-to-event analyses were not performed.

Results

Distribution of Renal Arterial Anatomy

Among 578 living-related donor kidney transplantations, 471 grafts (81.5%) had one renal artery and 107 grafts (18.5%) had multiple renal arteries. Within the multiple-artery group, 101 grafts (94.4%) had two arteries, two grafts (1.9%) had three arteries, and four grafts (3.7%) had four arteries. Thus, the evidence from the multiple-artery cohort primarily reflects grafts with two renal arteries, whereas grafts with three or four arteries were uncommon.

Revascularization Patterns

Table 2

Distribution of Multiple-Artery Anatomy and Revascularization Strategies

Arterial anatomy	n/N of MRA (%)	Revascularization pattern	n within anatomy subgroup (%)
2 arteries	101/107 (94.4%)	1+1	101/101 (100.0%)
3 arteries	2/107 (1.9%)	2+1	1/2 (50.0%)
3 arteries	2/107 (1.9%)	1+1+1	1/2 (50.0%)
4 arteries	4/107 (3.7%)	2+2	4/4 (100.0%)

Note. MRA = multiple renal arteries. In the 1+1 and 1+1+1 patterns, arteries were implanted separately. In 2+1, two arteries were combined into a common ostium and the third was implanted separately. In 2+2, four arteries were reconstructed into two paired arterial complexes.

The predominance of 1+1 reconstruction is important for interpretation: 101 of 107 multiple-artery grafts (94.4%) had two arteries and were managed with separate arterial anastomoses. Consequently, the present cohort provides only limited clinical experience with common-ostium reconstruction and does not validate the area-equivalent ostial diameter calculation.

Graft and Recipient Survival Status

At 6 months, graft survival was 461 of 471 (97.9%) in the single-artery group and 104 of 107 (97.2%) in the multiple-artery group. The absolute difference was -0.7 percentage points (95% CI [-5.9, 1.9]), and Fisher's exact test did not detect a statistically significant difference ($p = .716$). At 12 months, graft survival was 453 of 471 (96.2%) and 103 of 107 (96.3%), respectively; the absolute difference was 0.1 percentage points (95% CI [-5.6, 3.2]; $p = 1.000$).

Recipient survival at 6 months was 456 of 471 (96.8%) in the single-artery group and 103 of 107 (96.3%) in the multiple-artery group, corresponding to a difference of -0.6 percentage points (95% CI [-6.2, 2.5]; $p = .765$). At 12 months, recipient survival was 450 of 471 (95.5%) and 101 of 107 (94.4%), respectively, corresponding to a difference of -1.1 percentage points (95% CI [-7.4, 2.6]; $p = .613$).

ISSN: 2181-3337 | SCIENTISTS.UZ

Table 3

Unadjusted Fixed-Time Graft and Recipient Survival Outcomes

Outcome	Time	One artery n/N (%)	Multiple arteries n/N (%)	Difference, pp (95% CI)	Fisher p
Graft survival	6 mo	461/471 (97.9)	104/107 (97.2)	-0.7 (-5.9, 1.9)	.716
Graft survival	12 mo	453/471 (96.2)	103/107 (96.3)	0.1 (-5.6, 3.2)	1.000
Recipient survival	6 mo	456/471 (96.8)	103/107 (96.3)	-0.6 (-6.2, 2.5)	.765
Recipient survival	12 mo	450/471 (95.5)	101/107 (94.4)	-1.1 (-7.4, 2.6)	.613

Note. Difference is the multiple-artery survival proportion minus the single-artery survival proportion, expressed in percentage points (pp). Confidence intervals use the Newcombe method. p values are two-sided Fisher exact tests. Nonsignificant p values do not establish equivalence or noninferiority.

Illustrative Complex Reconstructions

Two complex reconstructions illustrate the institutional approach. One three-artery graft was implanted using three separate arterial anastomoses (1+1+1), with adequate early perfusion and no early thrombosis, stenosis, or segmental ischemia reported. One four-artery graft was reconstructed using a 2+2 strategy; cold ischemia time was 30 minutes and warm ischemia time was 42 minutes, with satisfactory early Doppler perfusion. These cases are presented as technical illustrations and do not provide comparative evidence regarding the safety or superiority of the reconstruction strategies.

Discussion

In this retrospective single-center cohort, no statistically detectable difference was observed in unadjusted graft or recipient survival proportions at 6 or 12 months between single-artery and multiple-artery living-related donor kidney grafts. The point estimates were close, but the confidence intervals were sufficiently wide to include clinically meaningful differences in either direction. Accordingly, these findings support feasibility in selected cases but should not be interpreted as proof of equivalence, noninferiority, or absence of an independent effect of arterial anatomy.

The direction of the present findings is broadly consistent with several living-donor studies. Garcia et al. (2021) reported no significant difference in postoperative complications, delayed graft function, renal function, or graft survival in a retrospective comparison of single- and multiple-vessel living-donor grafts. Roth et al. (2024) likewise reported acceptable short- and long-term outcomes after arterial vascular reconstruction in a specialized living-donor program. Most notably, Lim et al. (2023) pooled patient-level survival data from 14 studies and found no significant difference in overall survival or graft survival between single- and multiple-artery living-donor transplantation.

Nevertheless, the broader literature indicates that similar survival does not necessarily mean identical perioperative risk. Zorgdrager et al. (2016) found higher complication and delayed graft function rates and a small reduction in 1-year graft survival among multiple-artery grafts, although longer-term graft and patient survival were similar. George et al. (2026) similarly reported modestly lower 1- and 5-year live-donor graft survival and higher total and vascular complication rates in multiple-artery grafts. These data support a nuanced conclusion: multiple renal arteries are not an automatic contraindication, but they may increase technical and complication burdens that are not captured by survival proportions alone.

This distinction is especially relevant because outcomes in the present study were limited primarily to graft and recipient survival. Systematic comparative data were not available for delayed graft function, postoperative estimated glomerular filtration rate, arterial thrombosis, transplant renal artery stenosis, reintervention, ureteral complications, bleeding, ischemia times across both groups, or length of stay. These outcomes are clinically important in studies of multiple renal arteries. For example, Choudhary et al. (2024) identified ex vivo reconstruction of multiple renal arteries as an independent risk factor for

ISSN: 2181-3337 | SCIENTISTS.UZ

clinically significant transplant renal artery stenosis in a matched case-control study, underscoring the value of dedicated vascular follow-up when reconstruction is required.

Preoperative MSCT angiography remains a rational component of donor planning because it characterizes arterial number, caliber, branching, and spatial relationships that determine the feasibility of nephrectomy and implantation (Aghayev et al., 2019). The present study, however, cannot establish the diagnostic accuracy or outcome benefit of MSCT itself because every donor underwent the same imaging pathway and no reference-standard or alternative-imaging comparison was performed. The imaging component should therefore be interpreted as a description of the center's planning process, not as a comparative evaluation of MSCT efficacy.

The four-level vascular-anatomical framework has a similar status. It may help organize anatomical features that increase technical complexity, but the current data do not establish category reliability, calibration, discrimination, or association with complications. The category definitions contain potentially overlapping combinations of arterial number, diameter, and branching level. Future validation should prospectively define mutually exclusive assignment rules, assess interobserver agreement, and correlate categories with operative time, ischemia time, vascular and urological complications, graft function, and long-term outcomes.

The area-equivalent ostial diameter calculation is mathematically sound as a conservation-of-area relationship. For two circular lumens, $D_eq = \sqrt{(d_1^2 + d_2^2)}$ gives the diameter of a circle having the same total cross-sectional area. Its clinical meaning should not be overstated. Hemodynamic performance is also influenced by local geometry, suture configuration, branching angle, vessel compliance, pressure gradient, and downstream resistance. The present cohort offers very limited exposure to common-ostium reconstruction because 94.4% of multiple-artery grafts had two arteries and were implanted as separate anastomoses. The calculation is therefore best considered a hypothesis-generating morphometric aid until linked to Doppler velocities, computed tomography findings, pressure/flow measurements, stenosis, or graft perfusion outcomes.

Accessory polar arteries also require anatomy-specific judgment. Lower-pole arterial branches may contribute to ureteral blood supply and therefore warrant particular caution during donor nephrectomy and implantation, consistent with guideline principles for living-donor evaluation and preservation of clinically important arterial supply (Lentine et al., 2017). The present study does not validate a universal diameter threshold for accessory-artery ligation. Decisions regarding sacrifice or reconstruction should integrate diameter, perfusion territory, location, and the anticipated effect on renal parenchymal and ureteral perfusion.

Limitations

This study has several important limitations. First, its retrospective single-center design limits causal inference and generalizability. Second, the study period and completeness of consecutive case ascertainment were not reported, limiting assessment of temporal context and selection. Third, baseline donor and recipient characteristics were not available for adjusted analysis, and residual confounding therefore cannot be excluded. Fourth, time-to-event analyses were not performed; outcomes were evaluated at fixed 6- and 12-month points. Fifth, the number of grafts with three or four renal arteries was very small, preventing reliable subgroup comparisons of complex reconstruction strategies. Sixth, follow-up was limited to 12 months. Seventh, clinically relevant secondary outcomes—including delayed graft function, renal function, vascular and urological complications, stenosis, and reintervention—were not systematically analyzed. Finally, the proposed planning framework and area-equivalent ostial diameter were not prospectively or externally validated.

Clinical Implications and Future Research

The current data support continued consideration of living-related donor kidneys with multiple renal arteries when donor selection, imaging, and vascular expertise are appropriate. Future work should

ISSN: 2181-3337 | SCIENTISTS.UZ

prospectively capture donor and recipient baseline variables, exact arterial measurements, operative and ischemia times, reconstruction technique, serial renal function, Doppler parameters, vascular and urological complications, and time-to-event outcomes. A larger multicenter cohort would allow validation of an anatomy-based planning model and evaluation of whether measured reconstructed ostial area or diameter predicts transplant renal artery stenosis or segmental hypoperfusion.

Conclusion

In this single-center retrospective cohort of 578 living-related donor kidney transplantations, 107 grafts had multiple renal arteries. Unadjusted graft and recipient survival proportions at 6 and 12 months did not show a statistically detectable difference between single- and multiple-artery groups. These findings support the feasibility of selected multiple-artery grafts in an experienced center but do not establish equivalence, noninferiority, or an independent absence of risk. MSCT-based anatomical assessment and individualized reconstruction are clinically plausible components of surgical planning, whereas the proposed vascular-anatomical framework and area-equivalent ostial diameter should be regarded as descriptive tools requiring prospective validation. Future analyses should incorporate baseline covariates, time-to-event methods, graft function, and vascular and urological complications.

Data Availability

The datasets analyzed during the current study are available from the corresponding author upon reasonable request, subject to institutional and ethical requirements.

Author Contributions

Conceptualization: A. S. Suyumov and Z. T. Matkarimov. Surgery and clinical management: A. S. Suyumov, Z. T. Matkarimov, and M. O. Rustamov. Data collection: M. O. Rustamov. Statistical analysis: A. S. Suyumov and Z. T. Matkarimov. Writing - original draft: A. S. Suyumov and Z. T. Matkarimov. Writing - review and editing: all authors. All authors read and approved the final manuscript.

REFERENCES

1. Aghayev, A., Gupta, S., Dabiri, B. E., & Steigner, M. L. (2019). Vascular imaging in renal donors. Cardiovascular Diagnosis and Therapy, 9(Suppl 1), S116-S130. https://doi.org/10.21037/cdt.2018.11.02
2. Choudhary, D., Vijayvergiya, R., Kishore, K., Subramani, V. N., Banoth, M., Reddy Perugu, S. P., Mandwar, M., Bamaniya, B., Panjathia, A., Gupta, P., Patil, S. K. S., Sethi, J., Gorsi, U., Singh, S., Kenwar, D., & Sharma, A. (2024). Vascular reconstruction of multiple renal arteries-A risk factor for transplant renal artery stenosis: Insight from a matched case-control study. Transplant International, 37, 13298. https://doi.org/10.3389/ti.2024.13298
3. Garcia, L. E., Parra, N., Gaynor, J. J., Baker, L., Guerra, G., & Ciancio, G. (2021). Clinical outcomes following single vs. multiple vessel living-donor kidney transplantation: A retrospective comparison of 210 patients. Frontiers in Surgery, 8, 693021. https://doi.org/10.3389/fsurg.2021.693021
4. George, A. R., Dragan, Z., Gilliatt, F. R. J., Puttaswamy, V., & Saricilar, E. C. (2026). Multiple renal arteries in renal transplantation: A systematic review and meta-analysis. ANZ Journal of Surgery, 96(3), 440-448. https://doi.org/10.1111/ans.70408
5. Lentine, K. L., Kasiske, B. L., Levey, A. S., Adams, P. L., Alberú, J., Bakr, M. A., Gallon, L., Garvey, C. A., Guleria, S., Li, P. K.-T., Segev, D. L., Taler, S. J., Tanabe, K., Wright, L., Zeier, M. G., Cheung, M., & Garg, A. X. (2017). KDIGO clinical practice guideline on the evaluation and care of living kidney donors. Transplantation, 101(8S Suppl 1), S1-S109. https://doi.org/10.1097/TP.0000000000001769
6. Lim, E. J., Fong, K. Y., Li, J., Chan, Y. H., Aslim, E. J., Ng, L. G., & Gan, V. H. L. (2023). Single versus multiple renal arteries in living donor kidney transplantation: A systematic review and patient-level meta-analysis. Clinical Transplantation, 37(11), e15069. https://doi.org/10.1111/ctr.15069
7. Muharia, B. H. R., Situmorang, G. R., Rasyid, N., Rodjani, A., & Birowo, P. (2025). Comparing anastomosis techniques on ischemia time in multi-arterial kidney grafts: A systematic review and meta-analysis. Medical Journal of Indonesia, 34(1), 30-36. https://doi.org/10.13181/mji.oa.257527

ISSN: 2181-3337 | SCIENTISTS.UZ

8. Roth, N., Kalteis, M., Krause, A., Rösch, C. S., Huber, J., Enkner, W., Haller, M., Cejka, D., Függer, R., & Biebl, M. (2024). Vascular reconstructions in living donor kidney transplantation: A single-center experience over the last 17 years. Frontiers in Transplantation, 3, 1488277. https://doi.org/10.3389/frtra.2024.1488277
9. Zorgdrager, M., Krikke, C., Hofker, S. H., Leuvenink, H. G. D., & Pol, R. A. (2016). Multiple renal arteries in kidney transplantation: A systematic review and meta-analysis. Annals of Transplantation, 21, 469-478. https://doi.org/10.12659/AOT.898748

ISSN: 2181-3337 | SCIENTISTS.UZ

CONTENTS

Agzamova Shoira, Khaybullina Zarina, Babadjanova Faniya
GROWTH AND NUTRITIONAL STATUS IN YOUNG CHILDREN WITH CONGENITAL HEART DISEASE 4

Karimova Dilobar, Ibodullaev Z.
ASSESSING THE EFFECTS OF MULTIMODAL PSYCHOMOTOR REHABILITATION ON MOTOR FUNCTION AND FUNCTIONAL INDEPENDENCE IN CHILDREN WITH CEREBRAL PALSY: A RANDOMIZED CONTROLLED TRIAL 17

Khudayberganova Khulkar
COMPARATIVE MORPHOBIOLOGICAL ASSESSMENT AND LENGTH–WEIGHT RELATIONSHIPS OF GRASS CARP (Ctenopharyngodon idella VALENCIENNES, 1844) BROODSTOCK FROM THREE POND FARMS IN THE TASHKENT REGION 25

Musaeva Nargiza
CLINICAL PROGRESSION OF RHEUMATOID ARTHRITIS AND HEMOVASCULAR REMODELING: ASSOCIATIONS BETWEEN SEROSTATUS, FUNCTIONAL CLASS, ENDOTHELIAL DYSFUNCTION AND HEMOSTATIC ACTIVITY 31

Musaeva Nargiza, Babadjanova Shaira
PATHOGENETICALLY ORIENTED CORRECTION OF PLATELET ACTIVITY, COAGULATION IMBALANCE AND ENDOTHELIAL DYSFUNCTION IN RHEUMATOID ARTHRITIS 37

Sarimsakov Maksudkhon, Seitbayev Kuandik
COTTON YIELD AND IRRIGATION WATER PRODUCTIVITY UNDER DRIP AND SURFACE IRRIGATION REGIMES IN CALCISOLS OF UZBEKISTAN 46

Xudayberganov Munis, Sharipova Sarvinoz
MATERNAL PRE-PREGNANCY BODY MASS INDEX AMONG TERM NEWBORNS WITH PROLONGED JAUNDICE: CLINICAL AND LABORATORY FINDINGS 53

Turakulov Uktamjon, Mardonov Jamshid, Ergashev Farhod, Kurbonova Dilnoza, Sadikov Rustam
LOCAL MULTIFUNCTIONAL HYDROGEL THERAPY IN EXPERIMENTAL FIBRINOPURULENT PERITONITIS: ANTIBACTERIAL, FIBRINOLYTIC, AND REPARATIVE EFFECTS OF A NOVEL LEVOFLOXACIN-CUCUMAZINE-NA-CMC COMPOSITE 64

Jovliyev Behruz
EVALUATION OF THE CLINICAL EFFECTIVENESS OF PROFESSIONAL AND PERSONAL ORAL HYGIENE MEASURES IN THE TREATMENT OF CHRONIC CATARRHAL GINGIVITIS IN ADOLESCENTS 81

Ziyodullayev Samarddin
EVALUATION OF THE CLINICAL AND RADIOGRAPHIC OUTCOMES OF PULPITIS TREATMENT IN PRIMARY MOLARS USING DEVITALIZING PASTES 87

Makhmudov Lazizbek, Yakubova Rana, Tagayalieva Nigora
IN VIVO EVALUATION OF THE CHRONIC TOXIC EFFECTS OF REPEATED ADMINISTRATION OF THE C-4 COMPOSITION AT DIFFERENT DOSES IN RABBITS 95

Teshayev Rajabbek
AUTOMATIC SPEECH RECOGNITION AND CLINICAL DOCUMENTATION TIME IN TWO HEALTHCARE INSTITUTIONS IN BUKHARA, UZBEKISTAN: A WITHIN-CLINICIAN QUASI-EXPERIMENTAL STUDY 109

Ismoilov Iqboljon, Aliyeva G
MECHANISM OF DENTAL ENAMEL DEMINERALIZATION: THE ROLE OF ORGANIC ACIDS, PH, AND HYDROXYAPATITE DISSOLUTION 116

Karakhonova Sarvinoz
PSYCHOMOTOR THERAPY COMBINED WITH COGNITIVE-BEHAVIORAL TECHNIQUES FOR NEUROTIC SYMPTOMS IN VASCULAR DEMENTIA: A PROSPECTIVE COMPARATIVE PILOT STUDY 123

A. S. Suyumov, Z. T. Matkarimov, M. O. Rustamov, D. N. Komilova
EARLY OUTCOMES OF LIVING-RELATED DONOR KIDNEY TRANSPLANTATION WITH MULTIPLE RENAL ARTERIES: A RETROSPECTIVE COHORT STUDY WITH AN MSCT-GUIDED ARTERIAL RECONSTRUCTION FRAMEWORK 130

ISSN: 2181-3337 | SCIENTISTS.UZ



International Scientific Journal
Science and Innovation Series D
Volume 5 Issue 7

ISSN: 2181-3337

Published: 10.08.2026. Font: “Times New Roman”.

LLC “Science and innovation”
License Mass Media №:1597 27.04.2022
License Publisher №:455168 21.11.2024
Address: 100121, Uzbekistan, Tashkent city, Yakkasaroy district,
Shota Rustaveli Street 150, Vega Business Center, 6th floor, Room 2.
www.scientists.uz, info@scientists.uz, +998901259654